

Impact of polymeric additives on the functionality of Microfibrillar cellulose

Deepa Agarwal, MSc

Thesis submitted to the University of Nottingham for the
degree of Doctor of Philosophy

Division of Food Sciences
School of Biosciences
The University of Nottingham
Loughborough
LE12 5RD

March 2016

*The research leading to this thesis has received joint funding from
Borregaard AS and Oslofjordfondet regionale forskningsfond,
Norway (2012-2015).*



Abstract

The aim of the work presented in this thesis was to investigate the impact of different mechanical treatments on the structure and physical properties of microfibrillar cellulose (MFC) and examine further changes upon drying of these MFC suspensions. It has been demonstrated that depending on the type of homogeniser and number of passes through the homogeniser results in a different variety of MFC with a distinct degree of fibrillation. An entangled network structure of MFC plays an important role in maintaining the rheological properties as well as water mobility in the system. Spin-spin relaxation time (T_2) of the highly entangled microfibrils network indicates that the water mobility was higher in suspensions with a high degree of fibrillation, as compared to the low degree of fibrillation. It is now well established that during the drying stage MFC fibril-aggregates are formed due to strong intermolecular hydrogen bonds within the network structure. Due to a lack of redispersibility in water and the presence of fibril-aggregates, a non-homogenous distribution throughout the system was observed and the aqueous suspension of redispersed MFC shows a noticeable reduction in complex and shear viscosities.

Hence, the next stage of the study focused on to stabilise the fibril-networks of microfibrils upon the drying, where the impact of different polymeric additives *i.e.* carboxyl methylcellulose (CMC), locust bean gum (LBG) and a blend of CMC/LBG was investigated. The addition of polymeric additives

significantly improves the redispersibility of dried MFC in water with reduced fibrils aggregates. The interaction between microfibrils and additives are driven by surface OH-group-mediated hydrogen bonds; however the extents of these interactions are highly dependent on the type of additive used to stabilise the microfibrils. The point of the addition of polymeric additives plays an important role in terms of interaction between the polymeric additive and MFC. Co-processing of MFC and polymeric additives has a noticeable impact on the degree of fibrillation (visualised through light microscopy and degree of transparency) of the final MFC product. The presence of a charged polymeric additive such as carboxyl methyl cellulose (CMC) results in strong synergistic interaction with MFC, whereas weak synergistic interaction is reported with Locust bean gum (LBG). The addition of a CMC/LBG blend also showed strong synergistic interaction with MFC when added in a small amount.

The amounts of additive present in the system have a noticeable impact on the viscoelastic properties of the suspensions. At ambient temperature, the MFC/additives suspensions formed a weak gel-like network. It was found that a polymeric additive forms a surface coating on MFC fibrils which protects the fibrils, to form strong intermolecular hydrogen bonds during the drying process, resulting in improved redispersibility of the dry product in an aqueous medium. The interaction between MFC and polymeric additives leads to an increase in moisture uptake even after drying process. Increase in water accessibility within the microfibril network was evident with Dynamic

Vapour sorption analysis and low-temperature thermal transitions measured by Differential Scanning Calorimetry.

This research also features a preliminary study on the potential application of MFC produced from softwood spruce as a dietary fibre for food application. This includes a comparison between the microstructure and different physical properties of softwood MFC (flakes and powder) with food grade commercial dietary fibres *e.g.* citrus fibres. Softwood MFC (both flakes and powder form) showed similar rheological properties to other cellulosic dietary fibres such as citrus fibres. Due to a highly entangled network structure softwood MFC showed the highest water retention values (also known as water holding capacity) as compared to other cellulosic fibres. A comparison of the rate of taste *i.e.* salt perception was also carried out, and the structural features of MFC affect this and appear to be more similar to soluble hydrocolloid solutions than the particulate systems such as citrus fibres.

In summary, this thesis describes the mechanistic understanding of the interaction between MFC and different polymeric additives such as CMC and LBG. This research highlights the these interactions results in different microstructures affecting the functional properties of MFC such as redispersing behaviour, water mobility, low-temperature polymer-water interactions and rheological properties. Microfibrillar cellulose (MFC) are not only fundamentally interesting but most importantly they are practical, and certainly offers a more environmentally friendly, and cost-effective ingredient for various traditional commercial applications such as paints, composites and

adhesives. This work also proves, for the first time, that the MFC from softwood can also be used as an ingredient for food applications as a bulking agent, stabilising agent, texture and viscosity enhancer.

Acknowledgments

My first sincere appreciation and a deep sense of gratitude to Professor. Tim J. Foster for his thoughtful guidance, keen interest, patience and cooperation during the course of this PhD work. He gave the chance to present, and gain confidence to present this work in public forum/conferences. I am also extremely grateful of associate professor Dr Bettina Wolf, who has been always there to guide on technical aspects of rheology and invaluable discussion and suggestion during my internal annual reviews.

Special thanks to Dr William MacNaughtan for his help in the lab to understand and run different techniques and for all the discussion on a wide range of topics. I would like to extend special thanks to Dr Roger Ibbett for valuable inputs and feedback during the writing process of this thesis. Thanks to the technical staff of food science and Sensory Science Centre for technical support on different equipment and day-to-day lab.

I would like to express my gratitude to Borregaard AS and Oslofjordfondet regionale forskningsfond (Norwegian government) for financial and industrial support during this project. I am profoundly grateful to Dr Hans Henrik Øverbø, Dr Inger Mari Nygård Vold and all other staff members of Borregaard AS, Sarpsborg (Norway), for their constant encouragement and importantly for providing samples during this project.

And most importantly my eternal gratitude with immense love goes to my gracious and loving parents, brother, sister, brother-in-law, Rishith and Rivaan (my nephews) for their never ending support, love, care and affections throughout this journey. And finally, I acknowledge the presence of The Almighty for kind benedictions, blessings and his invisible, yet omnipresent, hand over my head so as to make me feel that he is always with me.

This thesis is dedicated to my loving grandmother Smt. Kiran Devi Goyal (1930-2016).

List of Abbreviations and Symbols

$ \eta^* $	Complex viscosity (Pas)
^{13}C or C	Carbon
2D	2-Dimension
3D	3-Dimension
atm	Atmosphere
BL1 or BL	Blend of CMC and LBG
CaCl₂	Calcium Chloride
Cell	Cellulose
CF100	CitriFi100
CMC	Carboxymethyl Cellulose
CMC(mix)	Carboxymethyl Cellulose (mixture)
CO₂	Carbon dioxide
cos	Cosine
CPKA	CP Kelco A CMC
CPMAS	Cross Polarization Magic Angle Spinning
CPMG	Carr-Purcell-Meiboom-Gill
CS	Cationic Starch
CTE (F)	Cellulosic Texture Enhancer (Flakes form)
CTE (P)	Cellulosic Texture Enhancer (Powder form)
CTE	Cellulosic Texture Enhancer
D	Dried and redispersed
DC	Dry Content (total solid content) (% w/w)
BMFC	Borregaard-Microfibrillar cellulose (concentrated to 8.97% w/w) produced by Borregaard Fibrillation technology
dMFC	d-Microfibrillar cellulose (2% w/w) produced by Borregaard Fibrillation technology
DS	Degree of Substitution
DTGA	Derivative Thermo-gravitational analysis
DW60	Dow Wolff 60000 CMC
FD	Freeze Drying
FTIR	Fourier transforms infrared spectroscopy
G	Galactose
gms	grams
G'	Storage Modulus (Pa)
G''	Loss Modulus (Pa)
GM	Galactose: Mannose ratio
H₂O	Water
HBAQ+	Herbacel AQ+
H-bonds	Hydrogen-bonds
hrs	hours
Hz	Hertz
HPMC	hydroxyl propyl methyl cellulose
K	kilo
LBG	Locust Bean Gum
M	Mannose
MFC/CMC	Microfluidics MFC with CMC(mix)
MFC/LBG	Microfluidics MFC with LBG

MFC/BL	Microfluidics MFC with Blend
MCC	Microcrystalline Cellulose
MFC	Microfibrillar cellulose
mMFC	Microfluidics MFC
mg	milligrams
mins	minutes
ml	milli-litres
mPa.s	milli-pascal seconds
ms	milli-seconds
N₂	Nitrogen gas
Na⁺	Sodium
NaCl	Sodium Chloride
NaOH	Sodium Hydroxide
ND	Never-dried system
nd	no-dimension reported
NiMFC	Niro-Microfibrillar cellulose produced by Niro-homogeniser
nm	nano-meter
NMR	Nuclear Magnetic Resonance
O (5, 6..)	Oxygen (5 or 6..)
OD	Oven Drying
1,2,3P	1, 2, or 3 Passes
Pa	Pascal
PC	Pair comparison test
ppm	parts per million
RMFC	Refined Microfibrillar cellulose
rpm	Rotation per minute
s⁻¹	per seconds
SD	Spray Drying
sec	seconds
sin	Sine
T	Time
Tanδ	Loss Tangent
T₁	Spin-lattice relaxation time
T₂	Spin-spin relaxation time
TGA	Thermogravimetric Analysis
T_m	Melting Temperature
Δt	length of time of excited nucleus
μm	micrometres
μs	microseconds
VOD	Vacuum Oven Drying
w/w	weight for weight
γ̇	Shear rate (1/s)
δ	Phase angle
η	Shear Viscosity (Pas)
θ	Theta (2θ)
σ	Shear stress
σ_o	Maximum shear stress
τ	tau (μs) CPMG pulse sequence
Υ	Strain
ω	Angular frequency

Contents	
I. Abstract	i
II. Acknowledgements	v
III. List of Abbreviations and Symbols	vi
IV. Contents	viii
V. List of Figure	xi
VI. List of Tables	xvii
Chapter 1: Introduction	01
1. General Introduction	02
1.1. Cellulose	05
1.1.1. Molecular structure	08
1.1.1.1. Cellulose – I (native cellulose)	09
1.1.1.2. Cellulose - II (Regenerated cellulose)	11
1.1.1.3. Cellulose – III and IV	15
1.2. Microfibrillar cellulose	15
1.2.1. Factors affecting the production of MFC	19
1.2.1.1. Source and extraction procedure of cellulose.....	19
1.2.1.2. Impact of drying	25
1.2.2. Suspension properties of MFC	28
1.3. Carboxymethylcellulose	32
1.4. Galactomannan	35
1.4.1. Locust bean gum	36
1.5. Cellulose/hydrocolloid mixtures	39
1.6. Brief Introduction to the thesis	41
1.7. Objectives	44
1.8. Thesis structure	45
2. Chapter 2: Materials and Methods	47
2.1. Introduction	48
2.2. Materials	48
2.3. Sample preparation	49
2.3.1. Microfibrillar cellulose (MFC)	49
2.3.2. Carboxymethyl cellulose (CMC)	50
2.3.3. Locust bean gum (LBG)	51
2.3.4. CMC/LBG blend	52
2.3.5. MFC/additive mixtures	52
2.4. Methods	53
2.4.1. Rheological Analysis	54
2.4.1.1. Flow behaviour	56
2.4.1.2. Viscoelastic behaviour	57
2.4.1.3. Equipment settings	60
2.4.2. Low Field (¹ H - Relaxation) NMR	61
2.4.2.1. Equipment settings	63

2.4.3.	Wide angle X-Ray Diffraction (WAXD)	64
2.4.3.1.	Equipment settings	68
2.4.4.	Differential scanning calorimetry (DSC)	68
2.4.4.1.	Equipment settings	69
2.4.5.	Derivative Thermo-gravitational analysis (DTGA)	69
2.4.5.1.	Equipment settings	70
2.4.6.	Microscopy	71
2.4.6.1.	Light microscopy	71
2.4.6.2.	Fluorescence microscopy	71
3.	Chapter 3: Microfibrillar cellulose: Impact of fibre network and drying on suspension properties	73
3.1.	Introduction	74
3.2.	Materials and Methods	77
3.2.1.	Sample preparation	78
3.2.1.1.	Drying Process	78
3.2.2.	Light microscopy	79
3.2.3.	Phase Separation and UV spectrophotometry	80
3.2.4.	Rheology	80
3.2.5.	Relaxation NMR	81
3.2.6.	Wide Angle X-ray diffraction (WAXD)	81
3.2.7.	Data analysis	81
3.3.	Results and Discussion	82
3.3.1.	Microstructure of MFC	82
3.3.2.	Rheological properties of MFC suspension	90
3.3.2.1.	Rheological properties of Never-dried MFC suspension	90
3.3.2.2.	Impact of number of passes on rheological properties.....	93
3.3.2.3.	Impact of drying on rheological properties of rehydrated MFC suspension	101
3.4.	Conclusions	105
4.	Chapter 4: Impact of Polymeric Additives on Stabilisation of MFC added “after” Homogenisation	108
4.1.	Introduction	109
4.2.	Materials and Methods	111
4.2.1.	Sample preparation	111
4.2.2.	Microscopy	112
4.2.3.	Rheology	112
4.2.4.	Relaxation NMR	112
4.2.5.	Differential Scanning Calorimetry (DSC)	112
4.2.6.	Derivative Thermo-gravitational analysis (DTGA)	112
4.2.7.	Dynamic Vapour Sorption (DVS)	113

4.2.8.	Data analysis	113
4.3.	Results and Discussion	114
4.3.1.	Rheological properties of BMFC/additives suspensions	114
4.3.1.1.	Viscoelastic behaviour BMFC/additive suspensions.....	114
4.3.1.1.1.	Impact of CMC as additive	118
4.3.1.1.2.	Impact of LBG as additive	122
4.3.1.1.3.	Impact of Blend (CMC/LBG) as additive	125
4.3.1.2.	Modulus-temperature dependence	130
4.3.1.3.	Viscous synergism of BMFC/additive mixtures.....	132
4.3.2.	Impact of additives on water mobility	136
4.3.3.	Thermal transitions of BMFC/additive at low moisture	141
4.4.	Conclusions	152
5.	Chapter 5: Impact of Polymeric Additives on Stabilisation of MFC added “before” Homogenisation	154
5.1.	Introduction	155
5.2.	Materials and Methods	156
5.2.1.	Sample preparation	156
5.2.2.	Microscopy	157
5.2.3.	Rheology	158
5.2.4.	Differential Scanning Calorimetry (DSC)	158
5.2.5.	Derivative Thermo-gravitational analysis (DTGA).....	158
5.2.6.	Wide angle X-Ray diffractometry (WAXD)	158
5.2.7.	Relaxation NMR	158
5.2.8.	Dynamic Vapour Sorption (DVS)	158
5.2.9.	Data analysis	159
5.3.	Results and Discussion	159
5.3.1.	Microstructure of suspensions	159
5.3.2.	Rheological properties of MFC/additive suspensions	166
5.3.2.1.	Viscoelastic behaviour MFC/additive suspensions ...	166
5.3.3.	Impact of additives on water mobility	173
5.3.4.	Thermal transitions of MFC/additive at low moisture	175
5.4.	Conclusions	186
6.	Chapter 6: Application of MFC as dietary fibre	188
6.1.	Introduction	189
6.2.	Materials and Methods	194
6.2.1.	Sample preparation	194
6.2.2.	Microscopy	195
6.2.3.	Rheology	195
6.2.4.	Water Retention Values (WRV)	195
6.2.5.	Sensory evaluation	196
6.2.6.	Data analysis	198
6.3.	Results and Discussion	199

6.3.1. Microstructure of fibres	199
6.3.2. Rheological properties of suspensions	202
6.3.3. Sensory perception	207
6.4. Conclusions	212
7. Chapter 7: Conclusions and Future Work	214
VII. References	224
VIII. Appendix	245

List of Figures

- Figure 1.1:** (A) Wood fibres consist of several layers (middle lamella (ML), primary wall (P), secondary wall (S1, S2, S3) and lumen (W) (Cote 1967). (B) Molecular organisation of primary plant cell wall (Ceres, 2014); and (C) Organization of the cellulose chains into microfibrils and fibril aggregates (adapted from Rowland and Roberts (1972), Kerr and Goring (1975)).----- **06**
- Figure 1.2:** The molecular structure and the inter- or intra-chain hydrogen bond present in cellulose I, where black broken lines: inter-chain hydrogen bonding and blue lines: intra-chain hydrogen bonding (adapted from Festucci-Buselli *et al.* 2007).----- **12**
- Figure 1.3:** Chain arrangement of Cellulose I α and Cellulose I β and NMR spectra of each component (adapted from Baker *et al.*, 1997, Baker *et al.*, 2000, Atalla and Vanderhart, 1984).----- **12**
- Figure 1.4:** Shows the ¹³CPMAS solid state NMR spectra, (A) original/native Cellulose I and (B) cellulose II for various samples. (a) Avicel, (b) α -cellulose, (c) cotton linters, (d) corn stover, and (e) amorphous cellulose (adapted from Mittal *et al.*, 2011).----- **14**
- Figure 1.5:** Different polymorphs of cellulose and the main processing steps (adapted from Lavoine *et al.*, 2012).----- **14**
- Figure 1.6:** Flow diagram of different methods to disintegrate cellulose pulp into microfibrillar celluloses (adapted from Lavoine *et al.*, 2012, Saito *et al.*, 2006).----- **18**
- Figure 1.7:** Different technologies to produce Microfibrillar cellulose (adapted from Lavoine *et al.* 2012).----- **25**
- Figure 1.8:** Structure of CMC with DS of 1.0 (Celluloseethers, 2013).----- **32**
- Figure 1.9:** Structure of locust bean gum (Cybercolloids, 2012).----- **37**
- Figure 1.10:** Model proposed for the interaction between helix forming polysaccharides and galactomannan (adapted from Morris *et al.*, 1995).----- **38**
- Figure 2.1:** A schematic representation of two-plate model for shear-strain deformation (adapted from Mezger 2006).----- **55**
- Figure 2.2:** Types of viscosity behaviour presented (a) as viscosity curves $\eta(\dot{\gamma})$ and (b) as flow curves $\tau(\dot{\gamma})$ (Mezger 2006).----- **58**
- Figure 2.3:** Bragg's law demonstration, according to the 2θ deviation, the phase shift causes constructive or destructive interferences. (Recreated from Suryanarayana *et al.*, 1998)----- **67**

- Figure 2.4:** WAXD diffraction spectra of cellulose illustrating the peak deconvolution method. ----- **67**
- Figure 3.1:** Light microscopy images of different varieties of MFCs produced from softwood spruce cellulose pulp (Cellulose) at 2%w/w concentrations, all scale bars are 200 μ m. ----- **83**
- Figure 3.2:** Light microscopy images of dMFC after 4, 5, 6 and 7 Passes at 2%w/w concentration, scale bar: 200 μ m.----- **84**
- Figure 3.3:** Visual inspection of phase behaviour after 24hrs of 7-Pass dMFC samples at; (a) 2.0% w/w and (b) 0.1% w/w concentration. The black arrows indicates the upper layer (supernatant) of phase separated aqueous suspension of MFC. ----- **86**
- Figure 3.4:** Visible transmittance of the upper layer of dMFC suspension after 1 to 7 Passes, where the buffer is water and path length of the cuvette was 1cm. All results are average data of 4 replicates with standard deviation 1%. ----- **86**
- Figure 3.5:** WAXD analysis (a) X-ray diffractogram patterns for Cell (starting material, solid line) and 1 Pass (---) dMFC, and (b) change in crystallinity with increase in number of passes through high pressure homogeniser (dMFC - parallel pattern), microfluidics (MFC - dotted pattern) and starting cellulose (solid bar). All results are average data of duplicates.----- **88**
- Figure 3.6:** The schematic models representing the effect of the number of passes (1, 2 and 3 Pass) through the high-pressure homogeniser (HPH) on the crystalline and amorphous regions of cellulose during MFC production. (A) Cellulose structure before homogenisation; change in structure after (B) 1Pass, (C) 2Pass and (D) 3Pass through high-pressure homogeniser.----- **89**
- Figure 3.7:** Mechanical spectra of aqueous suspensions of never-dried 2dMFC diluted to different concentrations *i.e.* (Δ) 0.8%, (\square) 1.0%, (\circ) 1.5% and (\diamond) 2.0% w/w, where G' - solid and G'' - unfilled symbols; (a) as a function of frequency at 20°C and strain 0.2%, (b) as a function of temperature at 1Hz frequency and strain 1% with heating rate of 1°C/min. All results are average data with standard deviation 1%. ----- **91**
- Figure 3.8:** (A) Shear viscosity as a function of shear rate (1/s) (slope: -1.04), (B) Shear viscosity as a function of increasing (unfilled-symbols) and decreasing (filled-symbols) shear rate (s^{-1}); of 1%w/w suspension of dMFC after a number of passes through the homogeniser at 20°C. All results are highly reproducible with a standard deviation less than 0.1%. ----- **95**
- Figure 3.9:** Impact of a number of passes (dMFC) through high-pressure homogeniser on 1%w/w suspension properties of MFC at 20°C, where; (A) viscoelastic behaviour (G' & G'') as a function of frequency at strain 0.2%; with standard deviation $\pm 1\%$. (B) Complex viscosity is taken at 0.2% strain and 1Hz frequency. The complex viscosity values are averaged from 2 replicates with standard deviation $\pm 1\%$.----- **97**

- Figure 3.10:** Impact of degree of fibrillation on the T_2 (ms) of water for 2% w/w dMFC suspension systems measured at $20 \pm 1^\circ\text{C}$, fitted with the single exponential curve. The T_2 values are averaged from 4 replications and are not statistically significant with $p\text{-value} = 0.3$ ($\alpha: 0.05$).----- **99**
- Figure 3.11:** Model illustration of particle dispersion state and distribution of associated/interacting water in MFC suspensions, (a) associated water and free water distribution in microfibril aggregate in MFC suspension with low degree of fibrillation; whereas (b) associated/interacting water is distributed in the vicinity of the microfibril surface due to high degree of fibrillation.-----
----- **99**
- Figure 3.12:** Effect of different drying process on the shear viscosity of the re-dispersed 1%w/w suspension of BMFC at 20°C , recorded at 1 s^{-1} shear rate. The shear viscosity values are averaged from 2 replications with standard deviation $\pm 1\%$.----- **102**
- Figure 3.13:** Light microscopy images of 1% w/w suspension of re-dispersed BMFC in water, where highlighted area shows the BMFC aggregates/agglomerates, scale bar: $200 \mu\text{m}$.----- **103**
- Figure 3.14:** Spin-Spin relaxation time (T_2) (ms) of (-●-) BMFC diluted from 8.97% in the never-dried state (as received) and (-○-) redispersed oven dried BMFC as a function of concentrations at 20°C .----- **104**
- Figure 4.1:** Storage (G' , solid symbols) and loss (G'' , open symbols) moduli of redispersed suspension of BMFC with different additives as a function of frequency (Hz) at 20°C , where (a) BMFC/CMC, (b) BMFC/LBG, and (c) BMFC/Blend. All results are highly reproducible with standard deviation less than 0.1%.----- **116**
- Figure 4.2:** Light microscopy images of 2% w/w aqueous suspensions of dried and redispersed MFC100 (BMFC), BMFC with different additives (*i.e.* CMC(mix), LBG and Blend) at different concentration levels, scale bar: $200 \mu\text{m}$. ----- **117**
- Figure 4.3:** Complex viscosity and $\text{Tan } \delta$ (at frequency: 1 Hz and 0.2% strain) as a function of CMC (CMC(mix)) proportion in aqueous suspension of BMFC, and redispersed MFC100 at same proportion to BMFC present in BMFC/CMC formulation. Data presented is average of 4 replicates with standard deviation less than 0.1%.----- **120**
- Figure 4.4:** (A) Storage moduli and loss moduli of redispersed BMFC with different CMC's as a function of frequency (Hz) at 20°C ; and (B) Complex viscosity as a function of different CMCs present in BMFC/CMC (85:15 ratio) suspension. Data presented is an average of 4 replicates with a standard deviation less than 0.1%. ----- **121**
- Figure 4.5:** (a) Complex viscosity (frequency: 1 Hz and 0.2% strain) and $\text{Tan } \delta$ (dried samples only) as a function of LBG proportion in aqueous suspension of BMFC (wet (solid) and dried (unfilled)), where "□" unheated LBG and "◇" heated LBG. (b) The impact of different concentration of LBG on the complex

viscosity of dried and redispersed BMFC/LBG suspension, the overall concentration of all suspensions is 2% w/w. Data presented is average of 4 replicates with standard deviation 1%.----- **124**

Figure 4.6: Storage (-●-) and loss (-○-) modulus as a function of frequency at 20°C of CMC/LBG blends at different ratios of CMC/LBG *i.e.* CMC50:LBG50, CMC65:LBG35 and CMC75:LBG25 in aqueous solution. The overall concentration of all suspensions was 2% w/w. All results are highly reproducible with a standard deviation ±1%.----- **126**

Figure 4.7: (a) Complex viscosity (frequency: 1Hz and 0.2% strain) as a function of blend (BL1) proportion in BMFC suspension, where (-○-) MFC100 and (-◇-) BMFC/BL1 (wet (solid) and dried (unfilled)), (b) Impact of different ratios of CMC/LBG blends on complex ($|\eta^*|$) and shear viscosity (η , at shear rate 1s⁻¹) of redispersed BMFC/BL1 (85:15) suspension. The overall concentration of all suspensions was 2% w/w. All results are highly reproducible with standard deviation less than ±1%.----- **128**

Figure 4.8: Storage (G') and loss (G'') module of redispersed suspension of BMFC with different additives as a function of temperature (°C) at 1°C/min heating rate, where (a) BMFC/CMC, (b) BMFC/LBG, and (c) BMFC/Blend. All results are highly reproducible with a standard deviation ±1%.----- **129**

Figure 4.9: Spin-spin relaxation time (T₂) as a function of additives proportion in (○) BMFC/CMC, (Δ) BMFC/LBG and (◇) BMFC/BL1 formulations at 20°C of 2% w/w overall suspension concentration. Data presented is an average of 4 replicates with not statistically significant (p-value>0.05). Where T₂ value of 2%w/w CMC100 is 1227ms and LBG100 is 846ms.----- **135**

Figure 4.10: (A) Shear viscosity (at 1 s⁻¹ shear rate); and (B) T₂ (ms) of (-◇-) MFC100 (wet (solid) and dry (unfilled)), (-○-) CMC15 (wet (solid) and dry (unfilled)) as a function of concentrations at 20°C. Data presented is an average of 4 replicates, highly reproducible with standard deviation less than 0.1%.----- **139**

Figure 4.11: Fluorescence microscopy images of 2% w/w suspension of (a, b) BMFC/CMC *i.e.* CMC15 & CMC50 respectively, (c) BMFC/BL1 (BL15), and (d) BMFC/LBG (LBG15), at scale bar: 200μm, where CMC and LBG are tagged with FITC (shown as green colour).----- **140**

Figure 4.12: DSC thermograms of BMFC/CMC, BMFC/LBG and BMFC/BL1 at (a) 2% and (b) 20% moisture content. All results are highly reproducible with standard deviation less than 0.1%.----- **143**

Figure 4.13: The thermal degradation under a nitrogen atmosphere of (a) CMC100, LBG100 and MF100 at low water content, and comparison between MFC100 (BMFC), BMFC/CMC, BMFC/LBG and BMFC/BL1 where (b) low, and (c) high water content. Data presented is highly reproducible.----- **146**

Figure 4.14: Thermal degradation of (a) BMFC/CMC, (b) BMFC/LBG, and (c) BMFC/BL1 under a nitrogen atmosphere with increasing amount of additives

in the system at low water content. Data presented is highly reproducible.----

- **149**
- Figure 4.15:** Sorption and desorption isotherms of different BMFC/additives powders (BMFC/CMC, BMFC/LBG, BMFC/BL1 and MFC100) obtained under dynamic conditions at 20°C temperature. Data presented is highly reproducible with standard deviation less than 0.1%.----- **150**
- Figure 5.1:** Light microscopy images of aqueous suspensions (2%w/w) of never-dried (wet) MFC produced in the presence of different additives: (a) CMC(mix), (b) Blend (BL), and (c) LBG; after (i) 1Pass, (ii) 2Pass, and (iii) 3Pass through homogeniser; scale bar: 200µm.----- **161**
- Figure 5.2:** Light microscopy images of (a) never dry (wet) and (b) dried and redispersed aqueous suspension of MFC/LBG(LV) (low concentration/viscosity *i.e.* 0.4%w/w) after (i) 1Pass, (ii) 2Pass, and (iii) 3Pass through homogeniser.----- **162**
- Figure 5.3:** Light microscopy of 2% w/w aqueous suspensions of dried and redispersed MFC with different additives: (a) CMC(mix), (b) Blend (BL), and (c) LBG after (i) 1Pass, (ii) 2Pass, and (iii) 3Pass through homogeniser. --- **162**
- Figure 5.4:** Crystallinity of MFC100 and MFC/additives when added before homogenisation as a function of a number of passes (1, 2 and 3 Passes) through microfluidic homogeniser. The data presented is average of duplicates and is highly reproducible.----- **166**
- Figure 5.5:** Storage (G' , -●-) and loss (G'' , -○-) modulus of dried and re-dispersed suspensions of MFC/CMC, MFC/LBG and MFC/BL after 3Pass; as a function of (a) frequency (Hz) at 20°C and strain 0.2%, (b) temperature (°C) at 1°C/min heating rate at frequency 1Hz and strain 1% . The data presented is an average of replicates with standard deviation $\pm 1\%$.----- **168**
- Figure 5.6:** Complex viscosity as a function of number of passes through the homogeniser at 0.2% strain and 1Hz frequency at 20°C of 2% w/w suspension of MFC/CMC, MFC/LBG (HV and LV) and MFC/BL1, where (a) never dry suspension, and (b) dried and redispersed suspension. The data presented is average of replicates.----- **171**
- Figure 5.8:** Spin-spin relaxation time (T_2 , ms) as a function of a number of passes through homogeniser of MFC/CMC, MFC/Blend, MFC/LBG and MFC/LBG(LV), measured at 20°C of overall 2%w/w overall suspension concentration. The data presented is average of 4 replicates, highly reproducible with standard deviation less than 0.1%.----- **174**
- Figure 5.9:** DSC thermograms of (a) MFC/CMC and (b) MFC/LBG at low moisture (2% w/w) after consecutive passes through the homogeniser (1 Pass, 2 Passes and 3 Passes). All results are highly reproducible with a standard deviation less than 0.1%. ----- **176**

- Figure 5.10:** DSC thermograms of MFC/Blend at low moisture (2% w/w) after consecutive passes through the homogeniser (1 Pass, 2 Passes and 3 Passes). All results are highly reproducible with a standard deviation less than 0.1%. ----- **177**
- Figure 5.11:** Comparison of the thermal degradation of (a) MFC/CMC, MFC/LBG and MFC/Blend after 3 Passes through the homogeniser, and (b) MFC/CMC after a number of passes and BMFC/CMC under a nitrogen atmosphere at low moisture content (2%w/w). All results are highly reproducible with standard deviation less than 0.1%.----- **179**
- Figure 5.12:** Comparison of the thermal degradation of (a) MFC/LBG, and (b) MFC/Blend after a number of passes through homogeniser, under a nitrogen atmosphere at low moisture content (2%w/w). All results are highly reproducible with standard deviation less than 0.1%.----- **180**
- Figure 5.13:** Sorption and desorption isotherms of different MFC/additives obtained under dynamic conditions at 20°C temperature, where (a) MFC/CMC, MFC/LBG and MFC/Blend after 3 Passes through the homogeniser, and (b) MFC/CMC after number of passes and BMFC/CMC.----- **183**
- Figure 5.14:** Sorption and desorption isotherms of different MFC/additives obtained under dynamic conditions at 20°C temperature, where (a) MFC/LBG and BMFC/LBG, and (b) MFC/BL and BMFC/Blend after a number of passes through homogeniser. ----- **184**
- Figure 6.1:** Optical microscopy images of 1.5% aqueous suspension of different cellulosic fibres stained with Congo red dye, scale bar: 200µm. ----- **200**
- Figure 6.2:** Water retention values of different cellulosic fibres, data presented is an average of replicates and highly reproducible. ----- **200**
- Figure 6.3:** Storage (-●-) and loss moduli (-○-) of 1.5%w/w aqueous suspension of different cellulosic fibres *i.e.*, CTE(F) flakes, CTE(P) powder, Herbacel AQ+ (HBAQ+) & CitriFi100 (CF100) as a function of (A) Frequency (Hz) at 20°C, strain: 0.2%, (B) temperature at 1°C/mins heating rate (frequency: 1Hz and strain: 1%). ----- **203**
- Figure 6.4:** Concentration dependence of shear viscosity (Pas) recorded at shear rate $50s^{-1}$ for four different cellulosic fibres. The viscosity values are averaged from 3 replicates. ----- **206**
- Figure 6.5:** Rank sum scores for each sample for saltiness perception; decreasing numerical value corresponds to an increase in the attribute. Herbacel AQ+ (HBAQ+), CitriFi100 (CF100), CTE flakes (CTE(F)) and CTE Powder (CTE(P)). Note: figure 6.5a has a smaller scale as a number of panellists involved in the study were 60 as compared to figure 6.5b and 6.5c have 74 panellists. ----- **208**
- Figure 7.1:** Predicted schematic representation of the MFC/additive interactions at a different ratio. ----- **219**

List of Tables

- Table 1.1:** Different types of plant raw materials studied in recent years, along with the procedures used for MFC extraction and dimensions (Samir *et al.* 2005; Tanem *et al.* 2006; Hubbe *et al.* 2008; Zimmermann *et al.*, 2010) ----
----- **21**
- Table 1.2:** Comparison of rheological parameters of aqueous MFC suspensions from different starter material (adapted from Shogren *et al.*, 2011); where HPH denotes high-pressure homogeniser; G' and G'' measured at 1 rad/s; η measured at 0.01s^{-1} .----- **29**
- Table 2.1:** List and codes of different variety of MFC, including dry weight (DC) and technology used to produce MFC. ----- **49**
- Table 2.2:** Composition of MFC/additives studied, where CMC(mix) used for CMC15, CMC25 and CMC50 is 75:25 (CPKA/DW60). Blend (BL) ratio used for all formulation is 75:25 (CPKA/LBG). ----- **53**
- Table 3.1:** Comparison between different MFC drying processes (Peng *et al.*, 2012a, Peng *et al.*, 2012b).----- **76**
- Table 3.2:** Sample code, technology and a number of passes used to produce wet MFC suspensions (note: these samples are never dried). ----- **78**
- Table 3.3:** Sample code, drying method, temperature and total time used to produce dried MFC. ----- **79**
- Table 4.1:** Rheological synergism of BMFC/CMC, BMFC/LBG, BMFC/BL1 mixtures in aqueous suspension at 20°C; where G' (Pa) is recorded at strain 0.2% and frequency 1Hz, and η recorded at a shear rate 1 s^{-1} . ----- **134**
- Table 5.1:** The MFC/additives formulation, number of passes through the homogenisers and the sample code.----- **157**

Chapter 1

Introduction

1. General Introduction

Developing eco-friendly, healthy and functional ingredients for different commercial applications for the food and personal care industry are one of the biggest targets for every ingredient and consumer application based company. Different natural plant based (starch, carrageenan, and guar gums) and bacterial (*e.g.* xanthan) polysaccharides are used as functional ingredients in various food applications. These polysaccharides are known to provide texture and stability to various food applications. Nevertheless, utilising waste raw materials to produce value-added products is always a key target of different commercial industries.

In recent years, cellulose based systems have increasingly been investigated. Aqueous suspensions of cellulosic fibres (refined cellulose, microfibrillar cellulose, nano-fibrillar cellulose) were shown to have a number of unique physical and mechanical properties such as very high specific surface area, low thermal expansion, low density and the formation of a highly porous network (Shogren *et al.*, 2011). It is also well established that aqueous suspensions of microfibrillar cellulose (MFC) from different sources show a stable viscoelastic gel-like behaviour over a wide concentration range

(>0.25%-3.5 wt%) , which makes it of interest for application in the food and personal care industry (Pääkkö *et al.*, 2007). Above 3.5 wt% the MFC suspensions tends to form paste which may affect the cost and formulation of final application. For example, the plant cell wall materials such as citrus fibres shows gel-like behaviour over wide range of concentration and are successfully being used to create soft solid structures particularly in the food, personal care and pharmaceutical industries which are also driven by their low cost, sustainability and “green” credentials (Foster 2011).

Microfibrillar cellulose is produced by subjecting the native cellulose fibres to chemical or physical processing and can be produced from regionally abundant materials and waste streams such as wood fibre, apple fibre and straw fibre *etc.*, and is, therefore, sustainable without using food crops (Habibi, Mahrouz and Vignon, 2009). For example, cellulosic fibre produced from apple or orange peel, which also contains naturally occurring polymeric additives such as pectin and hemicellulose, are used as a thickening and texturing agents in a wide range of food applications such as cooking sauces, tomato ketchup, mayonnaise, yoghurt and ice creams. Currently, a wide range of low-fat/reduced fat products are available in the market where food microstructure was designed/created by using cellulosic fibres in combination

with other polysaccharides, which mimics fat-like behaviour in terms of texture and stability (product portfolio of Fiberstar, 2005).

There are also many health benefits; a high intake of dietary fibre, traditionally defined as the portions of plant foods that are resistant to digestion by human digestive enzymes (*i.e.* polysaccharides and lignin), appears to significantly lower the risk of developing coronary heart disease, stroke, hypertension, diabetes, obesity and certain gastrointestinal diseases (Anderson *et al.*, 2009). Recommended intakes for healthy adults are between 20-35 g/day (Marlett, Mcburney and Slavin, 2002). Consumers struggle to reach such intake targets, for instance, less than half the recommended levels of dietary fibre daily is consumed by the majority of consumers in the US (Park *et al.*, 2005). Therefore, it would be beneficial to design the food systems with cellulose as an ingredient with unique rheological properties as well as control taste/flavour perception and controlling functionality in the system.

Hence, the aim of the work presented in this thesis was to investigate the impact of different mechanical treatments on the structural and physical properties of the microfibrillar cellulose and to find novel ways to stabilise the aggregation of microfibrillar cellulose upon drying. Finally, the potential of

MFC produced from softwood spruce in the food industry as a dietary fibre with unique functionality such as a viscosity enhancer, texture enhancer, and coating agent was explored.

In the rest of chapter 1 of the thesis, a comprehensive literature review of the three major topics: Cellulose and Microfibrillar Cellulose fundamentals and its morphology and interaction between cellulose and different additives are presented along with different fibrillation techniques. Current knowledge is reviewed, linking processing and microstructures of MFC related material properties of the suspensions. In addition, the physicochemical properties of the hydrocolloids used in this research are briefly reviewed.

1.1 Cellulose

The plant's primary cell wall is composed of various functional carbohydrates such as cellulose, hemicellulose and pectin. The cellulose microfibrils are linked via hemicellulose to form the cellulose-hemicellulose network, which is embedded in the pectin matrix (Figure 1.1a). The hemicelluloses may vary depending on plant source and maturity, and secondary cell walls are often lignified. Therefore, cellulose is a natural polymer available in large amounts; totally biodegradable and a supply of renewable biopolymers.

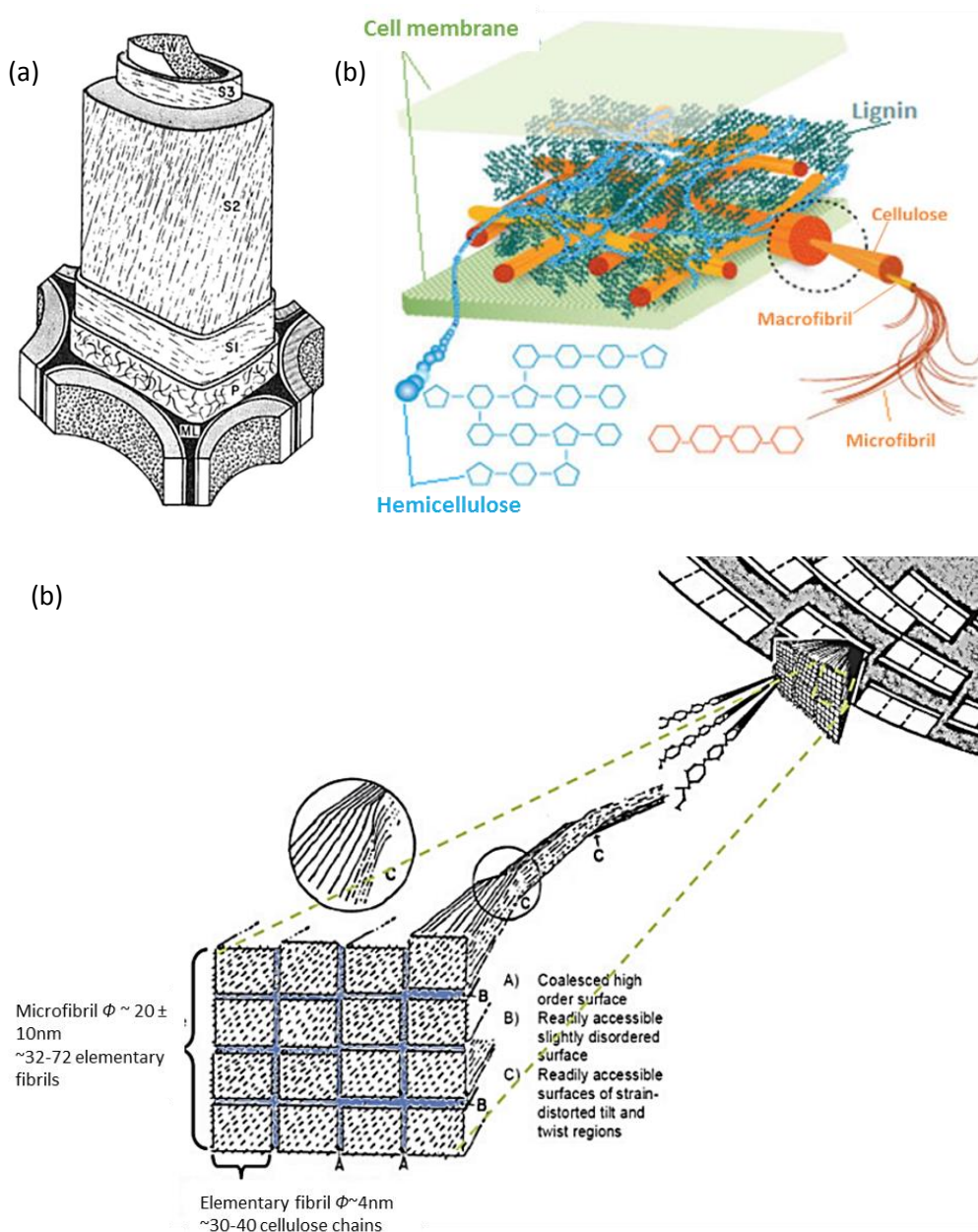


Figure 1.1: (a) Wood fibres consist of several layers (middle lamella (ML), primary wall (P), secondary wall (S1, S2, S3) and lumen (W) (Cote 1967). (b) Molecular organisation of primary plant cell wall (Ceres, 2014); and (c) Organization of the cellulose chains into microfibrils and fibril aggregates (adapted from Rowland and Roberts (1972), Kerr and Goring (1975)).

Cellulose is a structural polymer that provides mechanical properties to the plant cells. An important building block for this natural fibre is strength and

stiffness are the microfibrils within the cellulose structure (Figure 1.1b). Cellulose fibres can be divided into their structural micro-scale units by various chemical and mechanical means/processes. Naturally, cellulose does not occur as an isolated molecule but is found in the form of fibrils. Cellulose is synthesised in the cell as individual molecules which undergo self-assembly at the site of biosynthesis (Brown and Saxena, 2000). Approximately 36 molecules are then assembled into larger units known as elementary fibrils (protofibrils) (Habibi, Lucia and Rojas 2010).

These are then packed into larger units (approx. 64 elementary fibrils) commonly known as microfibrils, which are further assembled into the large macroscopic cellulose fibres termed as fibrils or fibrils aggregates (Figure 1.1c). The microfibrils of cellulose can be found as intertwined fibrils in the cell wall, with approx. 10-40nm diameter and >1000nm long depending on its source (Siró and Plackett, 2010). Another important feature of cellulose is its crystalline nature which means that cellulose chains have a structured order.

The production of commercial cellulose includes either non-enzymatic or enzymatic processes which remove the hemicelluloses and lignin leaving the pure cellulose pulp. Depending on the source of the cellulose pulp, the extraction procedure is selected. The pure cellulose pulp is later subjected to

either chemical or mechanical process resulting in chemically modified celluloses or MFC (Henriksson *et al.*, 2007). When the cellulose pulp is subjected to a harsh chemical process, the results are cellulose whiskers or microcrystalline cellulose, whereas just mechanical process (could be just classical refining or high-pressure homogenisation) of cellulose pulp results in microfibrillar cellulose. An unpacking of the cellulose fibrils into microfibrils or elementary fibrils depends on the severity of the process (Figure 1.1). Nowadays, cellulose is also biosynthesized by a wide variety of bacteria (*e.g.*, *Acetobacter xylinum*), photosynthetic algae (*e.g.*, *Valonia macrophysa* and *Oocystis apiculata*) and fungi (*e.g.*, *Microdochium nivale*) (Brown *et al.*, 1976, Hufnagel *et al.*, 2000).

1.1.1 Molecular structure

At molecular level, cellulose is a linear homo-biopolymer consisting of glucan chains (Kirk and Othmer, 1967). It is an unbranched polysaccharide composed of β -D-glucopyranose units linked by 1 \rightarrow 4 glucosidic bonds (Figure 1.2). Because of a large number of polar hydrogen and hydroxyl atoms, cellulose forms both inter- and intra-molecular hydrogen bonds. Two intramolecular hydrogen bonds, OH-3 \cdots O5 and OH-2 \cdots O6, can bind neighbouring glucose

units and thus provide the high stiffness of natural cellulose chains. Intermolecular hydrogen bonds are different in different polymorphs of cellulose.

Cellulose I is a natural polymorph, which can be divided into I α and I β polymorphs. In cellulose I (which has a parallel arrangement of the chains), the hydrogen bonds exist only between chains belonging to the same cellulosic fibre sheet (Nishiyama, Langan and Chanzy, 2002). Cellulose II (which features an antiparallel arrangement of chains) can be obtained from native cellulose. In this polymorph, the hydrogen bonds are found also between sheets, *i.e.*, they form a three-dimensional (3D) network.

1.1.1.1 Cellulose – I (native cellulose)

Native cellulose is a mixture of I α and I β whereas the ratio of these components depends on the source of the cellulose (Atalla and VanderHart, 1984). For example, cellulose I α rich cellulose is present in the cell walls of some algae and bacterial cellulose, whereas I β rich ones have been found in cotton, wood and ramie fibres. Another example, Tunicin (the small sea animal *Halocynthia roretzi*) consists of 90% I β phase (Mouro, Bizot and Bertrand, 2011) and cellulosic walls of alga *Valonia* consist of mainly 60% I α

phase (Atalla and VanderHart, 1984). Similarly, cellulose from the peel of prickly pear showed 60% cellulose I α and 40% cellulose I β phase with a degree of crystallinity of around 38% (Habibi *et al.*, 2009). In the case of a softwood cellulose source, in native spruce, cellulose I α crystalline form is almost three times the amount of I β , whereas, in kraft cellulose pulps, the amount of cellulose I β is twice the amount of I α cellulose (Liitia, Maunu and Hortling, 2000). Cellulose I α form corresponds to a single-chain triclinic crystallographic symmetry, whereas cellulose I β form is monoclinic and characterised by two parallel chains as shown in Figure 1.3 (Baker *et al.*, 1997, Sugiyama *et al.*, 1991, Baker *et al.*, 2000, Nishiyama *et al.*, 2002). Cellulose I α phase is metastable and could be converted into I β form by a hydrothermal treatment at 260°C (Yamamoto *et al.*, 1989).

These cellulose forms might co-exist in a system. For instance, the 2D FTIR of spruce and kraft cellulose showed the splitting of intermolecular bands, where the first peak represents cellulose I α , the second cellulose I β , and a third, in between, which also confirms that the native celluloses consist of a mixture of two crystalline phases I α and I β . The ratio of cellulose I α : cellulose I β defines the crystallinity of the cellulose, and it is directly related to the lateral size of microfibrils. These polymorphs are closely related in terms of

molecular conformations but different patterns of hydrogen bonding (Hinterstoisser and Salmen, 2000; Akerholm *et al.*, 2004; Fernandes *et al.*, 2011).

1.1.1.2 Cellulose - II (Regenerated cellulose)

Cellulose II, also known as regenerated cellulose is obtained by crystallisation of native cellulose and has an antiparallel arrangement of the chains. It can be prepared by two distinct routes: mercerisation (alkali treatment) and regeneration (solubilisation and subsequent crystallisation) (Aulin, 2009 and Siqueira *et al.*, 2010a). Cellulose II is thermodynamically more stable than cellulose I, however, recent studies show that cellulose II is more readily digested (during process such as enzymatic hydrolysis) than cellulose I. It has been suggested that the van der Waals interaction between hydrogen-bonded sheets in cellulose I is stronger than that in cellulose II and this acts as the main factor to resist hydrolysis (Wada *et al.*, 2010).

The standard ^{13}C CPMAS solid state NMR spectra of Cellulose I and cellulose II from various cellulose sources are shown in Figure 1.4. For Cellulose I, the upfield region from 60-70ppm is assigned to C6 carbon, the more intense

signals from 70-80ppm are assigned to C2, C3 and C5 carbons and the region from 80-90ppm corresponds to C4 carbon.

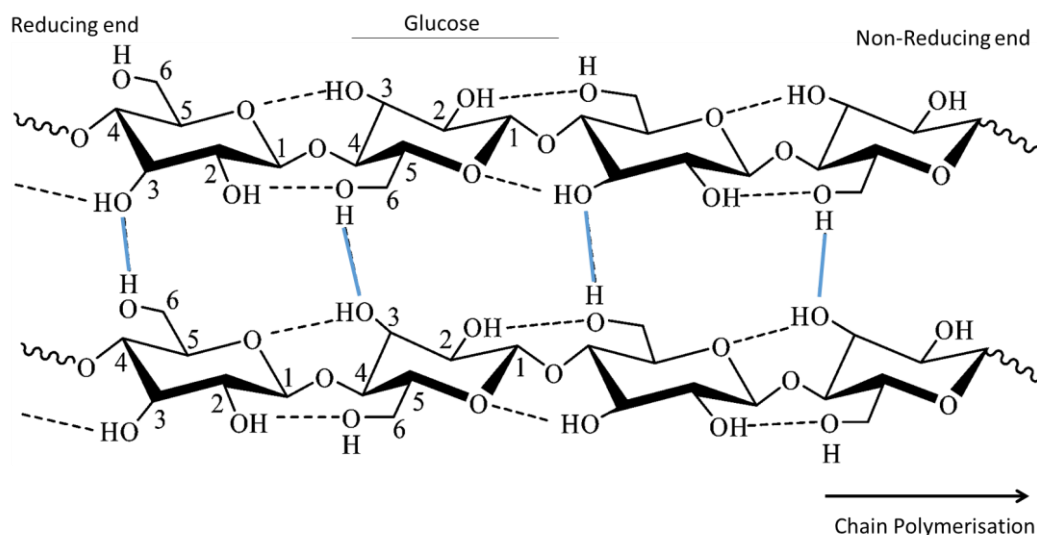


Figure 1.2: The molecular structure and the inter- or intra-chain hydrogen bond present in cellulose I, where black broken-lines: inter-chain hydrogen bonding and blue lines: intra-chain hydrogen bonding (adapted from Festucci-Buselli et al. 2007).

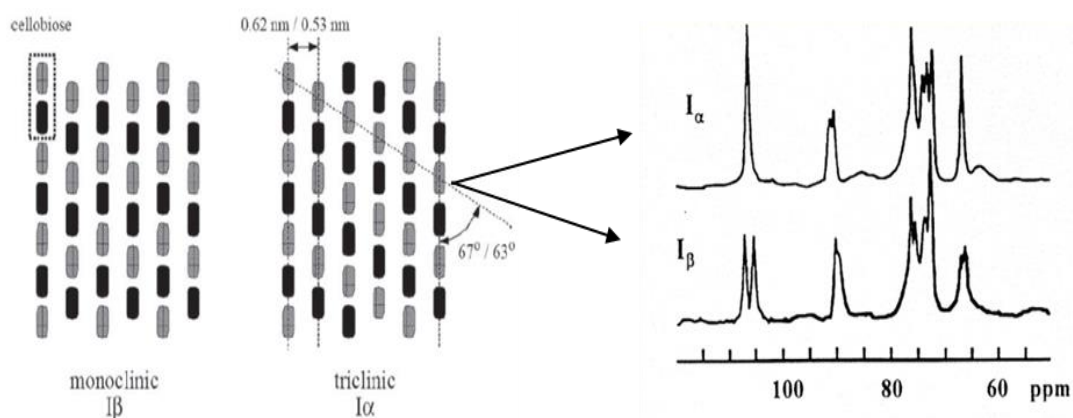


Figure 1.3: Chain arrangement of Cellulose I α and Cellulose I β and NMR spectra of each component (adapted from Baker et al., 1997, Baker et al., 2000, Atalla and Vanderhart, 1984).

The downfield signal at 105ppm is assigned to C1 carbon (Mauro *et al.*, 2003, Mauro *et al.*, 2011). Another variant among the different cellulose spectra is the proportion of the signal intensity between 86-92ppm and 78-86ppm assigned respectively to crystalline and surface chains of C4 carbons. The NMR spectrum of amorphous cellulose displays no signal in the C4 and the C6 resonance region assigned to the core crystalline material. Whereas for Cellulose II, the assignment of shifts associated with C4 crystalline sites is in the form of two convoluted peaks referenced at 89.4ppm and 88.3ppm believed to be due to two non-equivalent crystallographic positions within the cellulose II unit cell. The chemical shift of the C4 signals is particularly sensitive to the conformation of the glycosidic linkage (Ha *et al.*, 1998). It has been shown that the existence of two crystallographic phases for native cellulose, *i.e.*, I α and I β , induces distinct signals at separate chemical shifts: 105.5ppm and 103.8ppm for the C1 of the I α form.

The crystallinity of cellulose changes with the number of process steps the fibres are subjected which ultimately affects the functionality of celluloses (Heux *et al.*, 1999, Mittal *et al.*, 2011). During the processing of cellulose pulp (extraction process, refining, homogenisation, drying, milling and redispersing/hydration) two types of structural changes might occur in the

crystalline part of cellulose, *i.e.* conversion of I α into I β and conversion of cellulose I to cellulose II (Newman *et al.*, 2004; Walker and Wilson, 1991).

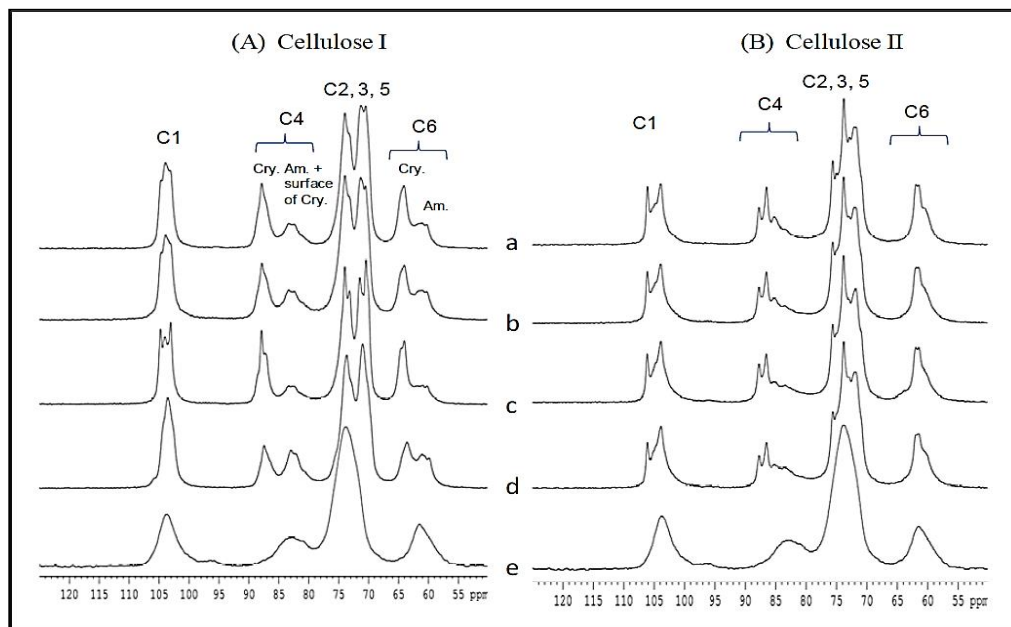


Figure 1.4: Shows the ^{13}C PMAS solid state NMR spectra, (A) original/native Cellulose I and (B) cellulose II for various samples. (a) Avicel, (b) α -cellulose, (c) cotton linters, (d) corn stover, and (e) amorphous cellulose (adapted from Mittal *et al.*, 2011).

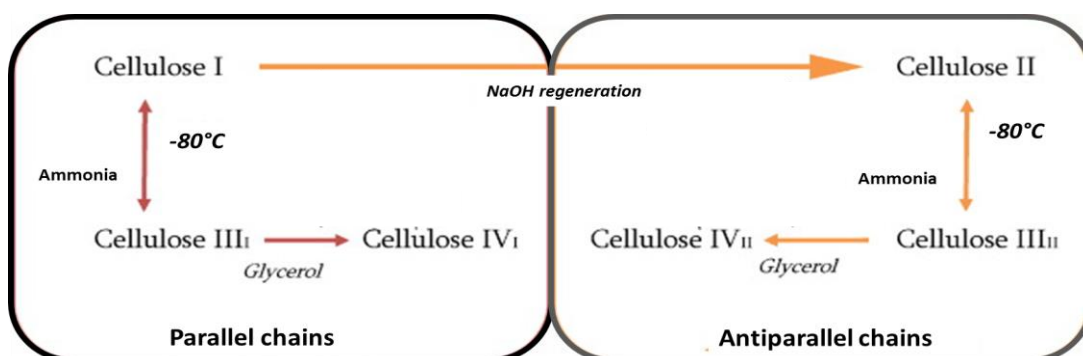


Figure 1.5: Different polymorphs of cellulose and the main processing steps (adapted from Lavoine *et al.*, 2012).

1.1.1.3 Cellulose – III and IV

The cellulose polymorphs III and IV are the reversible form of cellulose I and II. Celluloses III_I and III_{II} can be formed from celluloses I and II, respectively when cellulose pulp is treated with liquid ammonia in a reversible reaction as shown in Figure 1.5. Besides producing the different allomorphs of cellulose, this chemical treatment can also alter other physical properties of cellulose, such as the degree of crystallinity and therefore enhanced cellulase accessibility and chemical reactivity. The degree of conversion of cellulose I to cellulose III depends on the reaction period and the temperature used in the final stage of the treatment (Wada *et al.*, 2004b). Celluloses IV_I and IV_{II} can be produced by heating celluloses III_I and III_{II}, respectively (Gardiner and Sarko 1985; Aulin 2009) as shown in Figure 1.5. In general, cellulose IV could be prepared by treatment in glycerol at 260°C after transformed into cellulose II or III. Cellulose I cannot be transformed directly into cellulose IV (Wada, Heux and Sugiyama, 2004a).

1.2 Microfibrillar cellulose

Microfibrillar cellulose (MFC) is predominantly produced by subjecting cellulose fibres to a variety of mechanical processes including high-pressure homogenisers, refiner *etc.* (Henriksson *et al.*, 2007). Carrasco (2011) defined

microfibrillar cellulose (MFC) as material composed of nanofibrils, fibrillar fines, fibre fragments and fibres; however MFC with a high degree of fibrillation (properly produced) may contain nano-structures with diameters less than 40nm as a main component.

The classical way for producing MFC is just refining the cellulose pulp to produce MFC with a low degree of fibrillation. In the past decade, MFC has been produced by using more aggressive, high-pressure mechanical treatments such as homogenisation or microfluidisation, which leads to highly entangled, inherently connected microfibrils, fibril aggregates and mechanically strong networks. These processes generate high shear which cleaves the cellulose fibres along longitudinal axes resulting in a suspension with increased surface area. These long and flexible cellulosic fibrils have dimensions between 10–100nm diameter and length in the micrometre scale consisting of both crystalline and amorphous regions (Siqueira *et al.*, 2009)

The two methods to disintegrate cellulosic fibre pulp into microfibrils, cellulose whiskers and microcrystalline cellulose are shown in Figure 1.6. An aggressive acid hydrolysis leads to colloidal suspension of aggregated, highly crystalline, and low aspect ratio of fibril aggregates. Further hydrolysis and sonication break down the fibril aggregates to cellulose fibrils, *i.e.*, whiskers,

which form a weak physical network by hydrogen bonds. Whereas when this method incorporates either a long and intense mechanical treatment or an additional acid hydrolysis combined with the mechanical treatment it yields a mixture of predominantly cellulose-I fibrils (about 5nm thickness) and fibril aggregates (about 10-25 nm thickness) which have a significantly higher aspect ratio compared to the whiskers or MCC (microcrystalline cellulose). Microfibrillar cellulose or nano-fibrillar cellulose can also be produced by the pre-treatment of native cellulose with TEMPO (2,2,6,6-tetramethylpiperidine-1-oxyl radical)-mediated oxidation and successive mild disintegration in the water as shown in Figure 1.6 (Isogai *et al.*, 2011).

Mechanically, MFC is obtained by disintegrating the cellulose fibres at high shear/pressure, resulting in a high entangled network of micro/nano-scale size elements with a gel-like behaviour for water dispersions at 1% or lower concentrations. The most common mechanical method is where cellulose pulp is passed repeatedly through a high-pressure homogeniser or a microfluidiser to increase the degree of fibrillation (inevitably, the energy consumption increases with the number of passes) (Frone *et al.*, 2011, Lavoine *et al.*, 2012).

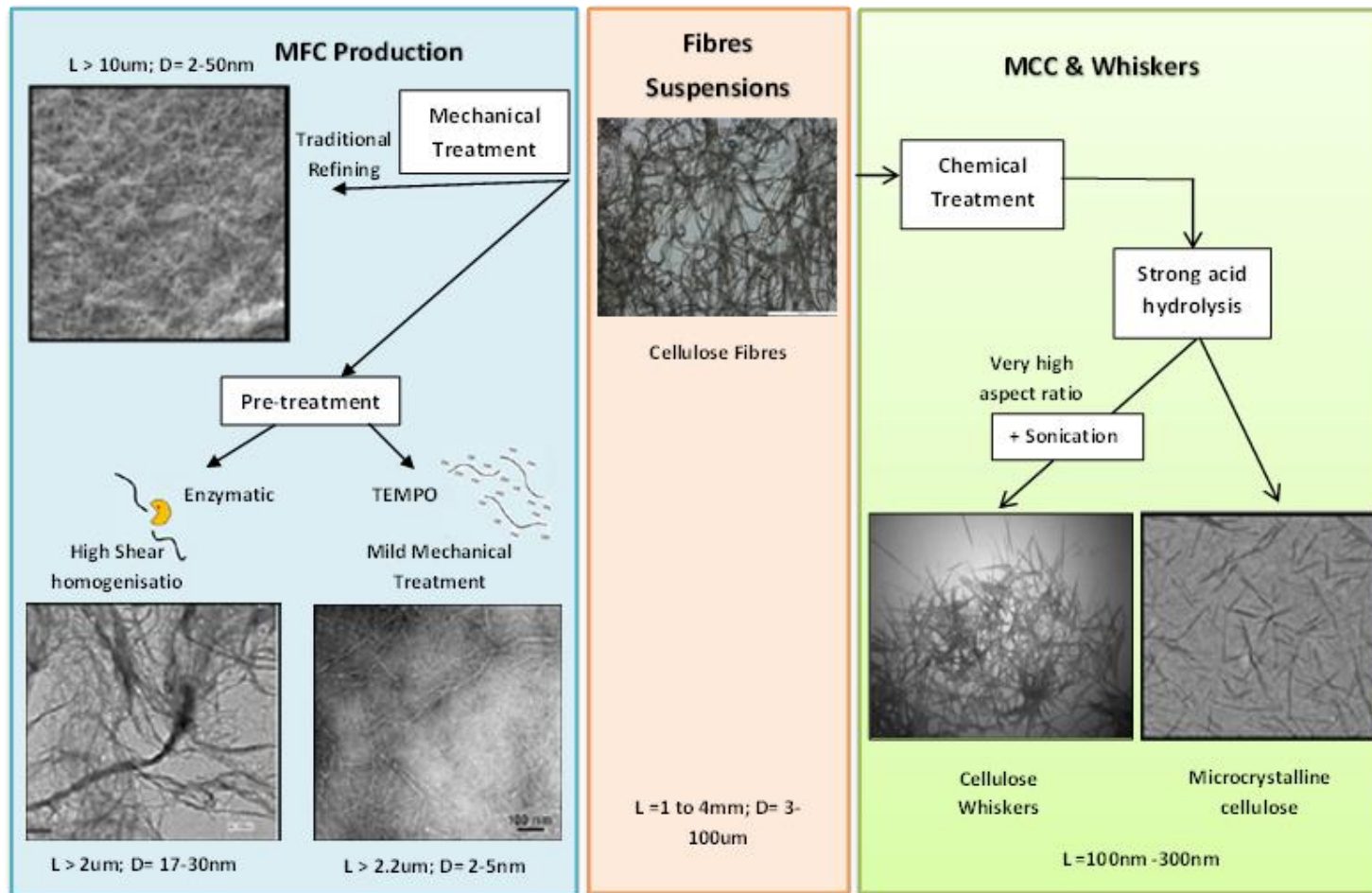


Figure 1.6: Flow diagram of different methods to disintegrate cellulose pulp into microfibrillar celluloses (adapted from Lavoine et al., 2012, Saito et al., 2006).

1.2.1 Factors affecting the production of MFC

There are various factors that affect the production and dimensions of MFCs, which include the source of cellulose, the extraction process of the cellulose pulp, the technology used for fibrillation of the fibres, the drying, milling and finally rehydration processes.

1.2.1.1 Source and extraction procedure of cellulose

A wide range of starting materials have been studied and used for the production of MFC. Apart from softwood and hardwood, a wide variety of bacteria, photosynthetic algae and fungi are used to biosynthesize cellulose. In terms of plant material, both softwood and hardwood are processed to produce cellulose pulp in different dimensions and specification for various applications (Table 1.1). The source of cellulose plays a significant role in terms of processing and further applications.

The first stage of MFC production is the extraction of the pure cellulose *i.e.* the bleaching process. During this stage hemicelluloses and lignin are removed from the starting material, resulting in a pure cellulose pulp. Depending on the type of starting material the bleaching process differs (either enzymatic or non-enzymatic process is selected, also shown in Table

1.1). The fibre diameter of chemically exposed pulp (bleached pulp) decreases more after refining followed by homogenisation as compared to a unbleached pulp. There is a significant difference between the bleached and unbleached celluloses in terms of the functionality (Spence *et al.*, 2010a; Spence *et al.*, 2011). The presence of hemicellulose and lignin influence the refining and homogenisation steps and their further applications (Silva *et al.*, 2000, Henriksson *et al.*, 2007, Bhattacharya *et al.*, 2008, Zuluaga *et al.*, 2007).

The excessive bleaching treatment reduces cellulose crystallinity and the degree of polymerisation, leading to the degradation of mechanical properties of isolated microfibers of cellulose (Iwamoto *et al.*, 2007; Abe and Yano, 2009). Hence, there are various parameters to be considered during the bleaching process and each parameter is critical for producing microfibrillar cellulose with appropriate properties.

The number of passes through the homogeniser or length of processing depends on the target degree of fibrillation. It was reported that the WRV (water retention value) of MFC was increased with the number of homogenisation rounds (Zhang *et al.*, 2012), which ultimately affects the suspension properties.

Table 1.1: Different types of plant raw materials studied in recent years, along with the procedures used for MFC extraction and dimensions (Samir et al. 2005; Andresen et al. 2006; Hubbe et al. 2008; Zimmermann et al., 2010).

Source	Procedure	Equipment	Nanofibre dimensions	References
Mechanical process				
Kraft pulp	Passing 2-30 times through a refiner with a gap of 0.1mm, subsequently passing through a high pressure homogeniser 2-30 times	15MR 2-stage homogeniser	50-100nm in width and several um in length	Iwamoto et al. (2007), Spence et al. (2010), Nakagaito and Yano (2004)
Soybean stock	Cryocrushing followed by 20 passes through a defibrillator at 500-1000 bar beating and refining in a PFI mill; 20 passes through a defibrillator at 500-1000 bar		50-100nm in width and several um in length	Wang and Sain (2007)
Wheat straw	Cryocrushing followed by fibrillation at 2000 rpm; homogenisation by 20 passes at pressure above 300 bar.	Cramer disintegrator	20-120 nm in width, the majority around 30-40nm	Ruigang et al. (2005)
Dried sugar beet pulp chips	Disintegration by high shear (24,000 rpm) and pressure	Ultra-Turrax and Microfluidics homogeniser	30-100 nm and a length of several um	lowys et al. (2001)
Maize bran	ND	Microfluidics	ND	Mouro et al. (2003)
Banana plant fibre	The banana fibres were ground to approximately 500 um size using a cutting mill with a 500um stainless	SM1 RetschGmbH cutting mill	ND	Elanthikkal et al. (2010)
Chemical process (after bleaching and extraction of cellulose)				
Bleached Kraft pulp	TEMPO-mediated oxidation, followed by disintegration	Waring blender	Few nm in width	Saito et al. (2006),
Sugar beet pulp	Disintegration in a Waring blender followed by 15 passes through a homogeniser at 500 bars and 90-75°C; TEMPO mediated oxidation	Microfluidics	ND	Habibi and Vignon (2008)
Enzymatic pre-treatment				
Bleached Kraft pulp	Enzymatic pre-treatment by fungus OS1 (isolated from infected Elm trees), followed by high shear refining	High shear refiner, cryocrushing	10-250 nm in width, majority is around 25-75 nm	Janardhnan and Sain (2006)
Bleached sulfite softwood cellulose pulp	Refining to increase the accessibility of the cell wall for enzymatic treatment, followed by refining and high pressure homogenising	Microfluidics	5-30 nm in diameter	Pääkkö et al. (2007)
Softwood sulfite pulp; softwood dissolving pulp	Beating in a PHI-mill, enzymatic treatment with endoglucanase (Novozyme 476) followed by high pressure homogenisation	Microfluidics	5-30 nm in diameter	Henriksson and Berglund (2007)

It was also reported with lemon fibres that the complex viscosity, loss and storage modulus increases with a decrease in particle size of fibres (Cordoba *et al.*, 2010). Currently, a number of technologies are present in the market which serves as a fibrillator for cellulose pulps. Depending on the pressure, flow rate, temperature, and the design and diameter of chambers used in high-pressure homogeniser or microfluidiser different degrees of fibrillation can be achieved (Lavoine *et al.*, 2012).

In general principle, the high-pressure homogeniser works by forcing cellulose suspensions through a very narrow channel or orifice under pressure. Subsequently, depending on the type of high-pressure homogenizer, the suspension may or may not impinge (strike) at high velocity on a hard-impact ring or against another high-velocity stream of suspension coming from the opposite direction. Disruption of the cellulosic fibre occurs by a combination of the large pressure drop, highly focused turbulent eddies, and strong shearing forces. The rate of fibre disruption is proportional to approximately the third power of the turbulent velocity of the product flowing through the homogenizer channel, which in turn is directly proportional to the applied pressure. Thus, the higher the pressure, higher the efficiency of disruption per pass through the machine. The operating parameters which affect the

efficiency of high-pressure homogenizers are pressure, temperature, the number of passes, valve design and flow rate (Ankerfors, 2012).

Common examples of mechanical treatments used to produce MFC are as follows (Figure 1.7):

Gaulin homogeniser: It was the first mechanical treatment used to prepare MFC (Herrick and Wash 1984; Turbak *et al.*, 1985). This homogeniser works at a pressure of 8000psi, where the cellulose pulp is passed through a small diameter orifice (nozzles); the high shearing action is followed by a high velocity decelerating impact. High velocity, pressure impact and shear forces on cellulose pulp generate shear rates in the stream resulting in a decrease in the fibrils size, to micro or nano scale depending on the number of passes (Frone *et al.*, 2011). High pressure or shear homogeniser results in high degree of fibrillation as compared to classical refiner or grinder. However, the big problem with using a homogeniser is the problem of clogging because of the small orifice size, this can be overcome by pre-treatment (mechanical) of cellulose pulp such as milling (Jonoobi *et al.*, 2010) or commonly used refining machines (Nakagaito *et al.*, 2004, Stelte *et al.*, 2009, Karande *et al.*, 2011).

Microfluidiser (Microfluidiser M110): This is a homogeniser where the pulp is forced through thin z-shaped chamber (with channel dimensions that are

usually 200–400 μm) under pressure as high as 2070 bars (Saarinen *et al.*, 2009; Siqueira *et al.*, 2010b) resulting in more uniform micro/nano-sized fibrils that have thinner dimensions or high degree of fibrillation as compared to refiner and grinder. The morphology of MFC produced from a microfluidiser is more homogenous as compared to a classical refiner, and the aspect ratio of cellulose fibre bundles increased with the number of passes (Lee *et al.*, 2009, Ferrer *et al.*, 2012).

Grinder (Masuko grinder): This uses the grinding mechanism where the cellulose pulp is passed between a static grindstone and a rotating grindstone, revolving at about 1500 rpm (Iwamoto *et al.*, 2007).

Cryocrushing: This is another method for mechanical fibrillation of cellulose pulp, in which process water swelled cellulosic pulp is immersed in liquid nitrogen followed by crushing the system with a mortar and pestle or a grinder. When the high impact forces are applied to frozen cellulosic fibres, fibres rupture releasing microfibrils (Frone *et al.*, 2011, Siró *et al.*, 2010).

All of the above mentioned mechanical treatments (including temperature) involves high consumption of energy, cost with relatively low both yield and degree of fibrillation. These technologies, individually, are limited to small scale

or laboratory scale production of MFC, hence, in general, a combination of two technologies are used to produce MFC (yet limited to small-scale production).

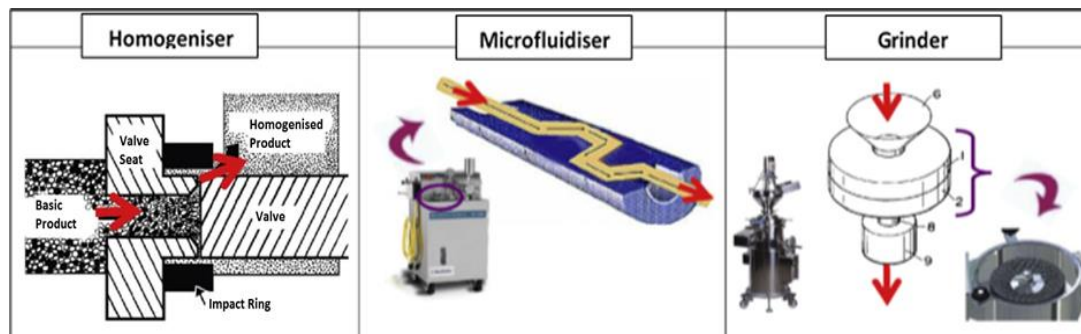


Figure 1.7: Different technologies to produce Microfibrillar cellulose (adapted from Lavoine et al. 2012).

1.2.1.2 Impact of drying

Due to various economic reasons such as easy transport and flexibility to blend with other ingredients, drying microfibrillar cellulose becomes important. Ideally, this is without losing rheological and other physical properties thus drying becomes a crucial processing stage. Homogenisation modifies the structure of the starting materials by creating a microfibrillar cellulose suspension and drying the MFC is known to modify the fibrillated state by causing hydrogen bonding between amorphous parts of the microfibrillar cellulose leading to the formation of some bundles and agglomerates (Quiévy et al., 2010, Kontturi et al., 2009, Kato et al., 1999, Iwamoto et al., 2008, and Young, 1994, Eyholzer, 2010).

The aggregation or agglomeration occurs to varying extents depending on the drying process. For instance, oven drying slowly evaporates water while atomization eliminates water by fast evaporation. Oven drying is a well-established process in the paper and pulp industry, generating hundreds of microns to millimetre particle sizes after drying. Freeze drying eliminates the water by sublimation after the sample has been frozen, in this case, the freezing temperature (-20°C or -80°C) plays a crucial role in the formation of agglomerates. Whereas a supercritical drying method consists of dehydration of MFC suspensions by replacing the non-aqueous media with CO_2 , with a later, subsequent removal of CO_2 (Peng *et al.*, 2012a); this method keeps the nano or micro size intact, but the high processing and solvent costs, the complicated method for solvent replacement and the impractical scale up makes this technique not so suitable for industrial applications.

In spray drying, the suspension is concentrated to an appropriate viscosity, pumped and dehydrated by hot gas (Peng, Ha and Gardner 2012b). The main advantage of this technique is the low cost and controllable size of the dry material, where this could be a big disadvantage as this technique does not protect from agglomeration. It was observed that gentle drying methods, in general, result in MFC with higher water binding capacities (Ulbrich *et al.*,

2014). It was also observed from thermogravimetric analysis (TGA) that the dried MFC samples do not behave or degrade like the original cellulose *i.e.*, the thermal stability of the dried MFC decreases after drying with the char level at the end of the pyrolysis was higher than original cellulose fibre (Quiévy *et al.*, 2010).

To protect the microfibrillar cellulose from collapse or agglomeration, a number of hydrocolloids (*e.g.* low and high methoxyl pectin, CMC and sodium polyacrylate) and salts (*e.g.* NaCl) (Lowys *et al.*, 2001; Tandjawa *et al.*, 2012a, Tandjawa *et al.*, 2012b; Missoum *et al.*, 2012) are used. Lowys (2001) reported an interaction between MFC and polymeric additives, where the additives are homogeneously distributed, forming weak bonds with MFC fibres, improving the redispersibility of MFC in water. It was reported with bacterial cellulose that addition of CMC leads to more homogeneous microstructures and a significant increase in the ζ -potential of the microfibrillar cellulose, preventing re-aggregation (Veen *et al.*, 2014). This interaction between the additive and MFC tends to stabilise the fibrils from collapsing or agglomeration during the drying process.

Rehydration of these dry materials is the final step of creating a functional ingredient, however redispersing MFC aggregates or agglomerates is very

difficult after the drying process even in the presence of additives. A variety of techniques or equipment have been employed to redisperse the MFC, where the most commonly used equipment produce a high shear for a short time (such as a high shear overhead mixer), low shear equipment for longer time (such as a low shear overhead stirrer) or ultrasonic dispersion device, where the ultrasonic cavitation generates high shear that breaks particle aggregates into smaller dispersed particles. Depending on the type of redispersing technique used the suspension will show differences in rheological properties. For instance, the yield stress of a MFC water suspension was greater with ultrasonic dispersion as compared to mechanical stirring (Lowys *et al.*, 2001).

1.2.2 Suspension properties of MFC

Microfibrillar cellulose dispersed in water shows a number of unique physical and mechanical properties. Rheological properties are some of the key characteristics which influence a wide range of commercial applications such as in food, cosmetics, pharmaceuticals, paints and composites as a coating application or a thickening agent. Depending upon the starting material and process the system is subjected to the rheological properties vary. In general, the rheological properties of aqueous MFC suspensions isolated from softwood, sugar beet pulp, corn cobs and cotton show gel-like behaviour where the

storage modulus (G') is higher than the loss modulus (G'') over a wide concentration range. It was also reported that the storage and loss modulus (G' and G'') show little frequency dependence at all concentrations (lowest till 0.01% w/w) (Pääkkö *et al.*, 2007, Tanjawa *et al.*, 2010, Cordabo *et al.*, 2010, Tatsumi *et al.*, 2002, Tatsumi *et al.*, 2007). The higher elastic modulus might be due to long fibrils and fibrils-aggregates and entangled microfibrils, forming strong network structures. These aqueous suspensions of MFC (source: fully bleached sulphate pulp mainly based on juvenile *Picea abies*) also exhibit shear thinning. There are several factors that affect the rheological properties of MFC suspension, *e.g.*, the degree of fibrillation (the unpacking of the cellulose fibrils), the process of cellulose production (enzymatic and non-enzymatic), the source of cellulose, temperature, pH and presence of salts.

Table 1.2: Comparison of rheological parameters of aqueous MFC suspensions from different starter material (adapted from Shogren *et al.*, 2011); where HPH denotes high-pressure homogeniser; G' and G'' measured at 1 rad/s; η measured at $0.01s^{-1}$.

Source	Processing	Concentration (%)	G' (Pa)	G'' (Pa)	η (Pa.s)
Corn cobs	Blender	0.5	0.7	0.3	-
Corn cobs	HPH, 2 passes	0.5	300	30	150
Softwood	HPH, 8 passes	0.5	20	3	10
Sugar beet pulp	HPH, 10 passes	0.5	30	3	8
Softwood	HPH, 10 passes	1	150	30	30 (0.1 s ⁻¹)
Corn bran	Colloid mill	3	250-700	-	-

A significant difference in viscosity, storage and loss modulus was observed with different starting materials (Shogren *et al.*, 2011), shown in Table 1.2.

Rheological behaviour of MFC suspensions also shows little dependency on increasing and decreasing temperature, depending on the source of the MFC.

For example, lemon fibre MFC has been reported to show no significant effect of temperature up to 20°C-40°C, but between 50°C to 80°C an increase in the suspension viscosity has been observed (Cordoba *et al.*, 2010). This indicates that at higher temperature strong networks are formed between fibre and fibre aggregates, and this appears to be dependent on the source of cellulose/MFC.

For instance, lemon fibre contains both soluble and insoluble components of the plant cell wall hence with an increase in temperature; there are possibilities of thermally induced interactions between the components which influence the viscosity of the system. In this case, the MFC suspension has been reported to show a total recovery of the properties on cooling from 80°C to 20°C, indicating the entire suspension is thermo-reversible. Similar trends were observed with freeze dried and never dried MFC produced from sugar beet pulp (Tandjawa *et al.*, 2010, Pääkkö *et al.*, 2007).

Aqueous suspensions of MFC (with hemicellulose) at higher pH showed a decrease in viscosity as at higher pH, the amount of charge increases leading to

higher electrostatic repulsion resulting in lower interaction. Whereas, at lower pH, the hydrogen ions neutralise the charge of hemicellulose associated with MFC which reduced the electrostatic repulsion resulting in increased interaction between fibres and thus an increase in viscosity (Pääkkö *et al.*, 2007). However, there is no significant effect of pH (4.5 to 9) on the MFC fibrils and fibre aggregates in the absence of hemicellulose (Tandjawa *et al.*, 2010). This indicates that the purity of MFC reflects the stability at different pH; pure MFC water suspensions do not exhibit a significant effect of pH, whereas various individual trends can be observed in the presence of hemicellulose and lignin. Just like the pH behaviour, as the salt concentration (NaCl or CaCl₂) is increased in MFC suspensions an increase in storage modulus was reported (Lowys *et al.*, 2001). This behaviour can be explained by the introduction of electrostatic repulsion by salts between the MFC fibrils allowing the microfibrils to come into slightly closer contact and increasing the inter-fibrillar friction (Saarikoski *et al.*, 2012). However, as the concentration of salts increases the G' and G'' of suspensions increases. Ono (2004) explained this behaviour as resulting from aggregation of the microfibrils. The aggregation of microfibrils leads to inhomogeneous suspension microstructure, and in the narrow gap of a rheometer may bridge the gap resulting in elevated moduli levels.

1.3 Carboxymethylcellulose

Carboxymethyl cellulose (CMC) (also known as cellulose gum or carboxymethyl ether) is a cellulose derivative with carboxymethyl groups (-CH₂-COOH) bound to the hydroxyl groups of the glucopyranose monomers of the cellulose backbone (Figure 1.8). Water-soluble CMC is a white granular substance available at various levels of viscosity (10-50,000 mPa.s in 2% solution) and is equally soluble in hot and cold water. The single most important property of CMC is viscosity building and highly shear-thinning behaviour (Ghannam *et al.*, 1997). The properties of CMC along with its versatility as a thickener, film former, protective colloid, and water-retaining agent have made CMC the most produced and widely used industrial cellulose ether. High-purity grades are employed as food additives; these are added as a thickener or as an emulsion stabiliser to some products such as frozen dairy, dry drink mixes, icing, syrups, and baked goods.

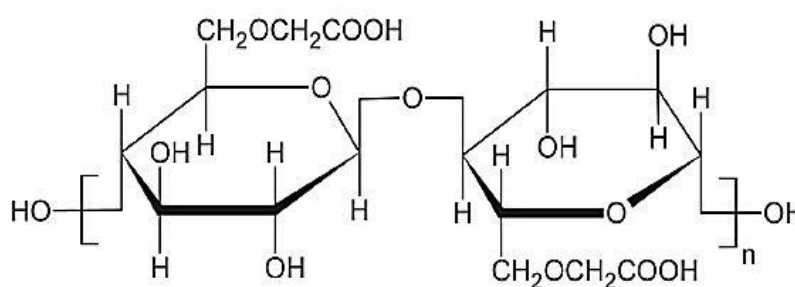
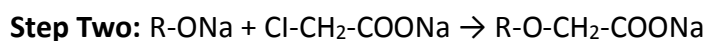


Figure 1.8: Structure of CMC with DS of 1.0 (Celluloseethers, 2013).

Carboxymethyl cellulose is produced by reacting alkali cellulose with sodium monochloroacetate under rigidly controlled conditions. Generally, CMC is produced in a slurry process, *i.e.* cellulose is suspended in a mixture of isopropanol/water, treated with aqueous NaOH solution and then converted with monochloroacetic acid or its sodium salt (Feddersen *et al.*, 1993).

The following two reactions represent the manufacture stages of the Na-CMC:



The average number of hydroxyl groups substituted per anhydroglucose unit is known as the degree of substitution or DS. Heinze (1999) reported that the change of concentrations or prolongation of reaction time significantly influences the overall DS. In a single processing step, the reaction of the cellulose with sodium monochloroacetate yields CMC with DS values as high as DS 2.2.

Technically, the optimum water solubility and other desirable physical properties of CMC are obtained at a much lower degree of substitution than 3 (Heinze *et al.*, 2001). The solution characteristics of CMC also depend on the average chain length which also determines the molecular weight of the polymer. As the molecular weight increases the viscosity of a CMC solution

increases rapidly. At the end of the reaction during CMC production, the reaction mixture is neutralised by controlling the pH of the mixture. The degree of neutralisation of carboxymethyl groups also impacts on solubility and further the viscosity of the solution. For instance, typically the neutral point of CMC is pH 8.25, the pH is generally adjusted around 7-7.5. If the CMC is neutralised to pH 6.0 or less, the dried CMC product will not have good solubility, and the solutions are hazy and will contain insoluble particles (Heinze *et al.*, 2001).

An aqueous solution of carboxymethyl cellulose (CMC) is known to build up viscosity with increasing concentrations. This increase in viscosity is due to the increase in the intermolecular interactions and polymeric space occupancy (hydrodynamic volume) of the CMC molecules (Benchabane *et al.*, 2008). CMC solutions show no evidence of a yield stress (Dolz *et al.*, 2007, Edali *et al.*, 2001). Rheological properties of CMC are highly affected by concentration, temperature and shear rate, for instance, it was reported that the apparent viscosity of CMC solution decreases with increasing temperature (Togrul *et al.*, 2003).

In addition to food applications, due to solubility and shear thinning behaviour CMC is a well-known additive to use in drilling fluids. CMCs are used to stabilise a clay suspension by increasing the viscosity and controls the mud losses,

finally, it maintains adequate flow properties at *in-situ* conditions. In cosmetic and pharmaceutical applications, CMC is used as a binding, thickening and stabilising agent in various commercial products such as creams (also acts as film forming agent to give moisturising effects), lotions, and toothpaste *etc.* In the textile industry, CMC is used as a coating agent, in resin emulsions/latex paints, adhesives and paint inks, and in coating colours for the pulp and paper industry (product specification of CMC by Aqualon®, Benchabane and Bekkour, 2008).

1.4 Galactomannan

The mannans, also referred to as gums, are generally found in numerous seeds. They are located mostly in the seed's cell wall or in the endosperm and regarded as cell wall components. The mannans represent an important group of neutral and water soluble polysaccharides structured as repeating mannose units linked $\beta(1\rightarrow4)$. The two naturally occurring variants of mannans, with galactose side chains, are known as galactomannans. Galactomannans such as Locust bean gum (LBG) and guar gum are commonly used in a wide range of food applications as a stabiliser, thickening agent *etc.* Different legume seeds have galactomannans with various mannose: galactose (M:G) ratio, molecular weight, and the distribution of galactose along the mannan backbone. For

example locust bean gum (LBG) has 4:1 (M:G) ratio, guar gum has 2:1 ratio *etc.*

Galactomannans are also produced by microorganisms or bacteria, however, their complex chemical structure compared to plant seed galactomannans makes them difficult to use in industrial applications (Mathur *et al.*, 2011).

1.4.1 Locust bean gum

Locust bean gum (LBG) or carob gum is extracted from endosperms of the leguminous Mediterranean tree carob (*Ceratonia siliqua*). Typically, locust bean gum is produced from fruit pods harvested, cleaned and broken from carob seeds, followed by rolling, splitting (chemically by hot concentrated sulphuric acid or physically by roasting at 450°C and removing the hulls mechanically) and separation of the endosperms by differential grinding. The endosperm is then milled, blended and graded with respect to the viscosity of the gum and particle sizes (Maier *et al.*, 1993; Fox 1992). Locust bean gum is partially soluble in water and can be fractionated on the basis of water solubility. Hui and Neukom (1964) reported that 30% of LBG was soluble in cold water, with an increase in temperature there is an increase in dissolution. The molecular structure of locust bean gum is composed of linear β -(1→4)-D-linked D-mannan chains with variable amounts of single D-galactose substituents attached to the main chain by α (1→6) linked (Herald, 1982) as shown in Figure 1.9. It has semi-

flexible/random coil conformation, higher galactose substitution increases the stiffness (that is, decreases the flexibility) (Petkowicz *et al.*, 1998).

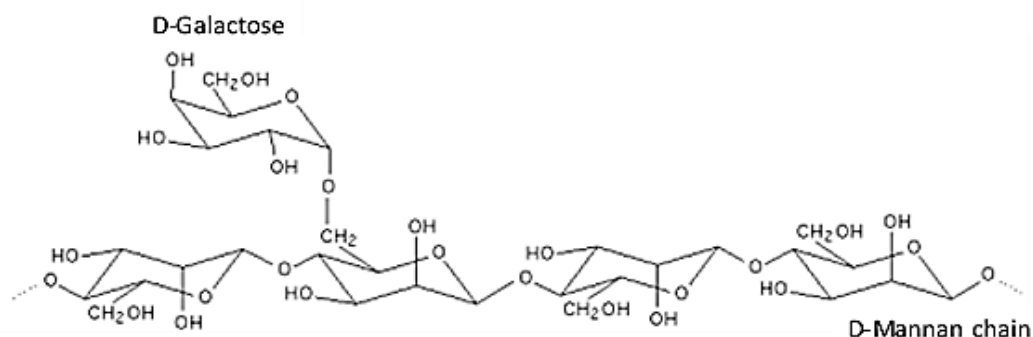


Figure 1.9: Structure of locust bean gum (Cybercolloids, 2012).

Locust bean gum (LBG) solutions are pseudo-plastic. The viscosity of LBG solutions is not influenced by salts and it is stable at a wide range of pH (Hoefler, 2004, Maier *et al.*, 1993). LBG is known to gel in the presence of a cross-linker such as borax, or forms gels synergistically in the presence of a second polysaccharide like κ -carrageenan, ι -carrageenan, agarose or xanthan. It was reported that G-free stretches of polymannan interact with helical regions of carrageenan, agarose and xanthan and terminated when a galactosyl-M residue is encountered, followed by the next polymannan sequence on the LBG chain to interact with different molecule present in the mixture (Figure 1.10).

The ratio between LBG and the other polysaccharide gives the opportunity to formulate a gel with controlled strength. Generally, these gels are prepared by

heating to 85°C to ensure solubilisation of the locust bean gum before leaving the mixture to set upon cooling. The gel set-temperature plays an important role in terms of its final functionality, for instance, when a xanthan and galactomannan mixture is heated to 70°C, the resulting storage moduli depend on the galactose content of the galactomannan, and resultant storage moduli are significantly higher than for an unheated system (Mannion *et al.*, 1992, Lundin *et al.*, 1994).

LBG also has a tendency to self-associate when M:G is high, promoted by freezing and thawing. At the correct concentration, this can result in gel formation (Richardson *et al.*, 1998; Goff *et al.*, 1999), which is utilised in the ice-cream industry for texture control. This is believed to be due to the mannan:mannan interactions of different chains and has been shown by Whitney (1998), to infer binding of LBG to cellulose.

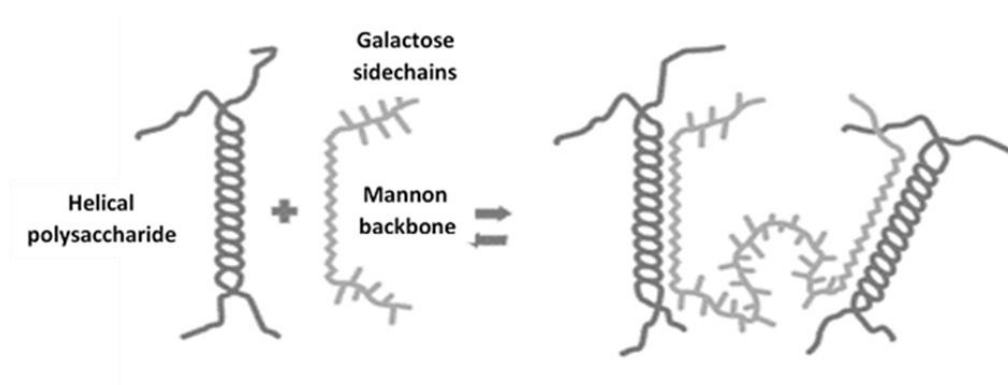


Figure 1.10: Model proposed for the interaction between helix forming polysaccharides and galactomannan (adapted from Morris *et al.*, 1995).

1.5 Cellulose/hydrocolloids mixtures

The effect of powdered cellulose on the viscosity of hydrocolloids solutions was first reported by Ang (1991) and Ang and Miller (1991). The addition of cellulose was able to increase the viscosity of guar, carboxymethylcellulose (CMC) and xanthan solutions of between 0.1 and 0.3wt%. There have been several studies reported the cell wall dispersions from a variety of sources such as tomato, apple and carrot are used to modify the viscosity of the hydrocolloid solutions for a specific application (Kunzek *et al.*, 2002). Similarly, the addition of hydrocolloids or polysaccharides exhibits a quite significant effect on the rheological properties of MFC or cellulose. For instance, the addition of CMC in MFC suspensions leads to higher viscosity than the sum of the viscosity of individual components in the suspension (these suspensions were not dried) (Vesterinen *et al.*, 2010, Lowys *et al.*, 2001). Vesterinen (2010) showed that cationic starch (CS) strengthens MFC suspensions, maintains the gel-like behaviour and shear thinning behaviour. But there is as yet no complete consensus as to what the binding mechanisms are between the cellulose/MFC and polymeric additives.

It was reported that the mixing of natural fibres with polysaccharides such as modified starch and/or cellulose derivatives improve their mechanical

properties (Curvelo *et al.*, 2001). These blends shows an increase in the tensile strength and the Young's modulus when the fibre content increases (Shaeb and Jog, 1999, Alvarez *et al.*, 2004). It was also reported that the addition of some hydrocolloids, such as xanthan and LBG, during co-processing (*e.g.* ball milling) protects the crystallinity of cellulose (Abbaszadeh *et al.*, 2014). The interaction between cellulose and other hydrocolloids has interested many researchers as it opens doors for a wide range of applications and also stabilises the MFC microfibrils from collapsing during drying (as mentioned earlier in Section 1.2).

Both hemicelluloses and pectin are naturally present in plant cell wall and likely to bind to cellulose but there is as yet no complete consensus as to what are the binding mechanisms. Depending on the hydrocolloid's molecular structure the interactions with cellulose varies. For instance, Newman (1998) reported that the interactions between the crystallite surface cellulose and adhering LBG result in blurring the distinction between two non-equivalent crystallographic sites. This indicates that the galactosyl residues of LBG are able to rotate around the bonds and link them to the mannan backbone, even when the backbone is bound to the cellulose crystallite surface. Unsubstituted mannan segments can bind to cellulose by undergoing a conformational transition to an extended 2-fold form (Whitney *et al.*, 1998, Newman *et al.*, 1998). It appears

that the interaction between microfibrillar cellulose and hydrocolloids (CMC and LBG) are still not well understood. There is a need for some systematic and fundamental work to understand the interaction between MFC and hydrocolloids and their impact on the degree of fibrillation and suspension properties when co-processed.

1.6 Brief introduction to the thesis

Different hydrocolloids are widely used in the food and personal care industry serving many different functions such as gelling, thickening, stabilising and coating agents (Foster, 2010). With growing environmental and health concerns as well as food shortages, there is increasing demand in cellulosic research and its sustainable applications. Cellulose is a major component of the plant cell wall, and the most abundant natural polymer on earth, but due to its poor solubility it has been limited to certain industries. Traditional methods of utilising cellulose involve harsh chemical treatments. In recent years, to produce materials with least environmental footprint (concerns) different mechanical treatments such as homogenisation and ball milling have been used to modify the native cellulose to the fibrillated form, unpacking cellulose fibrils to smaller units such as microfibrillar cellulose with unique functional properties.

The early studies highlighted a number of challenges using this mechanically modified native cellulose in different applications as mentioned in section 1.2.1.

The pure cellulosic fibres from softwood as an ingredient, which does not inherit any polymeric component (unlike citrus fibres), *e.g.*, microcrystalline cellulose (MCC) and microfibrillar cellulose, requires the addition of polysaccharides (depending on their thermodynamic compatibility) in order to achieve final functionality. Possible synergistic/functional interactions between the polymers and the cellulose microfibrils result in a complex system, and when stabilised may produce a stable and better functioning ingredient for food applications (Foster, 2010, Norton *et al.*, 2011).

Aggregation of microfibrils upon drying is a major challenge with microfibrillar cellulose application in food and personal care industry. In recent years, it has been tackled by the addition of polymeric additives and salts (Missoum *et al.*, 2012, Lowys *et al.*, 2001) to protect the microfibrils from aggregation during the drying process, resulting in better recovery of rheological or other functional properties. The interaction between the additive and MFC prevents the microfibrils from collapsing or agglomeration during the drying process. However, there is not enough evidence supporting how these polymeric

additives are interacting with and stabilising the microfibrils, and importantly what happens when MFC and additives are co-processed?

Carboxymethylcellulose (CMC) is one of the most studied hydrocolloids to stabilise microfibrillar cellulose during the drying stage (Vesterinen *et al.*, 2010, Lowys *et al.*, 2001). However, it is still hard to recover the maximum viscosity of the suspension after dispersing the dried MFC with CMC material, especially at low shear treatments, when compared with mixtures of never dried MFC with CMC suspensions. Besides carboxymethyl cellulose as an additive, it has previously been reported that some galactomannans and glucomannans, such as LBG and Konjac glucomannan show positive interactions with cellulose (Whitney *et al.*, 1998, Newman and Hemmingson 1998). Hence, during this research, LBG was used as an alternative additive to protect an aggregation of microfibrils after drying and its impact on the recovery of suspension properties (such as rheological properties, redispersibility *etc.*) was studied.

Therefore, the ultimate objective of this research was to explore the impact of different technologies used to produce MFC on the structure and functional properties of the suspension. In addition, an effort was invested to understand the interaction between MFC and carboxymethyl cellulose in water as well as the impact of drying on the functional properties of the suspension. This in-

depth understanding of the interaction between MFC/CMC was then transferred to a study of an interaction between MFC/LBG and triple blends (MFC/CMC:LBG). In the course of this research, the impact of drying and co-processing was considered to be another important aspect.

1.7 Objectives

To achieve the research aims as mentioned in Section 1.6, several specific objectives were undertaken and these included:

- Characterisation of physical properties (such as rheological properties, crystallinity and spin-spin relaxation times) and particulate structure through light microscopy of MFC in aqueous suspension. This includes:
 - Comparison between different qualities of MFCs produced by different technologies.
 - The impact of a number of passes through the homogeniser.
 - The impact of drying and rehydration of MFC.
- Investigate and characterisation of the interaction of MFC with carboxymethyl cellulose (CMC), locust bean gum (LBG) and a blend of CMC/LBG, to develop the most efficient system for a dry MFC, to prevent irreversible aggregation during drying when added post homogenisation.

- Investigate the structural effects and interactions between MFC/CMC, MFC/LBG and blend of CMC/LBG with MFC when co-processed with cellulose fibres.
- Explore the role of MFC as dietary fibre for food applications and its role in taste perception.

1.8 Thesis structure

This thesis is divided into multiple chapters, each chapter dedicated to a specific aim, however, all results in the results chapters are correlated with each other within the chapters and, later compared in the conclusions chapter.

Chapter 2 provides a general materials and methods chapter which itself includes a specific introduction and rationale behind the use of the techniques for a multidimensional characterisation used throughout this thesis.

The results of the study are presented in four separate results chapters. Each results chapter contains a specific introduction and brief description of the methodology used to justify the work presented. The first results chapter (Chapter 3) is aimed to characterise the suspension properties (such as rheological and phase behaviour) of MFC, also includes, the impact of processing and method used to produce MFC on particulate structure (through light microscopy), crystallinity and rheological properties of the suspension.

This enabled a rationalisation to the reasons behind the work presented in Chapters 4 and 5.

Chapter 4 and Chapter 5 are designed to gain a better understanding of the impact of polymeric additives to protect aggregation/ collapse of MFC fibres during the drying stage. Chapter 4 focus on an examination of the interaction of MFC with carboxymethyl cellulose (CMC), locust bean gum (LBG) and blend of CMC/LBG, when added post homogenisation. Chapter 5 explores the structural impact and interactions between MFC/CMC, MFC/LBG and blend of CMC/LBG when co-processed during the MFC production.

The last results chapter (Chapter 6) compares the suspension properties of MFC/CMC with commercial cellulosic dietary fibres such as citrus fibres, currently used in the food industry. Chapter 6 also includes the salt-reduction properties of MFC/CMC suspensions in a food model system in comparison with the commercial cellulosic dietary fibres. Finally, the general discussion, conclusions and suggestions for the future work are presented in chapter 7.

Chapter 2

Materials and Methods

2.1. Introduction

This chapter covers the materials and methods used to prepare the individual samples during this investigation; however the specific sample preparations are reported in the individual results chapters. A brief description of the basic principles of the techniques used to analyse the samples is presented in the methods section. The experimental conditions specific to individual chapters are reported in the methods section of each results chapter.

2.2. Materials

The different varieties of MFCs produced by different technologies and cellulose fibres (source: softwood spruce) at different dry content provided by Borregaard AS (Norway) are shown in Table 2.1. Refined MFC (RMFC/CMC) named as CTE(Flakes) and CTE(Powder) were provided by Borregaard AS, the type of CMC used in this formulation is confidential.

Low molecular weight carboxymethyl cellulose (CMC) named CP Kelco A (DP:10) was provided by C.P. Kelco (Finland) and high molecular weight carboxymethyl cellulose named Dow Wolff 60000 (DP:200) was provided by Dow Wolff (Germany). The degree of substitution (DS) of both CMCs is 0.7. Locust bean gum (Grindsted LBG®246) was provided by Danisco Ltd.

(Denmark). For a comparative study different food grade, the cellulosic fibres Herbacel AQ+ (HBAQ+) and CitriFi 100 (CF100) were supplied by CyberColloids Ltd (Ireland).

Table 2.1: List and codes of a different variety of MFC, including dry weight (DC) and technology used to produce MFC. No. of Passes means samples were passes through different technology and collected after every pass for analysis purpose.

Technology	No. of Passes	DC(%)	Code
Borregaard Fibrillation Technology	1 to 7 Pass	2.00	dMFC
Borregaard Fibrillation Technology + concentrated	2 Pass	8.97	BMFC
Microfluidics	1 to 3 Pass	2.00	mMFC

2.3. Sample preparation

This section gives details of the sample preparation and equipment used for preparing samples as standard protocol followed throughout this thesis.

2.3.1. Microfibrillar cellulose (MFC)

Never dried 2% or 8.97% microfibrillar cellulose (dMFC or BMFC) was diluted to target concentration by using distilled water and samples were treated with a high shear overhead mixer (source: IKA® Ultraturrax) at 15,000-18,000 rpm for 4 mins. All the diluted samples were stored at room temperature on a roller bed overnight before analysis.

Both MFCs (dMFC and BMFC) were also analysed in the dry state. In general, a thin layer (approx. 2 mm thick) of wet MFC was deposited on aluminium foil plates and dried by using the conventional oven (Gallenkamp hotbox oven, size 2) at 50°C for 12 hours. After drying, samples were kept in a silica desiccator (60 mins) for cooling before grinding (De'Longhi KG49 Coffee Grinder, UK) and storing. All dry MFC samples were redispersed in distilled water using the same process as for never-dried MFC. All of the samples were stored on the roller bed overnight before analysis. The dry weight (DC) was noted and corrected post-sample preparation.

2.3.2. Carboxymethyl cellulose (CMC)

Carboxymethyl cellulose (CMC) powder (CPKA and DW60) at required concentration (2% w/w) was dissolved in distilled water by adding the powder sample carefully maintaining the agitation of the solution using an overhead stirrer (IKA Eurostar 20 Digital Overhead Stirrer). The solution was stirred for 60 mins and allowed to sit at room temperature overnight before further formulation steps and analysis.

A mixture of two CMCs *i.e.* blend of low molecular weight CPKA and high molecular weight DW60 was formulated during this study, the blend was

named as CMC(mix). The two CMCs were dispersed in distilled water at 75:25 and 50:50 (CPKA:DW60) ratio resulting in an overall solution concentration of 2% w/w (IKA Eurostar 20 Digital Overhead Stirrer) at 20°C for 2 hrs. The pH of the solution was adjusted to 6.8 with NaOH (Sigma-Aldrich) and then left overnight at 4°C before mixing with MFC. The pH was cross-checked and maintained at 6.8, solutions contained 0.02% sodium azide (Sigma-Aldrich) was added to prevent bacterial contamination. The concentration of all samples was determined by calculating the dry weight content by using OHAUS MB25 moisture analyser (OHAUS, US).

2.3.3. Locust bean gum (LBG)

To prepare an unheated LBG solution, the LBG powder was dispersed (concentrations 1% or 2% w/w) in distilled water using a magnetic stirrer (20°C) and stored at room temperature for overnight before analysis. Whereas heated LBG solutions were prepared by dispersing the LBG powder (concentrations 1% or 2% w/w) in distilled water using a magnetic stirrer (20°C). The suspensions were stirred and heated at 80°C for 30 mins followed by storing the sample overnight at the room temperature before further formulations steps and analysis. The concentration of the LBG was cross-

checked on a w/w basis. The pH was maintained at 6.8 and sodium azide solution (0.02% w/v) was added to prevent bacterial contamination.

2.3.4. CMC/LBG blend

CMC/LBG blend (BL) was prepared by mixing previously prepared 2% w/w aqueous solutions of LBG and CPKA CMC (Section 2.3.2 & 2.3.3) at room temperature (20°C). CMC/LBG blends were made in three different ratios CMC/LBG *i.e.* 75:25; 65:35; 50:50. All mixtures were stirred using an overhead stirrer (IKA Eurostar 20 Digital Overhead Stirrer) for 60 mins at 20°C. The pH of the solution was adjusted to 6.8 with NaOH and then left overnight at 4°C before mixing with MFC. After this process, the pH and concentration were cross-checked and pH was maintained at 6.8. The solution contained 0.02% w/v sodium azide to prevent bacterial contamination.

2.3.5. MFC/Additive mixtures

MFC and different additives (MFC/CMC, MFC/LBG, MFC/BL1) were mixed in different proportions (as shown in Table 2.2) maintaining an overall 2% w/w mixture concentration of mixture. All samples were well mixed by using an overhead stirrer (Silverson) at 8000 rpm for 5 mins. The mixtures were stored overnight at room temperature; the pH (6.8) was cross-checked and

maintained. An approximately 2 mm thin layer of suspensions was prepared on aluminium plates and all samples were dried at 50°C for 12 hrs in an oven (Gallenkamp hotbox oven, size 2).

Table 2.2: Composition of MFC/additives studied, where CMC(mix) used for CMC15, CMC25 and CMC50 is 75:25 (CPKA/DW60). Blend (BL) ratio used for all formulation is 75:25 (CPKA/LBG).

Sample Code	% w/w suspension			
	MFC (%)	CMC (%)	LBG (%)	BL1 (%)
MFC100	2	0	0	0
CMC15	1.7	0.3		
CMC25	1.5	0.5		
CMC50	1	1		
CPKA15	1.7	0.3		
DW15	1.7	0.3		
CMC(1:1)	1.7	0.3		
LBG15	1.7		0.3	
LBG25	1.5		0.5	
LBG35	1.3		0.7	
LBG50	1		1	
BL15	1.7			0.3
BL25	1.5			0.5
BL35	1.3			0.7
BL50	1			1

2.4. Methods

During this research multiple techniques were used to characterise different samples, depending on moisture content different techniques was employed.

The rheological analysis was performed to study the suspension properties of MFC and correlated with microstructure produced from fluorescence and light microscopy. Water mobility in highly networked MFC suspension was studied by low resolution nuclear magnetic resonance spectroscopy

(relaxation NMR). In order to characterise the impact of drying on the physical properties of MFC different techniques were employed, for instance, Wide-angle X-ray diffraction (WAXD) analysis was performed to determine the crystallinity of the dried cellulosic fibres before and after homogenisation. Differential scanning calorimetry (DSC) analysis was performed to monitor thermally induced structure transition in the polymeric system whereas Derivative thermogravimetric analysis (DTGA) is a quick method to determine moisture content and degradation temperature of a sample. Detailed fundamental information and equipment setup used during this research are presented under this section.

2.4.1. Rheological Analysis

Rheology is the science of deformation and flow (Barnes *et al.*, 1989). Rheological properties are based on the flow and deformation responses of a system when subjected to stress. Simple rheological measurements can lead to extensive process characterisation and materials understanding. For instance, rheological analysis of different food applications helps in understanding the responses of food structure to applied force or deformation, which also provides information on the impact of overall

composition and interaction between the components on food microstructure (Norton *et al.*, 2011).

There are three fundamental parameters defined in rheology, *i.e.* shear stress, shear strain and shear rate. These are often explained with the two plate-model depicted in Figure 2.1. Shear stress (symbol: τ , unit: Pa) is the force required to produce the deformation divided by the cross-sectional area of the sample, whereas shear strain (γ) is defined as the distance moved by the sample divided by the original separation of the plates, which is dimensionless (Figure 2.1). The rate at which the deformation made is the shear rate (symbol: $\dot{\gamma}$, unit: s^{-1}) can simply be calculated by Equation 2.1.

$$\dot{\gamma} = \frac{v}{h} \quad \text{or} \quad \dot{\gamma} = \frac{d\gamma}{dt} \quad (\text{Equation 2.1})$$

v is the velocity of the upper movable plate [m/s] and h is the distance between the two plates.

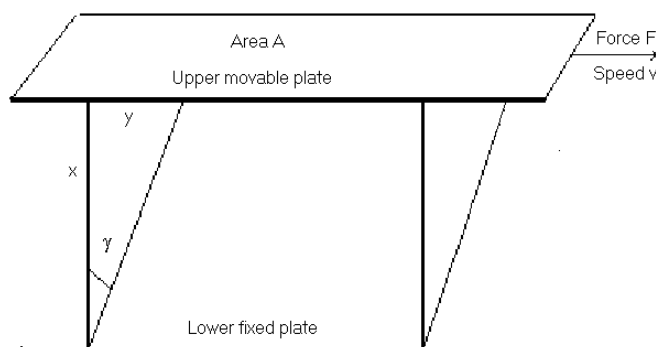


Figure 2.1: A schematic representation of the two-plate model for shear-strain deformation (adapted from Mezger 2006).

The two idealised extremes of the deformation behaviour are perfect elastic solids (Hookean solids) and perfect viscous liquids (Newtonian fluids). In the elastic solids (*e.g.* cross-linked rubber) the energy used during deformation is stored and released again when the stress is removed. The stress is directly proportional to the extent of deformation and independent of the rate of deformation applied (Hooke's law). In the case of viscous liquids (*e.g.* water, honey or cooking oil), the energy used during deformation is lost (dissipated as heat) and no recovery occurs when the stress is removed. The stress imposed flow is directly proportional to the rate of flow. An intermediate state of these two extremes of behaviour is viscoelastic behaviour; a viscoelastic material shows both viscous and elastic behaviour simultaneously. The viscous portion behaves according to Newton's law and elastic portion behaves according to Hooke's law (details are given in Section 2.4.1.2).

2.4.1.1. *Flow behaviour*

Newtonian fluids are characterised by a constant value of viscosity for a specific temperature and pressure. The viscosity (symbol: η , unit: Pa.s) of fluids by definition is a measure of the resistance to deformation by shear stress and is formulated as the proportionality constant between shear stress

(τ) and shear rate ($\dot{\gamma}$) (Equation 2.2). Although this viscosity will change with temperature, it does not change with the shear rate.

$$\eta = \frac{\tau}{\dot{\gamma}} \quad (\text{Equation 2.2})$$

As can be seen in Figure 2.2(a), there are three main types of viscosity behaviour: shear thickening (dilatant fluid) where the viscosity increases with increasing shear rate; shear thinning where the viscosity decreases with increasing shear rate, many polymers are classified in this group, *e.g.*, cellulosic suspensions; Newtonian where viscosity is independent of the shear rate, *e.g.*, water, oils, honey *etc.* There is also one type of material known as Bingham plastic that requires a minimum stress before the onset of flow, for example very high concentrated suspensions. This type of flow can be better illustrated in the form of a flow curve and has been included in Figure 2.2(b) (Mezger 2006, Lapasin and Pricl, 1995).

2.4.1.2. Viscoelastic behaviour

An aqueous suspension of microfibrillar cellulose tends to show viscoelastic gel-like behaviours (as mentioned in chapter 1). In order to characterise this behaviour, small deformation oscillatory tests were performed using a conventional rheometer. In oscillation measurements the sample is subjected to a low-amplitude, sinusoidal shear deformation, *i.e.* a time-dependent

strain waveform (Equation 2.3), the resulting shear stress wave will be a sin wave with a different amplitude and a phase shift (Equation 2.4).

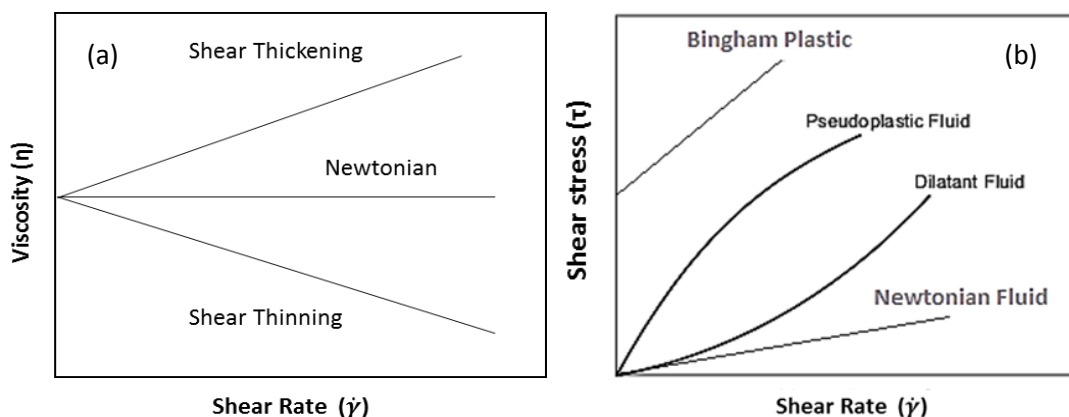


Figure 2.2: Types of viscosity behaviour presented (a) as viscosity curves $\eta(\dot{\gamma})$ and (b) as flow curves $\tau(\dot{\gamma})$ (Mezger 2006).

$$\gamma = \gamma_0 \sin \omega t \quad (\text{Equation 2.3})$$

where “ γ ” is the time dependent strain, “ γ_0 ” is shear strain amplitude and “ ω ” is the angular frequency (rad s^{-1}).

$$\tau = \tau_0 \sin(\omega t + \delta) \quad (\text{Equation 2.4})$$

where “ τ ” is the time dependent shear stress, “ τ_0 ” is the shear stress amplitude and “ δ ” is the phase angle between the shifted waves. This equation can be rewritten as Equation 2.5.

$$\tau = \tau_0 \cos \delta \sin \omega t + \tau_0 \sin \delta \cos \omega t \quad (\text{Equation 2.5})$$

For ideal elastic solids (stress is directly proportional to strain), the applied oscillatory strain and the stress generated by the sample resisting deformation are exactly in phase. Whereas for an ideal liquid, the stress

response is maximum at the midpoint of the cycle, where the net deformation is zero, but the rate of deformation is maximum. In this case, stress and strain are exactly (90°) out of phase. However, viscoelastic materials stand somewhere between, *i.e.* there are contributions from both the in-phase and out-of-phase components.

The ratio of in-phase stress (or energy stored) to applied strain is the **storage modulus (G')** (Equation 2.6); where the corresponding parameter for the out-of-phase (or energy loss) response is the **loss modulus (G'')** (Equation 2.7). A notation using complex variables can be used to define the **complex modulus (G^*)** according to Equation 2.8. A frequency-dependent viscosity function determined during forced harmonic oscillation of shear stress is corresponding to **complex viscosity ($|\eta^*|$)** derived according to Equation 2.9. The phase angle or **loss tangent ($\tan \delta$)** is then given by Equation 2.10. It is directly related to the energy lost divided by energy stored and it ranges between 0° to 90°. 0° indicates purely elastic behaviour and (no phase lag) and 90° indicates purely viscous material behaviour (out of phase).

$$G' = \frac{\tau_0 \cos \delta}{\gamma_0} \quad (\text{Equation 2.6})$$

$$G'' = \frac{\tau_0 \sin \delta}{\gamma_0} \quad (\text{Equation 2.7})$$

$$G^* = \sqrt{(G'^2 + G''^2)}/\omega \quad (\text{Equation 2.8})$$

$$|\eta^*| = G^*/\omega = \sqrt{(G'^2 + G''^2)}/\omega \quad (\text{Equation 2.9})$$

$$\tan \delta = G''/G' \quad (\text{Equation 2.10})$$

2.4.1.3. *Equipment settings*

The rheological measurements were carried out using a stress-controlled rheometer (Physica MCR 301, Anton Paar, Austria), with a serrated parallel plate geometry (50 mm diameter with a gap of 1 mm) at 20°C, controlled by a Peltier system. Amplitude sweeps were generated by log ramping strain between 0.01-100% at 1 Hz constant frequency, whereas frequency sweeps were performed over the frequency range of 0.1-15 Hz at constant strain (selected from the linear viscoelastic region: 0.2%). Rotational measurements were performed by increasing/decreasing the shear rate from 0.01-1000 s⁻¹. Finally, temperature sweeps were generated by heating the sample between the plates from 20°C to 90°C at 1°C/min heating rate. During these experiments, the strain was fixed to 1% and the frequency 1 Hz. A light mineral oil trap was used to prevent water evaporation. For each analysis two batches of samples were prepared and analysed in duplicate, hence the data presented is an average of 4 sets of data.

2.4.2. Low Field (^1H - Relaxation) NMR

Low field nuclear magnetic resonance spectroscopy (NMR) is a branch of spectroscopy in which radio frequency waves induce transitions between magnetic energy levels of nuclei of a molecule. The length of time the nucleus spends in the excited state is Δt . It is controlled by the rate at which the excited nucleus loses its energy of excitation and returns to the original state. The process of losing energy is called relaxation, and the rate at which the ensembles of nuclei return to equilibrium is the relaxation time. An excited nucleus may transfer its energy to a nearby unexcited nucleus of a similar molecule resulting in the excitation of the neighbouring nucleus and the relaxation of the original nucleus back to original state. This process, where there is no net change in energy of the system, is known as transverse or spin-spin relaxation (T_2). In general, a liquid component gives longer T_2 values whereas a solid component gives shorter T_2 values.

In contrast, if a nucleus loses its excitation energy to the surrounding molecules sometimes known as the lattice, the system will become warm since the energy is changed to heat. The excitation energy becomes dispersed throughout the molecular system, hence no radiant energy appears and no other nuclei are excited. As numerous nuclei lose their energy, the

temperature of the sample increases. This process is known as longitudinal or spin-lattice relaxation (T_1).

It has been demonstrated in previous work, that proton nuclear magnetic resonance (NMR) parameters such as spin-lattice-relaxation time (T_1) and spin-spin relaxation time (T_2) are sensitive to water binding and mobility in polymeric suspensions/dispersions (Ono *et al.*, 1997, Rachocki *et al.*, 2005, Vackier *et al.*, 1999). Spin-spin relaxation times are generally measured using the Carr-Purcell-Meiboom-Gill (CPMG) pulse sequences.

The CPMG sequence provides a more accurate measure of the liquid T_2 decay, free of artefacts such as magnetic inhomogeneity (Meiboom *et al.*, 1958, Carr-Purcell *et al.*, 1954). For example, the study by Ono (1997) showed that a microcrystalline cellulose (MCC) suspension contains both free- (bulk) water and water bound to the polymer chains interacting and exchanging protons with each other resulting in a shorter T_2 compared to pure distilled water, which has a T_2 at room temperature of approximately 2 seconds. MCC suspensions having a higher viscosity tend to have a shorter T_2 due to a direct effect of viscosity on the tumbling rate of the molecule and possibly a higher amount of interacting (associated) water. This may be restricted to the polymer interface (Ono *et al.*, 1998) however the allocation of

associated/interacting water fraction in systems such as these in controversial (Hills, 1991).

This study focuses on understanding the properties of model systems composed of polymeric mixtures, *i.e.* MFC/CMC, MFC/LBG or MFC/BL in aqueous suspension particularly with reference to the impact of water binding and mobility in the polymeric suspensions. The impact of CMC/LBG during the drying step is also investigated by correlating the suspension rheological properties of the suspension with the spin-spin relaxation time (T_2) in order to understand the mobility of water in the MFC/hydrocolloid matrix.

2.4.2.1. Equipment settings

Time domain measurements were carried out at 25 MHz using a Resonance Instruments (R.I.) Maran spectrometer. The temperature was controlled to $20 \pm 1^\circ\text{C}$ by a conventional gas flow system that was calibrated with an external thermocouple and controlled with a standard R.I. temperature unit. All measurements were conducted in standard 10 mm internal diameter NMR tubes. Spin-spin relaxation times (T_2) were recorded using CPMG (Carr-Purcell-Meiboom-Gill) pulse sequence *i.e.* sequence of pulse: $90^\circ x - (\tau - 180^\circ y - \tau - \text{echo})_n$ at tau (τ) 2048 μs . Typical 90° pulse lengths (x) were of

the order of 5 ms, and for 180° pulse lengths (γ) were of the order of 10 ms. A split time-base was utilised in order to ensure the most efficient sampling of the data (T_2 duplicate measurement were made 15 mins after the original measurement to check the reproducibility). Recycle delays were normally set to 10 sec to avoid saturation effects and 16 scans (n : in pulse sequence) were averaged.

2.4.3. Wide angle X-Ray Diffraction (WAXD)

An X-ray is an electromagnetic radiation that has a wavelength of between 0.1 Å and 100 Å which is similar to the interatomic distances in a crystal. The X-rays are produced by heating a tungsten filament inside a vacuum tube. Electrons are emitted and accelerated by an electric potential and impact on a metal target, often copper. These electrons disturb the metal atom's inner electrons, when the outer electrons fall to a lower orbital to take their place X-rays are emitted.

X-ray diffraction (XRD) is a tool for characterising crystallinity of dry or semi-dry material, *i.e.* to characterise the arrangement of atoms in crystals and distances between crystal faces. In an amorphous material, atoms have no order. When the atoms are hit by X-ray beams, the surrounding electrons will oscillate at the same frequency as the beam. Due to the lack of order, the x-

ray beams will be reflected at all angles resulting in destructive interference as the waves are out of phase of one another. However, crystals have an ordered structure. Due to the regular patterns in the crystal when X-ray beams hit the atoms, in some directions, the waves will be in phase which will cause constructive interference that can be measured by the detector (Figure 2.3).

In WAXD setup, a thin layer of the sample powder is placed on fixed stage in the path of monochromatic X-rays, an X-ray detector measures the X-rays diffracted from the sample over a wide range of angles (Figure 2.3). The sensors present in the detector collect the spike in X-rays at specific angles (satisfying the Bragg's Equation 2.11) representing the population of crystals. The output graph is X-ray intensity over 2θ , the angle of the detector (Chatwal and Anand, 2006).

Bragg's law gives the angles for coherent and incoherent scattering from a crystal lattice when X-rays are incident on an atom (as shown in Figure 2.3).

The Bragg's law is widely used for measuring wavelengths and determining the lattice spacing of crystals (Suryanarayana and Norton, 1998).

$$n\lambda = 2d\sin\theta \quad (\text{Equation 2.11})$$

where n is a positive integer, λ is the wavelength of the incident wave and θ is the scattering angle.

X-ray diffraction peaks are usually classified by peak position, peak width & peak intensity. From the intensity of these peaks the crystallinity of the system (also known as the peak height method) can be determined. The second approach is based on separation of the peak area contributions from the amorphous and crystalline portions known as the peak deconvolution method (Carrillo *et al.*, 2003, Park *et al.*, 2010). The Crystallinity Index is calculated as the ratio of the area arising from the crystalline phase to the total area.

In the peak deconvolution method, the peak contribution from the amorphous region and crystalline region was separated by using software (EvaV5 XRD software, UK). In order to fit the curves, a few assumptions are made such as of the shape and the number of peaks (for instance, it is hard to separate the peak 5 from peak 4 in Figure 2.4). In the case of cellulosic systems, five crystalline Gaussian peaks (101, 10 $\bar{1}$, 021, 002 and 040) can be separated. Crystallinity is calculated from the ratio of the area of all crystalline peaks to the total area (Figure 2.4). The presence of an amorphous region contributed to the broadening of peaks; however, an increase in crystallite

size and non-uniform strain within the crystals also influences the peak broadening (Ibbett *et al.*, 2013). The data manipulation was carried out using intensity vs. 2θ data in the Microsoft Excel software package with the Solver add-in. Figure 2.4 shows the results for fits using a cellulose type I pattern.

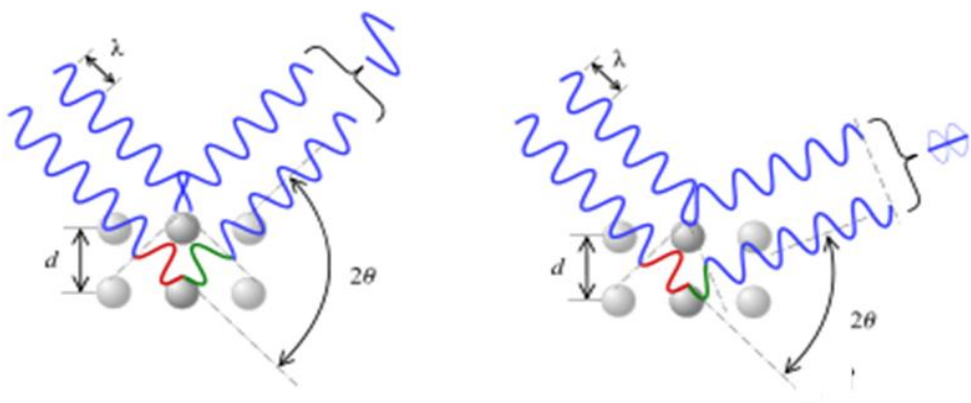


Figure 2.3: Bragg's law demonstration, according to the 2θ deviation, the phase shift causes constructive or destructive interferences. (Recreated from Suryanarayana *et al.*, 1998)

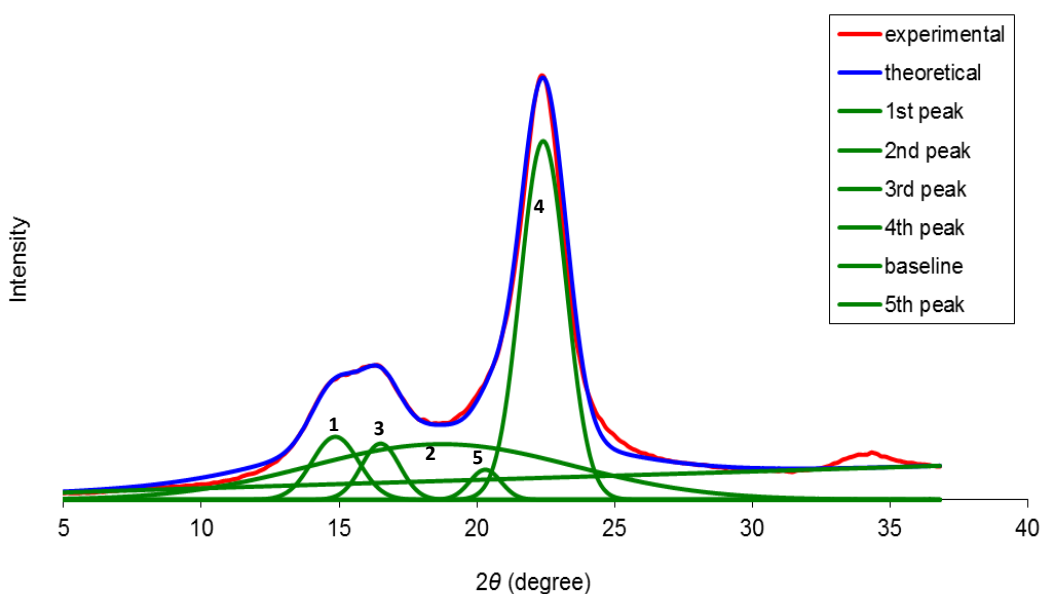


Figure 2.4: WAXD diffraction spectra of cellulose illustrating the peak deconvolution method.

2.4.3.1. Equipment settings

In this study, the crystallinity of cellulosic fibres (dry samples only) was measured using an X-ray diffractometer (Bruker AXS D5005) equipped with a copper tube operating at 40 kV and 50 mA produced in a Cu K α radiation of 0.154 nm wavelength. The data was recorded for a 2θ angular range between 3°-38° with an angular interval of 0.05°, the time spent at each angle was 2.5 sec, with a rotational speed of 60 rpm. The crystallinity of the test samples was calculated by using the peak deconvolution method. The analysis was made in duplicates; the peaks were individually fitted in Microsoft Excel software package with the Solver add-in. The presented crystallinity is an average of two sets of data.

2.4.4. Differential scanning calorimetry (DSC)

Differential scanning calorimetry (DSC) is a widely used thermal technique to measure the change in energy associated with material transitions that occur as the test sample is subjected to heating, cooling or held under isothermal conditions. The working principle of DSC is that the sample and an inert reference are heated separately, with the power supply to the sample heater variable so that the temperature difference can be maintained at zero even when endothermic or exothermic changes occur. The difference in power

supplied to the two heaters is monitored as the analytical signal. When the temperature of some amorphous materials is raised the polymer molecules will gain sufficient translational and torsional energy to reorganise into a crystalline structure which is a lower entropic state and therefore energy will be released which can be seen on the DSC as an exothermic transition.

2.4.4.1. *Equipment settings*

The DSC data presented in this thesis was recorded by using Differential scanning calorimeter (Mettler Toledo Ltd DSC823^e, UK). Approx. 10-20 mg of cellulosic material was weighed into stainless steel pans, and an empty steel pan was used as reference sample. The samples were heated from -30°C to 120°C at 5°C/min, followed by cooling the sample from 120°C to -30°C at 40°C/min followed by a re-heat from -30°C to 200°C. The onset, peak and end temperatures associated with thermal transitions occurring in the sample were reported. Analyses were made in duplicate to check the reproducibility and only single data is presented.

2.4.5. Derivative Thermo-gravitational analysis (DTGA)

In this technique, the sample is heated in a controlled environment where the temperature is changed in a predetermined manner, generally at a linear rate,

and the change in sample weight is recorded. Each stage of change in weight of the system signifies the specific thermal behaviour of the sample. For instance, with samples such as cell wall material (hemicellulose, cellulose *etc.*), the first set of weight loss corresponds to moisture loss from the system, followed by degradation of cellulosic materials. Hemicelluloses begin to decompose more easily with weight loss around 220°C-315°C, followed by cellulose pyrolysis in a higher temperature range *i.e.* 315°C - 400°C with maximum weight loss under controlled atmosphere (N₂ gas) (Yang *et al.*, 2007).

2.4.5.1. *Equipment settings*

Thermal stability of different cellulosic fibres and formulations were studied by using a Mettler Toledo model TGA/SDTA851e/LF1600 (Mettler Toledo, UK). Approximately 5–10 mg of the sample were subjected to a Nitrogen environment, a heating ramp from 20°C to 450°C at a rate of 10°C/min was applied to evaluate the peak temperature of DTG curve. The initial and final degradation temperatures and corresponding percentage weight loss for the samples were noted by using STARe Thermal Analysis Software package. Analyses were made in duplicate to check the reproducibility and single data is presented.

2.4.6. Microscopy

The microstructure of different MFC and MFC/additive suspensions was studied by using basic microscopy techniques such as brightfield light microscopy and fluorescence microscopy. The microscopy images presented in this thesis are indicative of structural impact or change in the microstructure of microfibrillar cellulose when cellulosic fibres are subjected to different processing stages such as the type of mechanical treatment used to produce MFC, a number of passes through homogeniser, drying *etc.*

2.4.6.1. *Light microscopy*

Light microscopy of all aqueous suspension of samples was performed by using Olympus BX5 bright field light microscopy. The microfibrils were dyed by using Congo red dye (Sigma-Aldrich). Congo red dye has a strong, though apparently non-covalent, affinity to cellulose fibres.

2.4.6.2. *Fluorescence microscopy*

Fluorescence microscopy was performed by using EVOS microscopy system in the fluorescence mode with a 20X objective. As both MFC and CMC do not exhibit fluorescence, it was necessary to attach a fluorescent label to at least

one of them. In the current study, CMC was tagged with FITC fluorescent dye as follows:

1 gm of CMC was dissolved in 10ml of dimethyl sulphoxide containing a few drops of pyridine. 0.1 gm of Isothiocyanato-fluorescein, followed by 20 mg dibutyltin dilaurate, was added. The whole mixture was heated at 95°C for 2 hrs. Free dye was removed from the system by a number of precipitations in ethanol, then the FITC-CMC was filtered and dried at 80°C (the protocol used is the same as that published by Belder *et al.*, 1973).

Chapter 3

Microfibrillar cellulose: Impact of fibre network and drying on suspension properties

3.1 Introduction

Cellulose from different raw materials can be disintegrated into various structural units such as microfibrillar or nanofibrils by using chemical or mechanical treatments. In current research MFC (softwood spruce) was produced by high-pressure mechanical treatment and different characterisation techniques were employed to examine the different suspension properties and microstructure. An important property of microfibrillar cellulose suspensions is their rheological properties as explained in Chapter 1; it is widely applicable in the food and personal care industries.

The type of technology used to produce MFC can result in different varieties of MFC specifically in terms of degrees of fibrillation, for example, typical mechanical treatments such as the number of passes through the homogeniser increases the degree of fibrillation. As the degree of fibrillation increases, the fibre size (particle size) decreases. The degree of fibrillation plays an important role in the physical properties of the system, *e.g.*, for a low degree of fibrillation of MFC, the particle size is larger with lower water binding capacity resulting in unstable phase behaviour, which ultimately has an effect on rheological properties of the suspension. Increasing the number of passes through homogeniser increases the fibrillation producing higher

water binding capacity and resulting in stable phase behaviour (Ulbrich *et al.*, 2014).

As the number of passes through a homogeniser increases the crystallinity of the system decreases due to breakage of hydrogen bonds present between the crystalline regions during the unpacking of cellulose fibrils (Kleinebudde *et al.*, 2000). Hence, the challenge for the large-scale industry is to produce MFC with a low number of passes through the homogeniser or refiner while at the same time achieving a high degree of fibrillation. However, the cost of production and energy consumption has to be considered in the MFC process.

Samples of MFC were produced for this project by two different types of fibrillation technologies. The first part of this chapter assembles the characterisation of MFC produced by using a different fibrillation technology, by studying the impact of the degree of fibrillation on the microstructure/fibril network of the MFC in suspension. The main hypothesis tested is “the technology used to produce MFC results in a broad range of MFC microstructures”. The understanding is further enhanced by the characterisation of MFC suspensions produced by multiple passes through one chosen homogeniser (Borregaard fibrillation technology). This was carried out as part of the sponsoring industry’s process development and the

processing steps are confidential. As discussed earlier the increase in the number of passes is thought to increase the water binding capacity due to an increase in microfibril network, hence low field NMR was performed to map the change in spin-spin relaxation time (T_2) in order to understand the mobility of water in the matrix.

Table 3.1: Comparison between different MFC drying processes (Peng et al., 2012a, Peng et al., 2012b).

Drying Method	Particle size after drying	Advantages	Disadvantages
Oven drying	Hundreds of microns	Well established in paper and pulp industry	Lose of micro/nano dimensions, aggregations
Freeze drying	Microns to millimeter length or width	homogenous dimensions of material and well established	High cost and agglomeration
Spray drying	few micro size	controllable size, continuous and easy scalable and low cost	agglomeration and non-homogenous particle size
Supercritical drying	micro-size fibrous MFC	Keep the dimensions intact	High cost, complicated method for solvent replacement and impractical
Atomisation drying	micro-size MFC	dimensions are intact	agglomeration and non-homogenous particle size distribution

Irreversible aggregation/agglomeration of MFC during the drying process results in fibrils too difficult to redisperse in water (Heux *et al.*, 2000). In recent years, a wide range of techniques has been used to dry MFC, aiming to achieve appropriate dimensions and suspension properties after rehydration (explained in Chapter 1 and summarised in Table 3.1). In this chapter, different conditions of oven drying were used to examine the impact of oven drying on the suspension properties, and a comparison was made with freeze

drying. The main reasons to use oven drying during this study are low cost and that it is extensively used in industry to produce dry material. In order to investigate the impact of temperature, different drying temperatures and times of drying were tested. This investigation also helped in defining the protocols used for the drying of different MFC/additive formulations presented in Chapters 4 and 5.

3.2 Materials and Methods

MFCs samples *i.e.* BMFC and dMFC used in this study were provided by Borregaard AS (Norway), where both samples were produced by using Borregaard Fibrillation technology. The BMFC is a concentrated form of MFC with approximately 8.97% w/w dry content whereas dMFC is a diluted form with dry content approximately 2% w/w. Processing of MFC to produce BMFC was carried out as a part of the sponsoring industry's process development and these processing steps are confidential. The NiMFCs were produced by subjecting 2% w/w cellulose (refined) pulp to a small scale Niro-homogeniser (panda 2K GEA Niro Soavi S.P.A. Germany) to distinguish from other products in this thesis named as NiMFC.

3.2.1 Sample preparation

The technologies used to produce MFC are presented in Chapter 2, Section 2.2 (Table 2.1). Sample codes used during this investigation are shown in Table 3.2. For each analysis, two batches of samples were prepared and analysed in duplicate.

Table 3.2: Sample code, technology and a number of passes used to produce MFC suspensions (note: these samples were never dried).

Sample	Technology	No. of Passes	Code
BMFC	Borregaard Fibrillation Technology	2	BMFC
dMFC	“	1	1dMFC
dMFC	“	2	2dMFC
dMFC	“	3	3dMFC
dMFC	“	4	4dMFC
dMFC	“	5	5dMFC
dMFC	“	6	6dMFC
dMFC	“	7	7dMFC
mMFC	Microfluidics	1	1mMFC
mMFC	“	2	2mMFC
mMFC	“	3	3mMFC
NiMFC	GEA Niro	3	3NiMFC
NiMFC	“	30	30NiMFC

3.2.1.1 Drying Process

Different drying methods were applied to 2% w/w BMFC suspensions diluted from 8.97% w/w. Approximately 2 mm thick layers of BMFC suspensions were poured onto aluminium plates and subjected to different drying processes

(Table 3.3). Oven drying (OD) was performed using a conventional drying oven (Gallenkamp hotbox oven, size 2, UK). Vacuum oven drying (VOD) was performed at 1 atm pressure by using vacuum oven (Gallenkamp Vacuum oven, UK). As a control, BMFC suspension was dried at room temperature (RTD) at $20\pm 1^\circ\text{C}$. Prior to freeze drying (FD), BMFC suspensions (about 10 ml) were frozen in a plastic beaker at a temperature of -20°C for 24 hrs. Frozen samples were then transferred to a freeze drier (Edward Freeze dryer Super Modulyo, UK) where the condenser temperature was set to -40°C and the vacuum pressure to 0.02 bar. Lyophilisation was continued for 24 hrs. Variable temperature and time were tested for all drying setups to monitor the influence these variables on the final product.

Table 3.3: Sample code, drying method, temperature and total time used to produce dried MFC.

Sample	Drying Method	Temperature ($^\circ\text{C}$)	Time (hrs)		Code
BMFC	Oven Drying	50°C	7.5	24	OD(50°C)
	Oven Drying	105°C	7.5	24	OD(105°C)
	Room Temperature Drying	$20\pm 1^\circ\text{C}$	48		RTD(20°C)
	Vacuum Oven drying	60°C	7.5	24	VOD(60°C)
	Freeze Drying	-20°C	24		FD(-20°C)

3.2.2 Light microscopy

Light microscopy as detailed in chapter 2, section 2.4.6 was used as an indicative tool to study the microstructure of aqueous suspensions.

3.2.3 Phase Separation and UV spectrophotometry

Phase separation was performed to monitor the liquid (in this case water) separated from highly networked MFC suspension. Phase separation was performed by placing 10 ml of 2% and 0.1% w/w sample suspensions in 10ml glass tubes and a measuring cylinder, respectively, and stored at 20°C temperature. Photographic images (Sony Cybershot 16.2 megapixel camera, India) were taken after 24hrs of storage. After 24 hrs, the upper layer from the 0.1% w/w phase separated suspension tube was introduced into quartz cuvettes and the transmittance was measured at 500 nm using a UV-Vis spectrophotometer (Varian Cary50 Bio-UV/Visible spectrophotometer, Australia), where water was used as blank. Samples were prepared and analysed in duplicate. An average of the readings is presented in the figure. UV-Vis spectrophotometry was performed to determine the presence of micro or nanofibrils in the upper (cloudy liquid) phase of phase-separated samples.

3.2.4 Rheology

Rheology measurements were made according to the method as detailed in chapter 2, section 2.4.1.3. Data presented is an average of 4 replicates.

3.2.5 Relaxation NMR

Spin-spin relaxation time (T_2) was measured according to the method as detailed in chapter 2, section 2.4.2.1. Data presented is an average of 4 replicates.

3.2.6 Wide Angle X-ray diffraction (WAXD)

WAXD was performed on the dried 1 to 7pass dMFC and MFC samples. 2% w/w aqueous suspensions were dried by using oven drying (OD) (Gallenkamp hotbox oven, size 2, UK) at 50°C for 7.5 hrs by placing a thin layer of BMFC suspension (2 mm thick) on aluminium plates. Details of equipment and measurements setting are presented in chapter 2, section 2.4.3.1. Data presented is an average of duplicates.

3.2.7 Data Analysis

Statistical data analysis was performed by using software Excel (Microsoft 2013, USA). Correlation analysis was performed to investigate the relationship between physical parameters (viscosity, complex viscosity, crystallinity, spin-spin relaxation time *etc.*) and a number of passes through homogeniser and different drying techniques using analysis of variance (ANOVA) with a minimum significance level defined as $p\text{-value} < 0.05$.

3.3 Results and Discussion

3.3.1 Microstructure of MFC

Figure 3.1 shows microscopy images of MFC aqueous suspensions produced from softwood cellulose pulp using different technologies. Light microscopy images show two distinct structures *i.e.* fibres fragments (large and small fibres) and microfibrils (entangled fibre network). The microscopy images indicate that as the number of passes through the homogeniser increased, the fibre size of cellulose decreased independent of the type of process used to produce the MFC. However, the type of process used to produce the MFC appears to have a significant impact on the resulting degree of fibrillation. For instance, the micrographs clearly indicate that dMFC had a higher degree of fibrillation, especially after 1 and 2 passes as compared to microfluidics MFC (mMFC) or 3 passes NiMFC.

The MFC suspension produced by using Niro-homogeniser (NiMFC) showed larger fibril-size (presence of large fibre fragments) even after 3 passes through the homogeniser as compared to the other MFCs. In order to achieve a high degree of fibrillation, multiple passes through Niro-homogeniser was required.

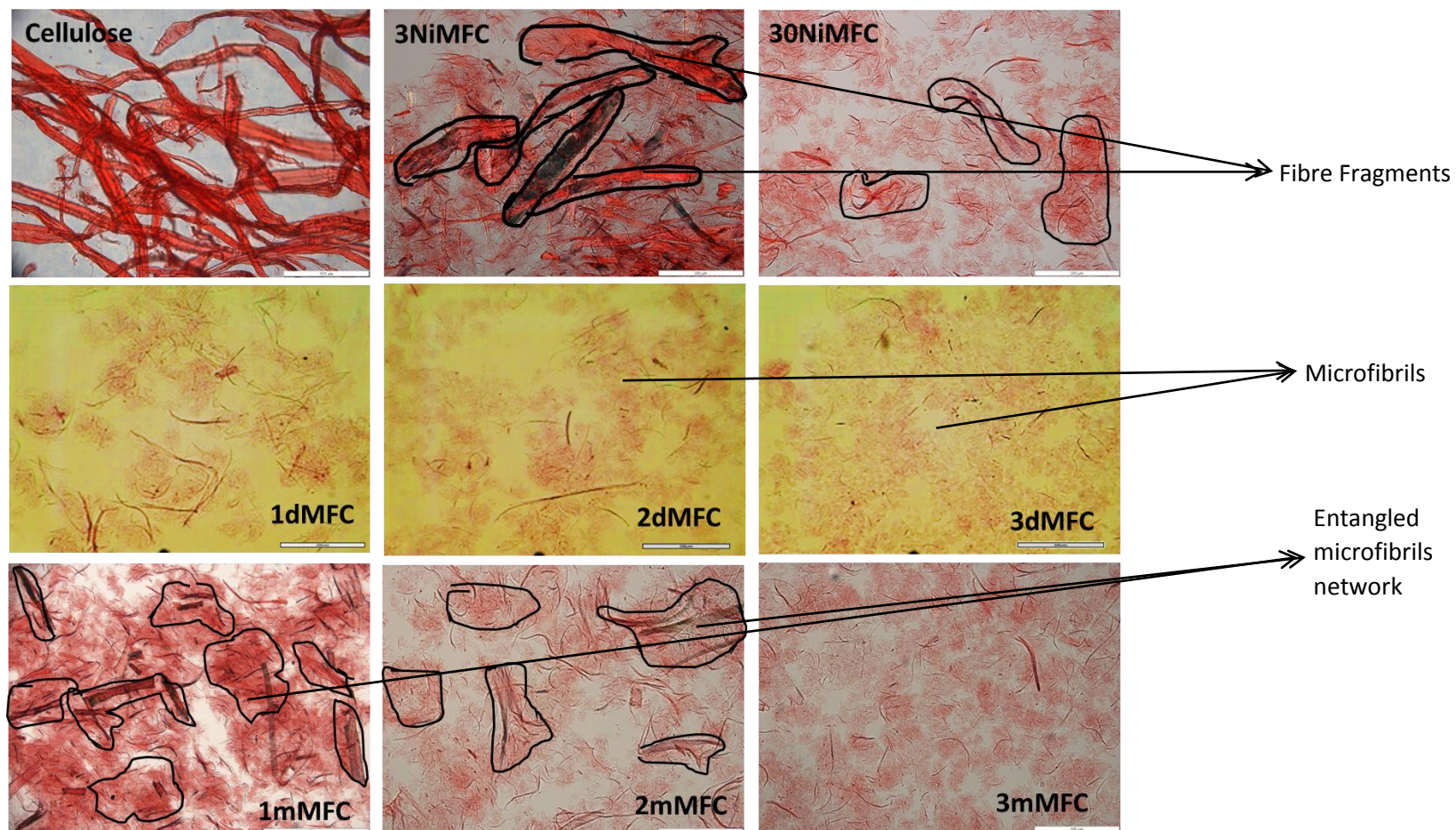


Figure 3.1: Light microscopy images of different varieties of MFCs produced from softwood spruce cellulose pulp (Cellulose) at 2% w/w concentrations, all scale bars are 200 μm .

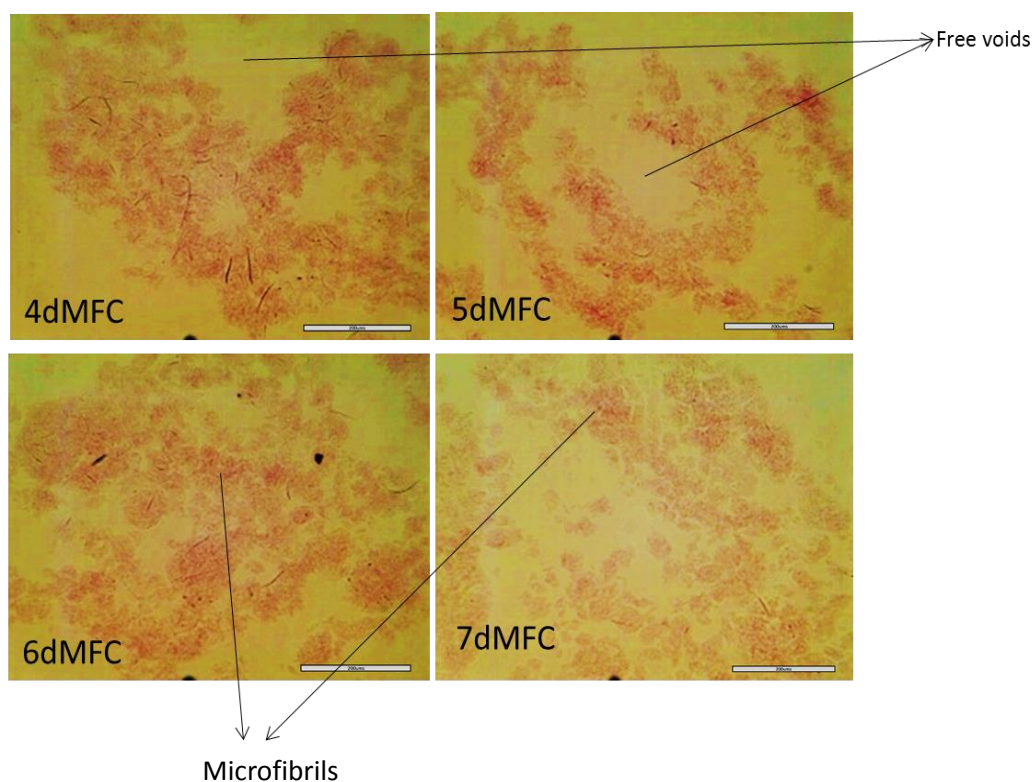


Figure 3.2: Light microscopy images of dMFC after 4, 5, 6 and 7 Passes at 2% w/w concentration, scale bar: 200 μm .

This supports the fact that the type of technique used to produce MFC has a noticeable impact on the degree of fibrillation or the fibril size in the suspension. In order to achieve that, a higher number of passes is recommended especially through a microfluidics homogeniser and a Niro-homogeniser. With further increase in the number of passes through high-pressure homogenisers, a noticeable reduction in fibril size and increase in the degree of fibrillation was observed for dMFC (Figure 3.1 and 3.2). In some cases, free space/voids (highlighted in Figure 3.2) were observed in the

suspension micrographs especially after 3 passes. Interestingly, these free voids have very small size individual fibrils which are difficult to view at low magnification; the presence of these fibrils was observed in micrographs recorded at higher magnification, but due to quality issues the images are not presented.

Light microscopy results are supported by the phase behaviour/sedimentation of the suspension as shown in Figure 3.3a. The aqueous suspensions of 1 to 7 pass dMFC at 2% w/w concentration showed no phase separation/sedimentation. However, at lower concentrations, these suspensions showed phase separation depending on the degree of fibrillation as shown in Figure 3.3b. For instance, the larger MFC fibrils sediment to the bottom of the tube as compared to samples produced with a higher number of passes through the homogeniser resulting in an upper layer with a visible cloudy phase. Hence, the presence of small fibrils/fibre fragments was evident from the transparency degree of the upper layer. Figure 3.4 shows the degree of transparency of upper layer (supernatant) of phase separated aqueous suspension of MFC. The UV-light scattering intensity is proportional to the sixth power of the particle size (diameter).

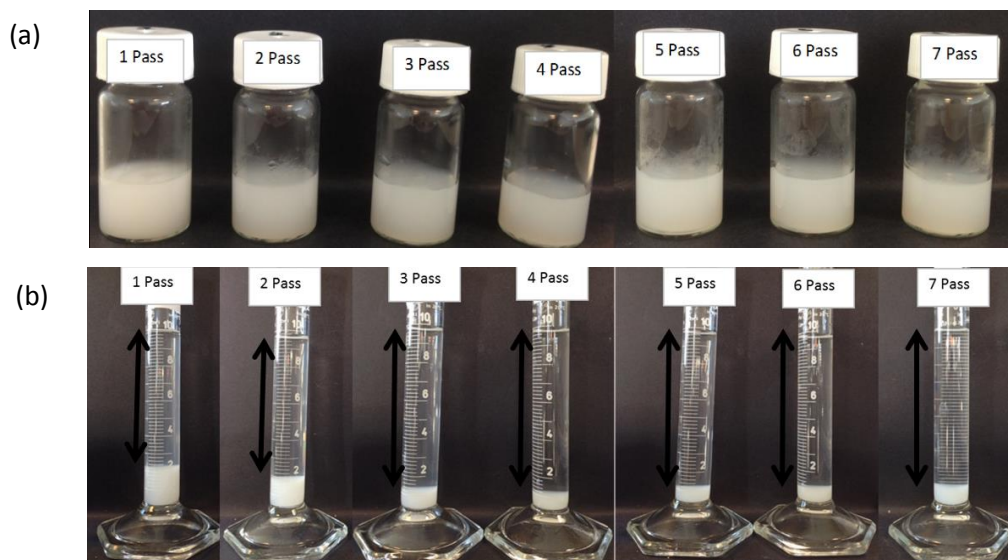


Figure 3.3: Visual inspection of phase behaviour after 24 hrs of 7-Pass dMFC samples at; (a) 2.0% w/w and (b) 0.1% w/w concentration. The black arrows indicate the upper layer (supernatant) of phase separated aqueous suspension of MFC.

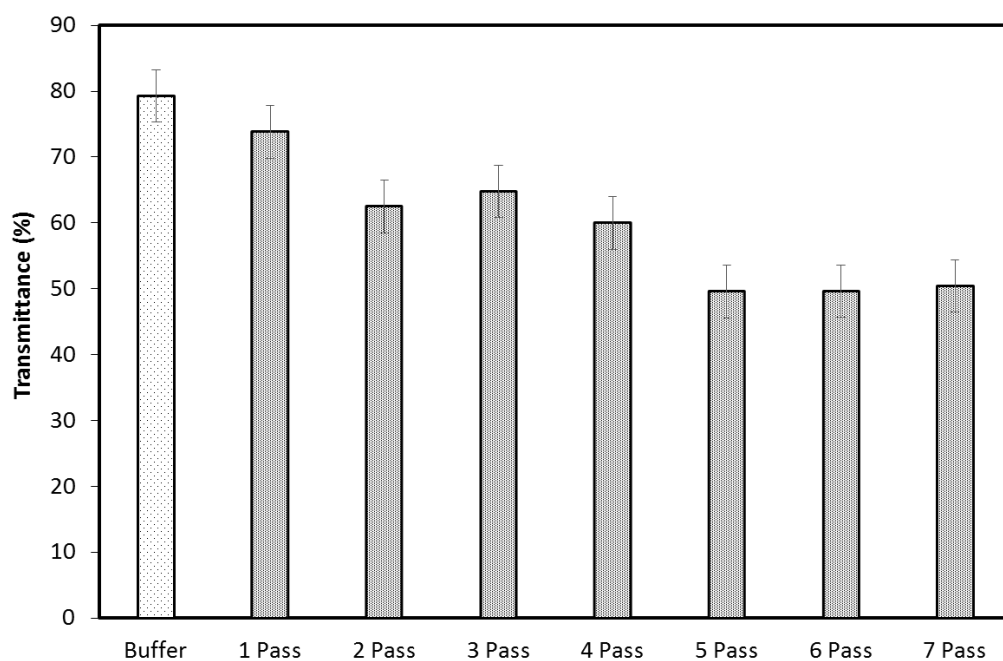


Figure 3.4: Visible transmittance of the upper layer of dMFC suspension after 1 to 7 Passes, where the buffer is water and path length of the cuvette was 1 cm. All results are average data of 4 replicates with standard deviation $\pm 1\%$.

When the light passes through the medium containing randomly dispersed particles, light is scattered by the particles causing a reduction in the degree of transparency (Alila *et al.*, 2013). Hence, the decrease in the transparency degree of the upper layer (supernatant) indicates the presence of micro-size fibrils (in terms of both diameter and length) (Figure 3.4).

It is known that with a high-pressure homogeniser, as the number of passes increases the crystallinity decreases. Hence, the crystal structure of the oven dried (OD) starting material cellulose (Cell) and 1 pass dMFC were compared and analysed by using wide-angle X-ray diffraction (WAXD). A noticeable reduction in signal intensity with increasing angle was observed in Figure 3.5a, indicating the impact of homogenisation on the molecular organisation of the starting cellulose material. A decrease in peak intensity corresponding to $2\theta=22.5^\circ$, 15.05° and 16.6° , indicates the reduction in the amount of crystalline region and an increase in the underlying amorphous response. A reduction in the degree of crystallinity by almost 50% was found after the first pass through the homogeniser, where 60% crystallinity of non-homogenised starting material was reduced to 37% after 1 pass independent on the type of homogeniser (evident in Figure 3.5b, while comparing mMFC and dMFC).

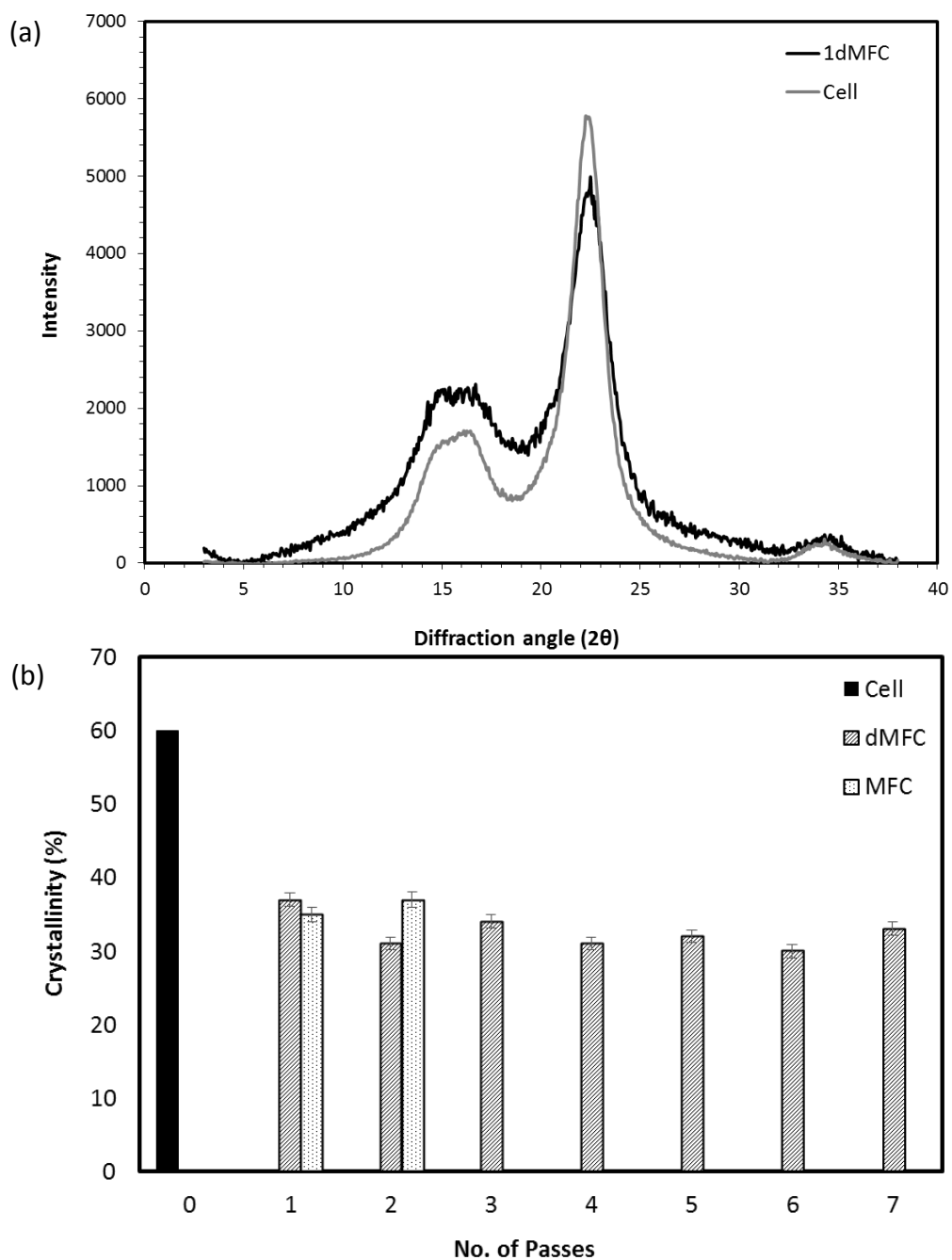


Figure 3.5: WAXD analysis (a) X-ray diffractogram patterns for Cell (starting material, solid line) and 1 Pass (---) dMFC, and (b) change in crystallinity with increase in number of passes through high pressure homogeniser (dMFC - parallel pattern), microfluidics (MFC - dotted pattern) and starting cellulose (solid bar). All results are average data of duplicates.

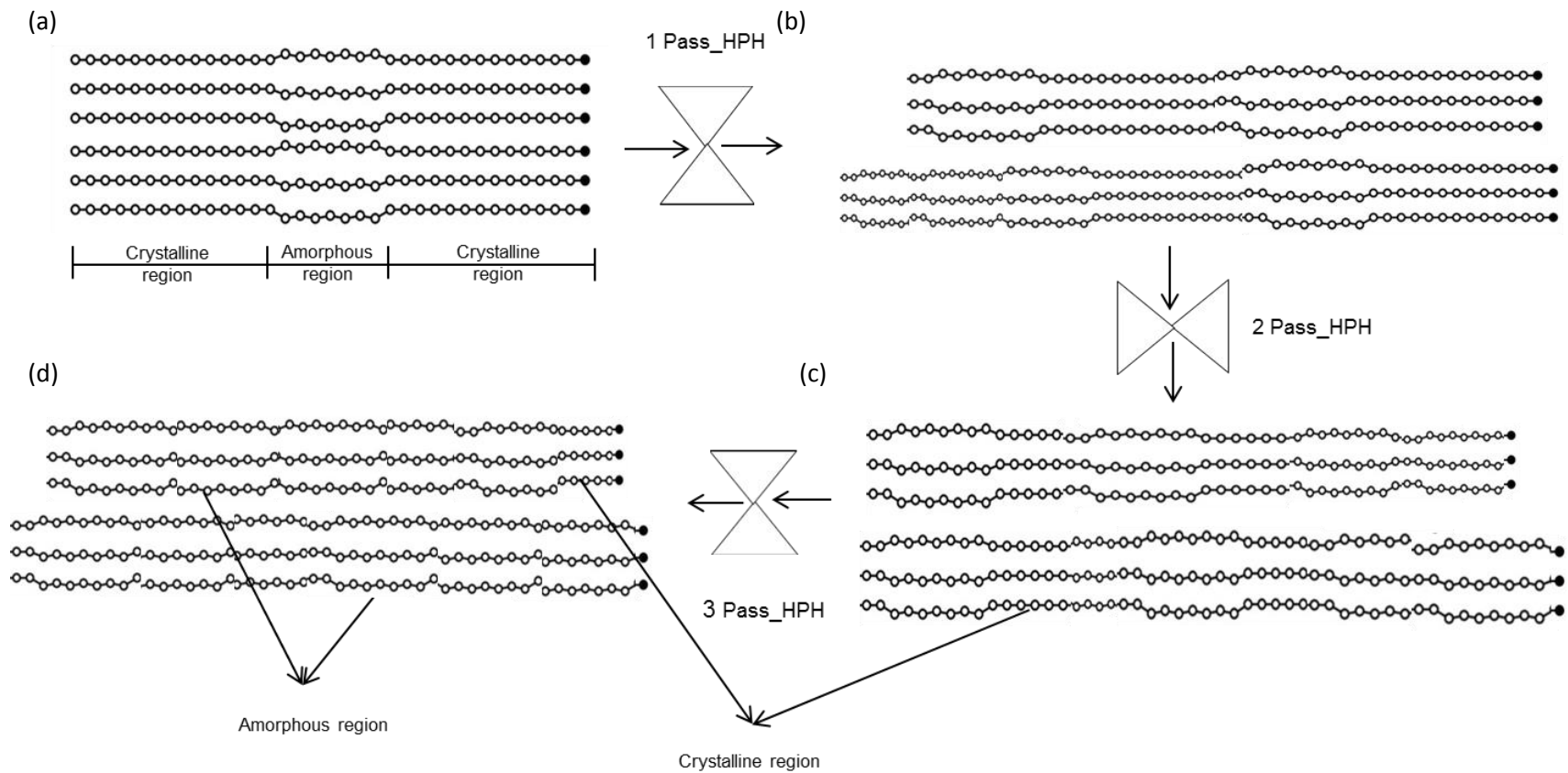


Figure 3.6: Schematic models representing the effect of the number of passes (1, 2 and 3 Pass) through the high-pressure homogeniser (HPH) on the crystalline and amorphous regions of cellulose during MFC production. (a) Cellulose structure before homogenisation; change in structure after (b) 1 Pass, (c) 2 Pass and (d) 3 Pass through high-pressure homogeniser.

However, when MFC was subjected to further passes through the homogeniser no further significant effect on crystallinity was observed, unlike the change in fibril size as indicated in microscopy images (comparing Figure 3.1, 3.2 and 3.5b). This indicates that a major change in crystallite structure occurs during the first homogenisation pass, and at this point, the fibrillation is achieved and further passes only serve to decrease the particle size. Hence, the consecutive passes through high-pressure homogeniser the further unpacking of microfibrils occur, targeting the amorphous region of the structure as shown in the mechanistic model in Figure 3.6.

3.3.2 Rheological properties of MFC suspensions

3.3.2.1 Rheological properties of Never-dried MFC suspension

Aqueous suspensions of MFC at various concentrations were subjected to small deformation dynamic viscoelastic measurements at 20°C and the results are shown in Figure 3.7a. Viscoelastic gel-like behaviour is observed where the storage modulus (G') is greater than the loss modulus (G''), showing similar dependency on frequency, *i.e.* both moduli increased slightly with increasing frequency. This indicates that the network structure formed by microfibrils, which are in an active mode of forming entanglements to form a stable network of fibrils, produces a suspension with gel-like properties.

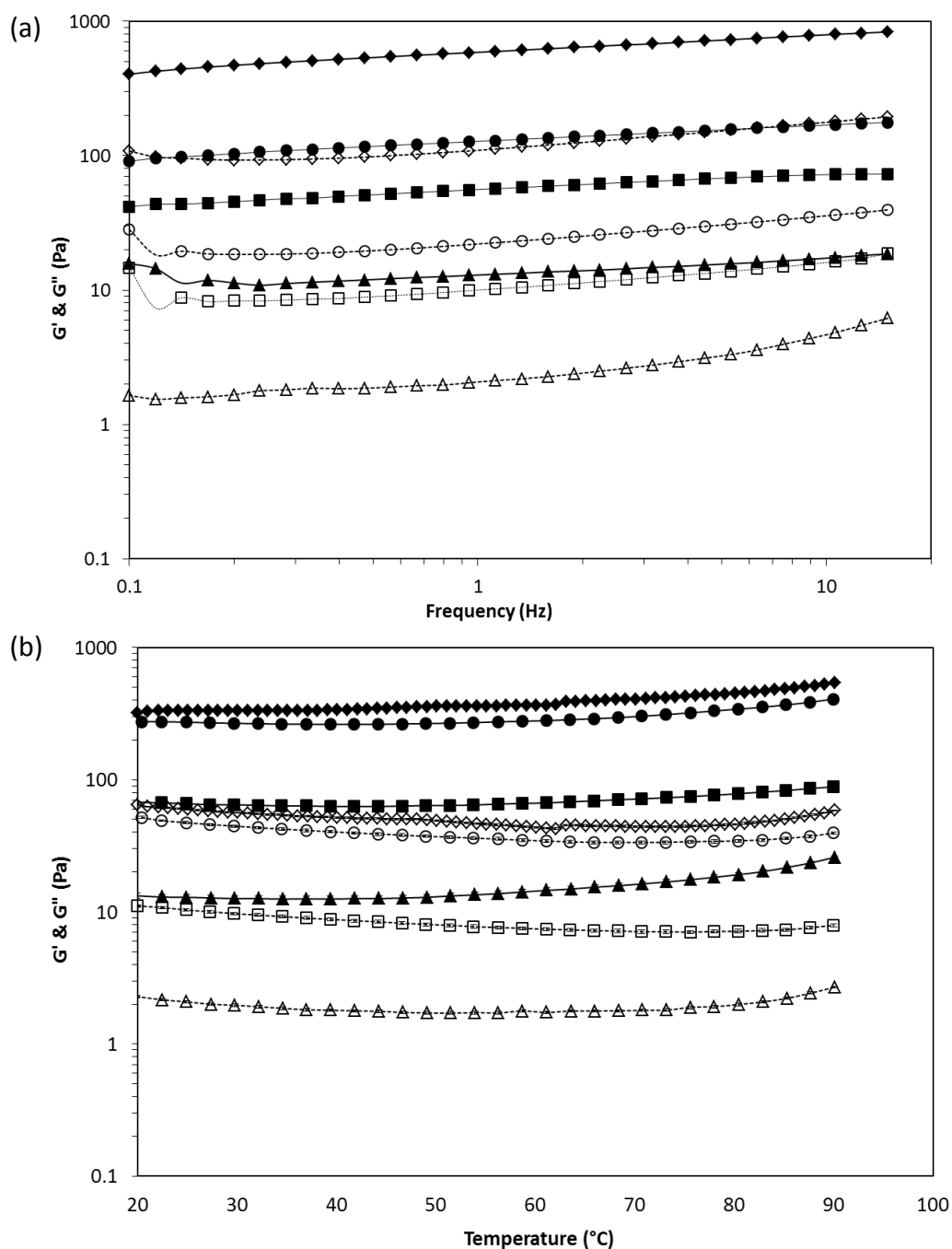


Figure 3.7: Mechanical spectra of aqueous suspensions of never-dried 2dMFC diluted to different concentrations i.e. (Δ) 0.8%, (\square) 1.0%, (\circ) 1.5% and (\diamond) 2.0% w/w, where G' - solid and G'' - unfilled symbols; (a) as a function of frequency at 20°C and strain 0.2%, (b) as a function of temperature at 1 Hz frequency and strain 1% with heating rate of 1°C/min. All results are average data with standard deviation $\pm 1\%$.

Lower concentrations *i.e.* 0.8% w/w, showed a higher dependency on the frequency, similar to the behaviour observed with cellulose nanofibers produced from poplar (Chen *et al.*, 2013). Chen (2013) suggested that high frequency increases the mobility of microfibrils in aqueous suspension, increased the mobility of the microfibrils results in increases in the entanglement and formation of the densely ordered network structure which reflects on viscoelastic behaviour of the suspension.

To characterise the structural changes with increasing temperature, small deformation dynamic viscoelastic measurements were performed from 20°C to 90°C at 1% strain and a frequency of 1 Hz at a heating rate 1°C/min (Figure 3.7b). Aqueous suspensions of MFC at concentrations between 0.8% to 2.0% w/w showed stable viscoelastic gel-like behaviour with increasing temperature. Slight increase in storage modulus (G') was observed with increasing temperature. There are possible two explanations for the increase in storage modulus of the suspension, when the temperature is increased: (1) the microfibrils of cellulose were dominated by temperature-induced thermal motion which initiates the network formation of the amorphous fibrils, and (2) swelling of microfibrils commonly known with cellulosic materials during the heating of the suspension. Similar results were also reported in the case

of MFC produced from poplar (Chen *et al.*, 2013), but contrasting with the work reported in the case of softwood Kraft pulp and sugar-beet pulp, where suspensions showed no temperature dependency (Pääkkö *et al.*, 2007, Tandjawa *et al.*, 2010). This indicates that the source of the cellulose plays a very important role in terms of temperature dependency.

3.3.2.2 Impact of number of passes on rheological properties

A comparison of equilibrium flow curves of 1%w/w suspensions of dMFC produced by a number of passes through the homogeniser are shown in Figure 3.8a. All suspensions exhibit shear-thinning behaviour, *i.e.* the viscosity of the suspension decreases with increasing shear rate. Under shear, fibre fragments and microfibril networks orient along flow lines causing a decrease of viscosity. When these suspensions are subjected to decreasing shear rate, the suspensions showed full recovery of the viscosity (Figure 3.8b), indicating the formation of new network or re-organisation of microfibrils in the suspension. Similar behaviour was reported MFC from bleached sulphate cellulose and pine tree cellulose (Dinand *et al.*, 1996; Iotti *et al.*, 2011). However, these changes in the network structure are reversible to the original state dependent on shear rate and time (Cordoba *et al.*, 2010). Such behaviour is very common with particulate dispersions, in this case the dMFC

suspensions, due to dense microfibrils network with a high specific area covered by hydroxyl groups that can take active part in the formation of temporary hydrogen bonds between the network particles (these interactions are similar to those holding together crystalline and amorphous cellulose). At a concentration of 1%w/w or above the microfibrils of MFC are close enough to structure themselves causing an increase in viscosity. No statistical significant difference (p -value=0.32; $\alpha = 0.05$) was observed in terms of shear viscosity between 1 pass to 7 pass MFC suspension (Figure 3.8a).

The impact of the number of passes through the Borregaard fibrillation homogeniser (dMFC) on viscoelastic behaviour and complex viscosity of the 1% w/w suspension are presented in Figure 3.9a and 3.9b. All suspensions showed stable viscoelastic gel-like behaviour *i.e.* G' was higher than G'' with little dependency on frequency. Unlike shear viscosity, the complex viscosity showed a slight increase as the number of passes through the homogeniser increases. However, after 4 passes there is a decrease which then remains stable up to 7 passes (Figure 3.9b). After the first pass through the homogeniser, a reduction in crystallinity and increase in the degree of fibrillation was observed promoting the formation of intermolecular networks

(Figure 3.1 and 3.5b) explaining the increase in complex viscosity from 1 pass to 3 passes.

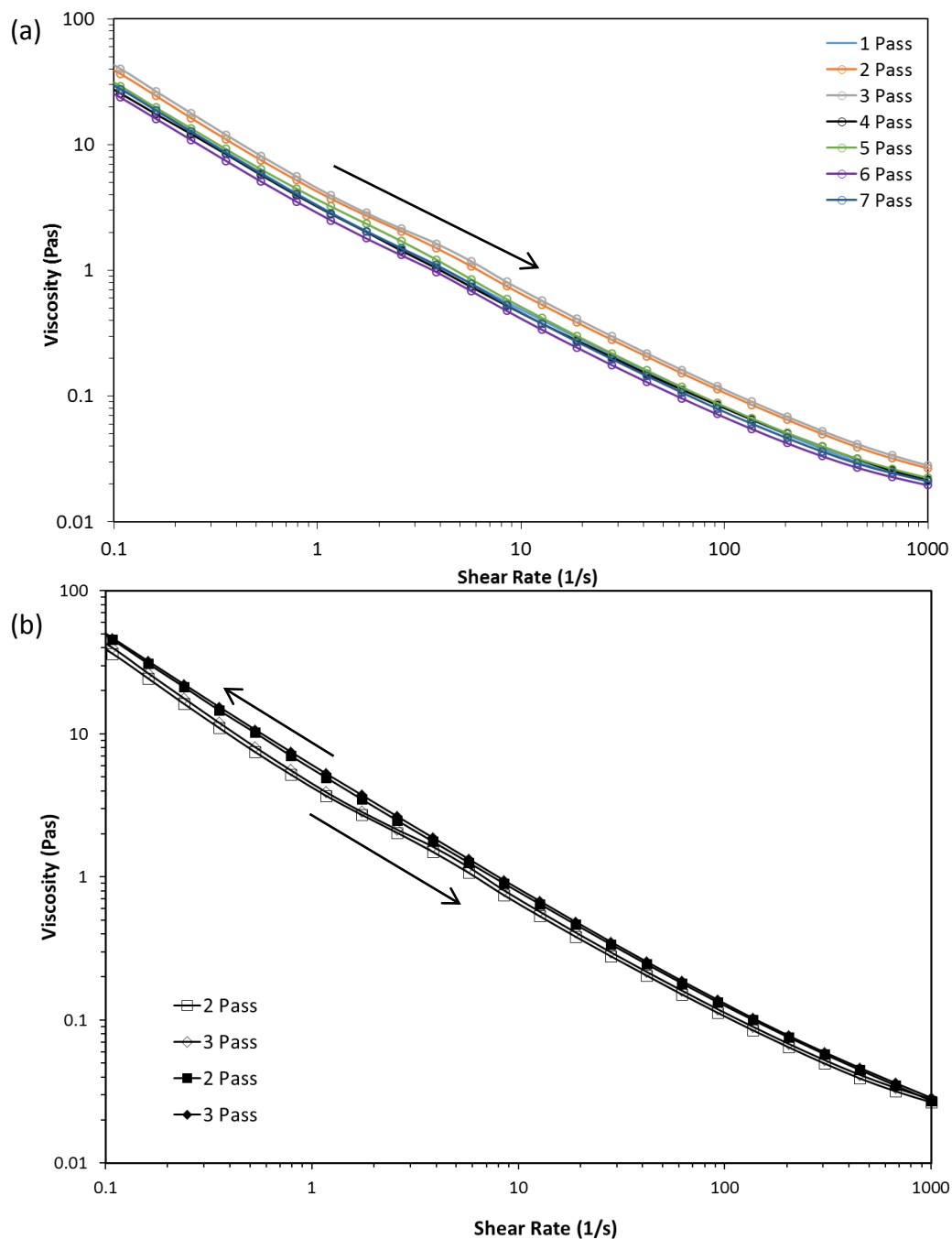


Figure 3.8: (A) Shear viscosity as a function of shear rate (1/s) (slope: -1.04), (B) Shear viscosity as a function of increasing (unfilled-symbols) and decreasing (filled-symbols) shear rate (s^{-1}); of 1% w/w suspension of dMFC after a number of passes through the homogeniser at 20°C. All results are highly reproducible with a standard deviation of less than 1%.

As explained earlier, highly networked and entangled microfibrils are the driving force behind the rheological properties of suspensions. After a number of passes (> 4Pass) through the homogeniser smaller microfibrils are produced. This results in more homogeneous or uniform structure and explains the slightly reduced (not statistical significant p -value>0.05) yet stable shear (p -value: 0.134) and complex viscosity (p -value: 0.372) as evident in Figure 3.8a and 3.9b. These results also indicate that a high degree of fibrillation is necessary to produce a homogenous/uniform network structure with resulting stable viscosity but low and minimum 4 passes through the high-pressure homogeniser were required where no further significant change in microstructure (at low-resolution microscopy) and resultant viscosity was observed.

In order to understand the particulate interactions further, the mobility of water was measured, which can be examined by T_2 (ms) relaxation times of the suspensions (shown in Figure 3.10). Spin-spin (T_2) relaxation times are sensitive to the mobility of the water molecules in the solutions, gels or the suspensions. As outlined in chapter 1, it is believed that the strong interaction between the microfibrils dispersed within the aqueous medium is the driving force for their rheological characteristics. Investigating the water binding and

mobility (interacting-water and free-water) may provide further information to explain the suspension properties.

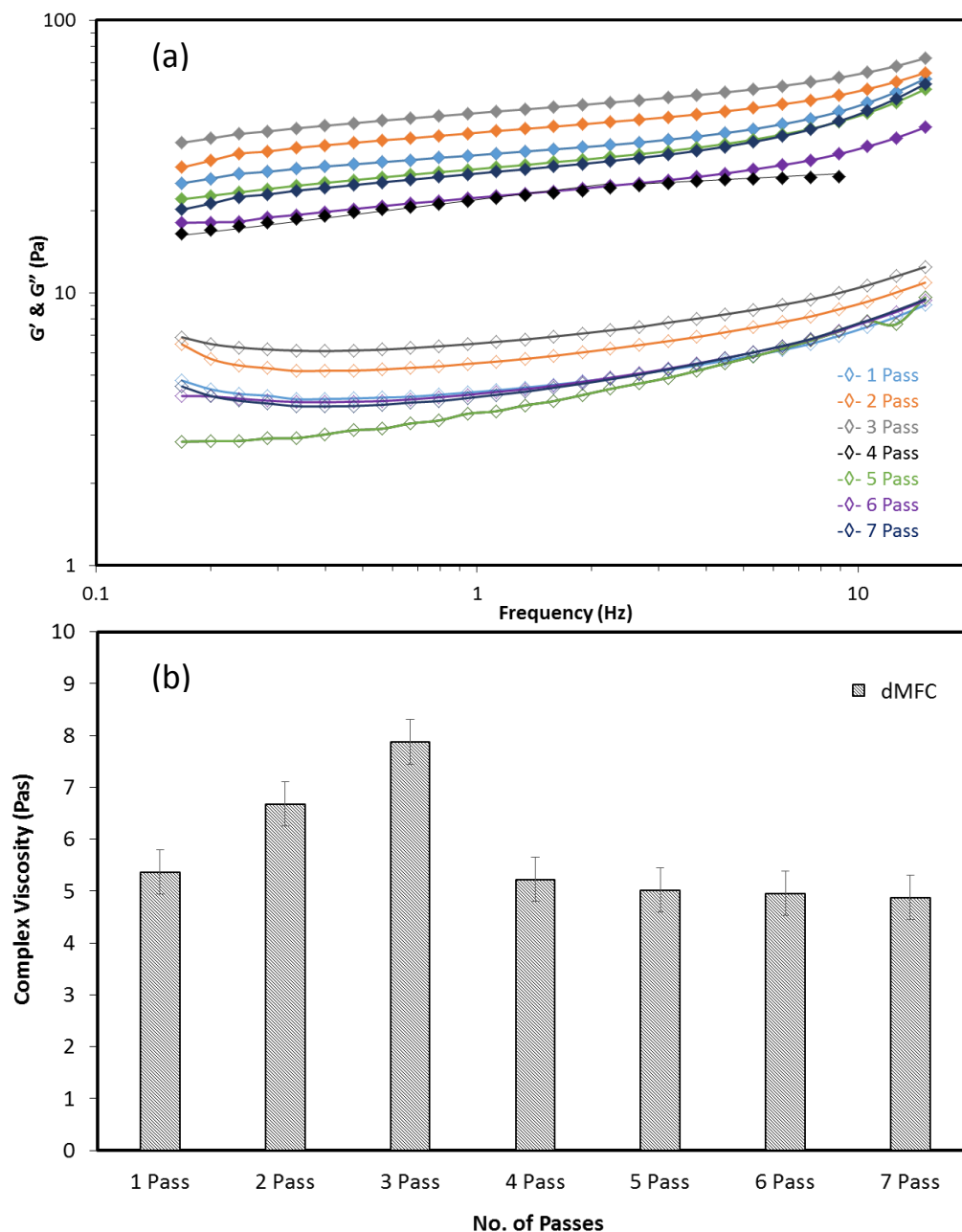


Figure 3.9: Impact of the number of passes (dMFC) through high-pressure homogeniser on 1% w/w suspension properties of MFC at 20°C, where; (a) viscoelastic behaviour (G' & G'') as a function of frequency at strain 0.2%; with standard deviation $\pm 1\%$. (b) Complex viscosity is taken at 0.2% strain and 1 Hz frequency. The complex viscosity values are averaged from 2 replicates with standard deviation $\pm 1\%$.

It was observed that during the first 3 passes through the homogeniser the T_2 value of the suspension decreased followed by an increase in T_2 values from 4 to 7 passes. This behaviour can be explained by the entangled microfibrils network of MFC and the homogeneity of the suspension.

In non-homogenous systems such as fluids gels, suspensions or dispersions, the water mobility can be defined as “interacting/associated water” and “free/bulk water”. The interacting/associated water is present in the polymer-rich regions whereas the free/bulk water molecules are found in polymer-poor regions or interstitial space between particles (Norton *et al.* 1998). It is evident in microscopy images (Figure 3.1), that the aqueous suspension of 1dMFC is a very non-homogenous system with both MFC-rich and MFC-poor regions. As the MFC-free region or the larger interstitial space between the fibre fragments/fibrils is higher in the case of 1dMFC, this could be a possible reason for longer T_2 value of the suspension. However, the aqueous suspensions of 2dMFC, 3dMFC and 4dMFC showed shorter T_2 values (*i.e.*, 776.68 ms, 761.74 ms and 765.75 ms respectively) which can be explained by the formation of a homogenous system where the fibril size is smaller (evident in Figure 3.1).

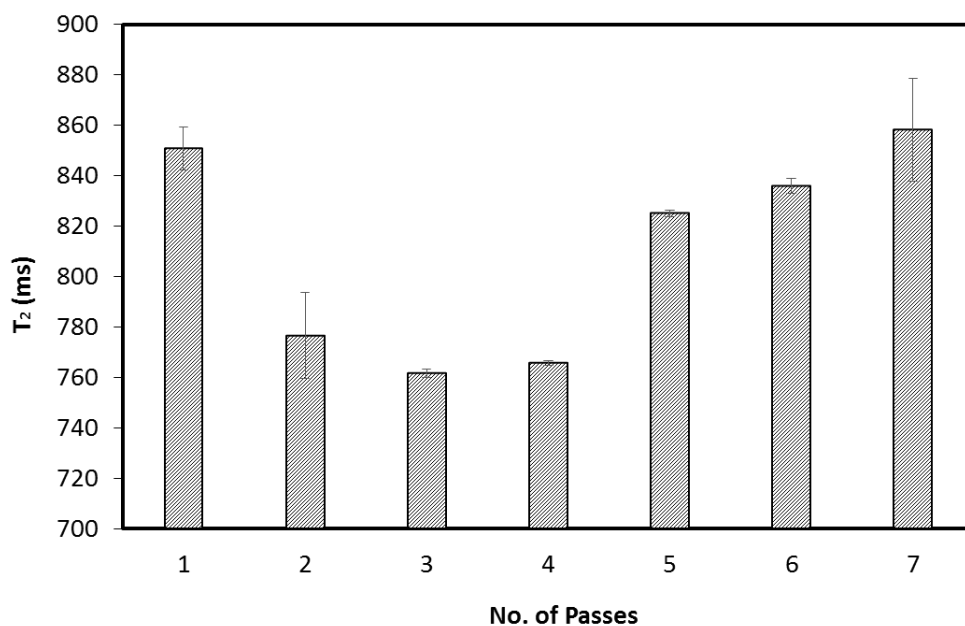


Figure 3.10: Impact of degree of fibrillation on the T_2 (ms) of water for 2% w/w dMFC suspension systems measured at $20 \pm 1^\circ\text{C}$, fitted with the single exponential curve. The T_2 values are averaged from 4 replications and are not statistically significant with $p\text{-value} = 0.3$ ($\alpha: 0.05$).

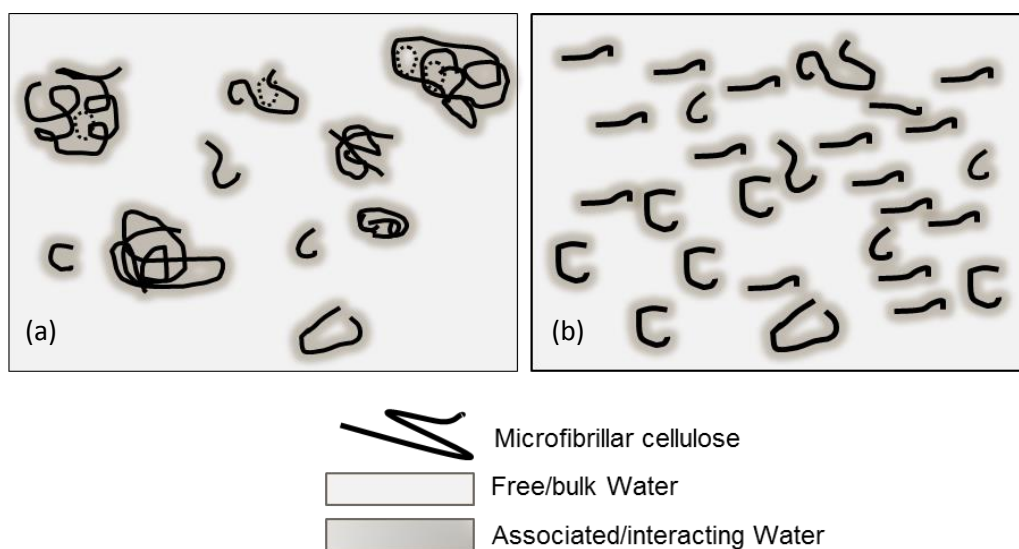


Figure 3.11: Model illustration of particle dispersion state and distribution of associated/interacting water in MFC suspensions, (a) associated water and free water distribution in microfibril aggregate in MFC suspension with low degree of fibrillation; whereas (b) associated/interacting water is distributed in the vicinity of the microfibril surface due to high degree of fibrillation.

Due to a high degree of fibrillation (evidenced by a decrease in crystallinity and change fibre size of dMFC in Figure 3.1 and 3.5b), the aqueous suspension shows stable phase behaviour and microfibril network structure (a higher viscosity, Figure 3.9). Therefore a higher amount of associated water in MFC-rich regions results in restricted water mobility in the system. Similar effects were observed with MCC, cellulose hydrogels (TCG) and silica gels by Ono *et al.*, 1998, Ono *et al.*, 2004, Martini, 1981.

A noticeable increase in T_2 values was observed as the number of passes increased. This increase in T_2 values can be explained by the fibril size of MFC decreasing, and the amount of individual microfibril particulate increasing in the system as evidenced by the decrease in the degree of transparency (Figure 3.4). Due to the small size of the microfibrils, the associated water with MFC is lower indicating the system is converting to a uniform polymeric suspension/dispersion resulting in longer T_2 values as demonstrated in the mechanistic model in Figure 3.11. From these results, it can be concluded that the increasing number of passes through the homogeniser increases the degree of fibrillation. This can result in a variety of different suspension properties, dependent on the proportion of microfibrils production.

3.3.2.3 Impact of drying on rheological properties of rehydrated MFC suspension

Homogenisation of cellulosic fibres is known to unpack the fibres to microfibrils, whereas drying of these suspensions is known to collapse the microfibrils and to form aggregates which are difficult to redisperse, as explained in detail in Chapter 1 and Section 3.1. Figure 3.12 shows the effect of different drying procedures on the shear viscosity of the suspension at 1% w/w concentration of BMFC (diluted from 8.97% concentrated stock).

A significant reduction ($p\text{-value} < 0.05$) in shear viscosity was observed after redispersing the dry BMFC material in water independent of the type of drying process used (Figure 3.12). This reduction can be explained by the aggregation/agglomeration of microfibrils due to irreversible stiffening of the polymer structure upon drying, evident in highlighted regions in micrographs (Figure 3.13). These results also indicate that there is little difference between the types of drying process used, and the resultant shear viscosity are in the similar range between 4 to 4.5 Pas (Figure 3.12). However, it is also observed that the prolonged drying time and high temperatures results in larger aggregates, shown in micrographs (Figure 3.13). For instance, oven drying at 105°C results in larger aggregates as compared to oven drying at 50°C,

especially when dried for a prolonged period of time. It is evident from the microscopy images (Figure 3.13) that little difference in the aggregation of microfibrils was observed when comparing the vacuum oven drying (VOD at 60°C), room temperature drying (RT at 20°C) and normal oven drying (OD at 50°C).

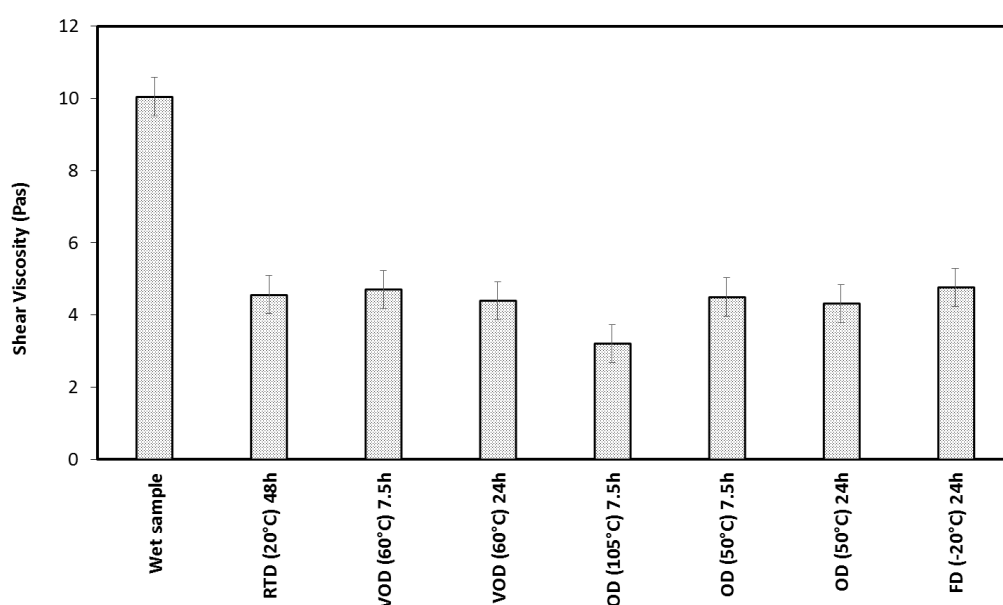


Figure 3.12: Effect of different drying process on the shear viscosity of the redispersed 1% w/w suspension of BMFC at 20°C, recorded at 1 s⁻¹ shear rate. The shear viscosity values are averaged of duplicates with standard deviation ±1%.

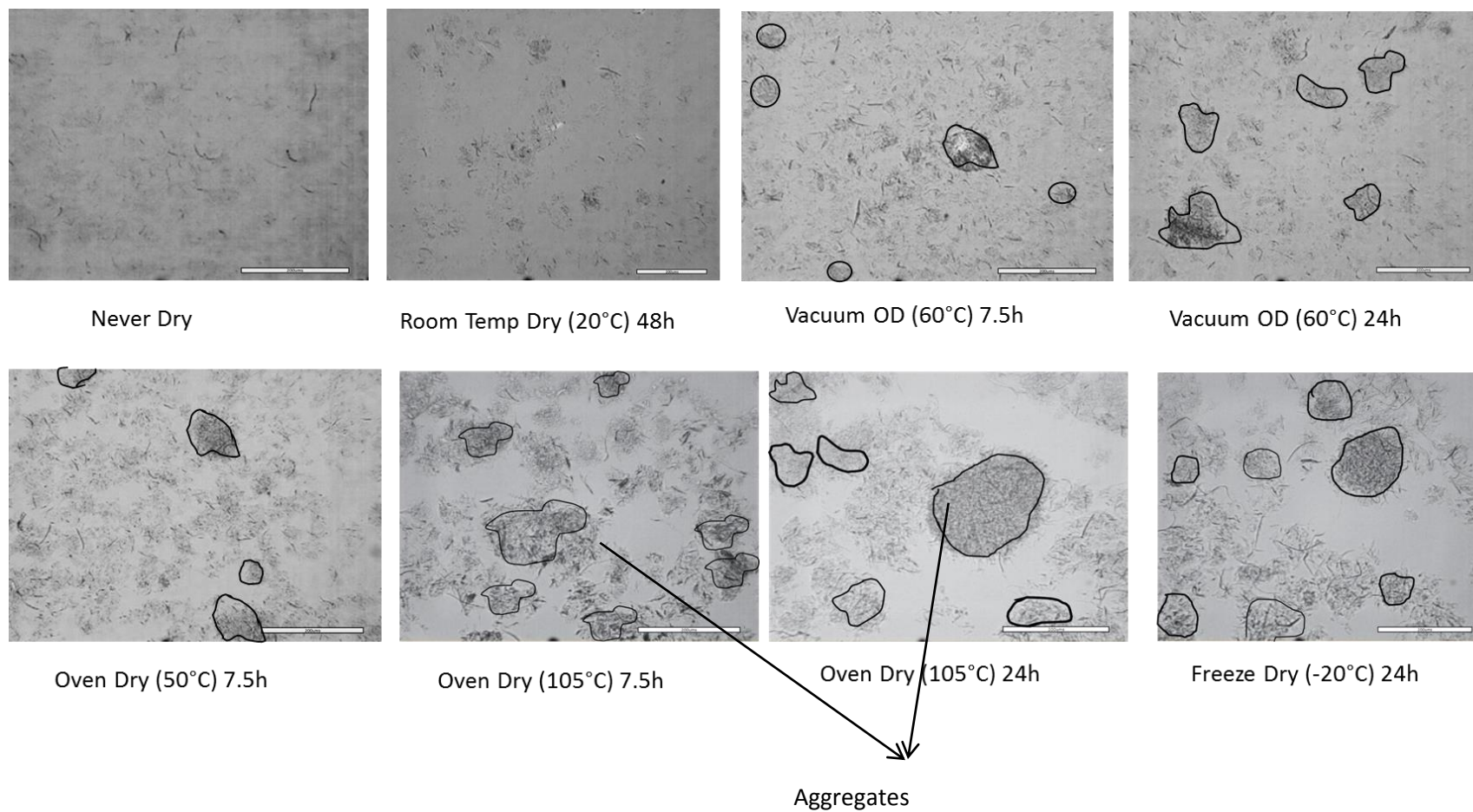


Figure 3.13: Light microscopy images of 1% w/w suspension of redispersed BMFC in water, where highlighted area shows the BMFC aggregates/agglomerates, and scale bar: 200 μ m.

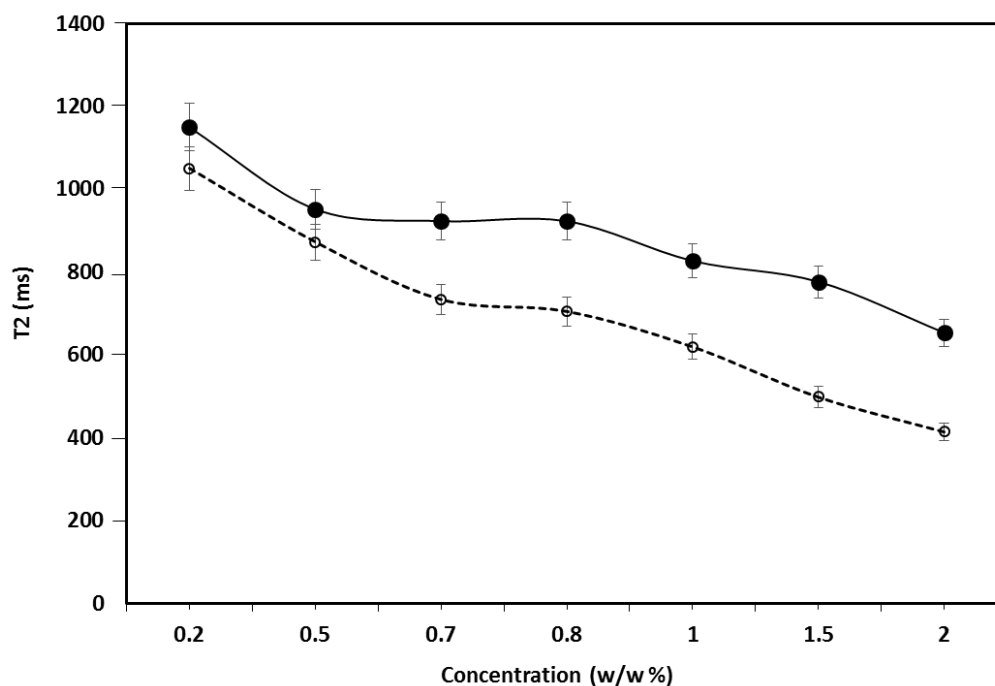


Figure 3.14: Spin-Spin relaxation time (T_2) (ms) of (●) BMFC diluted from 8.97% in the never-dried state (as received) and (○) redispersed oven dried BMFC as a function of concentrations at 20°C.

To examine the effect of drying on the mobility or accessibility of water in the microfibril network, the T_2 (ms) values, as a function of concentration were plotted to compare aqueous suspensions of redispersed oven-dried BMFC with never-dried BMFC (Figure 3.14). It was observed that as the concentration of MFC increased, the T_2 (ms) values of the suspensions decreased. This can be explained by the amount of “associated-water” and “free-water” in the system. As the concentration increases the suspension has higher polymer-rich regions, which due to high surface area of MFC can result in reduced water mobility (lower T_2 values) (Norton *et al.*, 1998).

The never dried suspensions show higher T_2 values than dried and redispersed MFC at all comparative concentrations. This is further evidence for the complex nature of the suspensions and the inherent role of the network of cellulose microfibrils in determining the suspension properties. Here the dried materials appear to be more heterogeneous, similar to the samples undergoing a low number of homogenisation passes, which leads to low T_2 values (comparing Figure 3.1 and Figure 3.13). However, in this case, the collapse in structure due to aggregation of microfibrils/fibre fragments upon drying and the subsequent poor re-dispersal of the aggregates promotes a suspension with lower shear viscosities (Figure 3.12). This then indicates that in the homogenisation work, the lower T_2 values are from a combination of both dense regions of cellulose microfibrils, with associated microfibrils and aggregated microfibrils limiting the water mobility in the network.

3.4 Conclusions

High-pressure homogenisation rapidly changes the structure of cellulose such as the degree of fibrillation, crystallinity and rheological properties of the suspensions. The new high-pressure fibrillation technology (Borregaard

fibrillation technology) produces a microstructure requiring the least number of passes and further processing; confirming the hypothesis stated earlier “the technology used to produce MFC results in a broad range of MFC microstructures”. The two main factors that affect the microstructure and suspension properties of the MFC are: the number of passes through the homogeniser and drying. As the number of passes through high-pressure homogeniser increases, the degree of fibrillation increases (independent on the type of homogeniser) and results in more uniform/homogenous MFC suspensions. These distinct microstructures of MFC’s have a noticeable impact on the water mobility within the microfibril network and its resultant properties. The maximum loss of crystallinity occurs after the first pass through the high-pressure homogeniser. Homogenisation is known to release and unpack the microfibrils from “mother-fibre”, whereas drying is known to collapse the microfibrils and result in aggregates, which are then very difficult to redisperse in water. The intermolecular hydrogen bonds formed between the microfibrils in aggregates dominate the mobility of water resulting shorter T_2 values and reduced shear viscosities.

It is therefore of interest to observe the impact of different additives on the redispersibility of MFC in aqueous suspension and their influence on different

physical properties with the question asked: can dry and redispersed samples be processed in such a way that they have the same (identical or similar) properties of never dried suspensions? Hence, the results presented in chapter 4 focus on the impact of different polymeric additives when added after homogenisation and on the redispersibility and physical properties of MFC.

Chapter 4

Impact of Polymeric Additives on Stabilisation of MFC added “after” the Homogenisation

4.1 Introduction

In chapter 3, it was concluded that each processing stage of MFC has a noticeable impact on the overall functionality of MFC suspensions. As discussed earlier, a significant reduction in water mobility and rheological properties of redispersed MFC suspension was observed due to aggregation of fibrils and microfibrils. This chapter focuses on protecting the aggregation of microfibrils during the drying stage by using different polymeric additives added after the homogenisation step. Various polymeric or non-polymeric additives have been used in the past to maintain and stabilise fibrillated textures following drying and rehydrating (as mentioned in chapter 1). For instance, MFC produced from sugar beet pulp showed a weak interaction with negatively charged low methoxyl pectin (Tandjawa *et al.*, 2012a) and sodium carboxymethyl cellulose (Lowys *et al.*, 2001). Similar interactions were observed with MFC produced from bacterial cellulose and Na-CMC (Veen *et al.*, 2014).

The purpose of the present study was to re-examine the effects of carboxymethyl cellulose (low and high molecular weight) on aggregation of MFC during drying considering the difference in microstructure and related physical properties highlighted in Chapter 3 and to examine the interaction

between the components. This study also explored the possibility of using locust bean gum as a polymeric additive to stabilise the fibrils and microfibrils against aggregation, based on the previously reported intermolecular interaction between cellulose and galactomannan (LBG) (Newman *et al.*, 1998). Finally, the question can be asked: what happens when dual additives, *i.e.* one which provides intermolecular interaction, the second providing charge and subsequent electrostatic repulsion are added together in the systems? Hence, the blend of low molecular weight CMC and LBG were formulated and used as an additive to investigate the possibility of stabilising the fibrillar texture by these combined mechanisms.

Rheological measurements have been widely used to investigate the suspension properties of microfibrillar cellulose in water, as a function of concentration and temperature as evident in chapter 3. This chapter shows the results of rheological analysis of MFC/additives as a function of frequency, temperature and increasing the concentration of additives. Rheological parameters such as shear viscosity and $\tan \delta$ were qualitatively correlated with spin-spin relaxation time (T_2) to understand the influence of additives on the mobility of water inside MFC/additives networks. MFC systems were studied by DSC and TGA analysis under controlled environments, which

allowed an understanding of the impact of polymeric additives on the structural stability and thermal transitions occurring upon drying of the system. Dynamic vapour sorption is also used to provide a further understanding of water uptake and release as a function of the changes in process and formulation in this study.

4.2 Materials and Methods

Materials used for this study are described in Chapter 2. During this chapter, MFC is produced by using the Borregaard fibrillation technology (2pass) named as BMFC with a dry content of 8.97% w/w.

4.2.1 Sample preparation

Samples were formulated according to Table 2.2 using the standard mixing protocol described in chapter 2, under section 2.3.5. All of the BMFC/additive mixtures were dried by using the conventional oven (Gallenkamp hotbox oven-size 2, UK) at 50°C for 12 hrs. Two batches of samples were prepared and analysis was performed in duplicate for the each batch. Data presented is an average of 4 replicates. To study the thermal behaviour of BMFC/additive combinations powders at approximately 20% moisture content were prepared by placing samples in a sealed desiccator with saturated KNO_3

(Sigma-Aldrich) salt solutions. All samples were stored at controlled relative humidity (RH) for 7 days at 20°C temperature before DSC and TGA analysis.

4.2.2 Microscopy

Light microscopy was used to study the microstructure of aqueous suspensions, images were recorded according to the method detailed in chapter 2, section 2.4.6.

4.2.3 Rheology

Rheological measurements were made according to the method detailed in chapter 2, section 2.4.1.3. Data presented is an average of 4 replicate analyses.

4.2.4 Relaxation NMR

Spin-spin relaxation time (T_2) was measured according to the method detailed in chapter 2, section 2.4.2. Data presented is an average of 4 replicate analyses.

4.2.5 Differential Scanning Calorimetry (DSC)

DSC thermograms were measured according to the method detailed in chapter 2, section 2.4.4.

4.2.6 Derivative Thermo-gravitational analysis (DTGA)

Thermal degradations were recorded according to the method detailed in chapter 2, section 2.4.5.

4.2.7 Dynamic Vapour Sorption (DVS)

DVS measures how quickly a solvent (often water) can be absorbed by a sample. The dynamic vapour sorption of BMFC/additives powder was studied by a Dynamic Vapour Sorption Analyser (DVS-I, Surface Measurements Systems Ltd., London, UK) equipped with a microbalance (Cahn D200, UK). This technique is ideal to measure the change in sample mass as low as 0.01 μg . Approximately 8 mg of the sample was loaded in the sample pan and introduced to the drying stage within the DVS setup by exposure to dry air (RH0%) for 6 hrs. The actual measurement was started at 0 a_w (water activity, RH0%), and terminated at 0.95 a_w (RH95%) with a step increase when thermodynamic equilibrium was reached (mass change <0.0005 mg/min). All samples were analysed in duplicate and data presented is an average of duplicates.

4.2.8 Data Analysis

Statistical data analysis was performed by using software Excel (Microsoft 2013, USA). Correlation analysis was performed to investigate the relationship between physical parameters (viscosity, complex viscosity, crystallinity, spin-

spin relaxation time *etc.*) and different drying techniques using analysis of variance (ANOVA) with a minimum significance level defined as $p\text{-value} < 0.05$.

4.3 Results and Discussion

4.3.1 Rheological properties of BMFC/additives suspensions

The rheology of the 2% w/w BMFC/additive aqueous suspensions was tested as a function of frequency (Hz) and temperature ($^{\circ}\text{C}$). Rotational measurements were also performed on all of the suspension at 20°C .

4.3.1.1 Viscoelastic behaviour BMFC/additive suspensions

The first part of this section correlated the viscoelastic properties of BMFC/additives suspensions with microscopy images followed by subsections presenting details on the impact of individual additives on BMFC suspension properties. Aqueous suspensions of different proportions of CMC/LBG blends along with BMFC at a total polymer concentration of 2% w/w were subjected to frequency ramping at 20°C . The results are presented in Figure 4.1.

All dried and redispersed BMFC/additives blend (*i.e.* BMFC/CMC, BMFC/LBG and BMFC/blend) suspensions showed viscoelastic gel-like behaviour where storage modulus (G') was higher than loss modulus (G'') with little

dependency on frequency. An explanation for such viscoelastic behaviour is the stable intermolecular network formed by the interaction between BMFC and the different additives. However, the type and level of additive used have a significant influence on the overall viscoelastic parameters (such as G' and G'' and complex viscosity).

It was evident in Figure 4.1 that all the suspensions with additives showed that both moduli (G' and G'') were higher as compared to MFC100 (BMFC dried without additive). This appears to be due to improved redispersibility (visual observation) and reduced aggregation of microfibrils in the suspension after drying, evident in micrographs presented in Figure 4.2. It was observed that the addition of CMC improves the redispersibility of the BMFC in water and forms a homogenous suspension by using the standard high shear mixing process. Whereas it was difficult to redisperse dried BMFC/LBG in water due to aggregation of microfibrils after the drying process, hence it was reflected by the reduced loss and storage moduli at all additive proportions for the BMFC/LBG suspension as compared to MFC100 and BMFC/CMC.

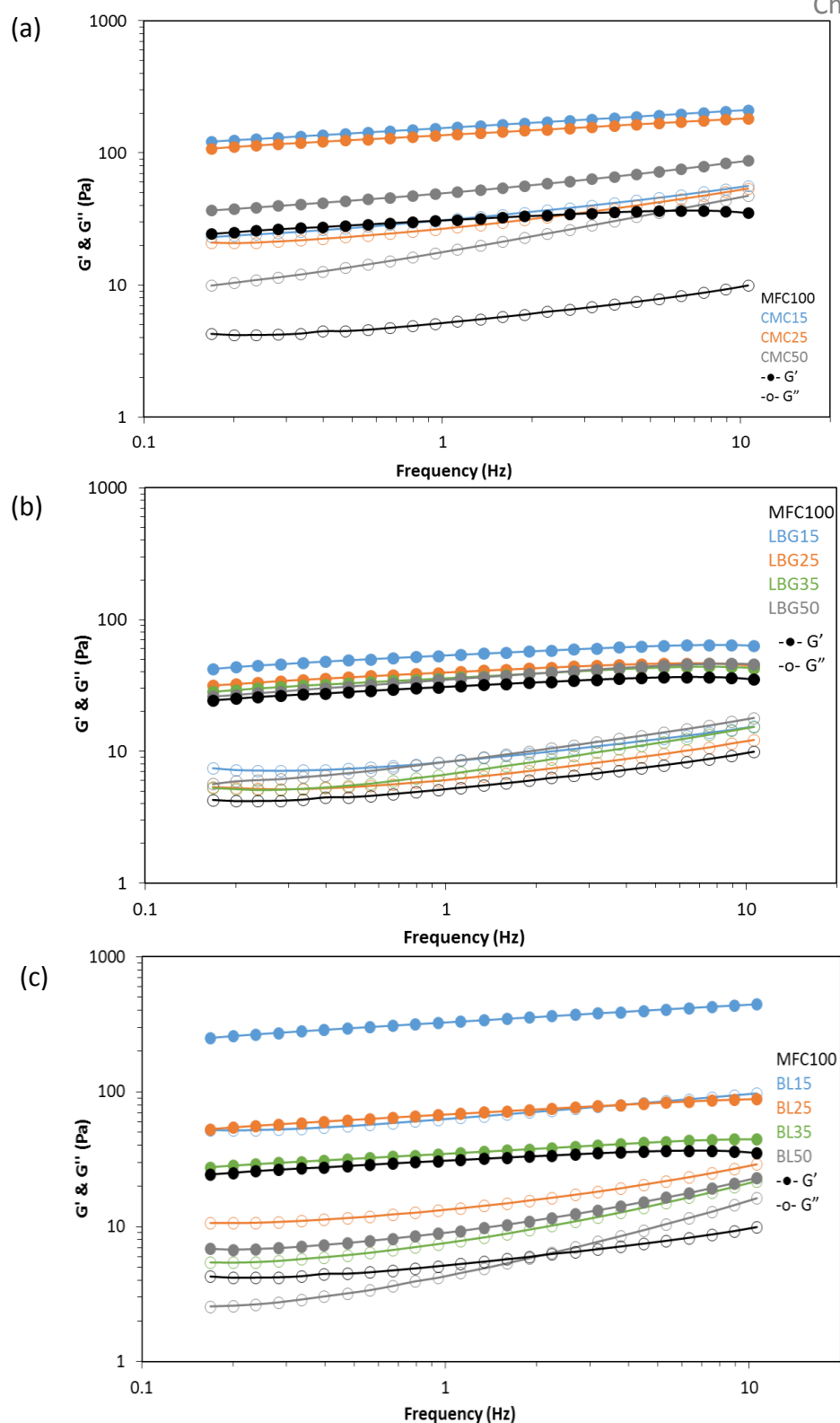


Figure 4.1: Storage (G' , solid symbols) and loss (G'' , open symbols) moduli of redispersed suspension of BMFC with different additives as a function of frequency (Hz) at 20°C, where (a) BMFC/CMC, (b) BMFC/LBG, and (c) BMFC/Blend. All results are highly reproducible with a standard deviation less than $\pm 1\%$.

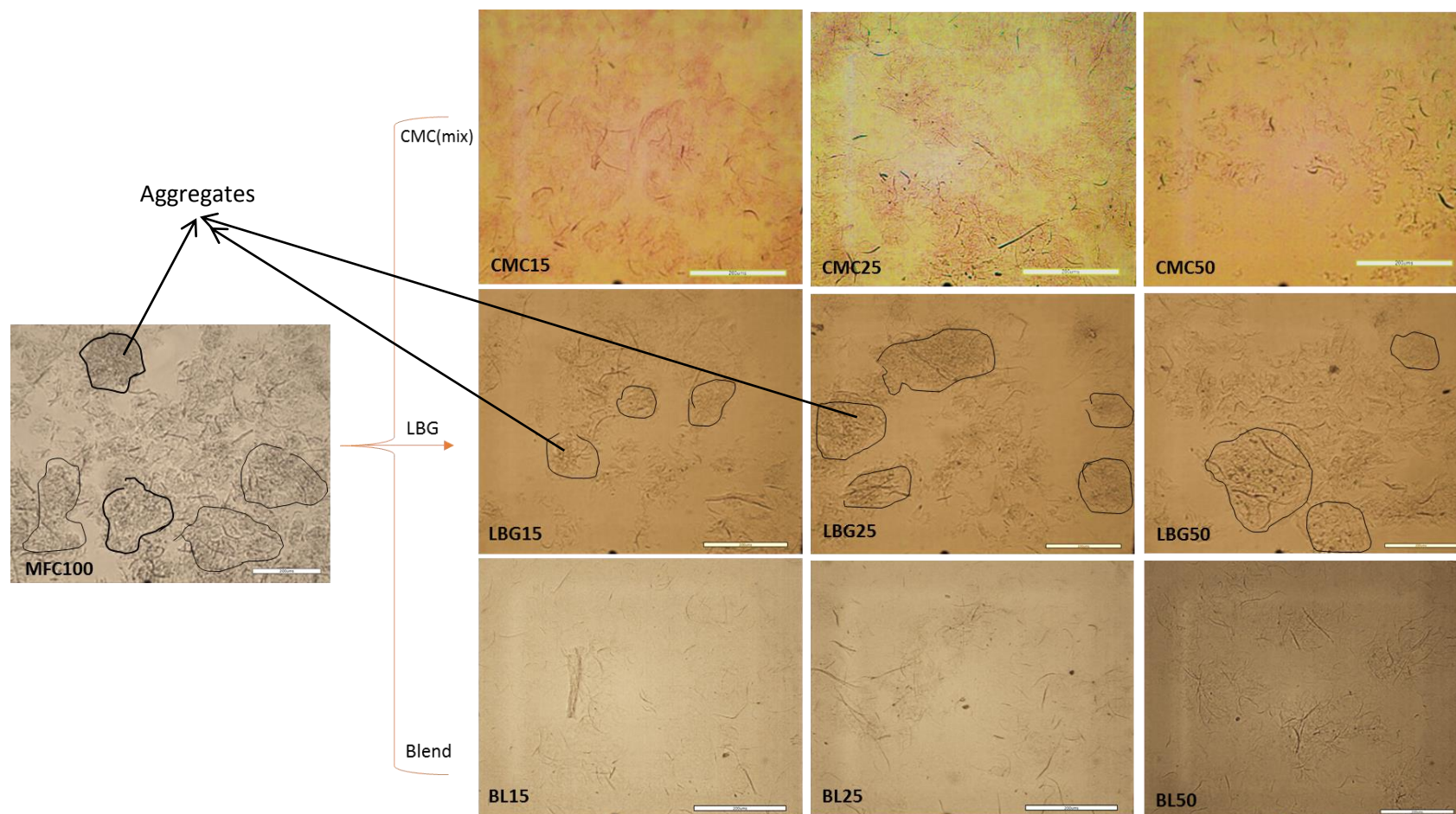


Figure 4.2: Light microscopy images of 2% w/w aqueous suspensions of dried and redispersed MFC100 (BMFC), BMFC with different additives (i.e. CMC(mix), LBG and Blend) at different concentration levels, scale bar: 200 μm .

Finally, when the blend of CMC/LBG was added to BMFC suspension, it was easier to redisperse the BMFC/Blend sample in water with least amount of aggregates and highly connected microfibril network evident in microscopy images (Figure 4.2). This indicates that the presence of charged additives (in this case CMC) plays an important role in maintaining the electrostatic repulsion between the microfibrils. Interestingly, an aqueous suspension of BMFC/Blend (BL15) showed higher G' and G'' as a function of frequency as compared to BMFC/CMC (CMC15) and BMFC/LBG (LBG15). This can be explained by properly redispersed microfibrils throughout the system as CMC provides charge to the microfibrils and LBG providing rigidity to the system, resulting in highly entangled network structure with higher viscoelastic parameters.

The impacts of individual additives on rheological properties are as follows:

4.3.1.1.1 Impact of CMC as additive

Figure 4.3, shows the change in complex viscosity (0.2% strain and 1Hz frequency) of MFC100 (dried BMFC without additive) made up at the same total concentration in water as the amount of MFC in comparative BMFC/CMC mixtures, plotted as a function of CMC proportion. It is observed that the complex viscosity ($|\eta^*|$) of the redispersed suspension initially

increases with an increase in CMC concentration within the suspension matrix, indicating that the BMFC forms an entangled network, crosslinking with CMC, resulting in higher complex viscosity (Figure 4.3) and higher viscoelastic moduli (Figure 4.1a). A slightly lower complex viscosity was observed while comparing never-dried (wet) and dried-redispersed BMFC/CMC formulations. But this reduction was minimal in the case of CMC50, however, CMC50 suspension showed weaker gel-like behaviour as evident in Figure 4.3 (slight frequency dependency on the moduli and the relatively large value of $\tan \delta$ ($G''/G' > 0.1$) can be defined as so-called weak gels (Ikeda and Nishinari, 2001)).

This indicates that when the negatively charged CMC was added in higher amounts, the CMC adsorption on BMFC microfibril surface leads to an increase in the charge effects. Similar behaviour was reported with bacterial cellulose/CMC systems where changes in zeta-potential were shown (Veen *et al.*, 2014). The increase in charge leads to better redispersibility of the BMFC/CMC formulations in water after drying, hence good recovery of complex viscosity. Weaker viscoelastic behaviour (where $\tan \delta > 0.1$) of CMC50 suspension can be explained by a dilution effect. As the dense network of microfibrils of BMFC plays an important role in maintaining

viscoelastic gel-like behaviour, when BMFC is diluted with CMC solution at a 50% dilution the BMFC concentration reduces to 1%, which without additives shows an order of magnitude decrease in G' and G'' (Figure 4.1), and the BMFC forms a weaker entangled network structure.

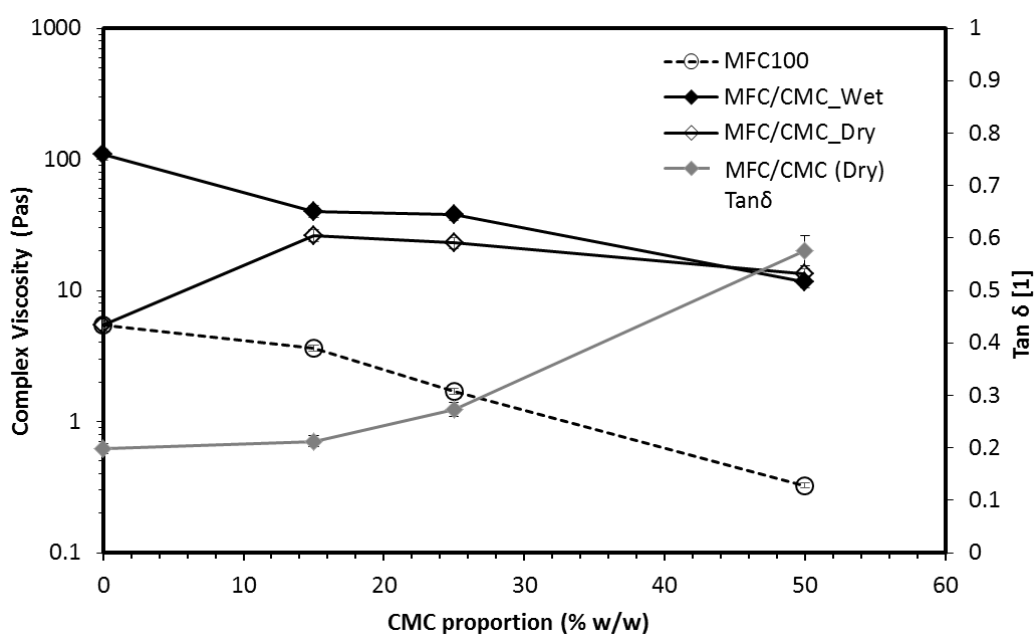


Figure 4.3: Complex viscosity and $\text{Tan } \delta$ (at frequency: 1 Hz and 0.2% strain) as a function of CMC (CMC(mix)) proportion in aqueous suspension of BMFC, and redispersed MFC100 at same proportion to BMFC present in BMFC/CMC formulation. Data presented is an average of 4 replicates.

Figure 4.4a and 4.4b show the impact of the molecular weight of CMC additive on microfibril redispersibility by blending two different molecular weight CMC products together in different proportions (75:25 and 50:50). Measurement of G' and G'' were taken before and after drying of

BMFC/additive mixtures as a function of frequency and complex viscosity of 2% w/w total solids concentration suspensions.

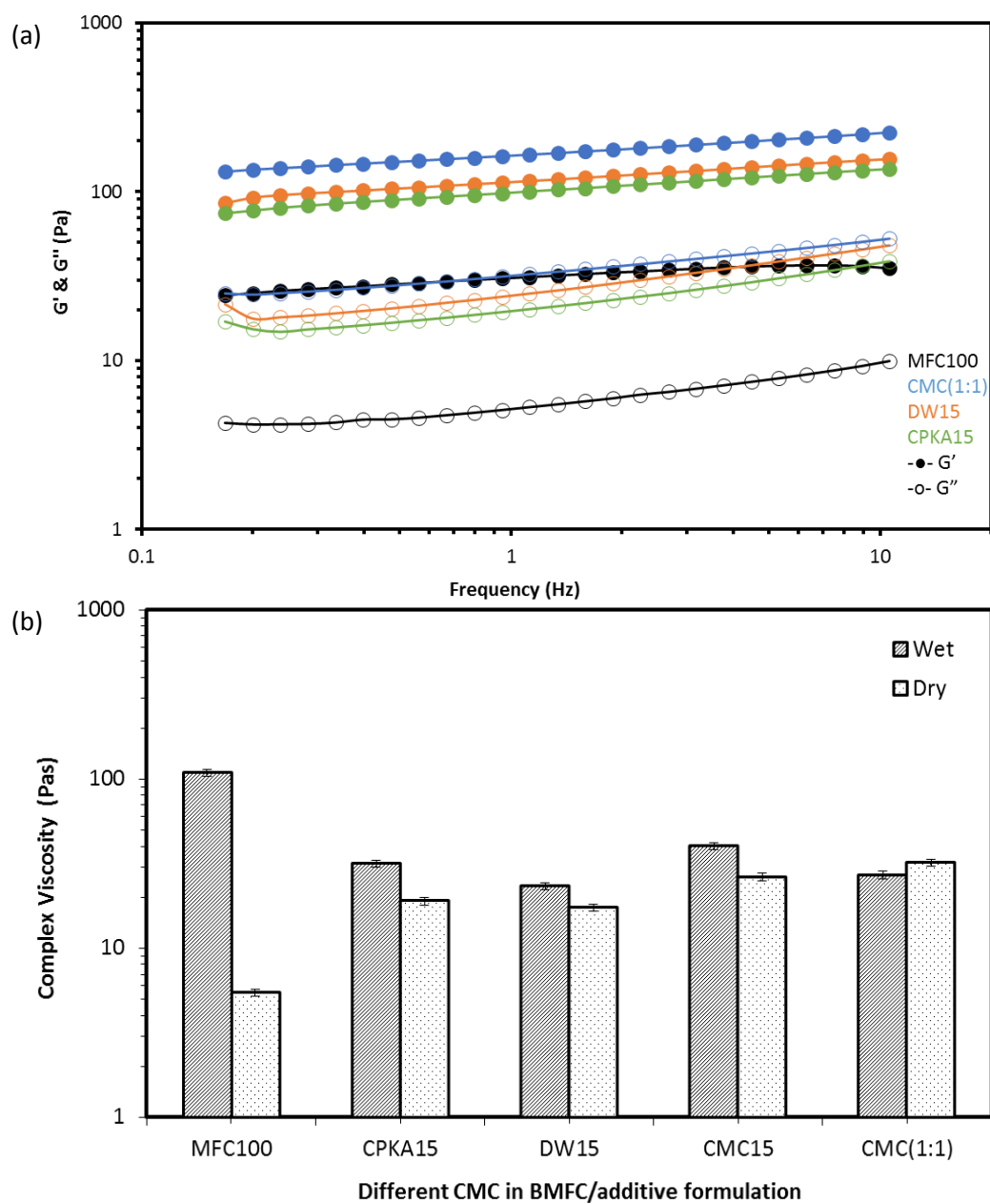


Figure 4.4: (a) Storage moduli and loss moduli of redispersed BMFC with different CMC's as a function of frequency (Hz) at 20°C; and (b) Complex viscosity as a function of different CMCs present in BMFC/CMC (85:15 ratio) suspension. Data presented is an average of 4 replicates with a standard deviation less than $\pm 1\%$.

It was evident that the change in molecular weight of CMC does not have any influence on the redispersibility of dry product and no significant change was observed in complex viscosity ($p\text{-value} > 0.05$). A similar behaviour was reported with sugar beet cellulose and CMC by Lowys *et al.*, 2001. The presented rheological data again indicates that the addition of CMC improves the overall redispersibility impacting on the recovery of the viscoelastic properties of never-dried materials, through charge interactions between BMFC and CMC.

4.3.1.1.2 Impact of LBG as additive

As mentioned earlier, unlike CMC, when LBG was added to BMFC in different proportions the redispersibility of the dried blend is not improved (visual analysis), which is also reflected by the complex viscosity of the suspensions (Figure 4.5a compared with Figure 4.3). Two forms of LBG solution were tested *i.e.* heated LBG and unheated LBG in order to examine the impact of LBG processing on its ability to interact with BMFC. A significant reduction (approximately 50%) in complex viscosity was observed when BMFC/LBG was redispersed as compared to never dry BMFC/LBG, independent processing of LBG (heated or unheated) evident in Figure 4.5a.

When comparing dried and redispersed BMFC/LBG with MFC100, the complex viscosity of the suspension showed a slight increase (by factor of 2) at lower concentration of LBG (15%) in the system, whereas at higher proportions of LBG in the matrix the complex viscosity of the suspension remains similar to that of MFC100 (BMFC) alone (Figure 4.5a). Similar trends were observed in terms of G' and G'' in Figure 4.1b. However, at this lower level of BMFC dilution, the LBG is possibly interacting with the large aggregates and contributing to the continuous phase viscosity. This can also be explained with reference to the micrographs presented in Figure 4.2 (BMFC/LBG), with the presence of aggregates non-homogeneously distributed throughout the system. As the amount of LBG increases, the amount and size of aggregates increases, which were very difficult to redisperse in water and results in significant reduction in complex viscosity (Figure 4.2 and Figure 4.5a).

Therefore, a test was performed where different starting LBG concentrations were used in the blending with 2% BMFC. To rule out the impact of LBG concentration a comparison was made between the BMFC/LBG formulation when two different concentrations of LBG *i.e.* 1% and 2% w/w were added to BMFC suspension to stabilise the microfibril material.

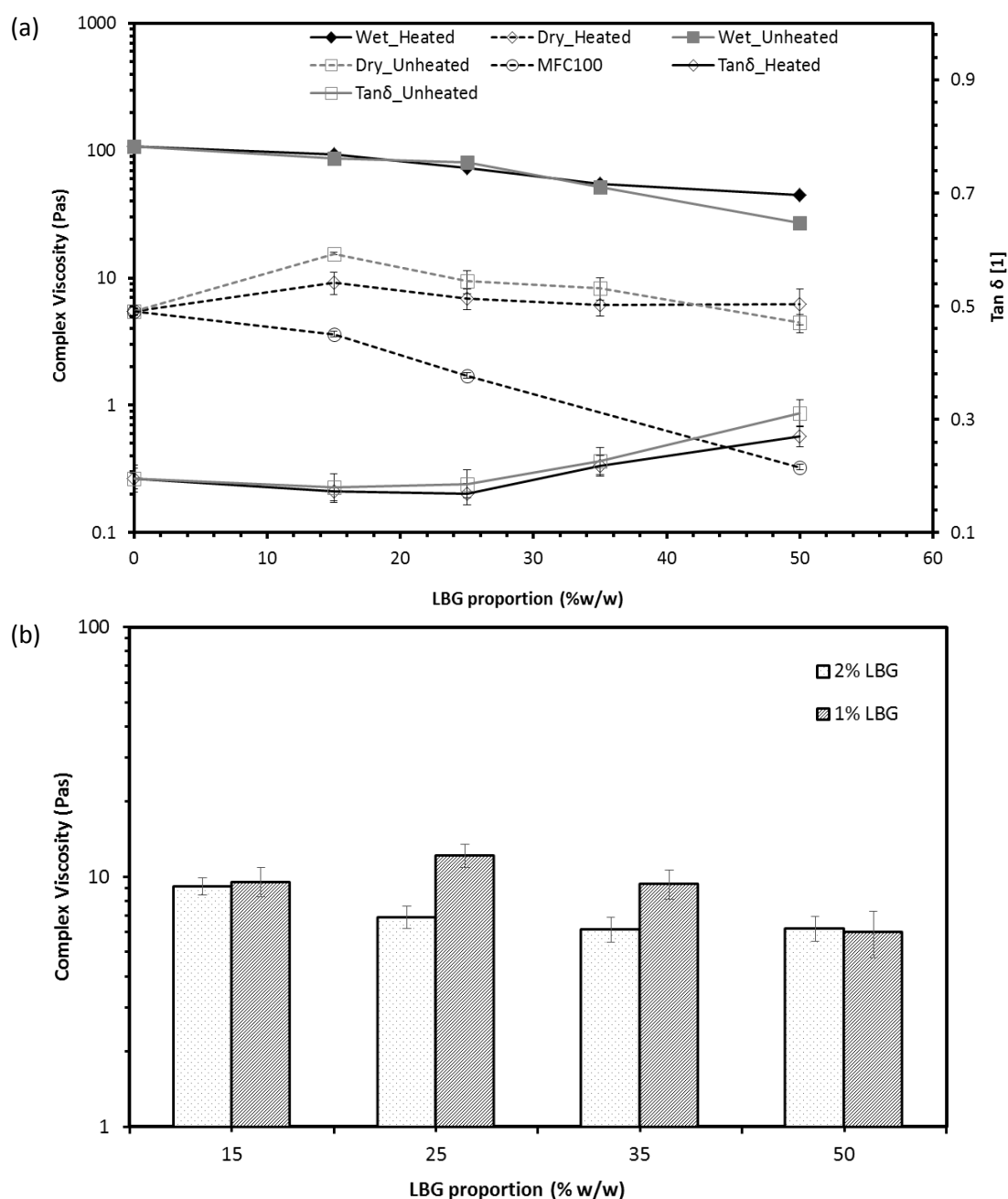


Figure 4.5: (a) Complex viscosity (frequency: 1 Hz and 0.2% strain) and Tan δ (dried samples only) as a function of LBG proportion in aqueous suspension of BMFC (wet (solid) and dried (unfilled)), where “ \square ” unheated LBG and “ \diamond ” heated LBG. (b) The impact of different concentration of LBG on the complex viscosity of dried and redispersed BMFC/LBG suspension, the overall concentration of all suspensions is 2% w/w. Data presented is an average of 4 replicates with a standard deviation $\pm 1\%$.

From Figure 4.5b, no significant impact of LBG concentration was observed in terms of complex viscosity ($p\text{-value} > 0.05$). Hence, from the rheological and microscopy data, an assumption can be that the addition of LBG does not have a significant impact on the suspension properties of dried BMFC as compared to CMC as an additive.

4.3.1.1.3 Impact of Blend (CMC/LBG) as additive

The blending of certain types of gums can produce the disperse system with greater viscosity compare to individual gum dispersions; this phenomenon is known as viscous synergism (Lapasin and Pricl, 1995). The addition of CMC in combination with other gums such as LBG or κ -carrageenan are used in the various application such as ice creams, custards, mayonnaises *etc.* Synergistic interaction between CMC and LBG was reported by Hernandez (2001). Typically both solutions at lower concentration show solution-like behaviour, but at higher concentration, LBG solutions show stable viscoelastic behaviour after the cross-over point of G' and G'' . It was evident in Figure 4.6, as the amount of LBG increases in the CMC solution, the mixture shows viscoelastic behaviour similar to LBG, indicating a shift from weaker viscoelastic behaviour to stable viscoelastic behaviour similar to LBG solutions.

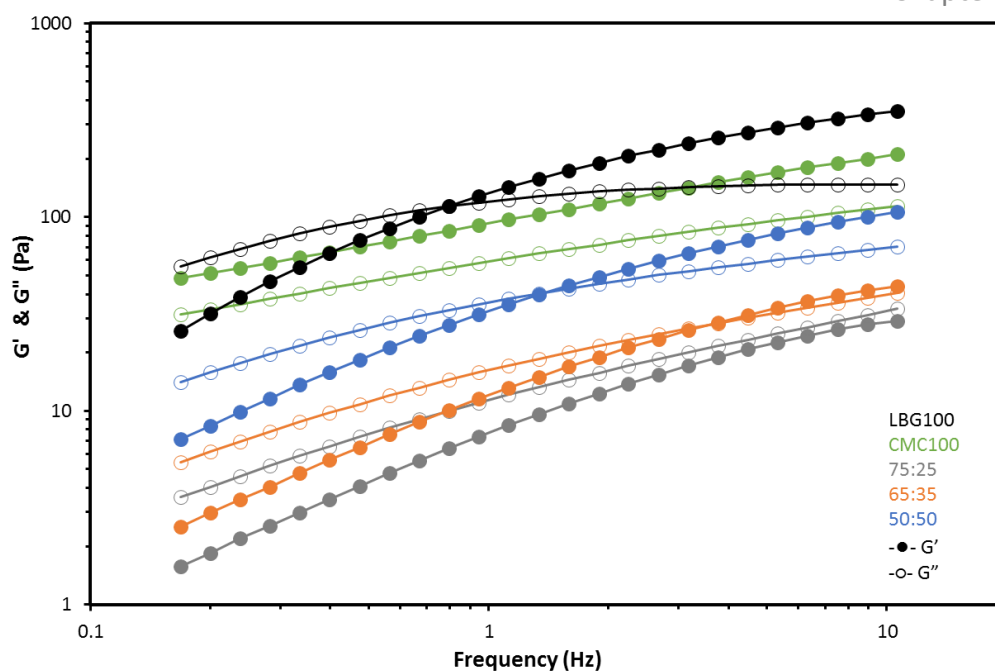


Figure 4.6: Storage (-●-) and loss (-○-) modulus as a function of frequency at 20°C of CMC/LBG blends at different ratios of CMC/LBG i.e. CMC50:LBG50, CMC65:LBG35 and CMC75:LBG25 in aqueous solution. The overall concentration of all suspensions was 2% w/w. All the results are highly reproducible with a standard deviation less than $\pm 1\%$.

Considering that CMC interacts with the microfibrils of BMFC and results in their taking on a negative charge, and LBG helps in inter-fibrillar networking as observed earlier (Newman *et al.*, 1998), the blend of CMC/LBG was formulated at different ratios and used as an additive mix to evaluate possible synergistic effect in the stabilisation of the BMFC. Figure 4.7a shows the change in complex viscosity as a function of the concentration of blend of CMC: LBG of 75:25, in a BMFC suspension. It was observed that BL15 showed higher complex viscosity as compared to MFC100 with both wet and

rehydrated suspensions. This behaviour can be explained by considering microscopy images in Figure 4.2, where redispersed BMFC/BL1 suspensions showed homogeneous and non-aggregated microstructures indicating a possible synergistic interaction between triple blend (BMFC:CMC/LBG). However, as a number of blend increases and the BMFC is diluted, the suspensions showed a noticeable decrease in complex viscosity. A possible explanation for this behaviour is that the synergistic interaction between CMC/LBG dominates over the interaction with BMFC, as the phase volume of microfibrils reduces with an increasing amount of added blend. Basically, when a high amount of blend is added to the BMFC suspension, the BMFC/CMC interaction ratio is less, as LBG interferes and tends to interact with both BMFC and CMC.

An alternative explanation might be that at the addition of 15% blend, the MFC benefits from the action of both CMC (charge) and LBG (interaction). However, at higher amounts of the blend, the LBG dominates the interaction with MFC and the lower viscosity CMC is then left in the non-interacting continuous phase. Then both a dilution effect and a lower viscosity continuous phase results in a viscosity lower than the individual polymers mixed with MFC at comparative MFC:polymer mixing ratios.

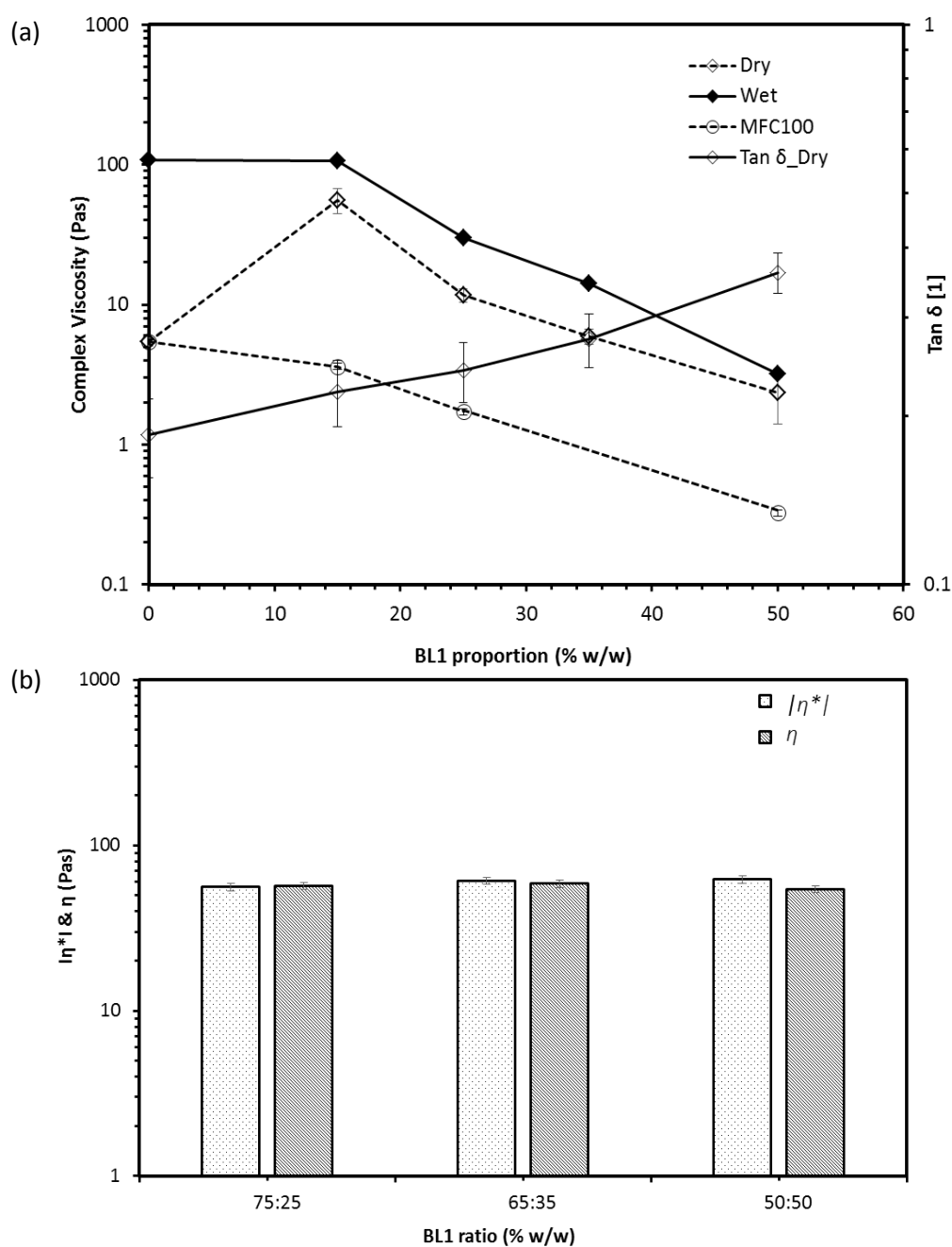


Figure 4.7: (a) Complex viscosity (frequency: 1Hz and 0.2% strain) as a function of blend (BL1) proportion in BMFC suspension, where (-o-) MFC100 and (- \diamond -) BMFC/BL1 (wet (solid) and dried (unfilled)), (b) Impact of different ratios of CMC/LBG blends on complex ($|\eta^*|$) and shear viscosity (η , at shear rate $1s^{-1}$) of redispersed BMFC/BL1 (85:15) suspension. The overall concentration of all suspensions was 2%w/w. All results are highly reproducible with a standard deviation less than 1%.

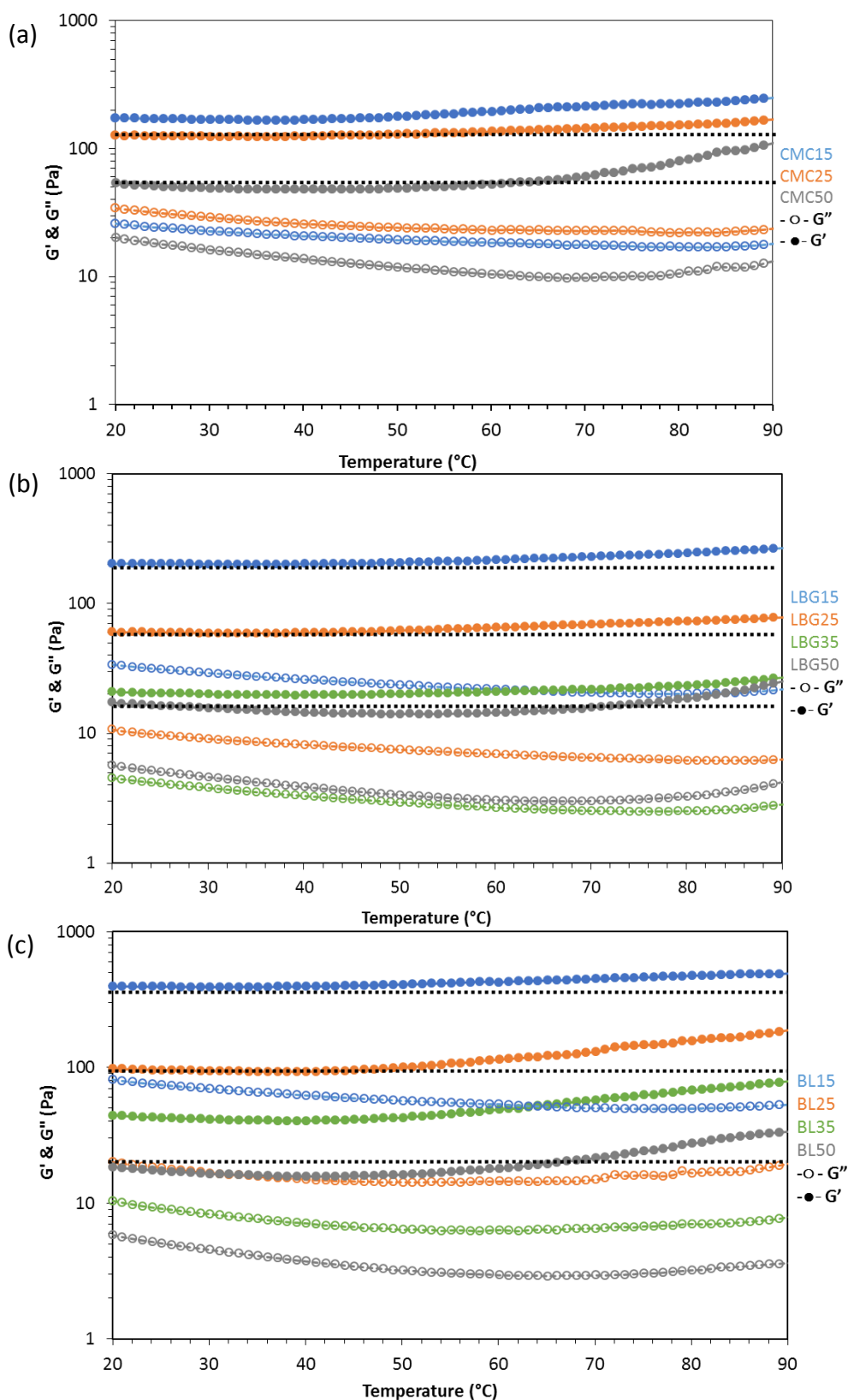


Figure 4.8: Storage (G') and loss (G'') module of redispersed suspension of BMFC with different additives as a function of temperature ($^{\circ}\text{C}$) at 1 $^{\circ}\text{C}/\text{min}$ heating rate, where (a) BMFC/CMC, (b) BMFC/LBG, and (c) BMFC/Blend. All results are highly reproducible with a standard deviation $\pm 1\%$.

In order to understand the impact of CMC/LBG ratio in the blend, it was evident from the Figure 4.7b that the ratio between CMC/LBG has no significant impact on complex and shear viscosity ($p\text{-value} > 0.05$) of dried and redispersed BMFC/BL1 suspensions.

4.3.1.2 Modulus-temperature dependence

The temperature dependence of G' and G'' for 2% w/w BMFC/CMC, BMFC/LBG and BMFC/Blend (BL1) aqueous suspension is shown in Figure 4.8. All suspensions showed stable viscoelastic gel-like behaviour with increasing temperature at constant frequency and strain. It is observed that on heating, both moduli (G' and G'') of all suspensions show firstly a slight decrease from 20°C to 40 °C, however after 40°C all formulations showed an increase in G' and G'' up to 90°C (can be visualised by deflection in G' and G'' from black-straight dotted-lines), independent of the amount of an additive in the individual suspensions. A similar increase in viscoelastic parameters was reported with cellulose nanofibers suspensions as a function of concentration by Chen *et al.*, (2013). These results are consistent with MFC100 (Figure 3.7b), however, slightly higher temperature dependency was observed with CMC50 and all Blends formulations

The first slight decrease in modulus may be due to thermal agitation/thermal motion of microfibrils, resulting in loosening of the fibrils within the network structure. However, the swelling of microfibrils with an increased temperature, while interacting with additives such as CMC, LBG and BL1 in the matrix, may strengthen the gel-like structure resulting in an increased G' and G'' of suspensions after 40°C. From Figure 4.8a, it is evident that as the amount of CMC increases (*i.e.* CMC50) in the suspension, G' and G'' increase to a greater extent after 40°C indicating a thermally induced synergistic interaction between BMFC/CMC. It is well known that polymeric solutions such as HPMC (hydroxyl propyl methyl cellulose) exhibit an increase thermal motion upon heating, leading to a weaker network and sometimes decrease in viscosity (Silva *et al.*, 2008).

The fact that the BMFC/CMC suspensions do not lose structure upon heating, even when the MFC proportion is lowered, indicates an interaction beyond the surface stabilisation of the microfibrils between CMC and MFC, although it is not yet clear what mechanisms are involved. Similar viscoelastic behaviour as a function of temperature was observed with MFC with LBG and blend (CMC/LBG). The interaction between microfibrillar cellulose and additives are driven by surface OH-group-mediated hydrogen bonds;

however, the extents of these interactions are highly dependent on the type of additive used to stabilise the microfibrils. An enhanced increase in both moduli (G' and G'') as a function of temperature with BMFC/additives as compared to MFC100 also indicates the presence of additional interaction between the two components.

4.3.1.3 *Viscous synergism of BMFC/additive mixtures*

Rheologically it is evident from the previous section that the presence of additives has a positive impact on BMFC suspension rheological parameters possibly due to synergistic interactions between the components and a subsequent development of mutually repulsive negative charge on the microfibril surfaces, through binding with CMC and steric stabilisation in the presence of LBG. Hence, for a quantitative analysis of these interactions between BMFC with CMC, LBG and Blend (BL1), the index on the basis of synergism known as viscous synergism (I_v) was used. Viscous synergism for two mixed polymers is defined by Equation 4.1a (Pellicer *et al.*, 2000, Hernandez *et al.*, 2001): where η is shear viscosity, i and j represents the polymers forming the mixed system, $i + j$.

$$I_v = \frac{\eta_{i+j}}{\eta_i + \eta_j} \quad \text{(Equation 4.1a)}$$

$$I_v = \frac{\eta_{i+j+c}}{\eta_{i+c} + \eta_{j+c}} \quad (\text{Equation 4.1b})$$

Viscous synergism for a blend of three polymeric components is defined by Equation 4.1b, which can be used to evaluate the interaction between the two polymeric and one fibrillar component, where “c” represents MFC, “j” is LBG, and “i” represents CMC. In all cases, the total blend concentration is fixed at 2% w/w. Typically, if I_v value is between 0 and 0.5, the viscosity of the mixed system will be less than the sum of the viscosities of its components, and less than one of the component, in this case, the system shows antagonistic interaction. If the I_v value is between 0.5 and 1.0, synergistic effects will occur, and lastly, $I_v > 1$, the viscosity of the mixed system would be greater than the sum of individual component viscosities, strong synergistic effects would result (Pellicer *et al.*, 2000). Furthermore, synergistic interactions can also be quantified by using a viscoelastic parameter *i.e.* G' (Tandjawa *et al.*, 2012a) by using the Equation 4.2a and 4.2b, where the synergistic effect is denoted by “R”.

$$R = \frac{G'_{c+i} - (G'_c + G'_i)}{G'_c + G'_i} \quad (\text{Equation 4.2a})$$

$$R = \frac{G'_{c+j} - (G'_c + G'_j)}{G'_c + G'_j} \quad (\text{Equation 4.2b})$$

Table 4.1 shows the quantitative evidence of synergistic interaction between the BMFC and different additives. The highest I_v value and positive R-value is for the BMFC/CMC formulation, indicating the strong rheological synergism ($I_v > 1$) between the two components, however as the amount of CMC is increased in the mixture a slight decrease in I_v and R-values was observed.

Table 4.1: Rheological synergism of BMFC/CMC, BMFC/LBG, BMFC/BL1 (BL1: is a blend of CMC/LBG) mixtures in aqueous suspension at 20°C; where G' (Pa) is recorded at strain 0.2% and frequency 1 Hz, and η recorded at shear rate 1 s^{-1} .

Sample	η (Pas)	G' (Pa)	I_v	R
MFC100	5.34	30.65	N/A	
CMC	3.23	3.39		
LBG	59.85	136		
BL1	6.64	8.053		
CMC15	53.85	162.75	6.28	3.78
CMC25	50.4	142.25	5.88	3.18
CMC50	36.9	80.9	4.31	1.38
LBG15	7.0675	57.42	0.11	-0.66
LBG25	5.335	43.3	0.08	-0.74
LBG50	5.705	38.27	0.09	-0.77
BL15	56.97	347	0.77	7.97
BL25	22.2	72	0.30	0.86
BL50	7.4	14	0.10	-0.64

In the case of BMFC/LBG, the I_v value was very low as compared to BMFC/CMC and R-value was negative, these values were reduced with increasing LBG proportion in the mixture, indicating weak synergistic effects, this can be explained by possible hydrogen bonding between the microfibrils and LBG. Finally, the I_v value of BMFC/Blend (BL1) is higher in the case of

BL15, indicating synergism, and start reducing as the amount of Blend (BL1)

increases with a greater reduction than that seen for BMFC/CMC.

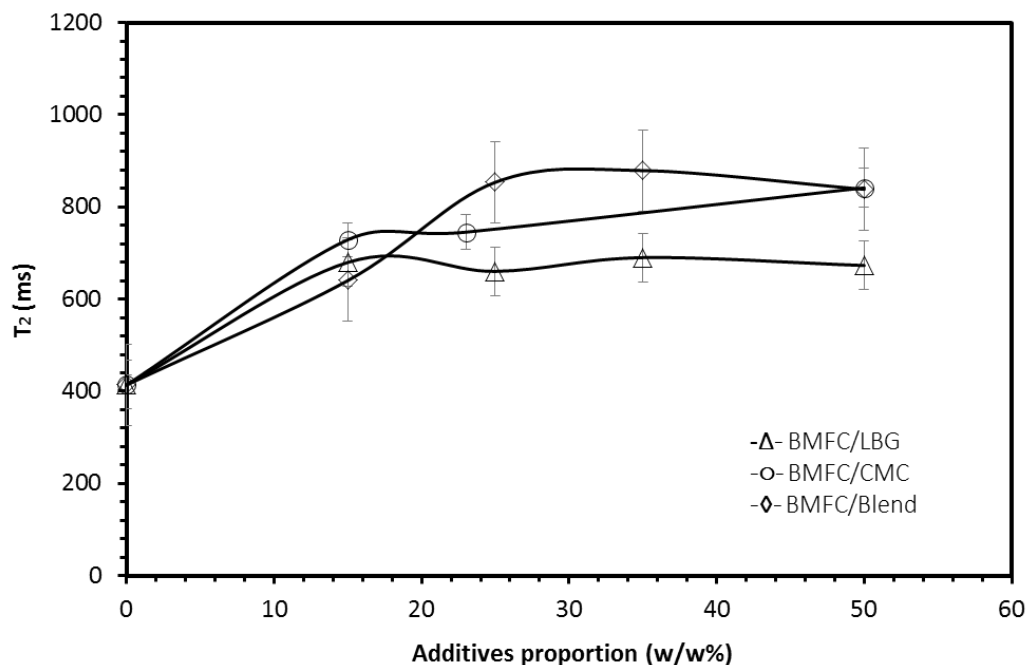


Figure 4.9: Spin-spin relaxation time (T_2) as a function of additives proportion in (○) BMFC/CMC, (Δ) BMFC/LBG and (◇) BMFC/BL1 formulations at 20°C of 2% w/w overall suspension concentration. Data presented is an average of 4 replicates with not statistically significant (p -value>0.05). Where T_2 value of 2% w/w CMC100 is 1227 ms and LBG100 is 846 ms.

The reduction in synergism index with increasing amount of the additive in the suspension confirms that a more ordered and entangled network structure is formed by a higher proportion of microfibrils. It is also evident that the presence of a charged additive *i.e.* CMC enhances synergism effects as compared to LBG, which is also reflected in the case of BL1. This is then

more evidence to suggest that the LBG and CMC in the blend have different roles, with the strong binding of the LBG and CMC having an influence on giving charge to the microfibrils.

4.3.2 Impact of additives on water mobility

The spin-spin relaxation times (T_2) of dried and redispersed suspensions show that addition of additives increases the T_2 value of the BMFC suspensions, in comparison with MFC100 (Figure 4.9). An explanation for the increase in relaxation time could be: as the amount of CMC/LBG or Blend (BL1) increases in the formulation it decreases the entangled network of BMFC, resulting in a much weaker gel-like behaviour ($\tan \delta$ presented in Figure 4.3, 4.5a and 4.7a) and synergism effects (decrease in I_v and R-values). The impact of different additives on the mobility of water in BMFC network structure, it was evident in Figure 4.9 that the CMC and Blend (BL1) showed higher T_2 values at all concentrations as compared to LBG. Lower T_2 values of BMFC/LBG suspensions can be explained by larger microfibril/fibrils aggregate structure formed due to strong intra- or inter- interactions between the microfibrils and LBG. Hence water mobility in the network structure of the suspensions was limited to the outer surface of the fibrils of BMFC/LBG suspensions, resulting in lower T_2 values. Similar water mobility (T_2 values) within the network

structure was observed with rehydrated BMFC *i.e.* MFC100. It appears to be the presence of microfibrils aggregates and inhomogeneity in the case of MFC100 and BMFC/LBG suspensions dominates the T_2 values. A small increase (not statistically significant) in water mobility was observed when comparing MFC100 and BMFC/LBG. The increases in the T_2 values can be explained by slight improve in the redispersibility of BMFC/LBG material as compared to MFC100 due to the surface interaction between the entangled microfibrils and LBG.

To further examine the effect of drying on the water mobility in the microfibril network in the presence and absence of additive (CMC), T_2 values as a function of total concentration are plotted to compare aqueous suspensions of blends of never-dried BMFC/CMC(ND) and redispersed BMFC/CMC(D) with pure MFC100 (never-dry (ND) and redispersed (D)) shown in Figure 4.10b, and also compared to the shear viscosity of the same systems (Figure 4.10a).

In chapter 3 (in section 3.3.2.2) it was shown that the drying of BMFC without additives resulted in the formation of strong intermolecular hydrogen-bonds between the fibrils and microfibrils, resulting in the formation of larger rigid fibrils aggregates of BMFC, which may limit water mobility within the

suspension resulting in lower T_2 values. Figure 4.10a shows that the addition of CMC to BMFC increases the shear viscosity of the dried and redispersed suspension as compared to MFC100 and leads to viscosities similar to the never dried MFC (MFC100(ND)). However, the water mobility in the redispersed BMFC/CMC was greater than MFC100 (ND) and MFC100 (D). Therefore the presence of CMC contributes to the increase in water mobility due to a reduction in the extent of aggregation, which must be present even in the MFC100 (ND).

Never-dried CMC15 shows highest T_2 values, since the addition of CMC protects the formation of strong H-bonds between BMFC fibrils, resulting in improved redispersibility of the BMFC/CMC in water. The highest T_2 values for CMC15(ND) indicate that the CMC is effective when mixed with MFC, and such effects are successful in providing good redispersibility once dried. However, as the overall concentration of BMFC/CMC is increased (from Figure 4.10b) the T_2 values decrease indicating that, as expected the extent of water-polymer interaction increases, which results in reduced water mobility in the system (Norton *et al.*, 1998).

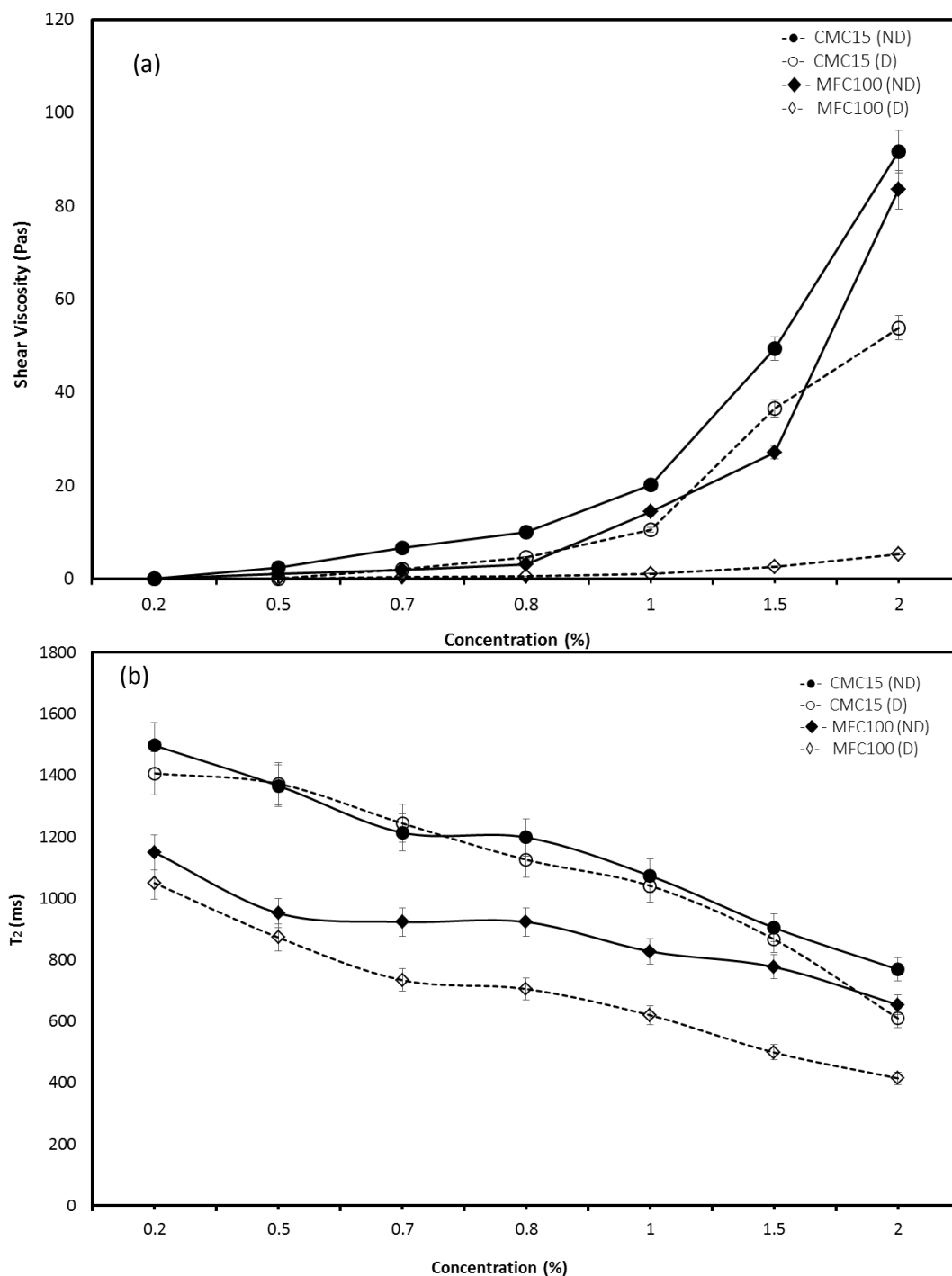


Figure 4.10: (a) Shear viscosity (at 1 s^{-1} shear rate); and (b) T_2 (ms) of (-○-) MFC100 (wet (solid) and dry (unfilled)), (-○-) CMC15 (wet (solid) and dry (unfilled)) as a function of concentrations at 20°C . Data presented is an average of 4 replicates, highly reproducible with a standard deviation less than 1%.

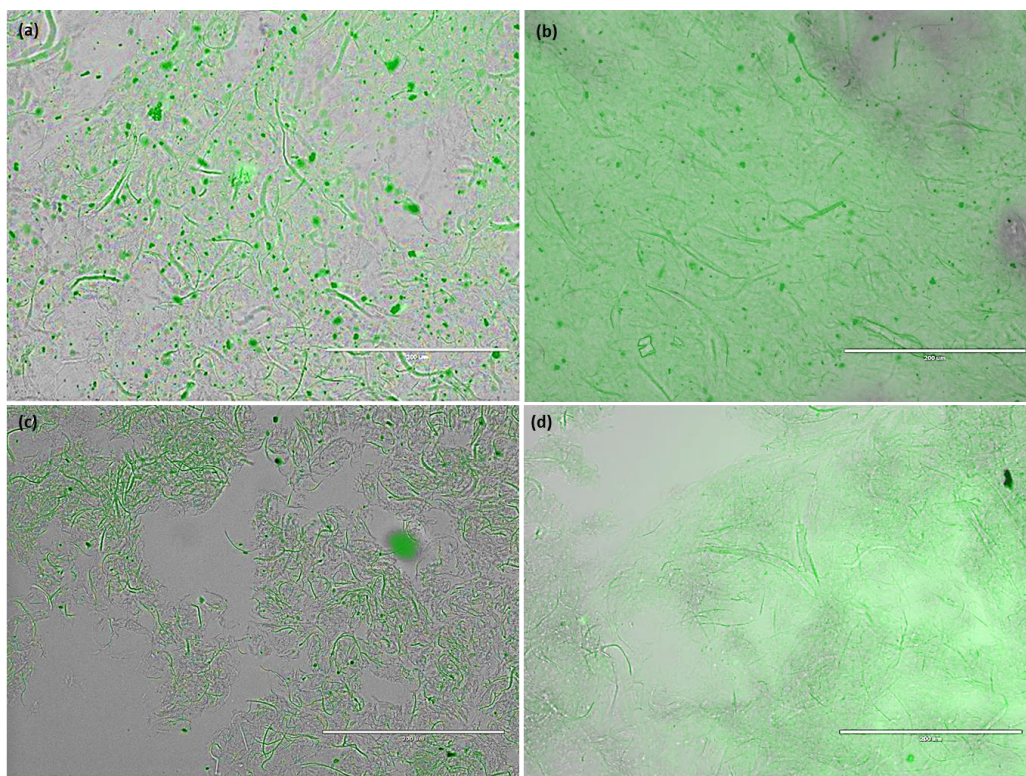


Figure 4.11: Fluorescence microscopy images of 2% w/w suspension of (a, b) BMFC/CMC i.e. CMC15 & CMC50 respectively, (c) BMFC/BL1 (BL15), and (d) BMFC/LBG (LBG15), at scale bar: 200 μ m, where CMC and LBG are tagged with FITC (shown as green colour).

Fluorescence microscopy images in Figure 4.11a and 4.11b of redispersed BMFC/CMC shows CMC coating the surface of the MFC fibrils. This CMC coating protects the formation of strong H-bonds between the MFC microfibrils resulting in a noticeable improvement in redispersibility of BMFC/CMC. Similarly, surface coating on microfibrils was observed with BMFC/BL1 and BMFC/LBG systems (Figure 4.11c and 4.11d). Therefore, these results indicate a complex and competitive nature of the addition of different

polymeric additives. CMC coats MFC and provides a charge and LBG binds and crosslinks with MFC. In a mixture with low levels of the blend of polymers appears to provide the dual effectiveness, but at higher additive levels the LBG seems to dominate. In some fluorescence microscopy images, small regions are uncoated; this is due to mixing limitation during mixing protocol.

4.3.3 Thermal transitions of BMFC/additive at low moisture

In previous sections, different BMFC/additive formulations were studied and characterised at high moisture levels, whereas in this section an attempt is made to understand the different physical properties of BMFC/additives at low moisture system (2% to 20% moisture content). The main objective of this study is to investigate the impact of different polymeric additives on temperature-induced structural transitions in MFC at low moisture environment in order to provide a further understanding of the complexity of interactions between the polymeric additives and the fibril/microfibril cellulosic material. Also, qualitatively determine the impact of additives on different water-populations (such as associated (interacting)-water and free (bulk)-water). In order to identify the low-temperature thermal transitions of BMFC/additive systems Differential Scanning Calorimetry (DSC) was used (Figure 4.12).

The DSC thermograms of BMFC/CMC and BMFC/Blend (BL1) at the lowest moisture (2%w/w) showed three distinct endothermic peaks (Figure 4.12a). During the first heating, a lower temperature shoulder between 30-40°C and a second higher temperature peak between 50-70°C was observed, however, both peaks disappear during the second heating, whereas during the second heating a new peak between 5-20°C is measured. In the case of BMFC/LBG, the system showed only one peak between 50-70°C during the first heating and which is also lost during second heating, with no peak observed between 5-20°C. An endothermic peak between 50-70°C is common for various polysaccharides at low moisture content; this peak is the result of the activation of processes associated with polysaccharide-water interactions and has also been ascribed to polymer relaxations (Gidley *et al.*, 1990, Abbaszadeh 2013).

For BMFC without the addition of polymers no peaks were observed in this region. This indicates that the addition of CMC and LBG induces low-temperature structural transitions in the system, *i.e.* associated with hydrogen bonding between BMFC-additive and BMFC/additive-water. This higher temperature endothermic peak disappears at higher moisture content (approx. 20%) as seen in Figure 4.12b, where the moisture content of

BMFC/additives was manipulated by equilibrating to constant weight under a controlled relative humidity (RH) 93%.

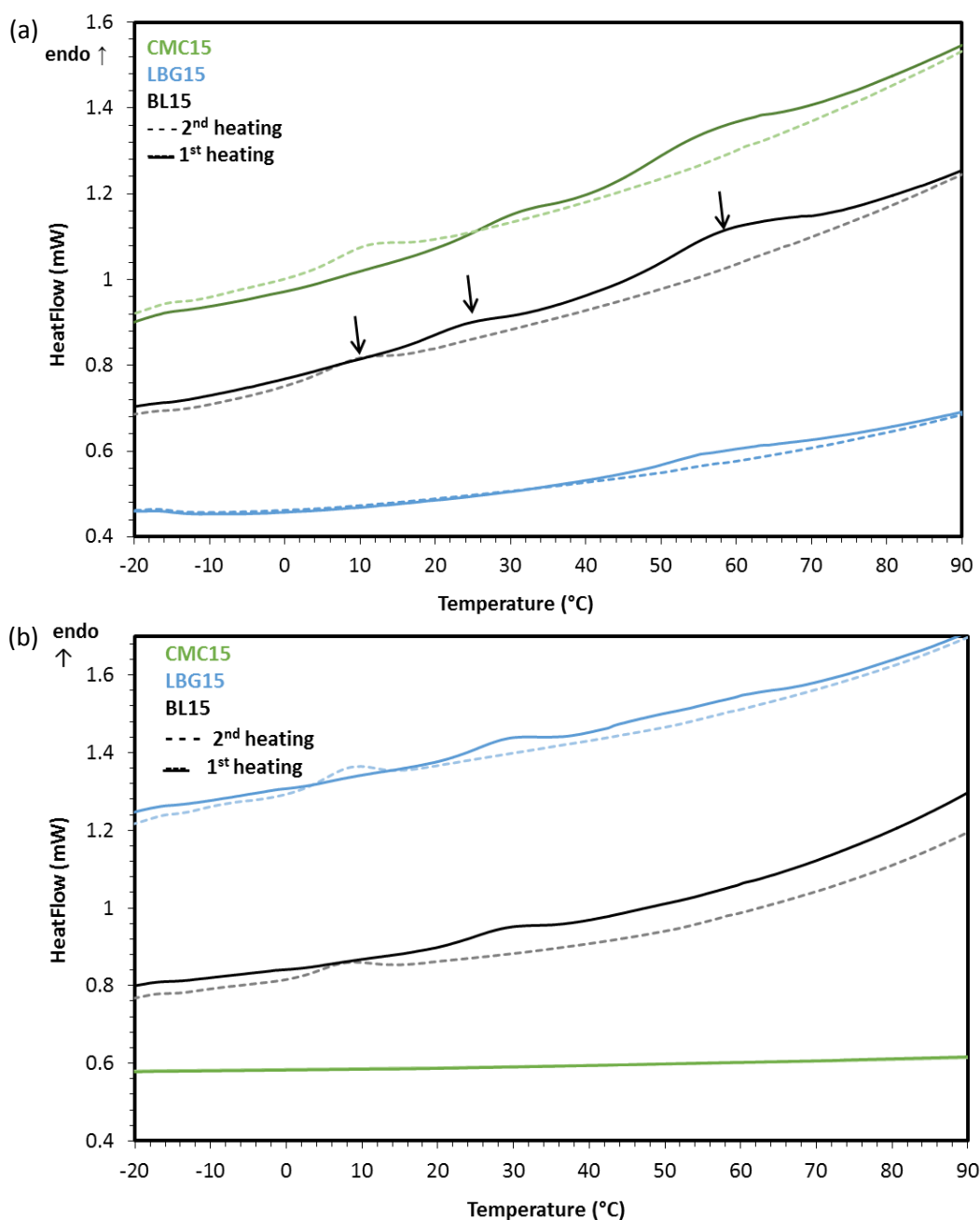


Figure 4.12: DSC thermograms of BMFC/CMC, BMFC/LBG and BMFC/Bend (BL1) at (a) 2% and (b) 20% moisture content. All results are highly reproducible with a standard deviation less than 0.1%.

This behaviour can be explained by the presence of excess freezable water in the system (evident in DTGA data in Figure 4.13b, an increase in the moisture loss between 50-150°C, discussed later), similar behaviour was observed with xanthan-water and starch-water systems (Raschip *et al.*, 2008 and Gidley and Cooke, 1991).

The second, lower temperature endothermic transition peak between 30-40°C indicates that the BMFC/CMC and BMFC/BL1 systems undergo thermal induced structural changes which will influence the extent of water interaction with the MFC:additives and cause a re-organisation of hydrogen-bonding. This transition was more pronounced at higher moisture levels evident in Figure 4.12b, and these transitions are considered as a liquid-crystal transition at low temperatures in hydrated hydrocolloid systems (similar behaviour was observed with the xanthan-water system (Abbaszadeh, 2013)). This structural transition was not observed with BMFC/LBG system at lower moisture but occurs at the higher moisture levels. An explanation for this behaviour is the presence of strong hydrogen bonds between the microfibrils and LBG after drying, resulting in a lower amount of interacting water in the system which is associated with a weaker transition. However, when the moisture content of the BMFC/LBG was increased, the transition in

the region of 30-40°C was observed (evident in Figure 4.13b). Therefore, the results indicate that like CMC, LBG is also capable of liquid-crystal type behaviours; however it is only initiated at higher moisture level.

Finally, an endothermic peak was observed between 5-15°C at both low and high moisture content with all BMFC/additive-water systems during the second heating cycle. BMFC in the presence of additives and varying amounts of water, therefore, undergoes a further structural reorganisation, which may also possibly be due to a combined water microfibril-additive liquid-crystalline state. Interestingly, the BMFC/CMC system at the higher moisture content does not show any thermal induced endothermic peak, which indicates that the liquid crystalline state is water content dependent.

Under inert atmosphere, the thermal degradation of cellulose/BMFC material is characterised by one mass loss step which results in one peak in the DTGA curve (Figure 4.13). Usually, the peaks are characterised according to the degradation of the different components of the samples. Typically, one peak between 300-350°C is related to the degradation of cellulose or in this case MFC, evident from both Figure 4.13a and also shown by Barneto *et al.*, (2010) and Moran *et al.*, (2008).

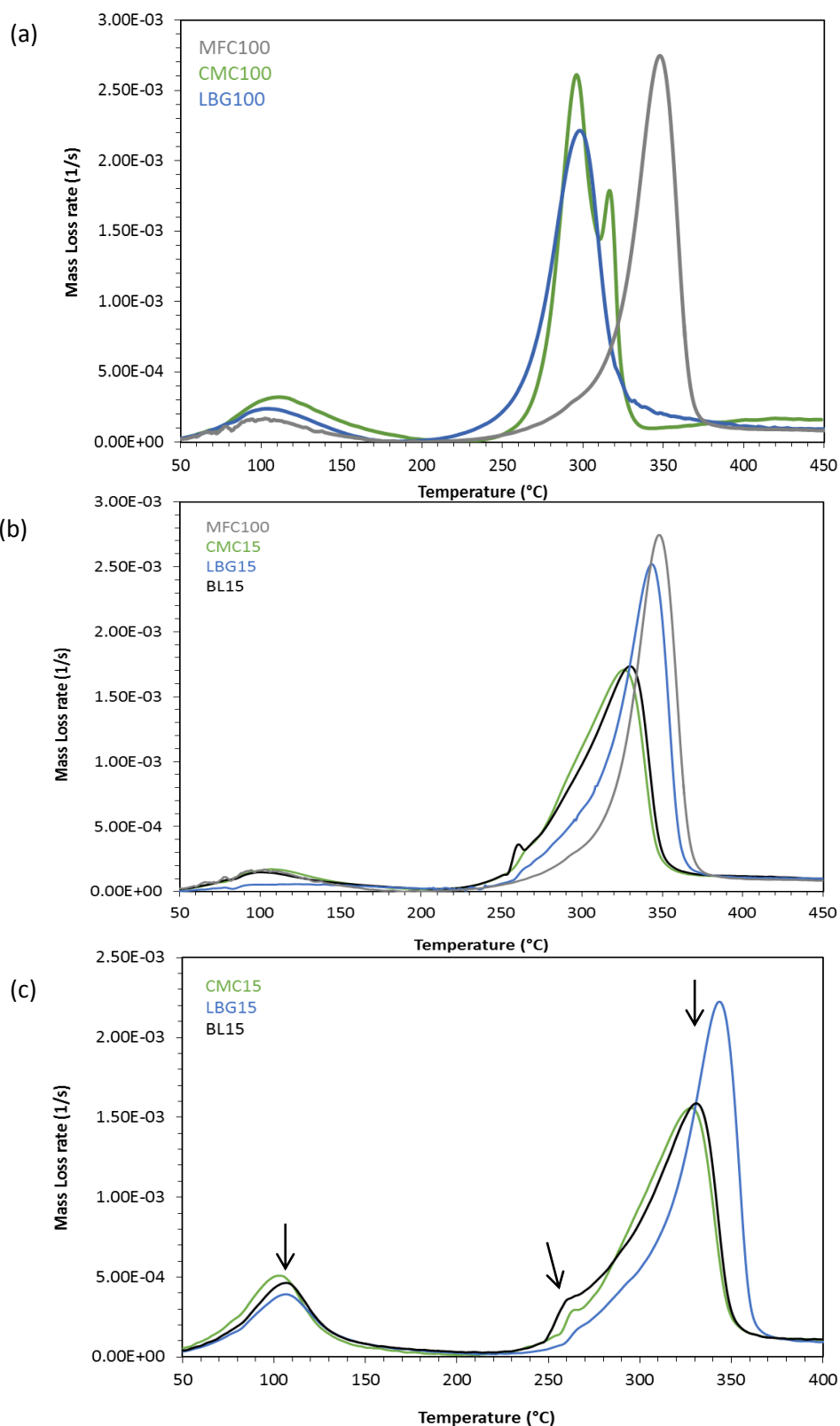


Figure 4.13: The thermal degradation under a nitrogen atmosphere of (a) CMC100, LBG100 and MF100 at low water content, and comparison between MFC100 (BMFC), BMFC/CMC, BMFC/LBG and BMFC/Blend (BL1) where (b) low, and (c) high water content. Data presented is highly reproducible.

It was also evident that the LBG100 and CMC100 degrade earlier as compared to MFC100. A shoulder peak between 250-300°C which is likely to belong to degradation of the additive (*i.e.* CMC, LBG and Blend (BL1)), as the temperature of degradation corresponds to CMC100, LBG100, and the peak size and area of this shoulder increases as the amount of additive increases in the BMFC/additive formulations evident in Figure 4.14a, 4.14b and 4.14c. This proves the theory that the synergistic interaction between BMFC/additives involves the formation of strong hydrogen bonds which break and degrades at a higher temperature close to MFC.

A comparison of these curves highlights a number of interesting features. One is around the lower temperature shoulder, which is more evident in the CMC and CMC/LBG blend systems, which also show the main exotherm maximum shifting to lower temperatures. This indicates that the interaction between cellulose and CMC is more thermally labile. Additionally, when looking at the peak at 100°C, which is indicative of water evaporation, these structures have higher amounts of “available” water than the system containing LBG (Figure 4.13b and 4.13c). At an equivalent additive content, the LBG system is less thermally labile than the CMC system, but with the addition of increasing amount of LBG to the system (Figure 4.14b) a pronounced increase in the

amount of more thermally sensitive material is seen (an increase in the size of the lower temperature shoulder), with a subsequent decrease in the size of the peak at the original cellulose degradation temperature. These observations support those measured by DSC, in that the CMC seems to be more effective than LBG in altering the properties of MFC, and either a higher water content and that an increased amount of added LBG are required to have similar effects.

These results correlate well with DVS moisture sorption and desorption isotherms of different BMFC/additive formulations (Figure 4.15a and 4.15b). From the dry state, the moisture uptake of MFC100 was relatively slow as compared to all BMFC/additive formulations, due to strong intermolecular hydrogen bonds present between the BMFC fibrils forming aggregates with lower diffusivity. The moisture sorption becomes higher during the second cycle of sorption independent of BMFC formulations indicating the after the first cycle of moisture sorption and desorption the fibril network hold some “associated” moisture (evident in desorption isotherm Figure 4.15b) which allows the higher moisture sorption during second sorption cycle.

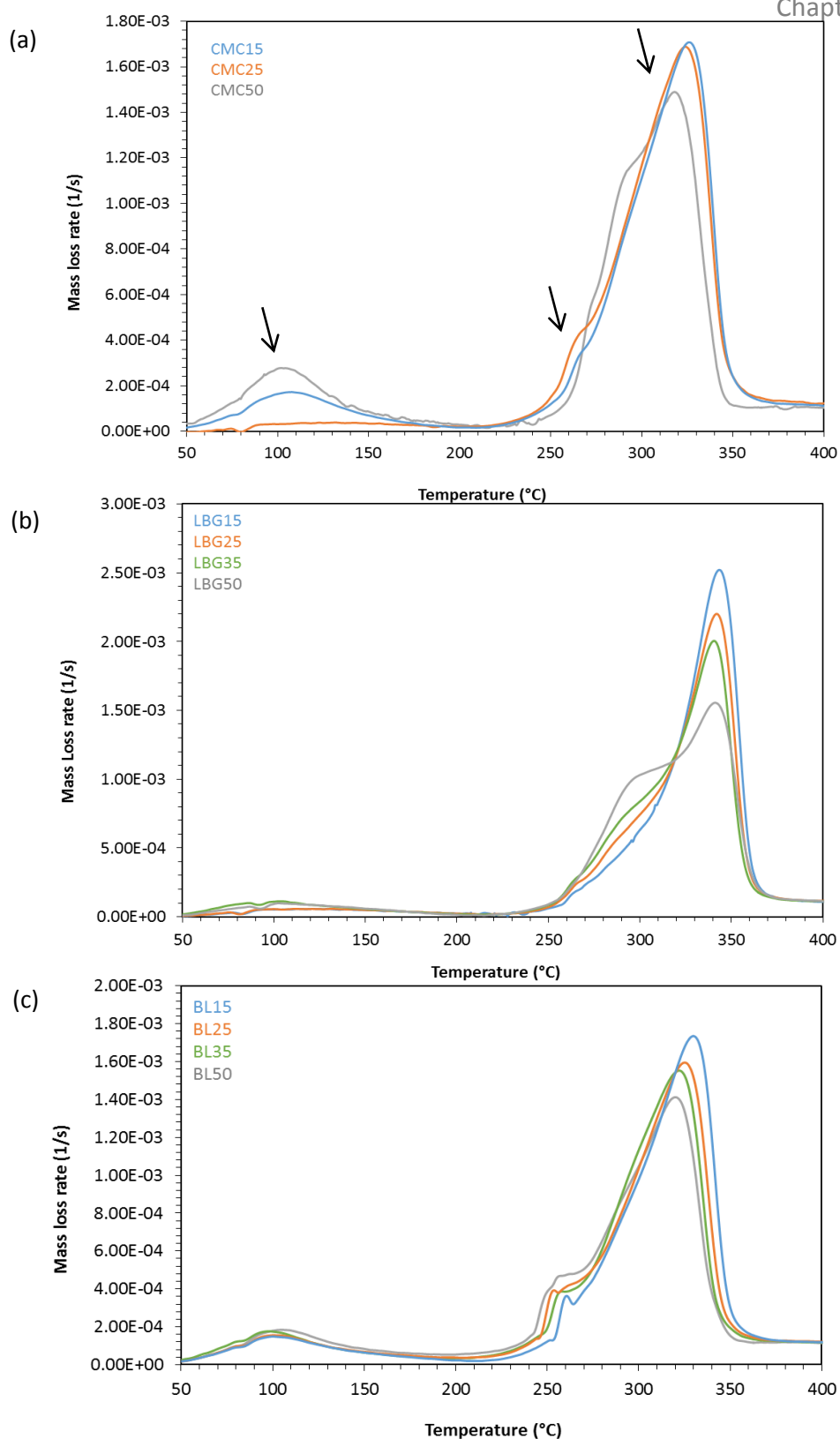


Figure 4.14: Thermal degradation of (a) BMFC/CMC, (b) BMFC/LBG, and (c) BMFC/Blend (BL1) under a nitrogen atmosphere with increasing amount of additives in the system at low water content. Data presented is highly reproducible.

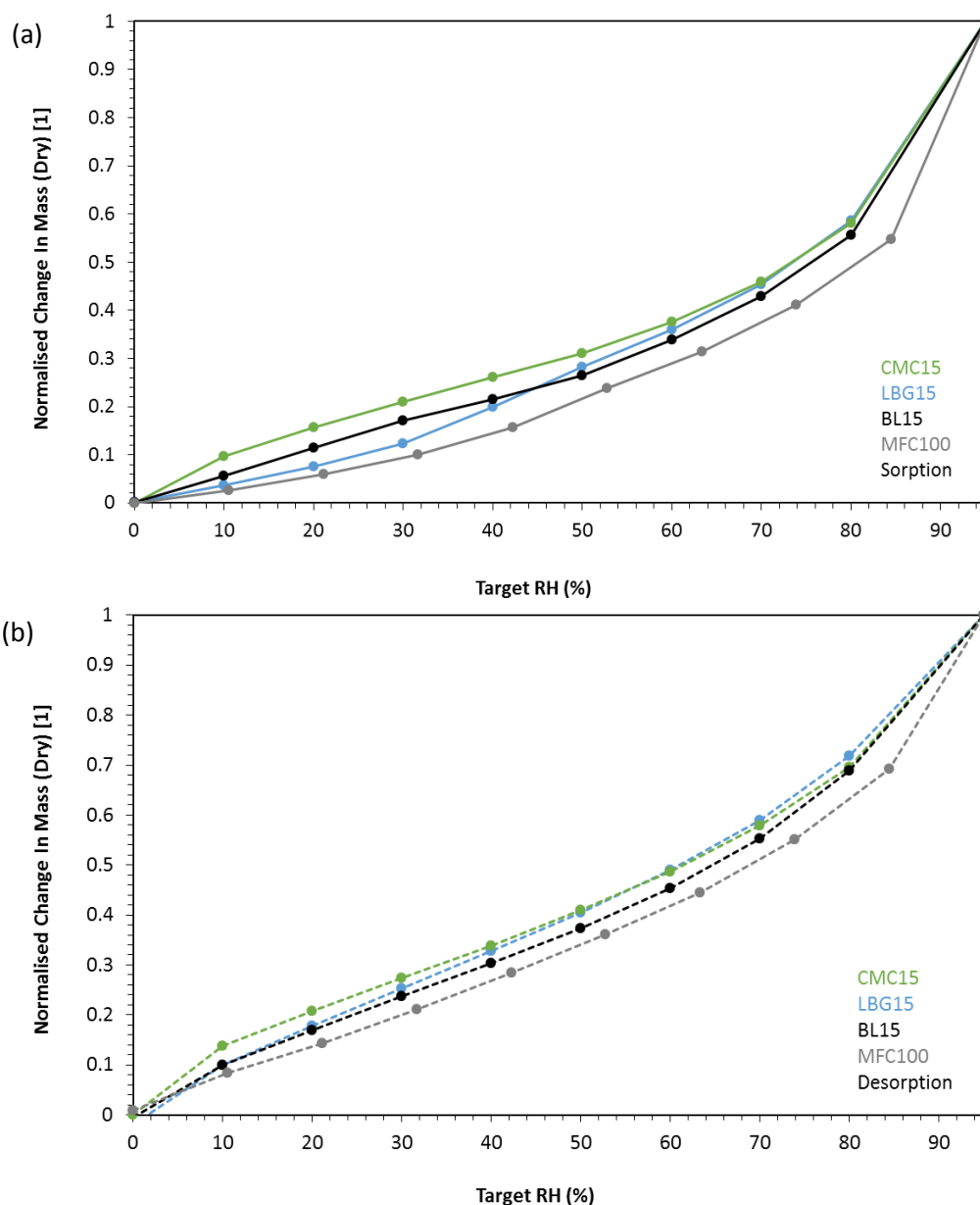


Figure 4.15: Sorption and desorption isotherms of different BMFC/additives powders (BMFC/CMC, BMFC/LBG, BMFC/Blend (BL1) and MFC100) obtained under dynamic conditions at 20°C temperature. Data presented is highly reproducible with a standard deviation less than 0.1%.

The BMFC/CMC system is able to take up more water (increase in mass) than the other systems, with increasing RH, and is able to retain that water upon drying of the system (desorption, Figure 4.15b). The next most effective system on sorption is the system containing the blend of CMC and LBG.

The LBG containing system is interesting as, at low RH levels, it is not much better than MFC alone. However, at RH~40% it then maps onto the blend, and at higher RH to that of BMFC/CMC. This suggests the finding of DSC and DTGA in that BMFC/LBG requires a higher water content to be effective at changing the MFC properties. Upon submitting the systems to drying (desorption, Figure 4.15b), there appears to be an ad-desorption hysteresis for all systems. While the BMFC/CMC system is most effective at retaining the water, the hysteresis is greater for BMFC and BMFC/LBG. Again this suggests that the water in the BMFC/CMC system is interacting, but can be removed successfully at elevated temperatures (100°C peak in DTGA curves), and that the water taken up by the BMFC/LBG system is more tightly “associated” (e.g., lack of a discernible 100°C peak for the low moisture content samples in Figure 4.13b) and not free for evaporation at elevated temperatures.

A translation of this finding into the much higher water content systems shown in the rheology and water mobility studies discussed earlier in this

chapter then may explain further the lower T_2 values of the aggregated/agglomerated, poorly dispersible LBG containing materials.

4.4 Conclusions

The addition of polymeric additives such as CMC, LBG and Blend (LBG:CMC) significantly improved the redispersibility of the dry material, which reflects its overall physical properties of the system. The addition of negatively charged CMC, a blend of LBG and CMC resulted in the maximum recovery of viscoelastic properties and shear viscosity upon drying as compared to LBG at comparable MFC/additive ratios. However, the amounts of additive present in the system also had a noticeable impact on viscoelastic properties of the suspensions. Both polymeric additives *i.e.* CMC and LBG form a surface coating on microfibrils (binds to cellulose) which protects the fibres to form strong inter-/intra-molecular hydrogen bonds upon drying process.

The reduced amount of fibril aggregates and proper redispersibility of the system results in higher mobility of water in the network structure of MFC. Even though promising results were observed in terms of redispersibility and recovery of viscoelastic properties with a blend of CMC/LBG as an additive, however, optimisation of formulation is required can be subjected to future

work. The results presented also showed the active involvement of polymeric additives in the formation of liquid crystalline structures by semi-flexible polymers when added to MFC in low moisture environments and offers an insight into the theory of synergistic interactions on the surface of cellulosic fibres, protecting the agglomeration of microfibrils present in the highly fibrillated suspension.

Chapter 5

Impact of Polymeric Additives on Stabilisation of MFC added “before” the Homogenisation

5.1 Introduction

The main purpose of the present chapter was to examine the impact of the polymeric additive on the degree of fibrillation and the interaction with MFC when the two components were co-processed. It is proposed that when the polymeric additives are added prior to homogenisation, the co-processing of the two components results in greater surface interaction and altered properties of the mixtures. Abbaszadeh *et al.* (2014) have recently shown that ball milling cellulose in the presence of polymeric additives can alter the crystallinity of cellulose in low water environments. Therefore, it is reasonable to assume that such additives might alter the properties of cellulose during a fibrillation process.

The addition of the CMC during mechanical fibrillation of bacterial cellulose to produce cellulose microfibrillar dispersions was first investigated by Veen *et al.*, (2014). It was reported that the presence of CMC during mechanical fibrillation resulted in gel-sol and direct gel-liquid crystalline structure transitions in dispersions. However, the change in microstructure after drying and the redispersibility of the dry product were not studied in the case of softwood spruce cellulose pulp. Hence the current work was aimed at understanding the structural impact of different polymeric additives such as

CMC, LBG and a Blend of CMC and LBG on the processing of cellulosic suspensions, and a direct comparison with the addition of these materials post-fibrillation, as reported in the previous chapter.

5.2 Materials and Methods

Materials used for this study are described in Chapter 2.

5.2.1 Sample preparation

Mixtures of pure softwood spruce cellulose and polymeric additives were prepared by the addition of 2% w/w CMC (mix), LBG and Blend to MFC at a ratio of 85:15 (85%MFC/15%additive). 0.4% w/w LBG solution (low viscosity) *i.e.* LBG(LV) was prepared by using the standard protocol as described in section 2.3.3 for MFC/LBG(LV) formulation. CMC(mix) is composed of two CMCs *i.e.* 75%CPKA/25%DW, whereas Blend (BL) is composed of 75%CMC/25%LBG, both solutions were prepared using the standard protocols described in chapter 2. These mixtures were passed through a Microfluidics homogeniser (Microfluidics Processor M-700) with a z-chamber with pressure at 2000 bar. All the mixtures were passed through the homogeniser three times, and after each pass 500 gm of the sample were collected and coded as mentioned in Table 5.1. A pH of 6.8 was maintained and all samples contained 0.02% w/v sodium azide to prevent bacterial contamination. The

concentration of all samples was determined by the dry weight. All of the MFC/additive mixtures were analysed in a wet and dry state. Only a single batch of samples was prepared for this set of work due to a limited time at the sponsor's production site, but all analyses were carried out in duplicate. The MFC/additive mixtures were dried according to the standard protocol, as described in chapter 2. All dry MFC samples were redispersed in distilled water using a high shear overhead mixer (Ultraturrax, UK) at 15000-18000 rpm for 4 mins. The same process step was also applied to the never-dried MFC. All of the samples were stored on a roller bed overnight before analysis.

Table 5.1: The MFC/additives formulation, the number of passes through the homogenisers and the sample code.

Sample Code	MFC/Additive	No. of Passes
MFC/CMC:1P	CMC(mix) (2%)	1
MFC/CMC:2P		2
MFC/CMC:3P		3
MFC/LBG:1P	LBG (2%)	1
MFC/LBG:2P		2
MFC/LBG:3P		3
MFC/LBG(LV):1P	LBG (0.4%)	1
MFC/LBG(LV):2P		2
MFC/LBG(LV):3P		3
MFC/BL:1P	BL (2%)	1
MFC/BL:2P		2
MFC/BL:3P		3

5.2.2 Microscopy

Light microscopy was used to study the microstructure of aqueous suspensions according to the method detailed in chapter 2, section 2.4.6.

5.2.3 Rheology

Rheological data presented is an average of 4 replicates and was measured according to the method detailed in chapter 2, section 2.4.1.3.

5.2.4 Differential Scanning Calorimetry (DSC)

Differential Scanning Calorimetry was performed according to the method detailed in chapter 2, section 2.4.4.

5.2.5 Derivative Thermo-gravimetric analysis (DTGA)

DTGA thermograms were measured according to the method detailed in chapter 2, section 2.4.5.

5.2.6 Wide angle X-Ray diffractometry (WAXD)

Crystallinity data presented is an average of 2 replicates and was measured according to the method detailed in chapter 2, section 2.4.3.

5.2.7 Relaxation NMR

Spin-spin relaxation time (T_2) data presented is an average of 4 replicates and was measured according to the method detailed in chapter 2, section 2.4.2.

5.2.8 Dynamic Vapour Sorption (DVS)

Dynamic vapour sorption isotherms were measured according to the method detailed in chapter 4, section 4.2.7.

5.2.9 Data Analysis

Statistical data analysis was performed by using software Excel (Microsoft 2013, USA). Correlation analysis was performed to investigate the relationship between physical parameters (viscosity, complex viscosity, crystallinity, spin-spin relaxation time *etc.*) and a number of passes through homogeniser and different drying techniques using analysis of variance (ANOVA) with a significance level defined as $p\text{-value} < 0.05$.

5.3 Results and Discussion

5.3.1 Microstructure of suspensions

In the earlier chapter 3, it was concluded that the fibrillation techniques used to produce the MFC (without additive) have a noticeable impact on the degree of fibrillation. As the number of passes through the homogeniser increased, the degree of fibrillation *i.e.* the amount of microfibrils released from the mother fibre increased in the suspension. Similar microstructures were observed with MFC/additive (never-dried) suspensions (Figure 5.1) when polymeric additives were added before homogenisation and mixtures were passed 3 times through the microfluidics homogeniser. However, it was also observed that depending on the type of additive used the degree of fibrillation of MFC was affected (Figure 5.1).

Homogenisation of cellulose pulp in the presence of CMC resulted in MFC suspension with a similar degree of visible fibrillation to MFC100 (compared Figure 5.1a to Figure 3.1). It is also observed in Figure 5.1ai that the 1Pass MFC/CMC suspension contained fewer fibre bundles compared to 1Pass MFC100 (Figure 3.1), and the degree of fibrillation was further increased with consecutive passes through homogeniser. Whereas a lower degree of fibrillation and larger fibril aggregates were observed when MFC was produced in the presence of LBG (MFC/LBG:1P in Figure 5.1ci). However, as the number of passes increased the degree of fibrillation increased (Figure 5.1cii and 5.1ciii).

Hence to control the effect of LBG viscosity on the degree of fibrillation, a lower viscosity LBG solution *i.e.* LBG(LV) (at 0.4% w/w concentration) was added to 2% w/w cellulose-pulp prior to homogenisation. The microscopy images presented in the Figure 5.2ai, show that never-dried MFC/LBG(LV):1P suspensions appeared to have a similar degree of fibrillation like MFC/LBG:1P (Figure 5.1ci), but with an increase in the number of passes through the homogeniser the fibrillation seemed to approach that of MFC/CMC (Figure 5.1a). This indicates that the viscosity of LBG affected the degree of fibrillation when co-processed.

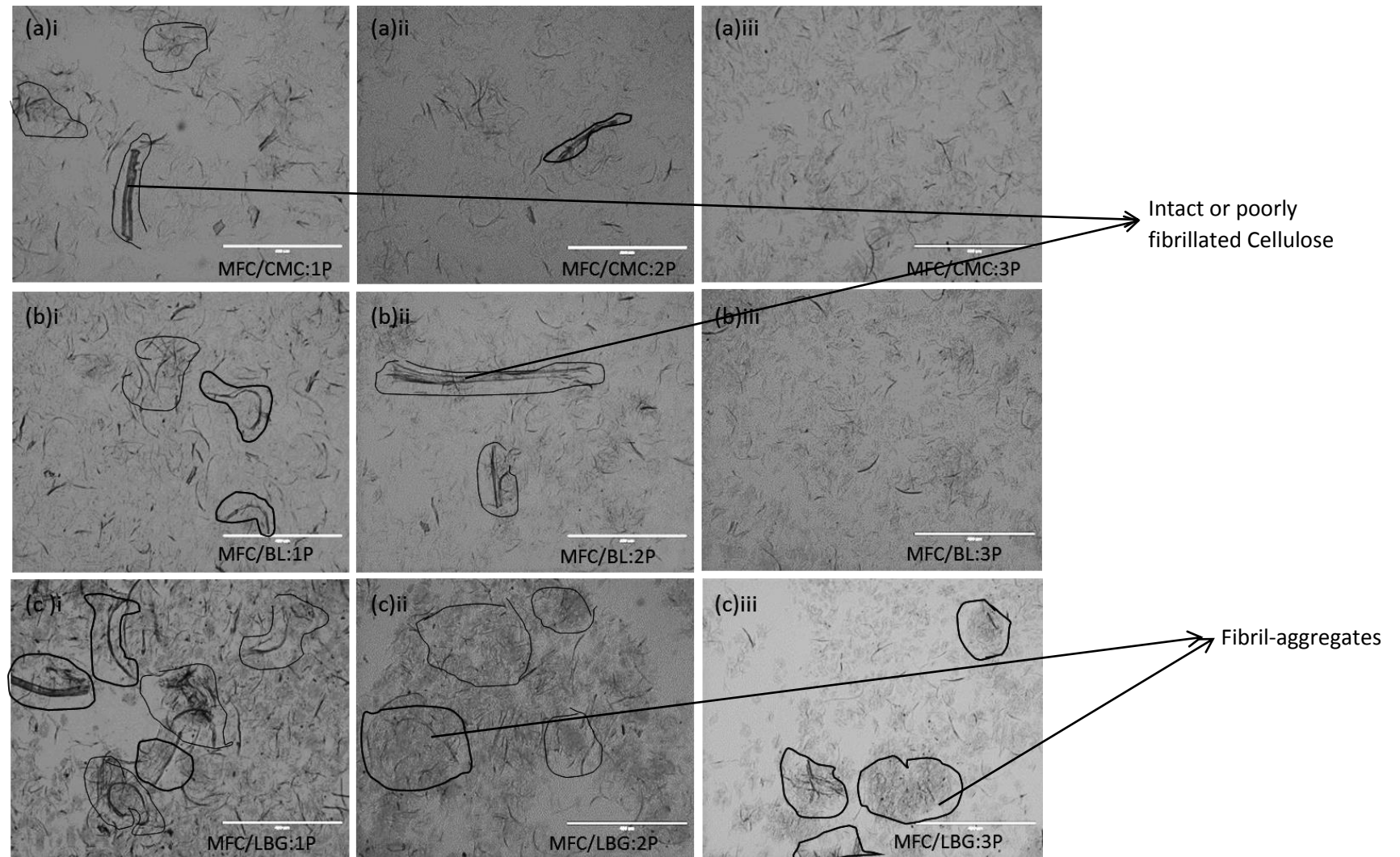


Figure 5.1: Light microscopy images of aqueous suspensions (2% w/w) of never-dried (wet) MFC produced in the presence of different additives: (a) CMC(mix), (b) Blend (BL), and (c) LBG; after (i) 1Pass, (ii) 2Pass, and (iii) 3Pass through homogeniser; scale bar: 200 μm .

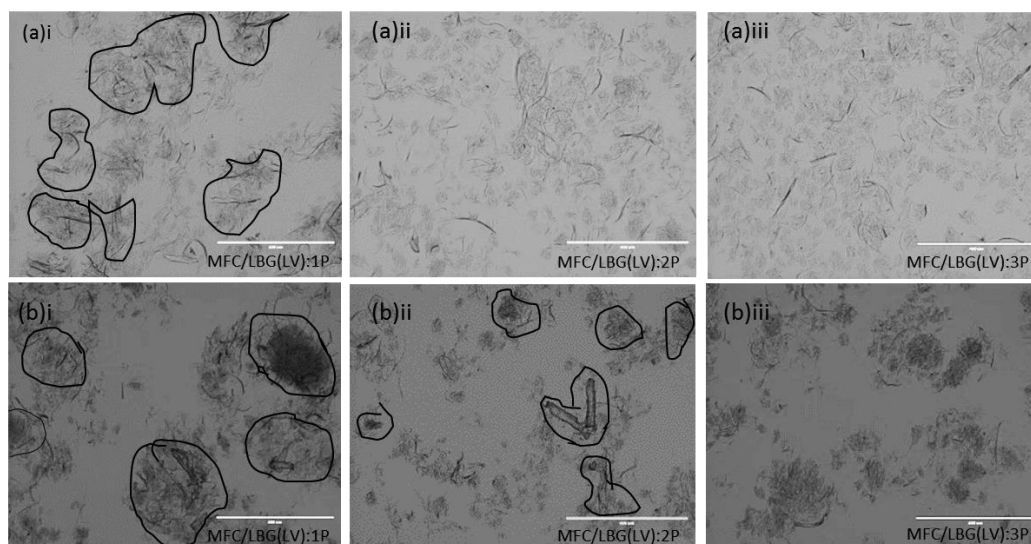


Figure 5.2: Light microscopy images of (a) never dry (wet) and (b) dried and redispersed aqueous suspension of MFC/LBG(LV) (low concentration/viscosity i.e. 0.4% w/w) after (i) 1 Pass, (ii) 2 Pass, and (iii) 3 Pass through homogeniser.

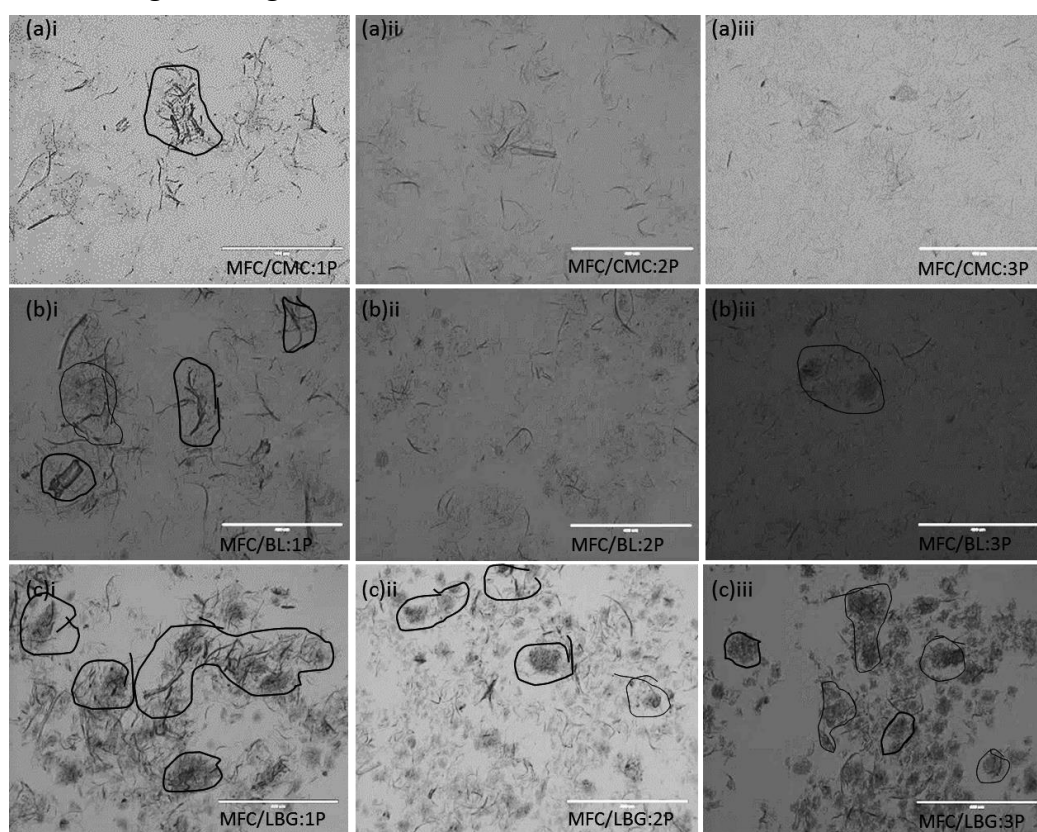


Figure 5.3: Light microscopy of 2% w/w aqueous suspensions of dried and redispersed MFC with different additives: (a) CMC(mix), (b) Blend (BL), and (c) LBG after (i) 1 Pass, (ii) 2 Pass, and (iii) 3 Pass through homogeniser.

Figure 5.1b shows the microscopy images of MFC produced in the presence of a BL *i.e.* blend of CMC:LBG. These images show an intermediate effect on the degree of fibrillation as compared to MFC/CMC and MFC/LBG. These microstructures indicate that the degree of fibrillation depends on the type of polymeric additive used in the system during mechanical co-processing, due to a combination of surface interaction between cellulosic fibres: additive and solution viscosity. It appears that high solution viscosity *e.g.* LBG (2% w/w) reduces the shear experienced by the cellulose upon homogenisation resulting in a lower degree of fibrillation.

A further processing step for all of the aqueous suspensions was drying and rehydration. Microscopy images of redispersed MFC/additive formulations are presented in Figure 5.2b and Figure 5.3. All dry samples *i.e.* MFC/CMC, MFC/LBG and MFC/Blend were easier to redisperse in water to form homogeneous suspensions than those studied in chapter 3 and 4 (visual observation). Comparing all 3Pass samples, the aqueous suspensions of MFC/CMC showed the least number of microfibrils aggregates. Similar microstructures of MFC/CMC microfibril-networks were observed when CMC was added before or after homogenisation (compare Figure 4.2 and Figure 5.3a).

From the microscopy images, the assumption can be made that the addition of CMC (independent of the point of addition *i.e.* before or after homogenisation) protects an aggregation of microfibrils during the drying process, resulting in a homogenous and entangled microfibrils suspension. Similar results were observed with MFC/Blend redispersed suspensions, where a few smaller aggregates were observed inherited from the never-dried MFC/Blend suspension (Figure 5.2b and 5.1b). The addition of LBG (2% or 0.4% w/w) prior to homogenisation does not protect the microfibrils against aggregation during the drying (Figure 5.2b and 5.3c), as compared to the MFC/CMC and MFC/Blend (Figure 5.3a and Figure 5.3b). After drying the microfibrils collapse and form larger microfibril aggregates independent of LBG concentration as compared to MFC/LBG systems when LBG is added after homogenisation (Figure 4.2). Besides a low degree of fibrillation and microfibril aggregation, the dry MFC/LBG powders (1 to 3 Pass) were easier to redisperse in water, when compared to the MFC/LBG system when the additive was added after homogenisation (visual analysis).

In chapter 3, it was reported that MFC produced by using a conventional homogeniser (microfluidiser or refiners) showed a maximum loss in crystallinity after 1Pass. After consecutive passes (*i.e.* 2P and 3P) through the

homogeniser no further effect on the crystallinity of the system was noted (Figure 3.5). Similar results were observed when MFC was produced in the presence of additives, where the maximum loss in crystallinity was observed after 1Pass and no further reduction is observed on consecutive passes through homogeniser (Figure 5.4). However, higher cellulose crystallinity is observed when additives are added prior to homogenisation.

After 1pass MFC100 showed crystallinity around 35%, whereas MFC/additive mixtures, independent of additive type when added before homogenisation, showed crystallinity values around 45% (Figure 5.4). Indeed, Abbaszadeh *et al.* (2014) showed that the presence of some polymeric additives protects the crystallinity of the cellulose during a harsh milling (ball milling) process when co-processed at low moisture. The results presented here indicate that the addition of polymeric additives protected the crystalline region of cellulosic microfibrils during high-shear homogenisation in the wet state. This can be explained by a surface interaction between MFC and additives which was observed in fluorescence microscopy images presented in chapter 4 (Figure 4.11) and supports the observations made by light microscopy.

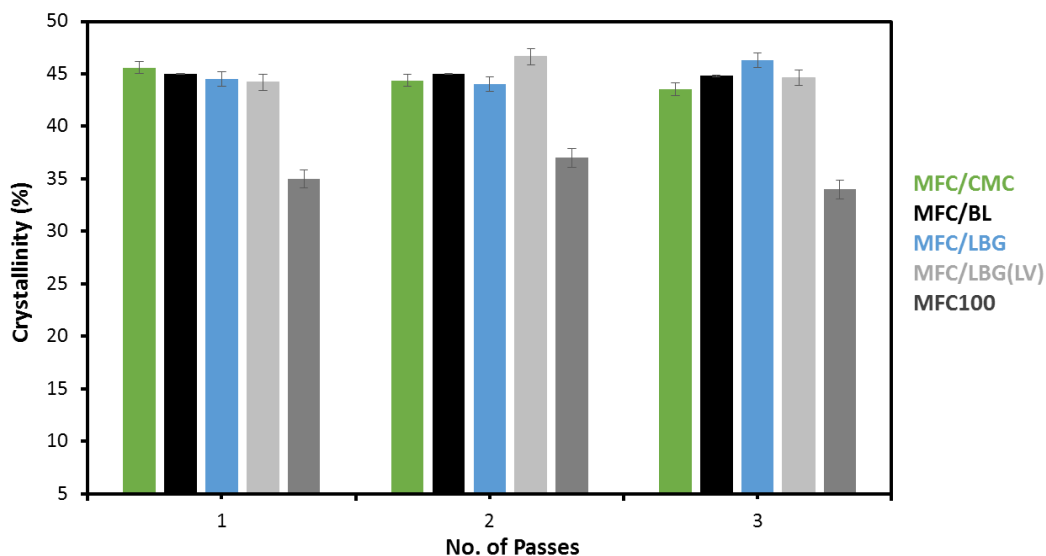


Figure 5.4: Crystallinity of MFC100 and MFC/additives when added before homogenisation as a function of a number of passes (1, 2 and 3 Passes) through microfluidic homogeniser. The data presented is an average of duplicates and is highly reproducible.

5.3.2 Rheological properties of MFC/additive suspensions

5.3.2.1 Viscoelastic behaviour MFC/additive suspensions

The aqueous suspensions of co-processed, dried and redispersed MFC/additive systems after 3 passes through a microfluidics homogeniser *i.e.* MFC/CMC, MFC/LBG and MFC/Blend, at 2% w/w concentration were subjected to frequency (Hz) ramping (Figure 5.5a). All suspensions showed viscoelastic gel-like behaviour as the storage modulus (G') was higher than the loss modulus (G'') with little dependence on frequency. This viscoelastic behaviour was consistent with BMFC suspensions when polymeric additives were added after homogenisation (in comparison with CMC15, LBG15 and

BL15 in Figure 4.1). Slight differences in G' and G'' were observed between additives added to MFC before and after homogenisation, which is likely due to the difference in the microstructure of the two systems.

Storage and loss moduli as a function of temperature for 2%w/w MFC/additive suspensions are shown in Figure 5.5b. All suspensions showed viscoelastic gel-like behaviour with increasing temperature (20-90°C) independent of the number of passes through the homogeniser. All redispersed suspensions showed first a slight decrease in both moduli up to 40°C and then an increase after 45°C up to 90°C while maintaining viscoelastic gel-like behaviour. These results are similar to MFC suspension when polymeric additives were added after homogenisation (compare with CMC15, LBG15 and BL15 in Figure 4.8). Thermal induced structural transitions, the formation of inter-connected microfibril networks and swelling of microfibrils during heating could be possible reasons for the changes in G' and G'' with increasing temperature.

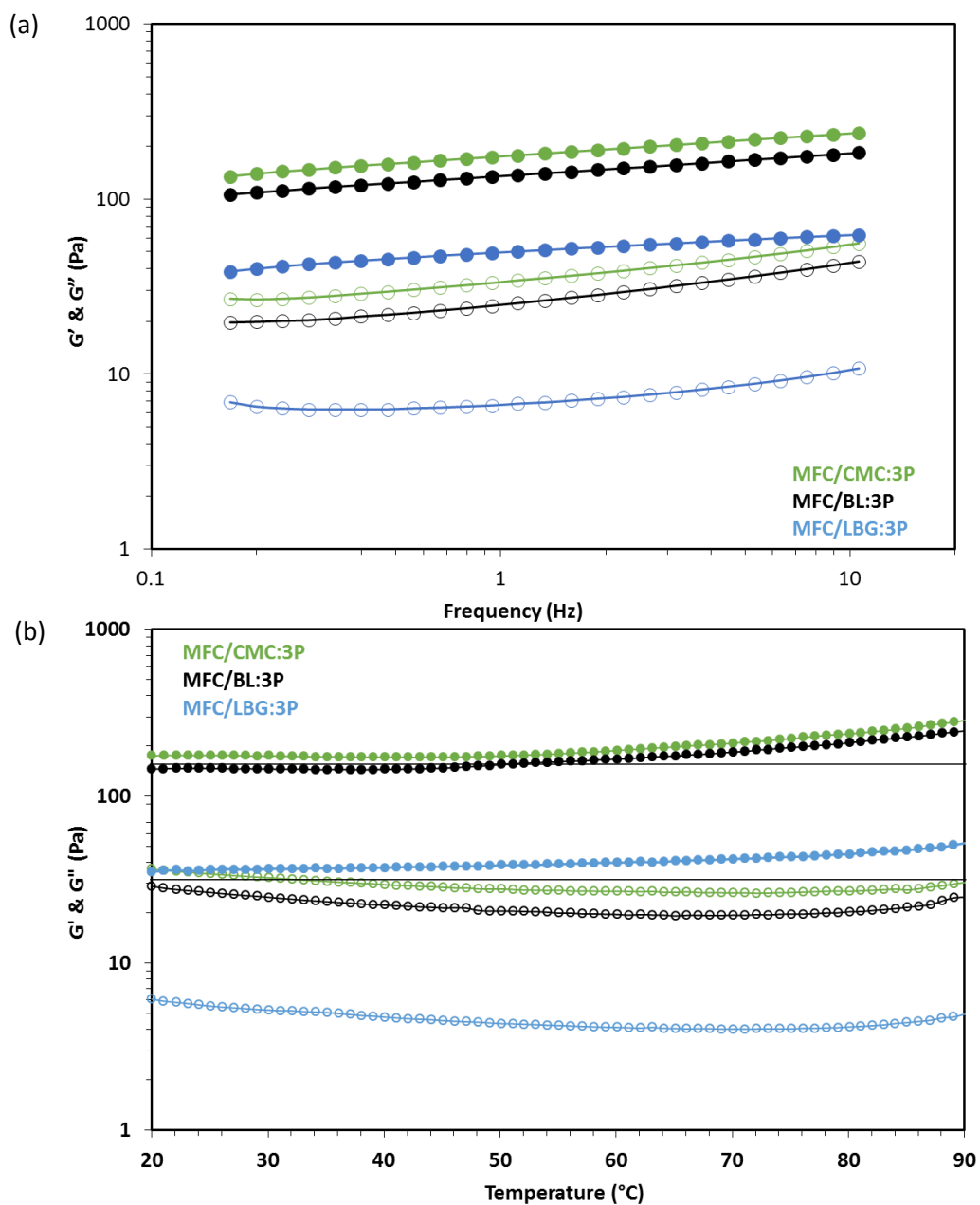


Figure 5.5: Storage (G' , -●-) and loss (G'' , -○-) modulus of dried and re-dispersed suspensions of MFC/CMC, MFC/LBG and MFC/BL after 3 Pass; as a function of (a) frequency (Hz) at 20°C and strain 0.2%, (b) temperature ($^{\circ}\text{C}$) at $1^{\circ}\text{C}/\text{min}$ heating rate at frequency 1 Hz and strain 1%. The overall concentration of all suspensions was 2% w/w. The data presented is an average of replicates with a standard deviation $\pm 1\%$.

As mentioned in the previous chapter, the recovery of viscoelastic parameters and shear viscosity after drying and redispersing depends on the type of additives used to stabilise the microfibrils in the system. A similar dependence of functional recovery on the MFC formulations was observed when polymeric additives were added before homogenisation (Figure 5.6a and 5.6b). Redispersed MFC/CMC suspensions showed a 20% reduction in complex viscosity after drying as compared to the never dry suspension. A similar behaviour was observed with BMFC/CMC (85:15) suspensions in chapter 4, which indicates that the addition of CMC before or after homogenisation has the same impact on complex viscosity. However, better redispersibility was observed when added before homogenisation and a noticeable increase in complex viscosity was observed when comparing MFC100 with MFC/CMC:3P. Similar behaviour was observed with 1Pass and 2Pass materials. The blend of CMC/LBG as an additive in the MFC suspensions (*i.e.* MFC/BL) also showed similar redispersibility and increase in complex viscosity over MFC100 (complex viscosity of dried and redispersed MFC100 is 5.43 Pas as reported in chapter 4).

Aqueous suspensions of never-dried MFC/LBG at both levels of LBG addition, after 1Pass and 2Pass through the homogeniser showed very high complex

viscosity as compared to both never-dried MFC/CMC and MFC/BL suspensions. This can be explained by a greater amount of fibril bundles/microfibrils aggregates in the suspension (Figure 5.1c and Figure 5.2a). Higher and non-homogenous fibril size leading to wall slip or wall depletion are well known in particulate systems and this could be a reason for the higher complex viscosity. These results also indicates that the high degree of fibrillation is important in order to achieve a homogeneous network structure with stable viscosity. In order to achieve this high number of passes through the microfluidics technology is recommended for MFC/LBG formulations. While comparing never-dried and redispersed suspensions a significant reduction (approximately 80%) in complex viscosity was observed independent of the number of homogeniser passes, indicating that any cellulose:LBG interactions cannot prevent aggregation of microfibrils upon drying; however these interactions were stable enough to improve redispersibility of dried product.

When comparing the viscoelastic parameters such as G' , G'' and complex viscosity of the different dried and redispersed MFC/additive formulations (Figure 5.5a and 5.6b), it is evident that the charged CMC (either alone or in a blend with LBG) showed higher complex viscosity as compared to MFC with

LBG after 2Pass and 3Pass (statistically significant p-value = 0.016; alpha: 0.05).

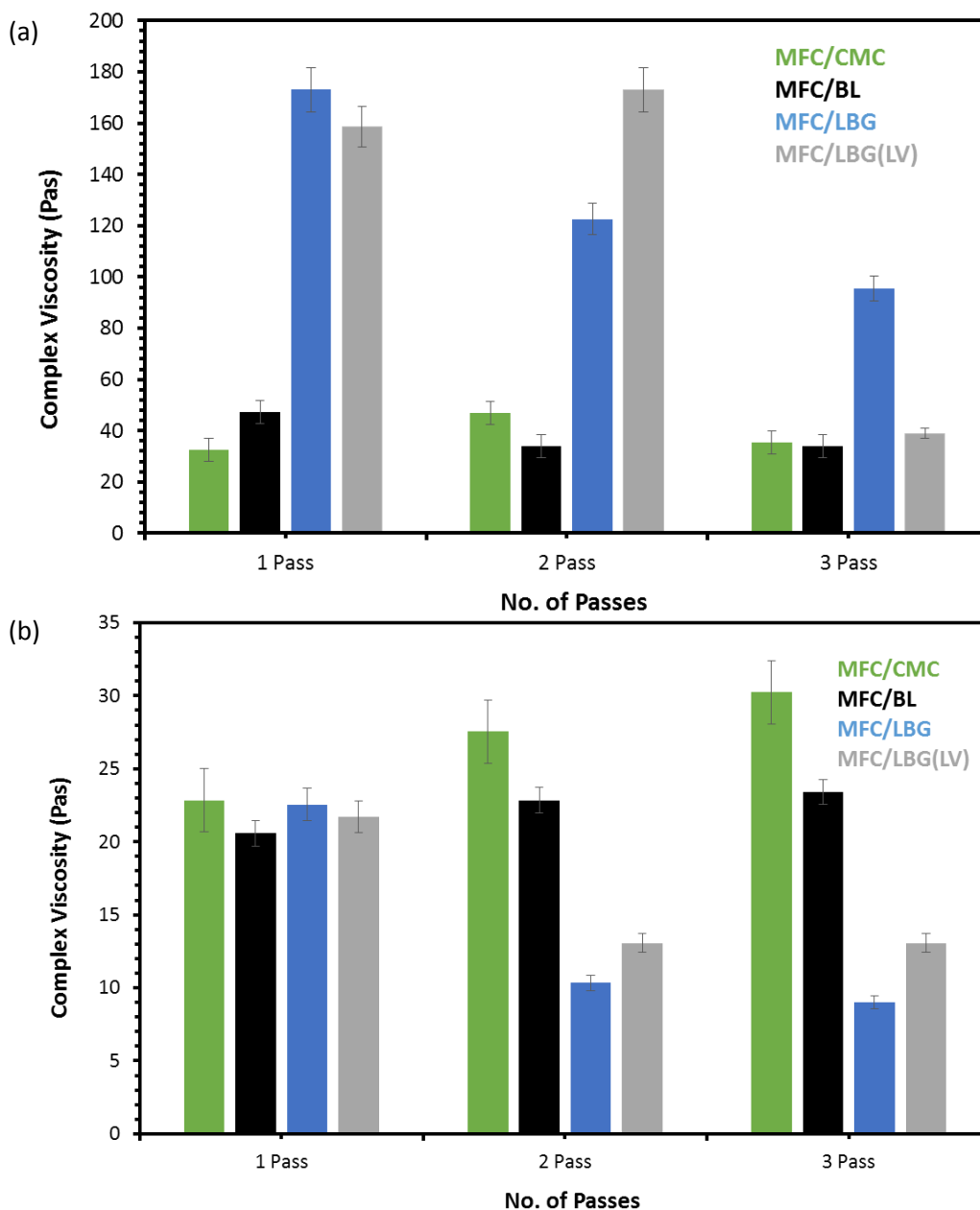


Figure 5.6: Complex viscosity as a function of number of passes through the homogeniser at 0.2% strain and 1Hz frequency at 20°C of 2% w/w suspension of MFC/CMC, MFC/LBG (HV and LV) and MFC/BL, where (a) never dry suspension, and (b) dried and redispersed suspension. The data presented is an average of replicates. Note: for proper visual comparison different Y-axis scale was used.

This viscoelastic behaviour is consistent with results presented in chapter 4, comparing different additives added after homogenisation. There are two possible explanations for the behaviour of the MFC/CMC and MFC/BL formulations. Firstly, the presence of negatively charged additive in the suspension protects the microfibrils from collapsing during the drying stage and, hence resulted in a good recovery of the microfibrils network. Secondly, consecutive passes through the homogeniser resulted in a decrease in the larger microfibril aggregates, explaining the slight increase in complex viscosity (Figure 5.3 and Figure 5.6b).

In the case of the MFC/LBG system, aggregates formed by stable inter and intra-molecular hydrogen bonds between the polymers and the microfibrils were difficult to redisperse as compared to MFC/CMC and MFC/BL, and resulted in a lower complex viscosity for MFC/LBG (comparing 2Pass and 3Pass samples). The complex viscosities of dried and redispersed MFC/additives in suspensions were similar to the suspensions produced when the polymers were added after homogenisation. Similar complex viscosities were observed when comparing the redispersed suspensions of MFC/CMC, MFC/LBG with CMC15 and LBG15 (Figure 4.3 and 4.5b), and lower than BL15 (Figure 4.8). However, the difference in the technology used to produce MFC

and its influence in microstructure cannot be discounted while interpreting the rheological properties of these suspensions.

5.3.3 Impact of additives on water mobility

The spin-spin relaxation times (T_2) as a function of a number of passes through the homogeniser for 2%w/w redispersed suspensions of MFC/CMC, MFC/LBG, MFC/LBG(LV) and MFC/Blend are presented in Figure 5.8. Figure 5.8 shows that the number of passes through the homogeniser did not have a statistically significant effect on the T_2 values of the suspension (p -value >0.05). However, all MFC/additive suspensions showed higher T_2 values as compared to MFC100 (T_2 value: 414ms; Figure 4.9). These results are consistent with the water mobility in the network structure of MFC/additives when the polymer was added after homogenisation at comparable ratios (85:15). Lower T_2 value of MFC100 suspensions can be explained by the fibril aggregates that formed due to strong intra- and intermolecular H-bonding between the microfibrils. The presence of charged polymeric additives *e.g.* CMC and Blend (CMC/LBG) during co-processing contributed to the increase in water mobility due to charge effects and surface interactions with microfibrils, resulting in a highly dispersed microfibrils network during rehydration upon drying.

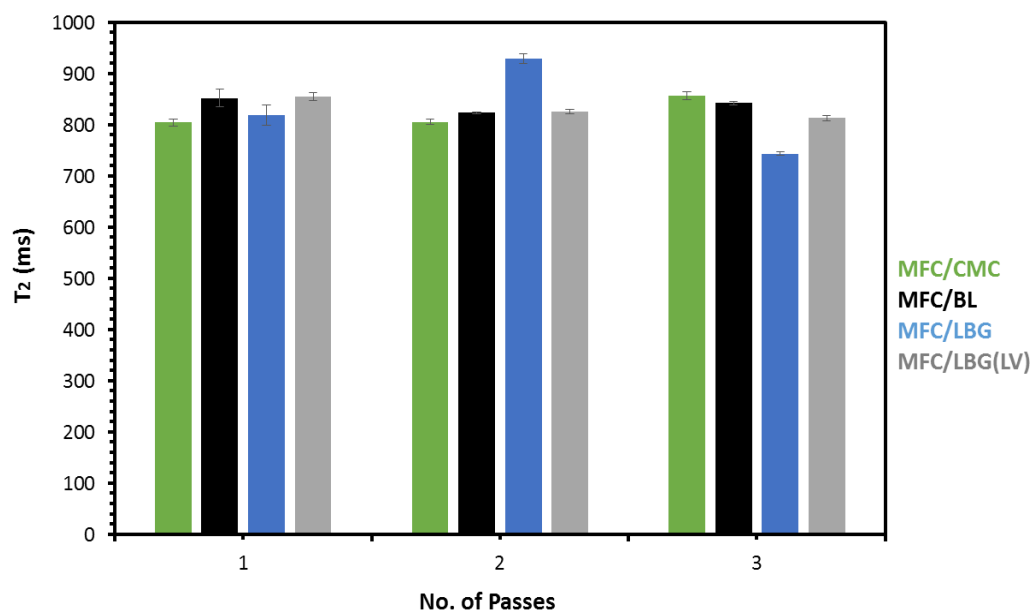


Figure 5.8: Spin-spin relaxation time (T_2 , ms) as a function of a number of passes through homogeniser of MFC/CMC, MFC/Blend, MFC/LBG and MFC/LBG(LV), measured at 20°C of overall 2% w/w overall suspension concentration. The data presented is an average of 4 replicates, highly reproducible with a standard deviation less than 0.1%.

Interestingly, MFC/LBG showed higher water mobility in the network structure compared to BMFC/LBG (when polymer added after homogenisation). The fibril aggregate structures and inhomogeneity were responsible for the lower T_2 values in the case of BMFC/LBG suspensions when LBG was added after homogenisation. It appears that the co-processing of MFC/LBG resulted in a more homogeneous microfibrils network providing improved redispersibility once dried. The reduced amount of fibril aggregates in the redispersed suspension increased the water mobility in the MFC/LBG through interstitial spaces within the microfibril network when compared

with BMFC/LBG when LBG was added post-homogenisation (Figure 4.2 and Figure 5.3c). Higher T_2 values were also observed in the case of MFC/CMC and MFC/BL redispersed suspensions. These results indicate that the co-processed MFC/additives systems produced a more homogeneous dispersion with active interactions between the two components resulting in the much-improved redispersibility and higher T_2 values as compared to MFC/additive systems when additives were added after homogenisation at comparable ratios (85:15).

5.3.4 Thermal transitions of MFC/additive at low moisture

In the previous chapter, different MFC/additive formulations at low moisture (2%w/w) showed low-temperature thermal transitions related to the water state (Figure 4.12). Similar temperature transitions were observed with MFC/additive when the additive was added before homogenisation (Figure 5.9 and Figure 5.10). The DSC thermograms of MFC/CMC, MFC/LBG and MFC/BL showed two distinct endothermic peaks independent of a number of passes through the homogeniser; the first peak between 30-40°C, and the second between 50-70°C. Both peaks disappeared during second heating, replaced by a new peak between 5-20°C (in some case between 10-20°C). Similar behaviour was noted and discussed in the previous chapter. The

absence of the 50-70°C peak in the case of MFC100 indicates that the addition of polymeric additives induces low-temperature structural transitions, *i.e.* associated with hydrogen bonding in the MFC/additive system.

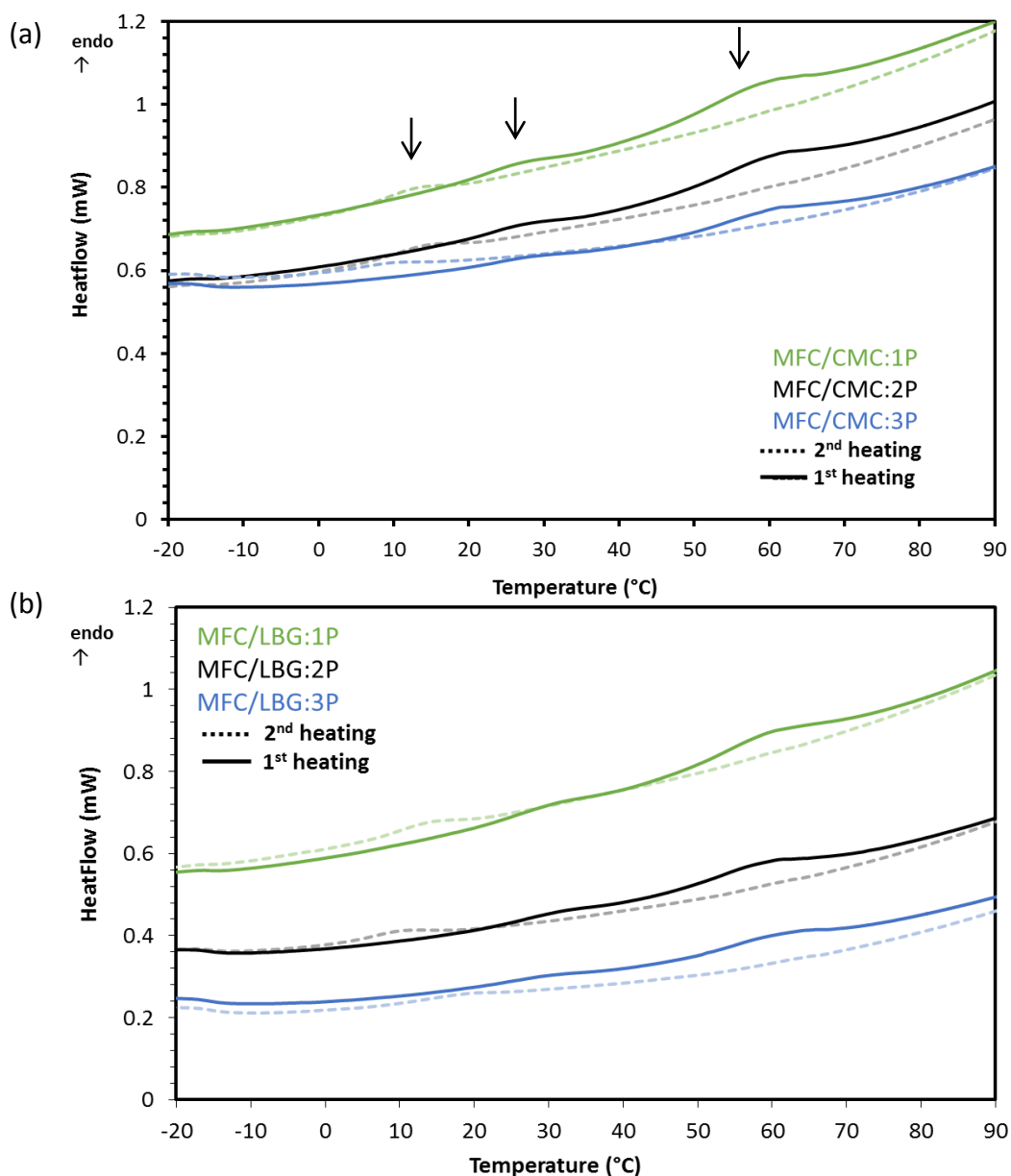


Figure 5.9: DSC thermograms of (a) MFC/CMC and (b) MFC/LBG at low moisture (2% w/w) after consecutive passes through the homogeniser (1 Pass, 2 Passes and 3 Passes). All results are highly reproducible with a standard deviation less than 0.1%.

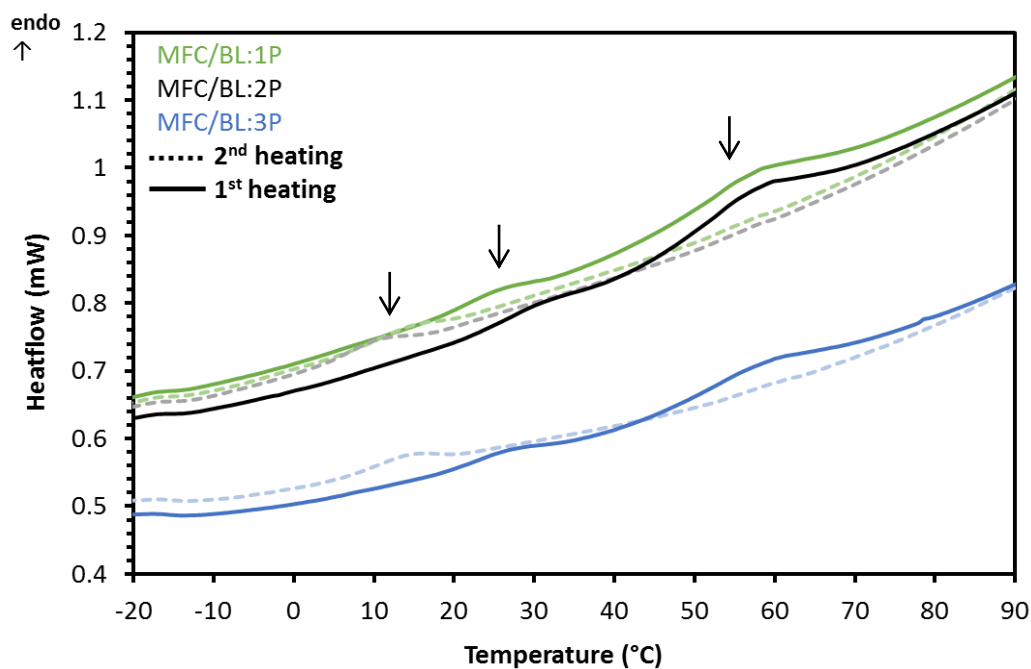


Figure 5.10: DSC thermograms of MFC/BL at low moisture (2% w/w) after consecutive passes through the homogeniser (1 Pass, 2 Passes and 3 Passes). All results are highly reproducible with a standard deviation less than 0.1%.

The endothermic transition peak between 30-40°C indicates that all MFC/additive MFC/CMC, MFC/Blend and MFC/LBG systems (independent of a number of passes) underwent thermally induced formation of the polymer/cellulose networks and a re-organisation of hydrogen-bonding influenced by the “associated water” in the system. This re-organisation is also considered as a liquid-crystal transition at low temperatures. These transitions were not observed for microfibrils aggregated structures in the case of MFC100 and BMFC/LBG (LBG added after homogenisation). An explanation for this behaviour is the presence of strong hydrogen bonds

between the microfibrils with LBG and within MFC after drying resulting in a lower amount of interacting water in the system. However, the presence of endothermic peaks when MFC was co-processed with LBG indicates the MFC's microfibrils structure incorporated LBG as a result of interactions between the two components, allowing more interacting water in the system during the drying process. The endothermic peak observed between 5-15°C in the second heating is evident for all MFC/additive-water systems. After the first heating cycle, the microstructure of the system loosened, either due to swelling or thermally induced reorganisation of interaction between the components. The DSC data, therefore, supports the theory that the co-processing of cellulose and polymeric additive mixtures had a structural impact.

Under an inert atmosphere of nitrogen using DTGA, the thermal degradation of cellulose/MFC material is characterised by one mass loss step which resulted in one peak between 300-350°C (MFC100 in Figure 5.11a), corresponding to degradation of the cellulosic components. In Figure 5.11a and 5.11b, the main degradation peak of MFC/additive presents at a temperature of 240-350°C, with a lower temperature shoulder peak at around 240°C, which is a result of the second component in the system.

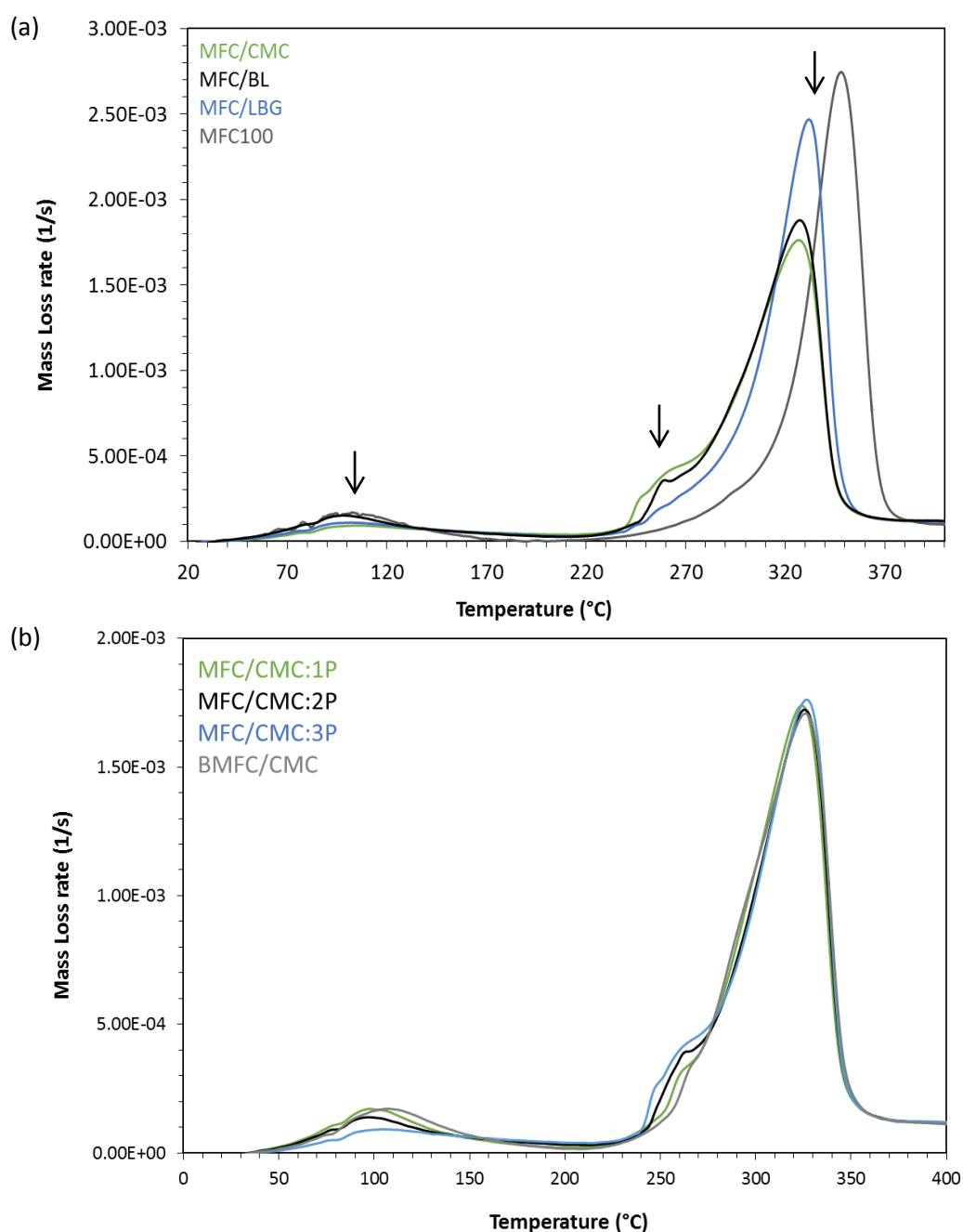


Figure 5.11: Comparison of the thermal degradation of (a) MFC/CMC, MFC/LBG and MFC/Blend (BL) after 3 Passes through the homogeniser, and (b) MFC/CMC after number of passes and BMFC/CMC under nitrogen atmosphere at low moisture content (2% w/w). All results are highly reproducible with a standard deviation less than 0.1%.

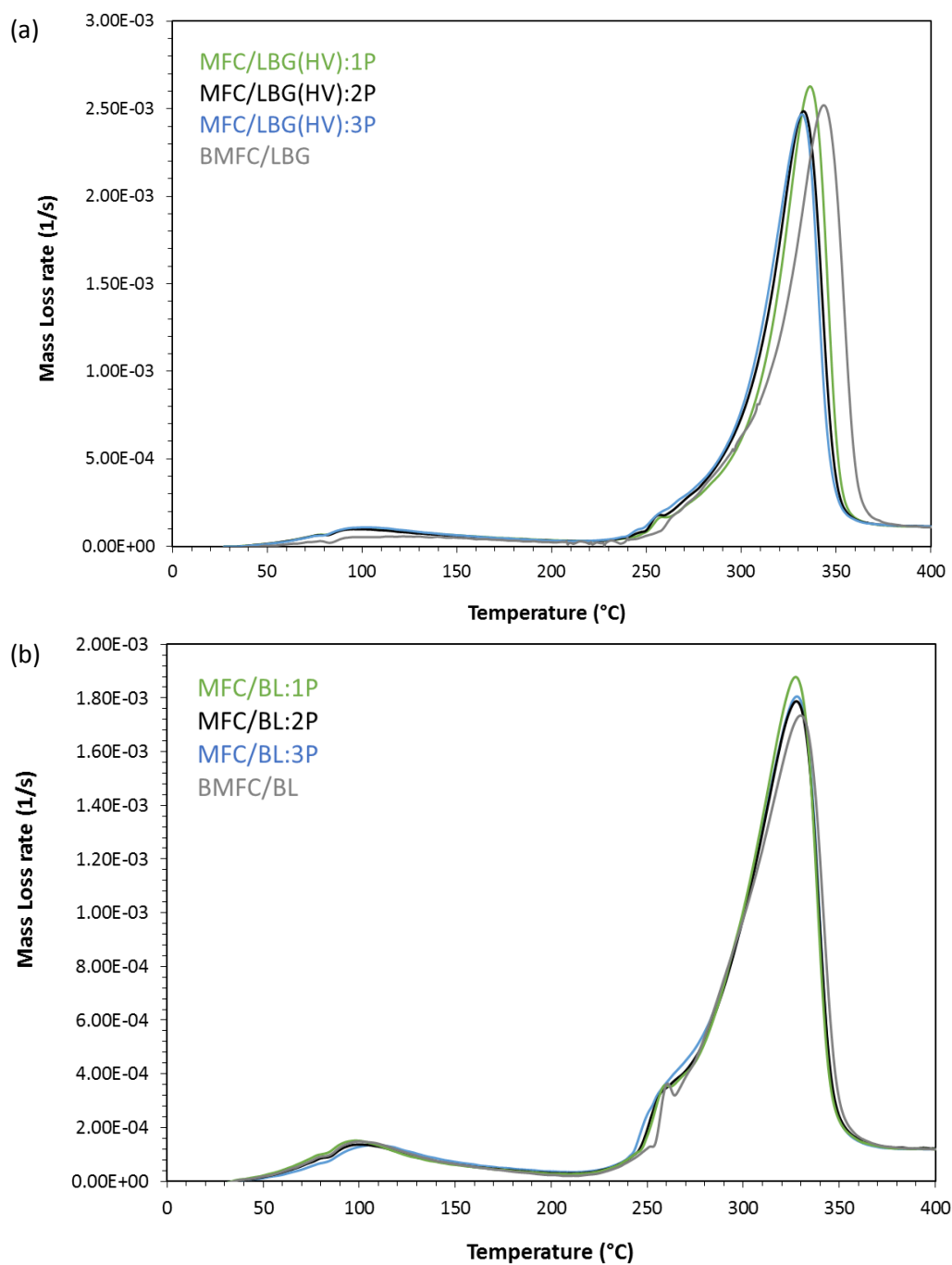


Figure 5.12: Comparison of the thermal degradation of (a) MFC/LBG, and (b) MFC/Blend after a number of passes through homogeniser, under a nitrogen atmosphere at low moisture content (2% w/w). All results are highly reproducible with a standard deviation less than 0.1%.

In this case, the second component-peak belongs to polymeric additives present in the system such as CMC, LBG and Blend. The TGA graph in Figure 5.11a shows that depending on the type of additive present in the system, the second component peak shifts and change in peak area. For instance, the synergistic interaction between MFC and CMC showed lower temperature degradation around 240°C, evident in the case of MFC/CMC and MFC/BL, whereas the presence of LBG in the MFC network shows degradation at higher temperatures close to the cellulose peak around 250°C. Similar results were observed with BMFC/LBG at the comparable additive proportion in the previous chapter (Figure 4.13).

The number of passes through the homogeniser when the two components were co-processed also had an impact on the thermal degradation of the system. For instance, it was observed that for the MFC/CMC system, as the number of passes through homogeniser increased, the peak size and area of the shoulder increased. Similar results were observed with MFC/Blend but not in the case of MFC/LBG (Figure 5.12a and 5.12b). This indicates that the interaction between MFC and CMC produced structural changes when co-processed resulting in degradation of the system at lower temperatures compared to MFC alone.

Due to intermolecular cross-linking between the polymers and the microfibrils and strong interactions between MFC and LBG during co-processing, a higher temperature is required by the system to initiate thermal degradation (Figure 5.12a). The DTGA data also supports the DSC data in showing that the interaction and resulting properties of a co-processed MFC/LBG system were different to that when LBG was added post-homogenisation. In the latter case, DTGA showed no “free/bulk” water at 50-150°C in the case of BMFC/LBG (when polymer was added after homogenisation), whereas when LBG was co-processed with MFC this peak appeared and was of similar magnitude to the system containing CMC or BL1 (Figure 5.11a).

These results correlate well with DVS moisture sorption and desorption isotherms of different MFC/additive formulations (Figure 5.13a). All co-processed MFC/additives systems showed similar water uptake (increase in mass) with increasing RH. Unlike the sorption and desorption profiles of BMFC/additives systems where additives were added after homogenisation shown in Figure 4.15a and 4.15b, BMFC/CMC was the most effective system as compared to others in terms of moisture uptake and retaining the water.

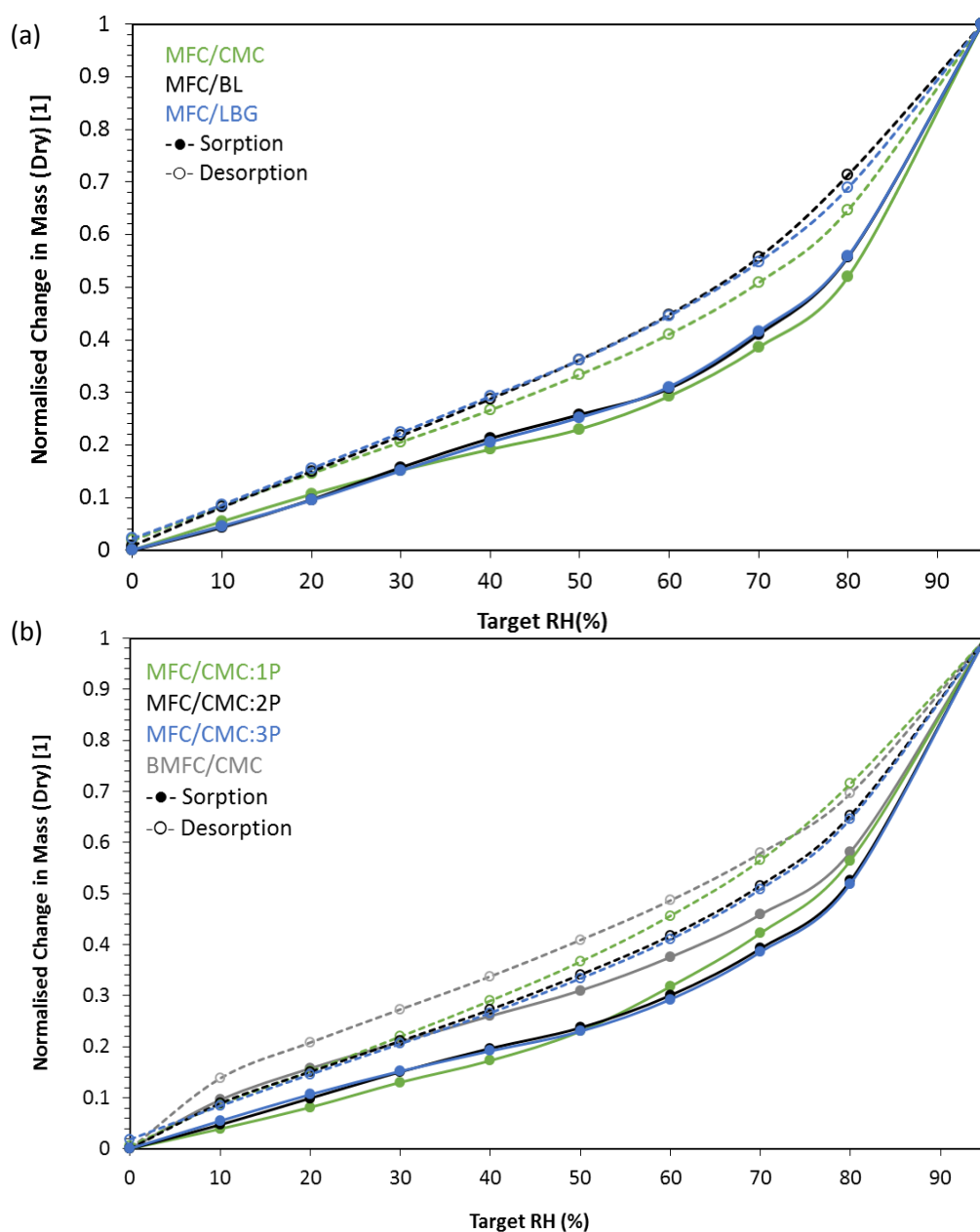


Figure 5.13: Sorption and desorption isotherms of different MFC/additives obtained under dynamic conditions at 20°C temperature, where (a) MFC/CMC, MFC/LBG and MFC/Blend (BL) after 3 Passes through the homogeniser, and (b) MFC/CMC after number of passes and BMFC/CMC.

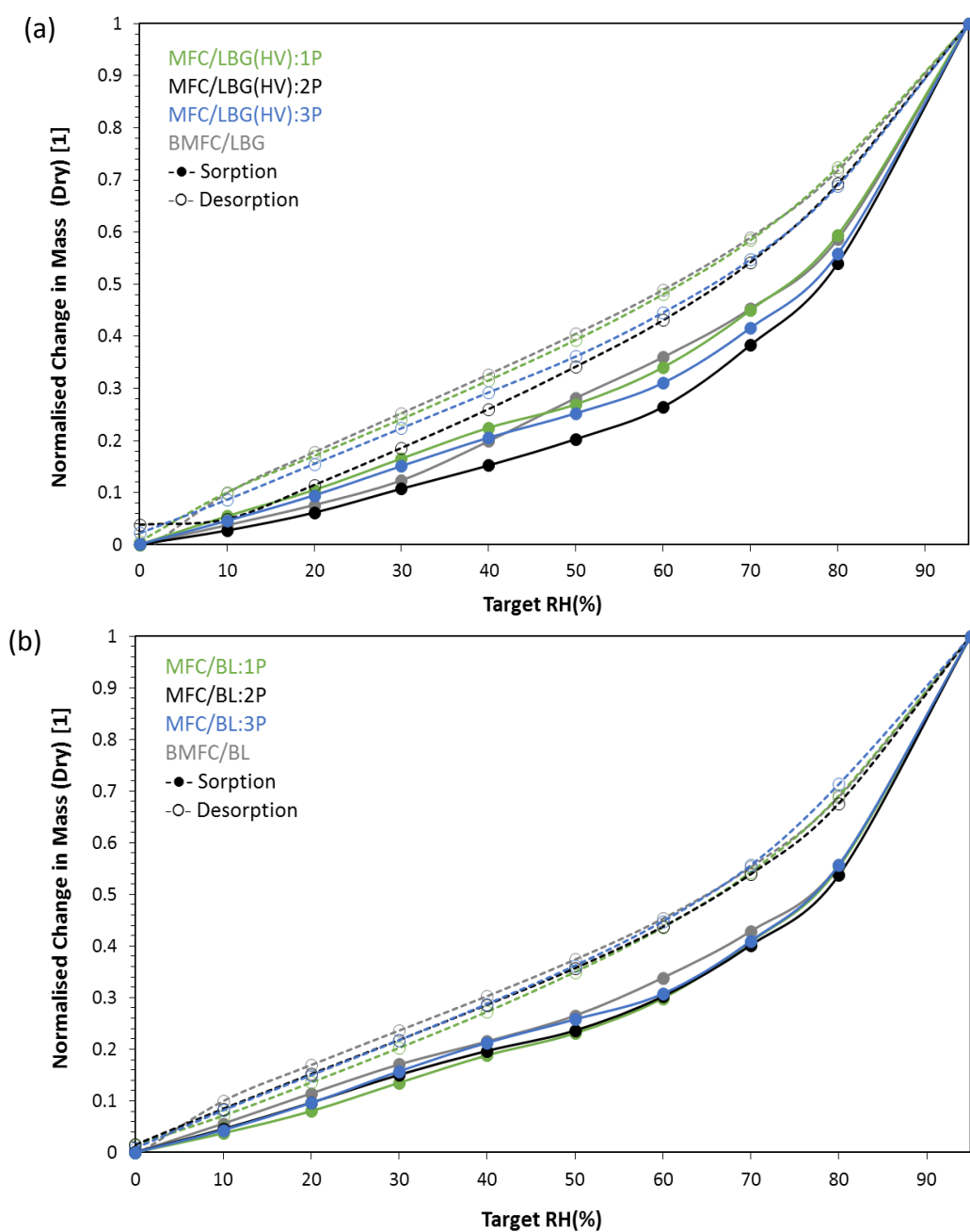


Figure 5.14: Sorption and desorption isotherms of different MFC/additives obtained under dynamic conditions at 20°C temperature, where (a) MFC/LBG and BMFC/LBG, and (b) MFC/Blend and BMFC/BL after a number of passes through homogeniser.

However, it is clearly evident in Figure 5.13b that the moisture uptake of BMFC/CMC (polymer added after homogenisation) was higher than MFC/CMC independent of a number of passes through homogeniser. Similar behaviour was observed with MFC/Blend and MFC/LBG (Figure 5.14a and 5.14b). It is well established that the moisture uptake of cellulosic material is very sensitive to crystallinity and surface area of the systems (Mihriyan *et al.*, 2004). The lowered sorption and desorption in the case of MFC/additives can also be explained by the higher crystallinity of the systems (Figure 5.4).

As explained earlier, the addition of the polymers during the homogenisation protected the crystallinity of the MFC. Systems with a higher crystallinity showed lower moisture uptake at RH below 75%. At higher RH the moisture uptake was reported to be associated with the filling of the large pore volume of the cellulose powder of higher crystallinity (Mihriyan *et al.*, 2004, Kachrimanis *et al.*, 2006). An increase in the number of passes through the homogeniser did not affect the rate of sorption and desorption of co-processed MFC/additives. For instance, it was observed that for the MFC/CMC system (Figure 5.13b), after 1Pass through the homogeniser, higher moisture uptake was observed at higher RH 50% and the system was able to retain that water upon drying (desorption). As the number of passes

increased, the system showed very similar moisture sorption and desorption. Similar results were observed with MFC/Blend and MFC/LBG (Figure 5.14a and 5.14b).

5.4 Conclusions

The co-processing of cellulose with polymeric additives such as CMC, LBG and a blend of CMC and LBG (Blend) resulted in highly fibrillated MFC/additives suspensions. Whilst there were some observable differences in the morphology between the co-processed suspensions of MFC in the presence of CMC, LBG and Blend, co-processing in the presence of LBG did not produce highly fibrillated MFC when compared with CMC and Blend. The degree of fibrillation of MFC/LBG can be increased by multiple passes through the homogeniser. Co-processed MFC/CMC and MFC/Blend were easy to redisperse in water. Suspension with fibrillated network with minimal fibril aggregates indicates that the charged CMC was a good stabilising agent for drying MFC. LBG did not decrease the aggregation of microfibrils upon drying. Interestingly, for co-processed MFC/LBG there was evidence from DSC (enhanced peak at 50-70°C and a liquid crystalline peak at a lower temperature) and DTGA (measurable “available water” between 50 -150°C)

that the structure created through interactions between MFC and LBG were different to post adding LBG.

Chapter 6

Application of MFC as dietary fibre

6.1 Introduction

Polysaccharides are used as functional ingredients in a wide range of commercial applications such as food, personal care and pharmaceutical products. In the food industry, polysaccharides are widely used as thickening, gelling, emulsifying, stabilisation and coating agents *etc.* (Foster, 2010). For these purposes different natural polysaccharides such as starch, carrageenan, guar gums and xanthan are used. Typically, a combination of two or more of these hydrocolloids is used to create a variety of microstructures to formulate stable foods with specific attributes such as acceptable mouthfeel and flavour perceptions. The processing conditions such as high shearing, heating and pumping of the polysaccharide mixtures result in the microstructures with unique rheological and sensory properties like fat mimicking (Tolstoguzov, 2003, Kokini *et al.*, 1977, Christensen, 1979).

These hydrocolloids are typically categorised as dietary fibres in the food and pharmaceutical industry. As defined by the American Association of Cereal Chemists (2000), dietary fibres refer to the edible parts of plants or analogous carbohydrates that are resistant to digestion and absorption in the human small intestine, with complete or partial fermentation in the large intestine (Tungland *et al.*, 2002). Fibres are often classified as soluble dietary fibres and

insoluble dietary fibres (Gorinstein *et al.*, 2001). These dietary fibres may consist of non-digestible carbohydrates, cellulose and lignin, that are an intrinsic part of plant cell walls (Slavin, 2003). Depending on the source of fibres, the amount of soluble and insoluble components vary, for instance, the fibre from fruits and vegetables are considerably higher in the proportion of soluble dietary fibres, whereas cereal and peel of fruits or other crops contain more insoluble components such as cellulose and hemicellulose (Herbafood, 2002). Dietary fibres play an important role in human health, where it is reported that high dietary fibre diets are associated with the prevention, reduction and treatment of some diseases, such as reducing cholesterol, and maintain gastrointestinal health (Anderson *et al.*, 1994, Gorinstein *et al.*, 2001).

The dietary fibre produced from fruit fibres (*e.g.* CitriFi and Herbacel AQ+) are widely used in various dairy products as fat replacers and in low-fat mayonnaise, salad dressing and ice-creams; also providing a fibre framework and a thickening agent. In bakery products (biscuits, croissants, muffins *etc.*) these fibres are used as fat and calorie reducing agents without compromising taste, texture and cost (Herbafood, 2002, Fiberstar, 2005). The rheological parameters such as flow behaviour and viscoelastic behaviour of the different

semi-solid food systems can be correlated with the sensory texture properties and stability of the products (Hill *et al.*, 1995, Maruyama *et al.*, 2007). Depending on the source, type and concentration of the fibres used, different rheological and texture properties can be achieved. For instance, the presence of xanthan gum improves the texture and physical shelf-life of oil-in-water emulsions such as salad dressings. Similarly, citrus fibre in combination with other stabilisers improves the physical, chemical and sensory properties of ice-cream. The suspension properties of cellulosic fibres from fruit fibres *e.g.* Citrus fibres are known to have multi-functionality (Herbafood, 2002; Fibrestar 2005). Previous chapters have shown the impact of different formulation and processing conditions on the physical properties of the MFC system, where all suspensions showed viscoelastic gel-like behaviour as a function of frequency and temperature and could be compared to the properties of the commercial dispersions.

In recent years, an increase in consumer demand for low-salt food products has been reported by the industry, due to continuous awareness from health professionals. Associations have been made between a high sodium diet and an increased risk of certain health conditions such as hypertension and cardiovascular disease (Cook *et al.*, 2007, Sacks *et al.*, 2001). Hence, due to

the World Health Organisation (WHO) recommending a daily salt intake limit of 5g, and the fact that many consumers exceed this limit (approx. > 10g) (Tian *et al.*, 2012), there is a need to improve product properties or formulations to enable salt reductions. However, salt plays many important roles in food products, not just as tastant, but also as a modification of flavour, prevention of fermentation and finally enhancement of shelf life (Lynch *et al.*, 2009). For example, in meat products, the salt contributes to water and fat binding, its reduction has an adverse effect on these parameters increasing cooking loss and weakening the texture (Ruusunen 2003). Different salt replacement strategies have been presented in the past, *e.g.* in bread NaCl was replaced with potassium or magnesium salts producing an unpalatable metallic, bitter and off-taste (Sullo *et al.*, 2014). Rama (2013) showed that the size of salt crystals has been found to influence the rate of salt release. It was reported that larger salts crystals dissolve slower than small salt crystals, prolonging the duration of tastant release, thus retaining saltiness.

It is well known that the viscosity of hydrocolloid thickened products affects the taste and flavour perception of the product with a decrease especially when hydrocolloid concentration exceeds the critical concentration *i.e.* c^*

(Baines *et al.*, 1987, Cook *et al.*, 2003, Hill *et al.*, 2008). This decrease in flavour perception is due to a reduction in the amount of the tastants and volatiles reaching the sensing organs (Hollowood *et al.*, 2002) due to the increase in viscosity. However this hypothesis is yet to be confirmed and numbers of researchers are using different imaging techniques to investigate the mechanism. The type of hydrocolloid used in the product has an impact on flavour and taste perception, for instance, it has been reported that products thickened with starch show good taste and flavour perception as compared to products thickened with xanthan and HPMC (Ferry *et al.*, 2006, Abson *et al.*, 2014).

Hence, the aim of the study presented in this chapter was to compare different physical properties of MFC produced from softwood spruce (CTE) with commercial food grade dietary fibres, such as citrus fibres (CF100 and HBAQ+), to examine the possible use of CTE as dietary fibres in food products. The second objective of the work was to test the impact of the entangled microfibril network of MFC on overall flavour/tastant perception from a basic food model system composed of MFC, water and salt.

6.2 Materials and Methods

For this comparative study, the two food grade cellulosic fibres Herbacel AQ+ (HBAQ+) and CitriFi100 (CF100) were provided by Cyber colloids Ltd (Ireland) and compared with CTE (Cellulosic Texture Enhancer; RMFC/CMC) provided by Borregaard AS. The CTE flakes and powder form is produced by using a refiner and different grades of CMC. The CTE powder form is produced by harsh milling of the CTE flakes form. Due to a strict confidential agreement with sponsors, formulation and equipment details cannot be disclosed.

6.2.1 Sample preparation

All dry MFC samples (all commercial cellulosic dietary fibres) were redispersed in distilled water at 1.5% w/w concentration by using a high shear overhead mixer (Ultraturrax, UK) at 15000-18000 rpm for 4 mins at room temperature.

All samples were stored on a roller bed overnight before analysis. The dry content was noted and corrected post-sample preparation. All samples were freshly prepared in two batches and all analyses were made in duplicate.

For sensory analysis, 0.2% w/w of stock solutions of NaCl were prepared in RO-water and different cellulosic fibres (*i.e.* CTE (flakes), CTE (Powder), CF100 and HBAQ+) were dispersed in 0.2% NaCl stock solutions at different

concentrations at comparable viscosity *i.e.* high (0.2 Pas) and low (0.01 Pas) at 50 s⁻¹ shear rate (as the viscosity at shear rate 50 s⁻¹ was chosen as it is most related to mouthfeel/texture perception, Wood, 1968, Richardson *et al.*, 1989). All samples were mixed by using a high shear mixer (Silverson, UK) at 5000 rpm for 5 mins. All samples were stored at 4°C overnight and stirred well before serving to panellists. For sensory analysis, no ethics approval was required as all of the products are commercially available and used in a variety of food products and listed under E460 ingredient (water-insoluble dietary fibres).

6.2.2 Microscopy

Light microscopy images were recorded according to the method detailed in section 2.4.6.

6.2.3 Rheology

Rheological measurements were made according to the method detailed in section 2.4.1.3. Data presented is an average of 4 replicates.

6.2.4 Water Retention Values (WRV)

Approximately 0.1 g (A) of powder was added to 100 g of water and mixed with an overhead mixer (Ultraturrax, UK) for 4 mins at 18000 rpm at room temperature. Approximately 45 g of the mixture was placed into a centrifuge tube and allowed to rest for 2 hrs followed by centrifugation (Beckman

Centrifuge machine, Model: J2-21) for 30 mins at 2141 g. The supernatant was removed and the sediment weighed (B). The analysis was performed in duplicate, WRV was calculated by using Equation 6.1 and average data is presented.

$$\text{WRV (\%)} = \frac{\text{Bottom Layer (B)} - \text{Starting material (A)}}{\text{Starting material (A)}} \quad (\text{Equation 6.1})$$

6.2.5 Sensory evaluation

The four samples were compared for saltiness perception using paired comparison (PC) test (BS EN ISO 5495:2007). The paired comparison test is used to identify directional differences: in order to determine the differences between two test samples for a specified attribute (for example more or less saltiness, Appendix 2). For this test, untrained panellists (n= 74, aged 20–40, mixed male and female volunteers) were recruited at the University of Nottingham. The sample size in each sample pot was 10 ml and the samples were served at room temperature (20°C). Three separate sessions were performed to examine the saltiness perception at a low viscosity (0.01 Pas at a 50 s⁻¹ shear rate, Panellists: 74), high viscosity (0.2 Pas at a 50 s⁻¹ shear rate, Panellists: 74) and one session at matched polymer concentration (1.5% w/w, Panellists: 60). The viscosity was also matched by a preliminary sensory test

for matching sensory viscosity by trained sensory panellists by using the paired comparison (PC) test as mentioned earlier.

For each test the panellist had to take the whole (10 ml) sample in their mouth on to their tongue, allow the sample to coat the roof of their mouth, hold in the mouth for a minimum of 5 sec before swallowing, and then cleanse their palate with mineral water (Evian, France) and unsalted crackers (99% Fat Free, Rakusen's, Leeds, UK) before tasting the next sample. Rest breaks were given between every third PC tests. The test was used in forced-choice mode, so panellists were required to give an answer even if the perceived difference was negligible. Panellists were asked to write comments such as smooth or grainy texture and any off-taste. All tests were carried out within individual sensory booths under controlled temperature and humidity conditions. The light of the room was red-light in order to avoid the discrimination of the samples on the basis of their colour.

To detect the differences in the preferences between the samples, paired comparison of the rank sums scores analysis were carried out, whose critical values for a large number of judges can be found in Basker 1988. In this thesis, the rank sum scores method was used to distinguish between the salt (taste) perceptions between different cellulosic fibres. On the scale presented

in result's figure, the lower number is, the saltier the product perceived by the sensory panel.

6.2.6 Data Analysis

Statistical data analysis was performed by using software Excel (Microsoft 2013, USA). Correlation analysis was performed to investigate the relationship between physical parameters (viscosity, complex viscosity, crystallinity, spin-spin relaxation time *etc.*) using analysis of variance (ANOVA) with a minimum significance level defined as $p < 0.05$. Sensory data was statistically analysed by using FIZZ 2.0 sensory software (Biosystems, Couternon, France) (P -value < 0.05). Analysis of variance (ANOVA) is a useful method which can be used to investigate product differences in sensory. The main purpose of the ANOVA test was to identify and quantify the factors which are responsible for the variability of the response. In addition, where appropriate, Tukey's HSD multiple comparison tests (significant level $\alpha = 0.05$) were performed to determine which samples were significantly different for rated intensity of each of the attributes.

6.3 Results and Discussion

6.3.1 Microstructure of fibres

Light microscopy images of different cellulosic dietary fibres at 1.5% w/w concentration are presented in Figure 6.1; the fibres were stained with Congo red dye. Noticeable differences in the microstructures were observed while comparing CTE(F) or CTE(P) with the citrus fibres CF100 and HBAQ+. The aqueous suspension of the citrus fibres showed multiple components in the system inherited from the citrus cell walls, such as short fibre bundles of cellulose and globular structures which are pectin and other cell wall material (similar microstructures were observed by Córdoba *et al.*, 2010).

The aqueous suspension of CTE(F) showed a dense entangled microfibril network, whereas larger fibril aggregates and fibre bundles were observed with CTE(P). CTE(P) samples were produced by harsh milling of the CTE(F) product. During the milling process, the system exhibited moisture loss, hence fibrils form strong intermolecular hydrogen bonding, which explains the higher amount of fibril aggregates upon rehydration. The presence of fibril aggregates post-milling process was supported by the low water retention values of these suspensions (Figure 6.2).

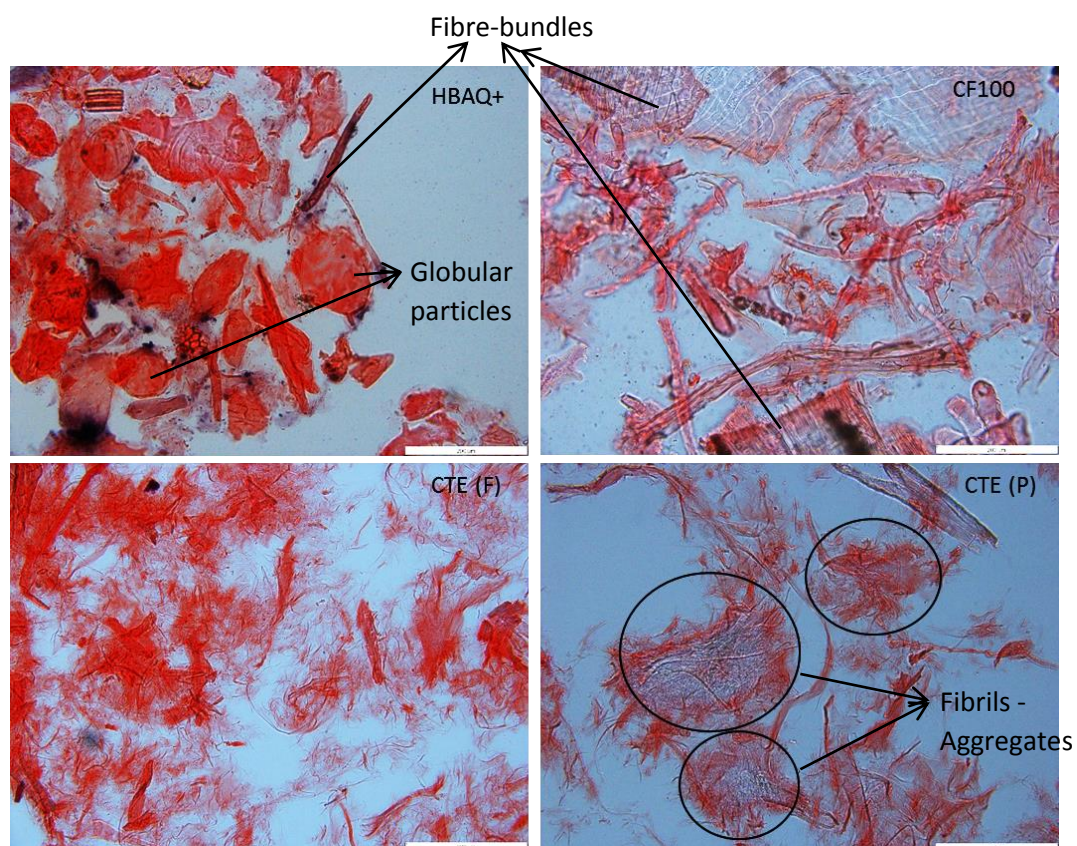


Figure 6.1: Optical microscopy images of 1.5% w/w aqueous suspension of different cellulosic fibres stained with Congo red dye, scale bar: 200 μm.

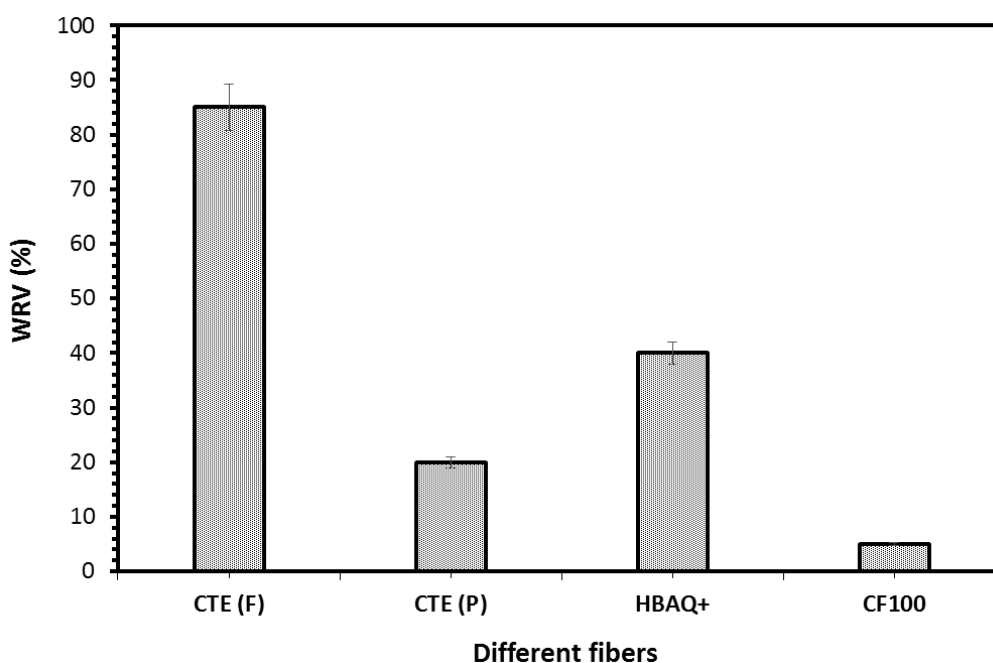


Figure 6.2: Water retention values of different cellulosic fibres, data presented is an average of replicates and highly reproducible.

Water-retention values (also known as water holding capacity) are an important property of dietary fibres from both a physiological and technological point of view. WRV of the suspension can be affected by the formulation (soluble and insoluble components in the system) and different processing. Sangnark & Noomhorm (2003) and Elleuch (2011) reported that the grinding can damage the regions of potential water retention capacity and, therefore, decrease the capacity to hold water. For instance, in this case, lower water was retained in the CTE(P) microfibril network (milled product) whereas higher water was retained in CTE(F) network structures and least with CF100.

Low water retention values of citrus fibre suspensions can be explained larger fibre bundles and a noticeably less interconnected microfibril network and the presence of other soluble and insoluble components (Figure 6.2; similar behaviour with other citrus fibres was reported by Grigelmo-Miguel *et al.*, 1999). The high WRV of CTE(F) suspension suggested that the material could be used as a functional ingredient to avoid syneresis and to modify the viscosity and texture of formulated products in addition to reducing calories by the total or partial substitution of high-energy ingredients (just like citrus fibres).

6.3.2 Rheological properties of suspensions

Storage modulus (G') and loss modulus (G'') as a function of frequency (Hz), of an aqueous suspension of CTE (Flakes and powder form) and the commercial food grade citrus fibres *i.e.* HBAQ+ and CF100 are presented in Figure 6.3a. All suspensions showed viscoelastic gel-like behaviour, where storage modulus was higher than loss modulus with little dependency on frequency. CTE(F) showed highest G' and G'' followed by HBAQ+ and CTE(P), lowest values for both moduli were observed with CF100.

Highly entangled fibre networks which retain a higher amount of water in the network, in the case of CTE (RMFC/CMC), explains the higher values found for both moduli (G' and G''), as compared to other cellulosic fibres. Interestingly, CTE(F) flakes showed higher moduli when compared to CTE(P) powder form, and can be explained by the agglomeration of microfibrils during the milling process which was observed in microscopy images (Figure 6.1). The lowest water retention value was observed with CF100 suspension, and relatively larger fibre particulates in the matrix, explaining the weak viscoelastic behaviour of this suspension at comparable concentrations.

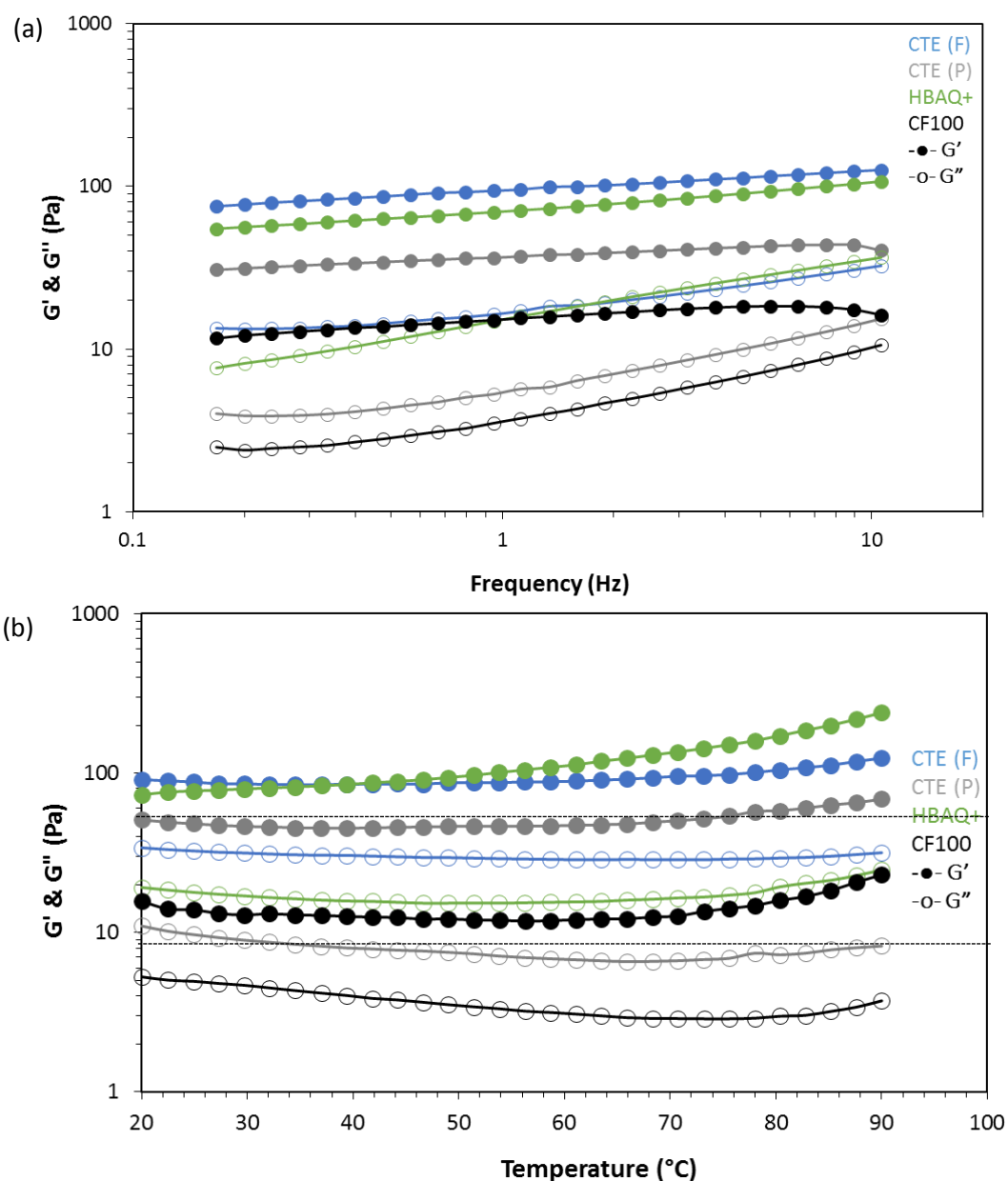


Figure 6.3: Storage (-●-) and loss moduli (-○-) of 1.5% w/w aqueous suspension of different cellulosic fibres i.e., CTE(F) flakes, CTE(P) powder, Herbacel AQ+ (HBAQ+) & CitriFi100 (CF100) as a function of (a) Frequency (Hz) at 20°C, strain: 0.2%, (b) temperature at 1°C/mins heating rate (frequency: 1 Hz and strain: 1%).

It was also evident in Figure 6.3a that the moduli acquired for the aqueous suspension of CTE(F) and HBAQ+ showed less dependency on frequency compared to CTE(P) and CF100. Frequency dependency of CF100 can be explained by the noticeable difference in network structure and low water holding capacity of the fibre suspensions at comparable concentration. Figure 6.3b shows the storage and loss modulus as a function of increasing temperature of the aqueous suspensions of the different fibres at 1.5% w/w concentration. All of the aqueous suspensions showed viscoelastic gel-like behaviour with increasing temperature. Slight increases in both moduli *i.e.* G' and G'' were observed with increasing temperature independent of the type of cellulosic fibres.

However, the fruit fibres HBAQ+ and CF100 showed higher temperature dependency compared to the CTE suspensions. For instance, the aqueous suspension of HBAQ+ showed a noticeable increase in G' and G'' with increasing temperature after 40°C up to 90°C. Whereas the aqueous suspension of CF100 showed a stable storage modulus (G') and a slight decrease in loss modulus (G'') up to 70°C and then a noticeable increase in both moduli up to 90°C. As observed in the earlier chapters that the MFC suspensions tended to undergo thermally induced microfibril network

formation, depending on the microfibril size and additives present in the system. The following results clearly indicate that the source and composition of cellulosic fibres also have a noticeable impact on the temperature-induced structural changes in the suspension. For instance, CF100 and HBAQ+ showed a noticeable increase in both moduli with increasing temperature (Figure 6.3), this likely suggests the increase in synergistic interaction between soluble and insoluble components present in the system upon heating along with the occurrence of some microstructural rearrangement at this temperature range.

The texture is one of the main components of food palatability and it is one of most extensively studied parameters by both sensory descriptive analysis and instrumental analysis. Food researchers tend to combine and correlate the results from both techniques to understand the texture properties of different food products. The rheological properties of liquid and semi-solid foods such as mayonnaise, yoghurts *etc.* have been extensively studied to relate with their mouthfeel perceptions (Richardson *et al.*, 1989, Wood 1968). A number of researchers reported that for weak gels the dynamic viscosity at a frequency of 50 rads^{-1} or shear rate 50 s^{-1} correlate closely with panel scores of thickness perceptions (Richardson *et al.*, 1989, He, Hort and Wolf 2016).

Considering the following studies, the concentration dependence of shear viscosity at 50 s^{-1} shear rate is shown in Figure 6.4 and was dependent on the type of cellulosic fibres. From Figure 6.4, the critical concentration (c^*) of the four cellulosic fibres is considered to be close to 0.8% w/w, after which a noticeable increase in shear viscosity is observed, this concentration dependence is very common with and can be related to the packing of the particles in the suspensions. Highest shear viscosity was observed with CTE(F) followed by HBAQ+, CTE(P) and least with CF100 suspensions at comparable concentrations.

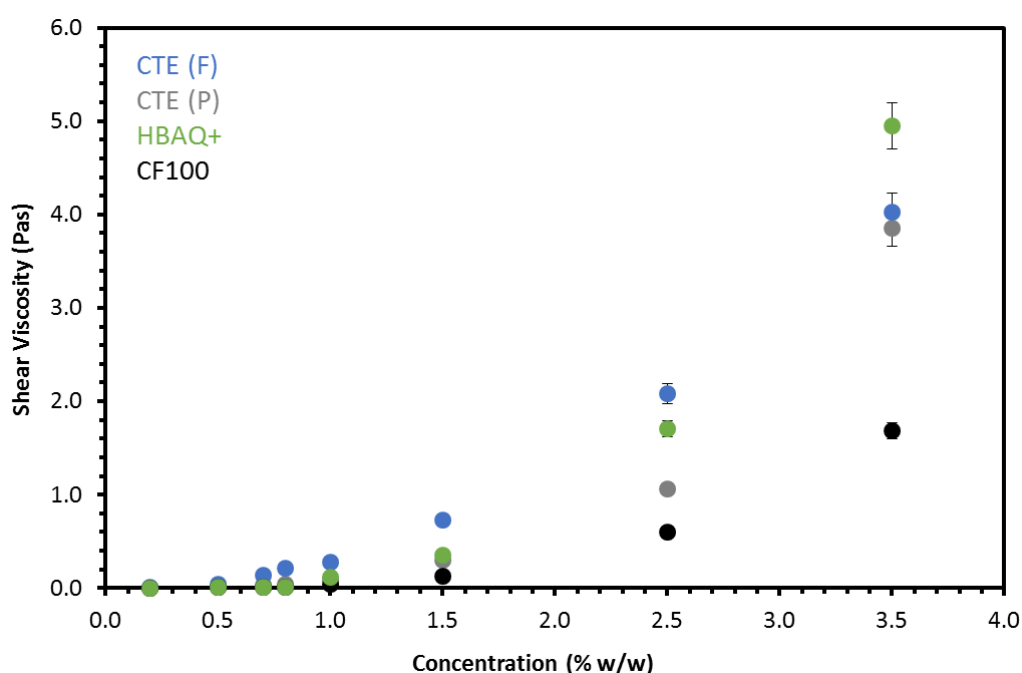


Figure 6.4: Concentration dependence of shear viscosity (Pas) recorded at shear rate 50 s^{-1} for four different cellulosic fibres. The viscosity values are averaged from 3 replicates.

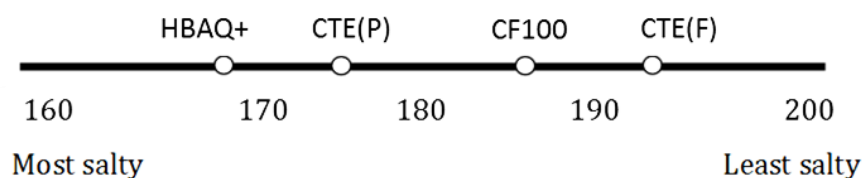
However, due to lack of water during the rehydration process, the presence of large aggregates and fibre bundles was observed with CTE(F) at higher concentration *i.e.* above 2.5% w/w, resulting in lower shear viscosity as compared to HBAQ+ suspension. From the following concentration dependence curves on shear viscosity, all of the suspensions showed a rapid increase in shear viscosity at a concentration higher than 0.8% w/w and dependent on the microstructure of the cellulosic fibres present in the suspension. These results also indicate that the amount of CTE(F) required to produce a particular viscosity can be achieved at lower concentrations as compared to the other fibres. The results have been considered when matching the viscosity and texture for a model system for taste/flavour perception analysis.

6.3.3 Sensory perception

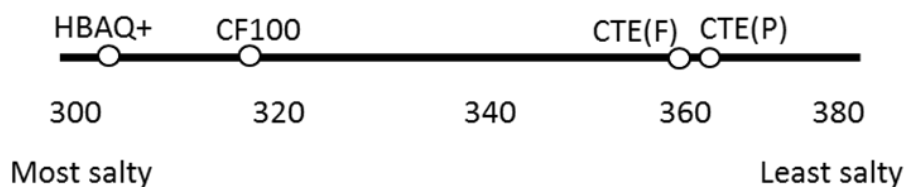
Figure 6.5 summarises the results from the sensory panel at the same concentration and at matching viscosities (low and high viscosity) of the four cellulosic fibre suspensions. Data presented in Figure 6.5, is analysed via rank sum scores method, where lower value represents the sample was perceived saltier in comparison with samples with higher values. In Figure 6.5a, no

significant difference ($p\text{-value} > 0.05$) was found between the saltiness perception of the four products at the same concentration *i.e.* 1.5% w/w.

(a) Constant Concentration



(b) Low Viscosity



(c) High Viscosity

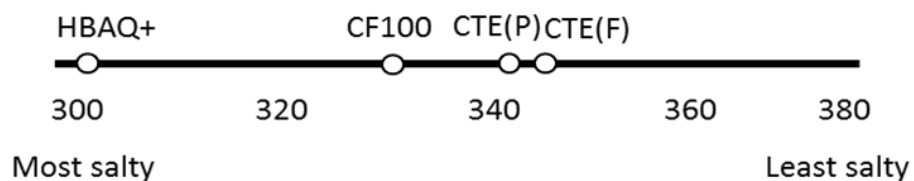


Figure 6.5: Rank sum scores for each sample for saltiness perception; decreasing numerical value corresponds to an increase in the attribute. *Herbacel AQ+* (HBAQ+), *CitriFi100* (CF100), *CTE flakes* (CTE(F)) and *CTE Powder* (CTE(P)). Note: figure 6.5a has a smaller scale as a number of panellists involved in the study were 60 as compared to figure 6.5b and 6.5c have 74 panellists.

Similar behaviour was reported with guar gum and HPMC (Baines and Morris 1987, Taylor *et al.*, 2000, Hollowood *et al.*, 2002), the perceived taste and flavour was affected by the addition of guar gum or HPMC respectively above critical concentration (c^*). One of the considered hypotheses for this behaviour was an increased viscosity that may result in a reduced rate of tastant reaching the receptors in the tongue and palate. This behaviour is highly dependent on the type of thickeners used in the product (Hill *et al.*, 1995, Ferry *et al.*, 2006, Pangborn *et al.*, 1973). For instance, as mentioned earlier (section 6.1), starch thickened systems showed smaller suppression in flavour and taste perception as compared to systems with linear hydrocolloids such as HPMC.

During the pair comparison test at a concentration of 1.5% w/w, in Figure 6.5a, the panellists found CTE(F) suspensions were much thicker texture as compared to other cellulosic fibres suspensions (comments provided during the sensory session). It was evident from the rheological analysis in Figure 6.4, that aqueous suspensions of CTE(F) showed higher shear viscosities at all concentrations (except at very high concentration) as compared to the other systems. This difference in shear viscosity of the different fibres at similar concentration explained the difference thickness (mouthfeel) perception

comments by the panellists during the sensory analysis. Figureuerola (2005) showed that the texture was strongly dependent on the particle size in the case of citrus fibres. This may explain the grainy texture reported by the panellists in the comments section of the study. In the comments section, most of the panellists reported a strong off-taste (citrus/lemon flavour) with CF100 and little off-taste with HBAQ+ suspensions. Whereas an absence of such off-taste in the case of CTE(F) and CTE(P) suspensions was reported by the panellists.

In order to rule out the impact of a difference in viscosities at the same concentration, different suspensions were formulated with matched viscosity (low and high) but different fibre concentrations. The viscosity was first matched by physical measurement (rheology) followed by a preliminary sensory test for matching sensory viscosity by trained sensory panellists. Using the paired comparison test, it was found that at low viscosity *i.e.* 0.01 Pas at a 50 s^{-1} shear rate, a significant reduction ($p\text{-value} < 0.05$) in saltiness perception was observed with CTE(F) and CTE(P) suspensions as compared to CF100 and HBAQ+ (Figure 6.5b). In Figure 6.5b the CF100 and HBAQ+ samples were rated very similar and much saltier (lower scores) as compare to CTE(F) and CTE(P). No significant difference in terms of saltiness perception was

observed between CTE(F) and CTE(P) as $p\text{-value} > 0.05$ (Figure 6.5b). However, a grainy texture and citrus off-taste were reported for CF100 and HBAQ+.

Similar taste perceptions were observed for suspension at the matched higher viscosity *i.e.* 0.2 Pas at a 50 s^{-1} shear rate of different cellulosic fibres (Figure 6.5c). It was found that at matched high viscosity, CTE(F) and CTE(P) showed significantly reduced saltiness perception (higher scores in Figure 6.5c) as compared to HBAQ+ followed by CF100 ($p\text{-value} < 0.05$). Similar behaviour was found in particulate suspensions such as starch and xanthan, that if the granular structure was maintained during processing, the system did not reduce the taste perception at high concentration (Ferry *et al.*, 2006, Morris, 1993, Abson *et al.*, 2014). It appears that in the case of CTE(F) and CTE(P) suspension the lower taste perception was driven by both presence of a dense microfibrillar cellulose network and the interaction between the polymer (*i.e.* MFC as well as CMC present in the formulation) with the salt (NaCl). This behaviour was independent on the suspension viscosity as taste perception was consistent with both low and high viscosity. However at higher concentrations (concentration exceeding c^*), this difference become smaller which is correlating well with the other food grade hydrocolloids such as xanthan, starch and CMC *etc.*

6.4 Conclusions

In the present study, softwood MFC (CTE) at low and high particle size was compared with the food grade dietary fibres HBAQ+ and CF100. All cellulosic suspensions showed very similar viscoelastic gel-like behaviour. Due to a highly dense fibre network and high water retention behaviour, the aqueous suspensions of CTE(F) showed higher viscoelastic behaviour as compared to all other fibres. Conversion of CTE(F) to a small particulate form by a milling process *i.e.* CTE(P) did not appear to improve the rheological properties and optical microscopy confirmed the presence of fibre aggregates in the suspensions which were difficult to redisperse in water.

The sensory viscosity (thickness) of CTE(F) was higher even at lower concentrations as compared to citrus fibres. Aqueous suspensions of CTE(F) products at matched viscosity showed a reduction in saltiness perception as compared to citrus fibres. However, no significant difference was observed between CTE(F) and CTE(P) on saltiness perception. A hypothesis that could explain the results for the CTE products is that CTE had dense microfibril networks actively interacting with CMC, which is also interacting with the salts (NaCl). This may have implication on slow taste (salt) release while mixing with saliva in a similar way to other negatively charged

polyelectrolytes, however, this has yet to be tested and should be the subject of future work.

Chapter 7

Conclusions and Future Work

The aqueous suspensions of microfibrillar celluloses (MFC) from softwood have a wide range of applications in the field of composites, paints and varnishes. However, it has been reported in recent years that microfibrillar or refined celluloses from appropriate raw materials (*e.g.* citrus plant) can be used as eco-friendly and functional ingredients in applications such as food and personal care. One of the most challenging goals in the production and processing of microfibrillar cellulose from softwood is the development of appropriate network structures with desirable properties and functionality after drying processes and re-dispersion. The present work has been focused on the formulation and processing of softwood microfibrillar cellulose (dry and redispersed) for food and personal care products as target applications.

The main conclusions with regard to this objective are summarised under 3 headings: (1) The characterisation and understanding of the suspension properties of different varieties of MFC and the impact of drying on the suspension properties; (2) The investigation of the interaction between different polymeric additives and MFC with particular reference to the physical properties of dried and redispersed systems; and finally (3) The examination of the possibility of using MFC/polymeric system as dietary fibre in food applications.

The characterisation and understanding of the suspension properties of different varieties of MFC and the impact of drying on the suspension

properties. The main findings from the first section of this work are:

- An increasing number of passes through the homogeniser resulted in an increased degree of fibrillation *i.e.* a noticeable decrease in the size of the cellulose fibres and the loss of crystalline structure of the system.
- The entangled network of MFC played an important role in maintaining the rheological properties as well as the water mobility of the system.
- Aqueous suspensions of microfibrillar cellulose showed viscoelastic gel-like behaviour where storage modulus (G') was higher than loss modulus (G''), with little dependency on frequency and temperature. However, after a certain number of passes (*e.g.* 5pass with Borregaard fibrillation technology) through the homogeniser, the aqueous suspension did not show any significant change in the complex and shear viscosities of the suspensions.
- The aqueous suspension of MFC with longer fibril size (low degree of fibrillation) had a shorter relaxation time (T_2) compared to suspensions with a high degree of fibrillation.

- Drying MFC suspensions resulted in the formation of microfibril aggregates due to strong intermolecular hydrogen bonds within the network structure.
- The lack of redispersibility in water and the presence of microfibril aggregates (upon drying) as well as the non-homogenous distribution of aggregates throughout the system, resulted in a significant reduction in the shear viscosities and water mobility of aqueous suspensions.

The investigation of the interaction between different polymeric additives

and MFC with particular reference to the physical properties of dried and

redispersed systems. Due to noticeable microfibril aggregates upon drying

reducing the redispersibility and functionality of the suspension properties of

MFC, the interaction between MFC with polymeric additives such as CMC,

pectin *etc.*, and salts can result in a reduction of microfibril aggregates. The

two polymeric additives chosen in the present work were the negatively

charged carboxymethylcellulose (CMC), which provides the charge-effect to

the microfibrils, and LBG, which interacts with cellulose forming highly inter-

connected network framework, and the blend of both polymeric additives *i.e.*

CMC and LBG (named as Blend) added as additive to never-dry MFC

suspension. Results showed that:

- The addition of polymeric additives significantly increased the redispersibility of dried MFC in water and reduced the size of microfibril aggregates.
- The point of the addition *i.e.* post or pre-homogenisation of polymeric additives played an important role in terms of the interaction between the polymeric additive and MFC.
- Co-processing of MFC and polymeric additives had a noticeable impact on the degree of fibrillation of the final MFC product. For instance, co-processing in the presence of CMC resulted in a higher degree of fibrillation as compared to LBG.
- The presence of a charged polymeric additive (CMC) resulted in a strong synergistic interaction with MFC, whereas a weak synergistic interaction was reported with LBG.
- The amount of additive present in the system had a noticeable impact on viscoelastic properties of the suspensions. At ambient temperature, the MFC/additive suspensions formed weak gel-like networks.
- The interaction between MFC and polymeric additives led to an increase in moisture uptake even after drying.

- Both CMC and LBG appeared to form a coating on the microfibril surface which prevents the microfibrils from forming strong intermolecular hydrogen bonds during the drying process. Figure 7.1 shows the predicted MFC/additive interaction models on the basis of results presented in this thesis.

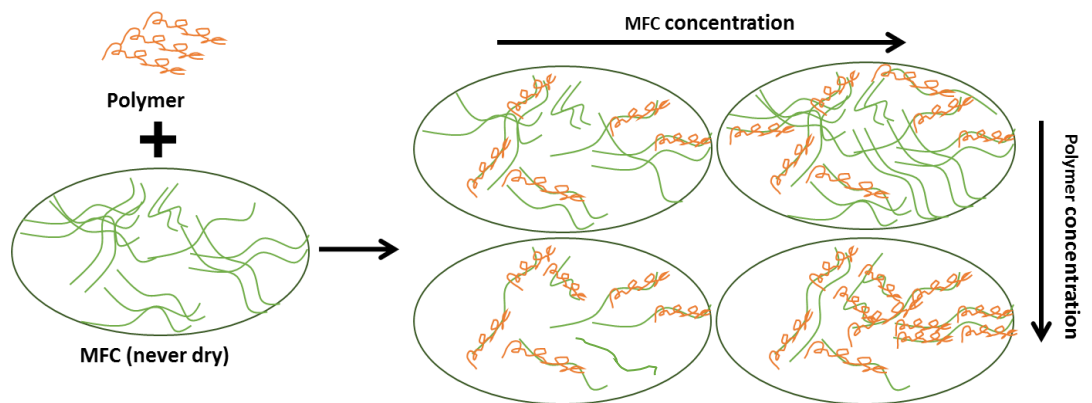


Figure 7.1: Schematic representation of the MFC/additive surface interactions at a different ratio.

The blend of CMC/LBG as a polymeric additive stabilised microfibrils of MFC in suspensions, however, the optimisation of the recipe and proper blending protocol has still to be carried out. In the present work, the degree of fibrillation and microstructures were studied by using light microscopy. Hence it would be interesting to map the change in microstructure and interaction behaviour by using advanced microscopy techniques such as environmental

scanning electron microscopy (ESEM) which allows collecting electron micrographs of "never-dried or wet" suspensions to enhance fundamental understanding of newly created structure.

During this study, the rheological properties of the aqueous suspensions of MFC/additive showed a noticeable increase in viscoelastic parameters such as G' and G'' with an increase in temperature. This behaviour was explained by the hypothesis that the increase in temperature results in the increase in thermal motion within the fibre network and the swelling of microfibrils. To verify this hypothesis, mapping the water mobility by measuring the spin-spin relaxation time (T_2) with increasing and decreasing temperature is recommended. Solid state NMR should also be carried out to check on the mobility of polymers in low moisture environments. And finally, the influence of low-temperature transitions at the low moisture on food application should be the subject of further study.

The examination of the possibility of using MFC/polymeric system as dietary

fibre in food applications. The final part of this study tested the potential use of MFC as dietary fibre for food applications similar to the other cellulosic fibres produced from citrus fibres. The rheological properties of these aqueous suspensions are compared as they are key parameters to test the

applicability of ingredients in high moisture food applications such as yoghurt, mayonnaise, ketchup and salad dressing *etc.*

- Softwood MFC in both flaked and powdered form showed similar rheological properties to other cellulosic fibres such as citrus fibres.
- Due to a highly entangled network structure, the softwood MFC showed the highest water retention values (also known as water holding capacity) compared to other cellulosic fibres.
- To achieve a target viscosity (or functionality) for a specific product, lower amounts of softwood MFC were required compared to other citrus fibres.
- Like other dietary fibres such as starch, CMC *etc.*, softwood MFC (CTE) also reduced taste perception, much slower than citrus fibres. It appeared that the particulate structure of the other fibres released the tastant more effectively and faster compared to highly-network (fibrillated) systems such as CTE.

On the basis of the physical measurements and sensory results, CTE can be used as a textural and viscosity enhancer in different food products. However to classify CTE products as dietary fibre for food products a fundamental study would have to be carried out. This would include increasing

understanding of how the MFC structures interact with saliva and the breakdown in the GI tract would give design rules for the release of not only tastants but also aromas and other functional actives. Finally, to categorise CTE products as dietary fibres for food application, it is critical to study these cellulosic products during digestion.

The application study presented here has focussed on the properties of MFC/additives in high water systems. In the present work, the findings at low water indicate that the type of additive and point of addition during the process can create different properties, such as liquid-crystalline phases. An understanding of these parameters on the performance of MFC in low moisture environments *e.g.* baked goods is recommended.

The work discussed in this thesis concerns the use of microfibrillar cellulose (MFC) from softwood, targeting the food and personal care applications. The MFC produced by high-pressure fibrillation technology developed by Borregaard Ltd. (Norway), is a revolutionary technology which results in highly fibrillated and entangled network structure of microfibrils from softwood with least amount of high energy consuming processing stages (number of passes through homogeniser). Addition of different polymeric additives at various processing stages results in the unique microstructure of

microfibrillar cellulose (MFC) which can be used in various application depending on their target properties. With the fact that the taste perception of these MFC samples is similar to other dietary fibres allows further application of MFC from softwood as “green/healthy” ingredient in food applications. For example, highly redispersed MFC/CMC can be used in high moisture applications such as mayonnaise, yoghurts, ketchup as bulking, stabilising agent, texture enhancer and viscosity enhancer, whereas MFC/LBG can be used for much dry/low moisture applications such as cakes, biscuits as fat-replacer and texture enhancer. Functional and healthy dietary fibre is required in food products of the future and the molecular control of MFC by the choice of additive and process offers flexibility and control in such products.

References

- Abbaszadeh, A., MacNaughtan W., Foster T.J. (2014).** The effect of ball milling and rehydration on a powdered mixture of hydrocolloids. *Carbohydrate Polymers*. 102, 978-985.
- Abbaszadeh, A.H. (2013).** Polysaccharide interactions providing structure control at high and low moisture contents. PhD thesis, University of Nottingham, UK.
- Abe, K., Yano H. (2009).** Comparison of the characteristics of cellulose microfibril aggregates of wood, rice straw and potato tuber. *Cellulose*. 16(6), 1017-1023.
- Abson, R., Gaddipati, S.R., Hort, J., Mitchell, J.R., Wolf, B., Hill, S.E. (2014).** A comparison of the sensory and rheology properties of molecular and particulate forms of xanthan gum. *Food Hydrocolloids*. 53, 85-90.
- Akerholm, M., Hinterstoisser B., Salmena L. (2004).** Characterization of the crystalline structure of cellulose using static and dynamic FT-IR spectroscopy. *Carbohydrate Research*. 339, 569–578.
- Alila, S., Besbes, I., Vilar, M.R., Mutje, P., Boufi, B. (2013).** Non-woody plants as raw materials for the production of microfibrillated cellulose (MFC): A comparative study. *Industrial crop and products*. 41, 250-259.
- Alvarez, V.A., Vazquez A. (2004).** Thermal degradation of cellulose derivatives/starch blends and sisal fibre biocomposites. *Polymer degradation and stability*. 84, 13-21.
- Andersen, M., Johansson L.S., Tanem B.S., Stenius P. (2006).** Properties and characterization of hydrophobized cellulose. *Cellulose*. 13, 665-677.
- Anderson, J. W., Baird, P., Davis, R. H., Jr., Ferreri, S., Knudtson, M., Koraym, A., Waters, V. & Williams, C. L. (2009).** Health benefits of dietary fibre. *Nutrition Reviews*. 67, 188-205.
- Anderson, J. W., Smith, B. M., & Guftanson, N. S. (1994).** Health benefit and practical aspects of high-fibre diets. *American Journal of Clinical Nutrition*, 59(5), 1242–1247.
- Andresen, M., Johansson L.S., Tanem B.S., Stenius P. (2006).** Properties and characterisation of hydrophobized microfibrillated cellulose. *Cellulose*. 13(6), 665-677.
- Ang, J. F. (1991).** Water retention capacity and viscosity effect of powdered cellulose. *Journal of Food Science*. 56, 1682-1684.

- Ang, J. F. Miller, W. B. (1991).** Multiple functions of powdered cellulose as a food ingredient. *Cereal Foods World*. 36, 558-564.
- Ankerfors, M. (2012).** Microfibrillated cellulose: Energy-efficient preparation techniques and key properties. Licentiate Thesis. KTH Royal Institute of Technology and Innventia AB.
- Aqualon® (1999).** Sodium carboxymethyl cellulose: physical and chemical properties, © Hercules incorporated. Viewed on 25th November 2014. e-link: <http://www.ashland.com/products/aqualon-sodium-carboxymethylcellulose> >.
- Atalla, R. H., & Vanderhart, D. L. (1984).** Native cellulose: A composite of two distinct crystalline forms. *Science*. 223, 283–287.
- Aulin C. (2009)** Novel oil resistant cellulosic materials (Pulp and paper technology). KTH Chemical Science and Engineering, Stockholm, Sweden.
- Baines, Z. V., & Morris, E. R. (1987).** Flavour/taste perception in thickened systems: the effect of guar gum above and below c^* . *Food Hydrocolloids*. 1 (3), 197-205.
- Baker, A.A., Helbert W., Sugiyama J., Miles M.J. (1997).** High-Resolution atomic force microscopy of native *Valonia* cellulose-I microcrystals. *Journal of Structural Biology*. 119(2),129–138.
- Baker, A.A., Helbert W., Sugiyama J., Miles M.J. (2000).** New insight into cellulose structure by atomic force microscopy shows the α crystal phase at near-atomic resolution. *Biophysical Journal*. 79(2), 1139-1145.
- Barnes, H.A., Hutton, J.K., and Walters, K. (1989).** An Introduction to rheology. Amsterdam. Elsevier: Distributors for the U.S. and Canada, Elsevier Science Pub. Co.
- Barneto, A.G., Carmona J.A., Blanco M.J.D. (2010).** Effect of the previous composting on volatiles production during biomass pyrolysis. *Journal of Physical chemistry A*. 114, 3756-3763.
- Basker, D. (1988).** Critical values of differences among rank sums for multiple comparisons. *Food Technology*, 79–84.
- Belder, De. N.A, Granath K. (1973).** Preparation and properties of fluorescein-labelled dextrans. *Carbohydrates Research*. 30, 375-378.
- Benchabane, A., Bekkour, K. (2008).** Rheological properties of carboxymethyl cellulose (CMC) solutions. *Colloid Polymer Science*. 286, 1173–1180.

- Bhattacharya, D.,** Germinario L.T., Winter W.T. (2008). Isolation, preparation and characterization of cellulose microfibrils obtained from bagasse. *Carbohydrate Polymers*. 73(3), 371–377.
- Brown, R.M.,** Willison J.H.M., Richardson C.L. (1976). Cellulose biosynthesis in *Acetobacter xylinum*: visualisation of the site of synthesis and direct measurement of the in-vivo process. *Proceedings of the National Academy of Sciences*. 73(12), 4565-4569.
- Brown, R. M.,** Saxena, I. M. (2000). Cellulose biosynthesis: A model for understanding the assembly of biopolymers. *Plant Physiology and Biochemistry*. 38, 57-67.
- BS EN ISO 5495:2007.** Sensory analysis. Methodology. Paired comparison test.
- Carr, H.Y.,** Purcell E.M. (1954). Effect of diffusion on free precession in nuclear magnetic resonance experiments. *Physical Review*. 94 (3).
- Carrasco, G.C.** (2011). Cellulose fibres, nanofibrils and microfibrils: The morphological sequence of MFC components from a plant physiology and fibre technology point of view. *Nanoscale Research letters*. 6(11), 417-423.
- Carrillo, F.,** Colom X., Sunol J.J., Saurina J. (2003). Structural FTIR analysis and thermal characterization of lyocell and viscose-type fibres. *European Polymer Journal*. 40, 2229-2234.
- Celluloseethers,** (2013). Properties of Sodium Carboxymethyl Cellulose viewed on 20th March 2014, e-link <<http://celluloseether.com/properties-of-cmc-carboxymethylcellulose/>>.
- Ceres,** (2014). The structure of plant cell wall viewed on 14th April 2014, e-link <<http://www.ceres.net/AboutUs/AboutUs-Biofuels-Carbo.html>>.
- Chamberlain, E.K.,** Rao, M.A. (1999). Rheological properties of acid converted waxy maize starches in water and 90%DMSO/10%water. *Carbohydrate Polymers*. 40, 251-260.
- Chatwal, G.R.,** Anand, S.K. (2006). *Instrumental methods of chemical analysis*. Himalaya publishing, India, 304- 319.
- Chen, P.,** Yu, H., Liu, Y., Chen, W., Wang, X., & Ouyang, M. (2013). Concentration effects on the isolation and dynamic rheological behaviour of cellulose nanofibres via ultrasonic processing. *Cellulose*. 20, 149–157.

- Cheng, G., Varanasi P., Li C., Liu H., Melnichenko Y.B., Simmons B.A., Kent M.S., Singh S. (2011).** The transition of cellulose crystalline structure and surface morphology of biomass as a function of ionic liquid pretreatment and its relation to enzymatic hydrolysis. *Biomacromolecules*. 12, 933–941.
- Cheng, Q., Wang, S., & Rials, T. G. (2009).** Poly (vinyl alcohol) nano-composites reinforced with cellulose fibrils isolated by high-intensity ultrasonication. *Composites: Part A*. 40, 218–224.
- Christensen, C. M. (1979).** Oral perception of solution viscosity. *Journal of Texture Studies*. 10 (2), 153-164.
- Cook, D. J., Hollowood, T. A., Linforth, R. S. T., & Taylor, A. J. (2003).** Oral shear stress predicts flavour perception in viscous solutions. *Chemical Senses*. 28 (1), 11-23.
- Cook, N. R., Cutler, J. A., Obarzanek, E., Buring, J. E., Rexrode, K. M., Kumanyika, S. K., Appel, L. J., & Whelton, P. K. (2007).** Long term effects of dietary sodium reduction on cardiovascular disease outcomes: Observational follow-up of the trials of hypertension prevention (TOHP). *British Medical Journal*. 334, 885–888.
- Cordoba, A., Camacho M.D.M., Navarrete N.M. (2010).** Rheological behaviour of an insoluble lemon fibre as affected by stirring, temperature, time and storage. *Food and Bioprocess Technology*. 5 (3), 1083-1092.
- Cote, W. A. (1967).** Wood ultrastructure. University of Washington Press, Syracuse, NY, USA.
- Cowan, B. (1997).** Nuclear magnetic resonance and relaxation. Cambridge university press. UK.
- Curvelo, A.A.S., de Carvalho A.J.F., Agnelli J.A.M. (2001).** Thermoplastic starch-cellulosic fibre composites: preliminary results. *Carbohydrate Polymers*. 45, 183–188.
- Cybercolloids, (2012).** The structure of locust bean gum viewed on 20th March 2014, e-link <<http://www.cybercolloids.net/information/technical-articles/carob-and-locust-bean-gum-structure>>.
- Dinand, E., Chanzy, H., and Vignon, M.R. (1996).** Parenchymal cell cellulose from sugar beet pulp: Preparation and properties. *Cellulose*. 3 (3), 183-188.

- Dolz**, M., Jiménez J., Hernandez M.J., Delegido J., Casanovas A. (2007). Flow and thixotropy of non-contaminating oil drilling fluids formulated with bentonite and sodium carboxymethyl cellulose. *Journal Petroleum Science Engineering*. 57, 294-302.
- Edali**, M., Esmail, M.N., Vatistas, G.H. (2001). Rheological properties of high concentrations of carboxymethyl cellulose solutions. *Journal of Applied Polymer Science*. 79, 1787-1801.
- Elanthikkal**, S., Gopalakrishnanpanicker U., Varghese S., Guthrie J.T. (2010). Cellulose microfibrils produced from banana plant wastes: Isolation and characterization. *Carbohydrate Polymers*. 80, 852-859.
- Elleuch**, M., Bedigian D., Roiseux O., Besbes S., Blecker C., and Attia H. (2011). Dietary fibre and fibre-rich by-products of food processing: Characterisation, technological functionality and commercial applications: A review. *Food Chemistry*. 124, 411–421.
- Eyholzer**, C. (2010). Preparation and properties of dried nano-fibrillated cellulose and its nanocomposites. Licentiate Thesis, chapter 1. Luleå university of technology. Sweden.
- Feddersen**, R.L., Throp, S.N., (1993). Whistler R.L., BeMiller J.N., (ed). *Industrial gums, polysaccharides and their derivatives*, 3rd edition. San Diego, Boston, New York, USA: academic press, Inc., 537.
- Fernandes**, D.J.M.B., Gil M.H., Castro J.A.A.M. (2004). Hornification-its origin and interpretation in wood pulps. *Wood Science and Technology*. 37, 489-494.
- Fernandes**, A.N., Thomas L.H., Altaner C.M., Callow P., Forsyth V.T., Apperley D.C., Kennedy C.J., Jarvish M.C. (2011). Nanostructure of cellulose microfibrils in spruce wood. *PNAS*. 108 (47), 1195-1203.
- Ferrer**, A., Filpponen, I., Rodríguez, A., Laine, J., & Rojas, O. J. (2012). Valorization of residual Empty Palm Fruit Bunch Fibers (EPFBF) by microfluidization: Production of nanofibrillated cellulose and EPFBF nanopaper. *Bioresource Technology*. 125, 249–255.
- Ferry**, A. L., Hort, J., Mitchell, J. R., Cook, D. J., Lagarrigue, S., & Pamies, B. V. (2006). Viscosity and flavour perception: why is starch different from hydrocolloids? *Food Hydrocolloids*. 20 (6), 855-862.
- Festucci-Buselli**, R.A., Otoni W.C., Joshi C.P. (2007). Review: Structure, organisation, and functions of cellulose synthase complexes in higher plants. *Brazilian Journal of Plant Physiology*. 19, 1-13.

- Fiberstar.** (2005). The product portfolio of Fiberstar Inc., US. Available at <http://fiberstar.net/>.
- Figureuerola, F., Hurtado, M.L., Estevez M.A., Chiffelle, I., Asenjo, F.** (2005). Fibre concentrates from apple pomace and citrus peel as potential fibre sources for food enrichment. *Food Chemistry*. 91, 395–401.
- Foster, T. J.** (2011). Natural structuring with cell wall materials. *Food Hydrocolloids*. 25, 1828-1832.
- Foster, T.J.** (2010). Technofunctionality of hydrocolloids and their impact on food structure. *Gums and stabilisers for the food industry 15*, Williams, P.A., and Phillips, G.O. (Eds). RSC: Cambridge. 103-112.
- Fox, J. E., & Imeson, A.** (1992). Thickening and gelling agents for food. Blackie Academic and Professional, London, 153-171.
- Frone, A. N., Panaitescu, D. M., & Donescu, D.** (2011). Some aspects concerning the isolation of cellulose micro- and nano-fibers. *U.P.B. Science Bulletin, Series B*. 73 (2), 133–152.
- Gardiner, E.S., Sarko A.** (1985). Packing analysis of carbohydrates and polysaccharides. 16. The crystal structures of celluloses IV_i and IV_{ii}. *Canadian Journal of Chemistry*. 63(1), 173-180.
- Ghannam, M.T., Esmail M.N.** (1997). Rheological properties of carboxymethyl cellulose. *Journal of Applied Polymer science*. 64(2), 289–301.
- Gidley, M.J. and Cooke, D.** (1991). Aspects of molecular organisation and ultrastructure in starch granules. *Biochemical Society Transactions*. 19, 551-555.
- Goff, H.D., Ferdinando D., Schorsch C.,** (1999). Fluorescence microscopy to study galactomannan structure in frozen sucrose and milk protein solutions. *Food Hydrocolloids*. 13 (4), 353-362.
- Gorinstein, S., Zachwieja, Z., Folta, M., Barton, H., Piotrowicz, J., Zember, M., Weisz, M., Trakhtenberg, S., & Martin-Belloso, O.** (2001). The comparative content of dietary fibre, total phenolic, and minerals in persimmons and apples. *Journal of Agricultural and Food Chemistry*. 49, 952–957.
- Griguelmo-Miguel, N., Gorinstein, S., and Martín-Belloso, O.** (1999). Characterisation of peach dietary fibre concentrates as a food ingredient. *Food Chemistry*. 65, 175–181.

- Ha**, M.A., Apperley D.C., Evans B.W., Huxham M.I., Jardine G.W., Viëtor R.J., Reis D., Vian B., Jarvis M.C. (1998). Fine structure in cellulose microfibrils: NMR evidence from onion and quince. *The Plant Journal*. 16(2), 183–190.
- Habibi**, Y., Mahrouz M., Vignon M.R. (2009). Microfibrillated cellulose from the peel of prickly pear fruits. *Food Chemistry*. 115, 423-429.
- Habibi**, Y., Vignon, M.R., (2008). Optimisation of cellouronic acid synthesis by TEMPO-mediated oxidation of cellulose III from sugar beet pulp. *Cellulose*. 15, 177–185.
- Habibi**, Y., Lucia L. A., Rojas O. J. (2010). Cellulose Nanocrystals: Chemistry, Self-Assembly, and Applications. *Chemical Reviews*. 110, 3479-3500.
- He**, Qi., Hort J., Wolf B. (2016). Predicting sensory perceptions of thickened solutions based on rheological analysis. *Food Hydrocolloids*. 61, 221–232.
- Heinze**, T., Liebert, T. (2001). Unconventional methods in cellulose functionalization. *Progress in Polymer Science*. 26, 1689-1762.
- Heinze**, T., Pfeiffer K. (1999). Studies on synthesis and characterisation of carboxymethyl cellulose. *Angew Makromol Chem*. 266, 37-45.
- Henriksson**, M., Henriksson, G., Berglund, L. A., & Lindstrom, T. (2007). An environmentally friendly method for enzyme-assisted preparation of microfibrillated cellulose (MFC) nanofibers. *European Polymer Journal*. 43, 3434–3441.
- Herald**, C. T. (1986). Locust/carob bean gum. *Food Hydrocolloids*. 3, 161-170.
- Herbafood**. (2002). Herbacel AQ Plus. Apple and citrus fibre. Available from www.herbafood.de/eaqplus.pdf.
- Hernández**, M.J., Dolz, J., Dolz, M., Delegido, J., Pellicer, J. (2001). Viscous synergism in carrageenans (κ and λ) and Locust bean gum mixtures: influence of adding sodium carboxymethylcellulose. *Food Science Technology International*. 7 (5), 383-391.
- Herrick**, F.W., Wash S. (1984). Process for preparing microfibrillated cellulose. Patent no: US 4481077 A.
- Heux**, L., Chauve, G., & Bonini, C. (2000). Non-flocculating and chiral-nematic self-ordering of cellulose microcrystals suspensions in nonpolar solvents. *Langmuir*. 16, 8210–8212.

- Heux, L., Dinanad E., Vignon M.R.** (1999). Structural aspects in ultrathin cellulose microfibrils followed by ¹³C CPMAS NMR. *Carbohydrate Polymers*. 40, 115-124.
- Hill, M.A., Mitchell, J.R. and Sherman, P.A.** (1995). The relationship between the rheological and sensory properties of a lemon pie filling. *Journal of Texture Studies*. 26, 457-470.
- Hill, R.J.** (2008). The elastic modulus of microfibrillar cellulose gels. *Biomacromolecules*. 9, 2963-2966.
- Hills, B.P.** (1991). Multinuclear NMR studies of water in solutions of simple carbohydrates. *Molecular Physics: An International Journal at the interface Between Chemistry and Physics*. 72 (5), 1099-1121.
- Hinterstoisser, B., Salmen L.** (2000). Application of dynamic 2D FTIR to cellulose. *Vibrational Spectroscopy*. 22,111–118.
- Hoefler, A.C.,** (2004). *Hydrocolloids*. American Association of Cereal Chemists, St Paul, MN.
- Hollowood, T. A., Linforth, R. S. T., & Taylor, A. J.** (2002). The effect of viscosity on the perception of flavour. *Chemical Senses*. 27 (7), 585-591.
- Hubbe, M. A., Rojas, O.J., Lucia, L.A., Sain M.** (2008). Cellulosic Nanocomposites: A Review. *BioResources*. 3 (3), 929-980.
- Hufnagel, U.S., Ono T., Izumi K., Hufnagel P., Morita N., Kaga H., Morita M., Hoshino T., Yumoto I., Matsumoto N., Yoshida M., Sawada M.T., Okuyama H.** (2000). Identification of the extracellular polysaccharide produced by the now mould fungus *Microdochium nivale*. *Biotechnology Letters*. 22(3), 183-187.
- Hui, P.A. and Neukom, H.** (1964). Properties of galactomannans. *Tappi*. 47, 39-42.
- Ibbett, R., Gaddipati S., Hill S., Tucker G.** (2013). Structural reorganisation of cellulose fibrils in hydrothermally deconstructed lignocellulosic biomass and relationships with enzyme digestibility. *Biotechnology for Biofuels*. 6(33), 1-15.
- Ikeda, S., Nishinari K.** (2001). “Weak Gel”-Type Rheological Properties of Aqueous Dispersions of Non-aggregated K-Carrageenan Helices. *Journal of Agriculture Food Chemistry*. 49, 4436–4441.

- Iotti, M., Gregersen Ø. W., Moe S., Lenes M. (2011).** Rheological studies of Microfibrillar cellulose water dispersions. *Journal Polymer Environment*. 19, 137-145.
- Isogai, A., Saito T., Fukuzumi H. (2011).** TEMPO-oxidized cellulose nanofibres. *Nanoscale*. 3, 71-85.
- Iwamoto, S., Abe K., Yano H. (2007).** Obtaining cellulose nanofibres with a uniform width of 15nm from wood. *Biomacromolecules*. 8 (10), 3276-3278.
- Iwamoto, S., Abe K., Yano H. (2008).** The effect of hemicelluloses on wood pulp nanofibrillation and nanofiber network characteristics. *Biomacromolecules*. 9, 1022-1026.
- Janardhnan, S., Sain, M.M., (2006).** Isolation of cellulose microfibrils – an enzymatic approach. *BioResources*. 1 (2), 176-188.
- Jonoobi, M., Harun, J., Mathew, A. P., & Oksman, K. (2010).** Mechanical properties of cellulose nanofiber (CNF) reinforced polylactic acid (PLA) prepared by twin screw extrusion. *Composite Science and Technology*. 70 (12), 1742–1747.
- Kachrimanis, K., Noisternig, M.F., Griesser, U.J., Malamataris, S. (2006).** Dynamic moisture sorption and desorption of standard and silicified microcrystalline cellulose. *European Journal of Pharmaceutics and biopharmaceutics*. 64, 307-315.
- Karande, V. S., Bharimalla, A. K., Hadge, G. B., Mhaske, S. T., & Vigneshwaran, N. (2011).** Nanofibrillation of cotton fibres by disc refiner and its characterization. *Fibres and Polymers*. 2 (3), 399 - 404.
- Kato, K.L., Cameron R.E., (1999).** A review of the relationship between thermally-accelerated ageing of paper and hornification. *Cellulose*. 6, 23-40.
- Kerr, A. J., Goring, D. A. I. (1975).** The ultrastructural arrangement of the wood cell wall. *Cellulose Chemistry and Technology*. 9(6), 563–573.
- Kirk, R.E., Othmer D.F. (1967).** Cellulose, *Encyclopaedia of Chemical Technology* (2nd ed.), Wiley, New York. 4.
- Kleinebudde, P., Jumaa M., Saleh F.E. (2000).** Influence of degree of polymerization on the behaviour of cellulose during homogenization and extrusion/spheronization. *AAPS Pharmscience*. 2(3), 18-27.

- Kocherbitov**, V., Ulvenlund S., Kober M., Jarring K., Arnebrant T. (2008). Hydration of microcrystalline cellulose and milled cellulose studied by sorption calorimetry. *Journal Physical Chemistry B*. 112, 3728-3734.
- Koganti**, N. (2012). Solvent effects on the dissolution and regeneration of cellulose and starch. PhD thesis, University of Nottingham, UK.
- Kokini**, J. L., J. B. Kadane and E. L. Cussler., (1977). Liquid texture perceived in mouth. *Journal of Texture Studies*. 8 (2), 195-218.
- Kontturi**, E., Vuorinen T. (2009). Indirect evidence of supramolecular changes within cellulose microfibrils of chemical pulp fibres upon drying. *Cellulose*. 16, 65-74.
- Kuang**, Q. L., Zhao, J. C., Niu, Y. H., Zhang, J., & Wang, Z. G. (2008). Celluloses in an ionic liquid: The rheological properties of the solutions spanning the dilute and semidilute regimes. *The Journal of Physical Chemistry B*. 112, 10234–10240.
- Kunzek**, H., Muller, S., Vetter, S., Godeck, R. (2002). The significance of physicochemical properties of plant cell wall materials for the development of innovative food products. *European Food Research and Technology*. 214, 361-376.
- Lapasin**, R., Prici S. (1995). Rheology of polysaccharide systems. *Rheology of Industrial Polysaccharides: Theory and Applications*. Springer US. 250-494
- Lavoine**, N., Desloges I., Dufresne A., Bras J. (2012). Microfibrillated cellulose – Its barrier properties and applications in cellulosic materials: A review. *Carbohydrate Polymers*. 90(2), 735–764.
- Lee**, S. Y., Chun, S. J., Kang, I. A., & Park, J. Y. D. (2009). Preparation of cellulose nanofibers by a high-pressure homogenizer and cellulose-based composite films. *Journal of Indian Engineering Chemistry*. 15, 50–55.
- Liitia**, T., Maunu S.L., Hortling B. (2000). Solid state NMR studies on cellulose crystallinity in fines and bulk fibres separated from refined kraft pulp. *Holzforschung*. 54, 618-624.
- Lowys**, M.P., Desbrières, J., Rinaudo, M. (2001). Rheological characterization of cellulosic microfibril suspensions: Role of polymeric additives. *Food Hydrocolloids*. 15, 25-32.

- Lue, A., Zhang, L. (2009).** Rheological behaviours in the regimes from dilute to concentrated in cellulose solutions dissolved at low temperature. *Macromolecular Bioscience*. 9, 488-496.
- Lundin, L., Hermansson A.M. (1994).** Supermolecular aspects of xanthan-locust bean gum gel based rheology and electron microscopy. *Carbohydrate Polymers*. 26, 129-140.
- Lynch, E.J., Bello, F.D., Sheehan, E.H., Cashman, K.D., Arendt, E.K. (2009).** Fundamental studies on the reduction of salt on dough and bread characteristic. *Food Research International*. 42, 885-891.
- Maier, H., Anderson, M., Karl, C. and Magnuson, K. (1993).** Guar, locust bean, tara and fenugreek gums, in Whistler, R.L. and BeMiller, J.N. (ed) *Industrial Gums*, Chapter 8, Academic Press, New York, USA.
- Mannion, R.O., Melia, C.D., Launay, B., Cuvelier, G., Hill, S.E., Harding, S.E., Mitchell J.R. (1992).** Xanthan/locust bean gum interactions at room temperature. *Carbohydrate Polymers*. 19, 91-97.
- Marlett, J. A., Mcburney, M. I. & Slavin, J. L. (2002).** The position of the American Dietetic Association: Health implications of dietary fibre. *Journal of the American Dietetic Association*. 102, 993-1000.
- Martini, G. (1981).** The state of water absorbed on silica gel as determined by ESR of transient metal ion probe. *Journal of Colloid Interface Science*. 80, 39-48.
- Maruyama, K., Sakashita, T., Hagura, Y., and Suzuki, K. (2007).** The relationship between rheology, particle size and texture of mayonnaise. *Food Science and Technology Research*. 13 (1), 1-6.
- Mathur, N. K. (2011).** *Industrial galactomannan polysaccharides*. CRC Press, LLC.
- Mazeau, K., & Heux, L. (2003).** Molecular dynamics simulations of bulk native crystalline and amorphous structures of cellulose. *The Journal of Physical Chemistry B*. 107 (10), 2394-2403.
- Meiboom, S. and Gill, D. (1958).** A Modified spin-echo method for measuring nuclear relaxation times. *Review of Scientific Instruments*. 29, 688-691.
- Mezger, T.G. (2006).** *The Rheology handbook*. Edition: 2, Vincentz Network GmbH & Co KG: Germany.

- Mihiranyan, A., Llagostera, A.P., Karmhag, R., Stromme, M., Ek R. (2004).** Moisture sorption by the cellulose powder of varying crystallinity. *International Journal of Pharmaceutics*. 264, 433-442.
- Missoum, K., Bras J., Belgacem N. (2012).** Water re-dispersible dried nanofibrillated cellulose by adding sodium chloride. *Biomacromolecules*. 13 (12), 4118-4125.
- Mittal, A., Katahira R., Himmel M.E., Johnson D.K. (2011).** Effects of alkaline or liquid ammonia treatment on crystalline cellulose: changes in crystalline structure and effects on enzymatic digestibility. *Biotechnology for biofuels*. 4 (41), 2-16.
- Moon, R.J., Martini, A., Narin, J., Simonsen, J., Youngblood, J. (2011).** Cellulose nanomaterials review structure, properties and nanocomposites. *Chemical Society review*. 40, 3941-3994.
- Moran, J.I., Alvarez V.A., Cyras V.P., Vazquez A. (2008).** Extraction of cellulose and preparation of nanocellulose from sisal fibres. *Cellulose*. 15, 149-159.
- Morris, E.R. (1990).** Shear thinning of 'random coil' polysaccharides: Characterisation by two parameters from a simple linear plot. *Carbohydrate Polymers*. 13, 85-96.
- Morris, E.R. (1993).** Rheological and organoleptic properties of food hydrocolloids. *Food hydrocolloids: Structures, Properties, and Functions*. 201-210.
- Morris, E.R. (1995).** Polysaccharide synergism – more questions than answers, in Harding, S.E., Hill, S.E., and Mitchell, J.R. (ed) *Biopolymer mixtures*, chapter 14, Nottingham university press, Nottingham, UK.
- Morris, E.R., Cutler, A.N., Ross-Murphy, S.B., Rees, D.A., and Price, J. (1981).** Concentration and shear rate dependence of viscosity in random coil polysaccharide solutions. *Carbohydrate Polymers*. 1, 5-21.
- Mouro, C.R., Bizot H., Bertrand D. (2011).** Chemometric analyses of the $1\text{H}-13\text{C}$ cross-polarization build-up of celluloses NMR spectra: A novel approach for characterising the cellulose crystallites. *Carbohydrate Polymers*. 84, 539–549.
- Mouro, C.R., Bouchet B., Pontoire B., Robert P., Mazoyer J., Buleon A., (2003).** Structural features and potential texturizing properties of lemon and maize cellulose microfibrils. *Carbohydrate Polymers*. 53, 241-252.

- Nakagaito, A. N., & Yano, H. (2004).** The effect of morphological changes from pulp fibre towards nano-scale fibrillated cellulose on the mechanical properties of high-strength plant fibre based composites. *Applied Physics A – Material Science Process.* 78, 547–552.
- Newman, R.H. (2004).** Carbon-13 NMR evidence for co-crystallization of cellulose as a mechanism for hornification of bleached kraft pulp. *Cellulose.* 11, 45-52.
- Newman, R.H., Hemmingson J.A. (1998).** Interactions between LBG and cellulose characterised by ¹³C NMR spectroscopy. *Carbohydrate polymers.* 36, 167-172.
- Nishiyama, Y., (2009).** Structure and properties of the cellulose microfibril. *Journal of Wood Science.* 55, 241-249.
- Nishiyama, Y., Langan P., Chanzy H. (2002).** Crystal structure and Hydrogen-bonding system in cellulose I β from synchrotron X-ray and neutron fibre diffraction. *Journal of the American Chemical Society.* 124 (31): 9074–82.
- Norton, I.T., Foster, T.J., Brown, R. (1998).** The science and technology of fluid gel. *Gums and stabilisers for the food industry.* Ed. William, P.A., Phillips, G.O. Edition 9; 259-268.
- Norton, I.T., Spyropoulos, F., Cox, P. (2011).** *Practical Food Rheology: An interpretive approach.* Wiley-Blackwell: UK.
- Ono, H., Inamoto M., Okajima K., (1997).** Spin-lattice relaxation behaviour of water in cellulose materials in relation to the tablet forming ability of microcrystalline cellulose particles. *Cellulose.* 4, 57–73.
- Ono, H., Shimaya Y., Sato K., Hongo T., (2004).** ¹H spin-spin relaxation time of water and rheological properties of cellulose nano-fiber dispersion, transparent cellulose hydrogel (TCG). *Polymer Journal.* 36, 684-694.
- Ono, H., Yamada H., Matsuda S., Okajima K., Kawamoto T., Iijima H., (1998).** ¹H-NMR relaxation of water molecules in the aqueous microcrystalline cellulose suspension systems and their viscosity. *Cellulose.* 5, 231-247.
- Pääkkö, M., Ankerfors, M., Kosonen, H., Nykänen, A., Ahola, S., Österberg, M., Ruokolainen, J., Laine, J., Larsson, P.T., Ikkala, O., and Lindström, T. (2007).** Enzymatic Hydrolysis Combined with Mechanical Shearing and High-Pressure Homogenization for Nano-scale Cellulose Fibrils and Strong Gels. *Biomacromolecules.* 8, 1934-1941.

- Pangborn, R. M., Trabue I. M., Szczesniak A. S. (1973).** Effect of hydrocolloids on oral viscosity and basic taste intensities. *Journal of Texture Studies*. 4(2), 224-241.
- Park, S., Baker J.O., Himmel M.E., Parilla P.A., Jonhson D.K. (2010).** Cellulose crystallinity index: measurement techniques and their impact on interpreting cellulase performance. *Biotechnology Biofuels*. 3, 3–10.
- Park, Y., Hunter, D. J., Spiegelman, D., Bergkvist, L., Berrino, F., Van Den Brandt, P. A., Buring, J. E., Colditz, G. A., Freudenheim, J. L., Fuchs, C. S., Giovannucci, E., Goldbohm, R. A., Graham, S., Harnack, L., Hartman, A. M., Jacobs, D. R., Kato, I., Krogh, V., Leitzmann, M. F., Mccullough, M. L., Miller, A. B., Pietinen, P., Rohan, T. E., Schatzkin, A., Willett, W. C., Wolk, A., Zeleniuch-Jacquotte, A., Zhang, S. M. M. & Smith-Warner, S. A. (2005).** Dietary fibre intake and risk of colorectal cancer - A pooled analysis of prospective cohort studies. *Jama-Journal of the American Medical Association*. 294, 2849-2857.
- Pellicer, J., Delegido J., Dolz J., Dolz M., Hernández M.J. and Herráez M. (2000).** Influence of shear rate and concentration ratio on viscous synergism. Application to xanthan-locust bean gum mixtures. *Food Science and Technology International*. 6, 415–423.
- Peng, Y., Gardner, D. J., and Han, Y. (2012a).** Drying cellulose nanofibrils: In search of a suitable method. *Cellulose*. 19, 91–102.
- Peng, Y., Han, Y., & Gardner, D. J. (2012b).** Spray-drying cellulose nano fibrils: Effect of drying process parameters on particle morphology and size distribution. *Wood Fibre Science*. 44 (4), 1–14.
- Petkowicz, C.L.O., Reicher F., Mazeau K. (1998).** Conformational analysis of galactomannans: from oligomeric segments of polymeric chains. *Carbohydrate Polymers*. 37, 25-39.
- Quievy, N., Jacquet N., Sclavons M., Deroanne C., Paquot M., Devaux J. (2010).** Influence of homogenization and drying on the thermal stability of microfibrillated cellulose. *Polymer degradation and stability*. 95, 306-314.
- Rachocki, A., Markiewicz E., Goc-Tritt J. (2005).** Dielectric relaxation in cellulose and its derivatives. *Acta Physica Polonica A*. 108, 137-145.
- Rama, R., Chiu, N., Silva, M.C.D., Hewson, L., Hort, J., Fisk, I.D. (2013).** The impact of salt crystal size on the in-mouth delivery of sodium and saltiness perception from snack foods. *Journal of Texture Studies*. 44, 338-345.

- Raschip**, I.E., Yakimets, I., Martin, C.P., Paes, S.S., Vasile, C., and Mitchell, J.R. (2008). Effect of water content on thermal and dynamic mechanical properties of xanthan powder: A comparison between standard and novel techniques. *Powder technology*. 182, 436-443.
- Richardson**, P.H., Willmer J., Foster T.J. (1998). Dilute solution properties of guar and locust bean gum in sucrose solutions. *Food hydrocolloids*. 12 (3), 339-348.
- Richardson**, R. K., E. R. Morris, S. B. Ross-Murphy, L. J. Taylor and I. C. M. Dea. (1989). Characterization of the perceived texture of thickened systems by dynamic viscosity measurements. *Food Hydrocolloids*. 3(3), 175-191.
- Rochefort**, W. E., & Middleman, S. (1987). Rheology of xanthan gum: Salt, temperature, and strain effects in oscillatory and steady shear experiments. *Journal of Rheology*. 31, 337–369.
- Rowland**, S. P., Roberts, E. J. (1972). Nature of accessible surfaces in the microstructure of cotton cellulose. *Journal of Polymer Science, Part A-1: Polymer Chemistry*. 10(8), 2447–2461.
- Ruigang**, L., Yu H., Huang Y. (2005). Structure and morphology of cellulose in wheat straw. *Cellulose*. 12, 25-34.
- Ruusunen**, M, Vainionpaa J, Poulanne E, Lyly M, Lähteenmäki L, Niemistö M, Ahvenainen R. (2003). Physical and sensory properties of low-salt phosphate free frankfurters composed with various ingredients. *Meat Science*. 63, 9–16.
- Saarikoski**, E., Saarinen T., Salmela J., Seppala J. (2012). The flocculated flow of microfibrillated cellulose water suspension: an imaging approach for characterization of rheological behaviour. *Cellulose*. 19, 647-659.
- Saarinen**, T., Lille M., Seppälä J. (2009). Technical Aspects on Rheological Characterization of Microfibrillar Cellulose Water Suspensions. *Annual Transactions of the Nordic Rheology Society*. 17.
- Sacks**, F. M., Svetkey, L. P., Vollmer, W.M., Appel, L. J., Bray, G. A., Harsha, D., Obarzanek, E., Conlin, P. R., Miller, E. R., Simons-Morton, D.G., Karanja, N., Lin, P. H., Aickin, M., Most-Windhauser, M. M., Moore, T. J., Proschan, M.A., & Cutler, J. A. (2001). Effects on blood pressure of reduced dietary sodium and the dietary approaches to stop hypertension (DASH) diet. *The New England Journal of Medicine*. 344, 3–10.

- Saito**, T., Nishiyama, Y., Putaux, J.-L., Vignon, M., & Isogai, A. (2006). Homogeneous Suspensions of Individualised microfibrils from the TEMPO-catalyzed oxidation of native cellulose. *Biomacromolecules*. 7 (6), 1687–1691.
- Samir**, M.A.S.A., Alloin F., Dufresne A. (2005). Review of recent research into cellulosic whiskers, their properties and their application in nanocomposite field. *Biomacromolecules*. 6, 612-626.
- Sangnark**, A., and Noomhorm, A. (2003). Effect of particle sizes on functional properties of dietary fibre prepared from sugarcane bagasse. *Food Chemistry*. 80, 221–229.
- Shaeb**, D.N., Jog J.P. (1999). Natural fibre polymer composites a review. *Advance in Polymer Technology*. 18(4), 351–363.
- Shogren**, R.L., Peterson S.C., Evans K.O., Kenar J.A., (2011). Preparation and characterization of cellulose gels from corn cobs. *Carbohydrate Polymer*. 86, 1351-1357.
- Silva**, G.G., De Souza D.A., Machado J.C., Hourston D.J., (2000). Mechanical and thermal characterization of native Brazilian coir fibre. *Journal of Applied Polymer Science*. 76, 1197-1206.
- Silva**, S.M.C., Pinto, F.V., Antunes, F.E., Miguel, M.G., Sousa, J.J.S., Pais, A.A.C.C. (2008). Aggregation and gelation in hydropropylmethyl cellulose aqueous solutions. *Journal of Colloid and Interface Science*. 327, 333-340.
- Siqueira**, G., Bras J., Dufresne A. (2009). Cellulose whiskers versus microfibrils: influence of the nature of the nanoparticle and its surface functionalization on the thermal and mechanical properties of nanocomposites. *Biomacromolecules*. 10, 425-432.
- Siqueira**, G., Bras J., Dufresne A. (2010a). Cellulosic bionanocomposites: A review of preparation, properties and applications. *Polymer*. 2 (4), 728–765.
- Siqueira**, G., Tapin-Lingua S., Bras J., Da Silva Perez D., Dufresne A. (2010). Morphological investigation of nanoparticles obtained from combined mechanical shearing and enzymatic and acid hydrolysis of sisal fibres. *Cellulose*. 17(6), 1147–1158.
- Siró**, I., & Plackett, D. (2010). Microfibrillated cellulose and new nanocomposite materials: A review. *Cellulose*. 17, 459–494.

- Slavin, J.** (2003). The impact of the proposed definition of dietary fibre on nutrient databases. *Journal of Food Composition and Analysis*. 16, 287-291.
- Spence, K.L., Venditti R.A., Rojas O.J., Habibi Y., Pawlak J.J.** (2010a). The effect of chemical composition on microfibrillar cellulose films from wood pulps: water interactions and physical properties for packaging applications. *Cellulose*. 17, 835-848.
- Spence, K.L., Venditti R.A., Rojas O.J., Habibi Y., Pawlak J.J.** (2010b). The effect of chemical composition on microfibrillar cellulose films from wood pulps mechanical processing and physical properties. *Bioresource Technology*. 101, 5961 - 5968.
- Spence, K.L., Venditti R.A., Rojas O.J., Habibi Y., Pawlak J.J.** (2011). A comparative study of energy consumption and physical properties of microfibrillated cellulose produced by different processing methods. *Cellulose*. 18, 1097-1111.
- Stelte, W., & Sanadi, A. R.** (2009). Preparation and characterization of cellulose nanofibers from two commercial hardwood and softwood pulps. *Industrial and Engineering Chemistry Research*. 48, 11211–11219.
- Sugiyama, J., Vuong R., Chanzy H.** (1991). Electron diffraction study on the two crystalline phases occurring in native cellulose from an algal cell wall. *Macromolecules*. 24, 4168-4175.
- Sullo, A., Watson, R.L., Norton, I.T.** (2014). The design of colloidal foods for healthier diets. *Gums and Stabilisers for the food industry: Changing the face of food manufacture: the role of hydrocolloids -17*. Royal society of chemistry, Cambridge, UK. 289-299.
- Suryanarayana, C., Norton G.M.** (1998). *X-Ray Diffraction: A Practical Approach*. Edition.1. p50.
- Tandjawa, A.G., Durand S., Berot S., Blassel C., Gaillard C., Garnier C., Doublier L.J.** (2010). Rheological characterization of microfibrillated cellulose suspensions after freezing. *Carbohydrate Polymers*. 80, 677-686.
- Tandjawa, A.G., Durand S., Gaillard C., Garnier C., Doublier L.J.** (2012a). Rheological behaviour and microstructure of microfibrillated cellulose suspensions/low-methoxyl pectin mixed systems. Effect of calcium ions. *Carbohydrate Polymers*. 87(2), 1045–1057.
- Tandjawa, A.G., Durand S., Gaillard C., Garnier C., Doublier L.J.** (2012b). Properties of cellulose/pectins composites: Implication for structural

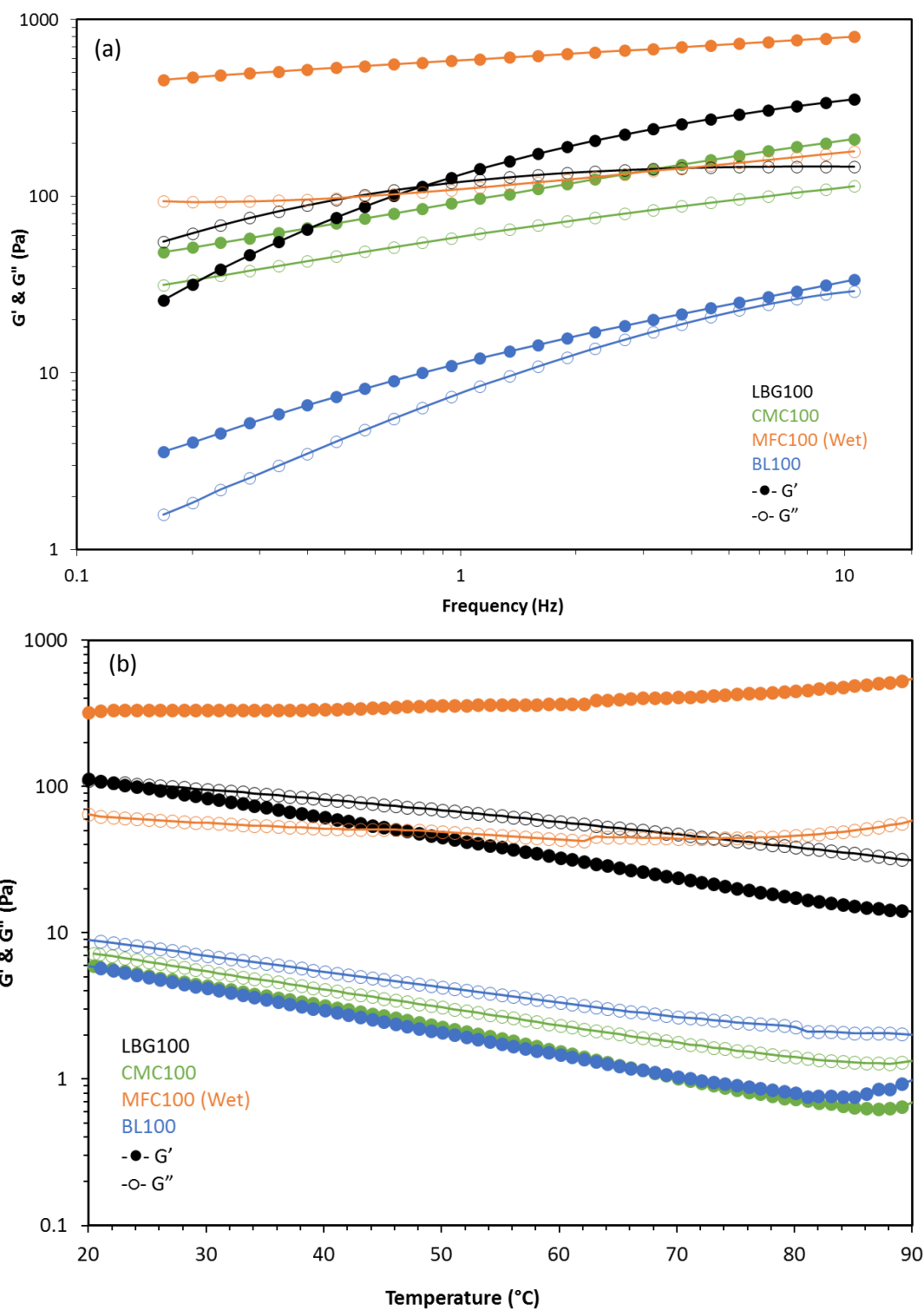
and mechanical properties of the cell wall. *Carbohydrate Polymers*. 90(2), 1081–1091.

- Tatsumi, D.** (2007). Rheology of cellulose fibre disperse systems and cellulose solutions. *Nihon Reoroji Gakkaishi*. 35 (5), 251–256.
- Tatsumi, D., Ishioka, S., & Matsumoto, T.** (1999). Effect of particle and salt concentrations on the rheological properties of cellulose fibrous suspensions. *Nihon Reoroji Gakkaishi*. 27 (4), 243–248.
- Tatsumi, D., Ishioka, S., & Matsumoto, T.** (2002). Effect of fibre concentration and axial ratio on the rheological properties of cellulose fibre suspensions. *Journal of the Society of Rheology Japan*. 30 (1), 27–32.
- Taylor, A. J., Linforth R. S. T., Harvey B. A., Blake B.** (2000). Atmospheric pressure chemical ionisation mass spectrometry for in vivo analysis of volatile flavour release, Udine, Italy, Elsevier Sci Ltd.
- Tian, X., Fisk, I.D.** (2012). Salt release from potato crisp. *Food and Function*. 3, 376-380.
- Togrul, H., Arslan, N.** (2003). Production of carboxymethyl cellulose from sugar beet pulp cellulose and rheological behaviour of carboxymethyl cellulose. *Carbohydrate Polymers*. 54, 73–82.
- Tolstoguzov, V.** (2003). Some thermodynamic considerations in food formulation. *Food Hydrocolloids*. 17(1), 1-23.
- Tungland, B.C. and Meyer, D.** (2002). Non-digestible oligo- and polysaccharides (dietary fibre): their physiology and role in human health and food. *Comprehensive Reviews in Food Science and Food Safety*. 1, 73-92.
- Turbak, A. F., Snyder, F. W., & Sandberg, K. R.** (1985). Micro-fibrillated cellulose and process for producing it. Patent no: CH 648071 (A5).
- Ulbrich, M., Floter, E.** (2014). The impact of high-pressure homogenisation modification of a cellulose based fibre product on water binding properties. *Food Hydrocolloids*. 41, 281-289.
- Vackier C.M., Hills B.P., Rutledge D.N.** (1999). An NMR Relaxation study of the state of water in gelatin gels. *Journal of Magnetic Resonance*. 138, 36–42.
- Veen, S.J., Kuijk, A., Versluis, P., Husken, H., Krassimir, P.V.** (2014). Phase transitions in cellulose microfibril dispersions by high-energy mechanical de-agglomeration. *Langmuir*. 30, 13362-13368.

- Vesterinen**, H.A., Myllytie P.,Laine J. Seppala, J. (2010). The effect of water-soluble polymers on the rheology of microfibrillar cellulose suspension and dynamic mechanical properties of the paper sheet. *Journal of Applied Polymer Science*. 116 (5), 2990-2997.
- Wada**, M, Heux L, Sugiya J. (2004a). Polymorphism of cellulose I family: Reinvestigation of cellulose IV_I. *Biomacromolecules*. 5, 1385-1391.
- Wada**, M., Chanzy H, Nishiyama Y, Langan P. (2004b). Cellulose III_I Crystal Structure and Hydrogen Bonding by Synchrotron X-ray and Neutron Fibre Diffraction. *Macromolecules*. 37(23), 8548-8555.
- Wada**, M., Ike M, Tokuyasu K. (2010). Enzymatic hydrolysis of cellulose I is greatly accelerated via its conversion to the cellulose II hydrate form. *Polymer Degradation and Stability*. 95, 543-548.
- Walker**, L.P., Wilson D.B. (1991). Enzymatic hydrolysis of cellulose: an overview. *Bioresource Technology*. 36, 3- 14.
- Wang**, B., Sain, M., (2007). Isolation of nanofibers from soybean source and their reinforcing capability on synthetic polymers. *Composites Science and Technology*. 67, 2521–2527.
- Whitney**, S.E.C., Brigham J.E., Darke A.H., Reid J.S.G., Gidley M.J. (1998). Structural aspects of the interaction of mannan-based polysaccharides with bacterial cellulose. *Carbohydrate Research*. 307, 299-309.
- Wood**, F. W. (1968). Psychophysical studies on the consistency of liquid foods. S.C.I. monograph: Rheology and texture of foodstuffs. 40-49.
- Yamamoto**, H., Horii F., Odani H. (1989). Structural changes of native cellulose crystals induced by annealing in aqueous alkaline and acidic solutions at high temperatures. *Macromolecules*. 22 (10), 4130–4132.
- Yang**, H., Yan, R., Chen, H., Lee, D.H., Zheng, C. (2007). Characteristics of hemicellulose, cellulose and lignin pyrolysis. *Fuel*. 86, 1781-1788.
- Young**, R.A. (1994). Comparison of the properties of chemical cellulose pulps. *Cellulose*. 1(2), 107-130.
- Zhang**, J., Song H., Lin L., Zhuang J., Pang C., Liu S. (2012). Microfibrillated cellulose from bamboo pulp and its properties. *Biomass and Bioenergy*. 39, 78-83.
- Zimmermann**, T., Bordeanu, N., Strub, E. (2010). Properties of nanofibrillated cellulose from different raw materials and its reinforcement potential. *Carbohydrate Polymers*. 79, 1086-1093.

- Zuluaga, R., Putaux J.L., Restrepo A., Mondragon I., Gañán P. (2007).** Cellulose microfibrils from banana farming residues: isolation and characterization. *Cellulose*. 14(6), 585-592.

Appendix



Appendix 1: Viscoelastic behaviour of 2% w/w suspension of LBG100, CMC100, MFC100 (never dried) and Blend100 (CMC/LBG) where; (a) as a function of frequency (Hz), and (b) as a function of temperature ($^{\circ}\text{C}$) at $1^{\circ}\text{C}/\text{min}$ heating rate.

You are provided with two samples, please taste them in the order from left to right, identify which one is more saltier of sample by placing a tick in the box marked with the sample's three digit code.

Cleanse your palate with the water after each sample with the water provided.

717 254

Any Comments:

Thank you for your participation!

Appendix 2: Pair comparison and comment card used in the sensory analysis.